Calcium measurement in living filamentous fungi expressing codon-optimised aequorin

Olga Kozlova-Zwinderman

Doctor of Philosophy

University of Edinburgh

2002

Dedicated to my parents and my husband

This thesis has been composed by myself. The research of which it is a record was carried out by myself. All sources of information have been acknowledged by means of references.

Olga Kozlova-Zwinderman

ACKNOWLEDGEMENTS

I want to thank my supervisor Dr. Nick Read who arranged this research and who helped me throughout my PhD.

Also I am grateful to my supervisor in Russia Prof. Sergey Egorov for his help and support.

I am very grateful to Darwin Trust who provided me with the Scholarship.

Also thanks for Prof. Trewavas for general advice and Prof. Christofi for help on biosensor project.

I am very grateful to Dan Cordova from DuPont for organising the project on fungicides mode-of-action and Dr. Chritoph Plieth for his help on the calibration and work with cold and heat shock.

Big thanks to everybody in the lab who helped me and cheered me up and people in Rutherford building for being always there to answer questions.

And finally very big thank you for my parents for their believe and support and my husband Mark for everything.

ABSTRACT

The aim of this study was to monitor changes in cytosolic free calcium ($[Ca^{2+}]_c$) in filamentous fungi using codon-optimised aequorin under different conditions in order to analyse Ca^{2+} signalling in these organisms, and to use the recombinant aequorin method in fungicide mode-of-action studies, and as novel toxicant biosensor.

Calcium signalling is little understood in filamentous fungi largely because easy and routine methods for Ca^{2+} measurement in living hyphae have previously been unavailable. Recently a new method for measuring cellular Ca^{2+} based on using codon-optimised recombinant aequorin, has been developed and used throughout the present study.

The calibration method to convert light detected from aequorin expressing strains into $[Ca^{2+}]_c$ concentrations was optimised and critically evaluated. It was concluded that codon-optimised aequorin can provide excellent qualitative measurements of fungal $[Ca^{2+}]_c$ but that precise quantification of $[Ca^{2+}]_c$ using this method need to be treated with caution.

Three external stimuli (mechanical perturbation, hypo-osmotic shock and high external $CaCl_2$, but not hyper-osmotic shock) were found to transiently increase $[Ca^{2+}]_c$ levels and to generate specific $[Ca^{2+}]_c$ signatures. Different parameters of the Ca^{2+} signature (rise time, amplitude and full width half maximum) were quantified. Transient $[Ca^{2+}]_c$ increases were also observed in response to cold and heat shock. Using Ca^{2+} channel blockers ($LaCl_3$, KP4, ryanodine, nifedipine, TMB-8, verapamil), the Ca^{2+} chelator BAPTA, and Ca^{2+} agonists (A23187, caffeine and cyclopiazonic acid), it was shown that the $[Ca^{2+}]_c$ increases resulting from hypo-osmotic shock and high external $CaCl_2$ are predominantly due to the influx of Ca^{2+} from the external media through plasma membrane Ca^{2+} channels. The $[Ca^{2+}]_c$ increases resulting from mechanical perturbation seem to arise from both extracellular and intracellular sources. My results indicate that filamentous fungi possess a number of the components of the calcium signalling machinery found in other eukaryotic cells.

Differences were noted in the $[Ca^{2+}]_c$ responses to physico-chemical stimuli and Ca^{2+} agonists in fungi grown in liquid medium compared with those grown on solid medium.

$[Ca^{2+}]_c$ plays an important role in signal-response coupling. I therefore investigated whether the external stimuli shown to transiently elevate $[Ca^{2+}]_c$ also induced changes in hyphal tip morphology, branching frequency, colony extension rate and sporulation. The short term increases in $[Ca^{2+}]_c$ resulting from mechanical perturbation, hypo-osmotic shock and high external $CaCl_2$ were found not to influence any of theses parameters. However the long term increase in $[Ca^{2+}]_c$ caused by A23187 resulted in the formation of bulbous hyphal compartments and hyperbranching. A23187 also inhibited growth of *A.awamori* and caused significant cell death.

The aequorin method was found to be useful in fungicide mode-of-action studies. A large number of commercial fungicides were shown to perturb $[Ca^{2+}]_c$ homeostasis. Evidence was obtained which suggested that a cell permeabilizing compound (viscosinamide) produced by antagonistic soil bacteria may inhibit the growth of soil fungi by perturbing Ca^{2+} signalling or $[Ca^{2+}]_c$ homeostasis.

The aequorin method was used as a novel eukaryotic toxicant biosensor. Three environmental pollutants (3,5-DCP, Cr^{3+} and Zn^{2+}) were tested and were each shown to influence in a unique manner the Ca^{2+}-signature in response to the addition of external $CaCl_2$. Preliminary results suggested that the fungal aequorin biosensor may be less sensitive for detecting these pollutants than the standard *Vibrio fischeri* luciferase biosensor.

ABBREVIATIONS

Standard SI (International System of Units) were used throughout this thesis. Non-SI units are as follows:

A23187	calcymycin
ADP	adenosine diphosphate
aeqS	synthetic apoaequorin gene
AMP	adenosine monophosphate
ATP	adenosine triphosphate
BAPTA	1,2-bis(2-AMinophenoxy)ethane-N,N,N',N'-tetraacetic acid
BAY(-)	(E)3-[(4-Methylaphynyl)sulfonyl]-2-propenenitrile
BSA	bovine serum albumin
cAMP	cyclic adenosine monophosphate
$[Ca^{2+}]_c$	cytosolic free Ca^{2+}
cADP	cyclic adenosine diphosphate ribose
CaM	calmodulin
Captan	N–tricholomethylthio–4–cyclohexene–1,2-dicarboximide
cDNA	complementary deoxyribonucleic acid
cf	compare figures
CICR	calcium-induced calcium release
CLSM	confocal laser scanning microscopy
CPA	cyclopiazonic acid
3D	three dimensional
DAG	diacylglycerol
3,5-DCP	3,5-dicholorphenol
dH_2O	distilled H_2O
DHP	dihydropyridine
DMSO	dimethylsulphoxide
EDTA	ethylenediaminetetraacetic acid
EGTA	ethyleneglycol-bis-(β-aminoethyl)-N,N,N',N'-tetraacetic acid
EtOH	ethanol
ER	endoplasmic reticulum

Exp	experiment
FDA	fluorescein diacetate
FWHM	full width half maximum
G-protein	guanosine triphosphate binding protein
GTP	guanosine triphosphate
h	hour(s)
IC_{50}	concentration of chemical which results in 50% inhibition
IP_3	inositol 1,4,5-triphosphate
M	molar
Manzate	manganese ethylenebis dithiocarbamate (polymeric)
MBC	methyl 2-benzimidasolecarbamate
MeOH	methanol
min	minute(s)
MM	minimal medium
M_r	relative molecular weight
Paba	*p*-aminobenzoic acid
PC	personal computer
PLC	phospholipase C
PM	plasma membrane
ppm	parts per million
psi	pounds per square inch
$PtdInsP_2$	phophotidylinositol 4,5-biphosphate
PZ	0.8% NaCl
RLU	relative light unit(s)
RMG	rich media with glucose
rpm	revolutions per minute
RyR	ryanodine receptor
s	seconds
SE	standard error
SERCA	sarco/endoplasmic reticulum
TFP	trifluroperazine
TMB-8	3,4,5-trimethoxybenzoic acid 8-(diethylamino)-octyl ester

UV	ultraviolet
VS medium	Vogel's media with sucrose
v/v	volume:volume
W-5	N-(6-aminohexyl)–1-naphthalenesulfonamide
W-7	N-(6-aminohexyl)-5-chloro-1-naphthalenesulfonamide

TABLE OF CONTENTS

1 INTRODUCTION

1.1 CALCIUM SIGNALLING IN EUKARYOTES

Eukaryotic cells possess very complex signalling systems. Whilst interacting with the environment, cells are exposed to numerous extracellular signals. In order to respond to these stimuli adequately, eukaryotes have developed a wide range of interconnected intracellular signalling pathways which are able to regulate all of an organism's functions.

Ca^{2+} is the most universal intracellular signalling molecule found in all organisms from prokaryotes to highly specialized animal cells. The reason why evolution chose this ion as an intracellular signalling molecule is still not known. One hypothesis suggests that at first cells developed mechanisms to maintain very low level of cytosolic free Ca^{2+} ($[Ca^{2+}]_c$), much lower then the millimolar concentrations that prevail in seawater (Sanders et al. 1999). The reason for this is that Ca^{2+} binds to phosphate groups, including those of ATP, ADP and AMP, which are essential for the energy metabolism of cells (Gadd 1995). The maintenance of $[Ca^{2+}]_c$ at a very low concentration was absolutely essential for phosphate-oriented metabolism to exist (Carafoli 1987). Thus, even very early during evolution cells had a transport system that exported Ca^{2+} from the cytosol to sustain steady state values of $[Ca^{2+}]_c$ in the submicromolar range. Another reason for Ca^{2+} becoming a second messenger is that this ion can coordinate a significant number of oxygen atoms (6-8) which enables protein conformational changes. These conformational changes can then elicit downstream events in signalling pathways (Sanders et al. 1999). So even small changes in Ca^{2+} can possibly trigger wide variety of signalling processes. The third reason why Ca^{2+} was chosen as a signal molecule may be the low rate that Ca^{2+} diffuses through the cytosol and also nonhomogenous distribution of intracellular Ca^{2+} stores (i.e. various Ca^{2+} -storage organelles). These factors provide spatial variation in Ca^{2+} concentration within different regions of the cytosol allowing

different $[Ca^{2+}]_c$ signals to be spatially separated from each other in the same cell (Bush 1995; Gilroy and Trewavas 2001).

1.2 CALCIUM SIGNALLING IN FILAMENTOUS FUNGI

Calcium is believed to be involved in the control of many important processes in fungi (Table 1.1). Although Ca^{2+} signalling has been implicated in regulating these processes little is known about the precise components and sequence of events involved into each signalling pathway.

1.3 CALCIUM SIGNAL TRANSDUCTION NETWORK

The general scheme of Ca^{2+}-mediating signalling pathway is shown in Fig. 1.1.

Extracellular signal	⇒	Receptor	⇒	Ca^{2+}-channel	⇒	$Ca^{2+} \pm$ CaM	⇒	Target proteins	⇒	Response

Figure 1.1 Simplified scheme showing components of a Ca^{2+}-mediated signal response pathway (Adapted from Gadd, 1995).

The normal resting level concentration of $[Ca^{2+}]_c$ is typically in the range of 50-200 nM (Bush 1995). The concentration of the Ca^{2+} in the extracellular environment is usually 10^4 times higher (Saporito and Sypherd 1991). Calcium-mediated signal transduction commonly involves a transient increase in $[Ca^{2+}]_c$, which is often localised within a specific region of a cell (Gadd 1995). The level of $[Ca^{2+}]_c$ increase often depends upon the strength of the stimulus (Bootman et al. 1994).

Species	Ca^{2+} -dependent processes	Reference
Aspergillus nidulans	cell cycle	Lu et al. 1992, Lu et al. 1993
A. fumigatus	hyperbranching	Gow et al. 1992
Botrytis cinerea	hyphal branching and growth	Hudecova et al. 1994
	phytoparasitism	Elad and Kirshner 1992
Ceratocystis (Ophiostoma) ulmi	dimorphism	Muthukumar et al. 1987, Gadd and Brunton 1992
Fusarium graminearum	hyphal extension and branching	Robson et al. 1991a, Robson et al. 1991b
Microsporum gypseum	phospholipid synthesis	Giri et al. 1994
Neurospora crassa	apical dominance	Dicker and Turian 1990
	circadian rhythm	Sadakane and Nakashima 1996
	Conidial germination	Muthukumar and Nickerson 1984, Rao et al. 1997
	hyphal branching	Reissig and Kinney 1983
Penicillium spp.	induction of conidiation	Pitt and Barnes 1993, Roncal et al. 1993
Sporothrix schenckii	germination	Rivera-Rodriguez and Rodriguez-Del Valle 1992
	dimorphism	Alsina and Rodriguez-Del Valle 1984
Trichoderma viride	conidiation	Krystofova et al. 1995

Table 1.1 Key studies providing evidence for Ca^{2+} regulating different aspects of the physiology in filamentous ascomycetes.

Most stimuli are extracellular and are mediated via a plasma membrane bound receptor (Bootman et al. 1996). Membrane bound receptors are predominantly G-protein linked. In response to stimulation, $[Ca^{2+}]_c$ is increased either from the entry into cells of Ca^{2+} through plasma membrane Ca^{2+}-channels, or through Ca^{2+} release from internal cell compartments acting as Ca^{2+} stores (Berridge 1997a).

When an extracellular ligand binds to a membrane receptor linked to a G protein the latter changes its conformation and commonly activates phospholipase C, which results in the hydrolysis of phosphotidylinositol 4,5-biphosphate ($PtdInsP_2$) into diacylglycerol (DAG) and inositol 1,4,5-triphosphate (IP_3). IP_3 acts as a second messenger and diffuses from the site of formation to an appropriate Ca^{2+} storage organelle. Here it binds to receptor on the membrane of this organelle, which activates Ca^{2+}-channels thus causing the release of Ca^{2+} from internal stores. The Ca^{2+} will interact with different Ca^{2+}-binding proteins (e.g. CaM). Commonly Ca^{2+} primarily binds to CaM, which can then interact with and activate or regulate the activity of various proteins involved in the final response. Alternatively Ca^{2+} may directly regulate the activities of specific proteins (e.g. protein kinase or ion channels) (Hancock 1997).

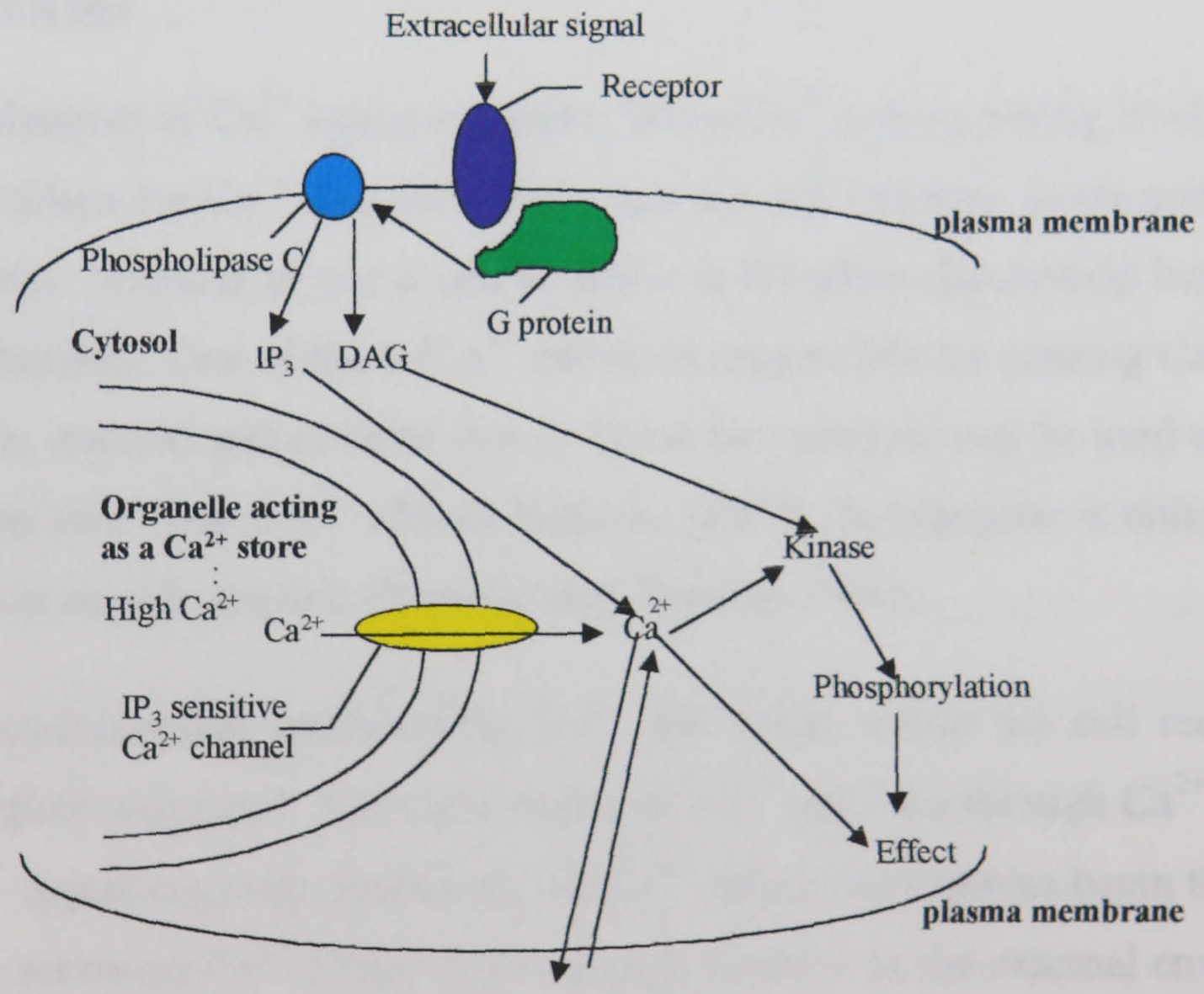

Figure 1.2 Simplified scheme showing the control and role of $[Ca^{2+}]_c$ within the cell (adapter from Hancock, 1997).

High levels of $[Ca^{2+}]_c$ are toxic to the cell due to Ca^{2+} reacting with phosphate-containing compounds (Campbell 1983). Hence Ca^{2+} ions are very actively pumped out of the cytosol by Ca^{2+} transporter proteins located in the plasma membrane and the membranes of organelles (e.g. endoplasmic reticulum (ER), vacuoles and mitochondria). which sequester Ca^{2+}. Ca^{2+} levels may be further regulated by Ca^{2+}-binding proteins in the cytosol. Because the concentration of free Ca^{2+} is up to 4 orders of magnitude lower in the cytosol compared with the external environment or within Ca^{2+} storage organelles (Hancock 1997), the transport of Ca^{2+} out of the cytosol needs to be energized, either by ATP hydrolysis or by proton gradient, which is itself ATP-generated (Johannes et al. 1991).

1.3.1 Ca^{2+} fluxes

The basic mechanism of Ca^{2+} action is simple. When Ca^{2+} is at its resting level the cell is quiescent, but when the Ca^{2+} concentration raises the cell becomes active and performs certain functions. Whether or not a cell is active is therefore determined between two different mechanisms. One of them (Ca^{2+} influx) is responsible for pouring Ca^{2+} into the cytoplasm from internal and external stores. These two sources may be used together or separately. The other one (Ca^{2+} efflux) removes $[Ca^{2+}]_c$ by pumping it either into the internal stores or outside the cell (Berridge and Bottman 1996).

The steep electrochemical gradients for Ca^{2+} that occur within the cell require Ca^{2+} influx to be tightly regulated. The main routes of Ca^{2+} entry are through Ca^{2+}-channels. Once the Ca^{2+} signal has been generated, the Ca^{2+} efflux mechanisms begin the process of recovery by returning Ca^{2+} either to the internal stores or to the external environment. These recovery pathways must be extremely active because they have to work against the 10000:1 electrochemical gradient of the Ca^{2+} across membranes.. This Ca^{2+} removal is carried out by Ca^{2+}-ATPases and Ca^{2+}/nH^{+} antiporters (Bush 1995).

Ca^{2+} influx and efflux in yeast are well described both on genetical and biochemical levels (Cunningham and Fink 1996). For filamentous fungi only some parts of the Ca^{2+} transportation system has been identified. Inward Ca^{2+} transport has been demonstrated in *Ophiostoma ulmi* (Gadd and Brunton 1992), *Penicillium notatum* (Pitt and Barnes 1993) and *Trichoderma viride* (Krystofova et al. 1996). There are several driving forces of Ca^{2+} influx. One of them is definitely the osmotic gradient of Ca^{2+}. Another driving force described is a Ca^{2+}/nH^{+} ($n<2$) antiporter, though a Ca^{2+} uniporter may also play a role. H^{+}/Ca^{2+} antiporter has also been found in yeast (Dunn et al. 1994) and plant vacuolar membranes (Dunn et al. 1994; Hirschi et al. 1996).

Calcium efflux from hyphae of *Trichoderma viride* has been described by Simkovic et al. (2000). Also accumulation of Ca^{2+} in the organelles has been shown in *Neurospora crassa* (Cornelius and Nakashima 1987; Miller et al. 1990).

Ca^{2+} efflux is thought to occur at the same time as Ca^{2+} influx. But the transport systems involved are different (Simkovic et al. 2000). Most Ca^{2+} efflux results from the activity of Ca^{2+}-ATPases (Hernandez et al. 1994; Stroobant and Scarborough 1979).

1.3.2 Ca^{2+}-channels

In animal and plant cells Ca^{2+} influx occurs through the activation of Ca^{2+}-channels that control either entry of extracellular Ca^{2+} or release of Ca^{2+} from internal stores (i.e. Ca^{2+}-storage organelles).

Ca^{2+}-channels may be classified by their intracellular location. Those found in the plasma membrane are classified as influx channels and those found on intracellular membranes are release channels (Bush 1995).

Plasma membrane Ca^{2+}-channels have been classified according to how their activities are controlled. Three types are distinguished: voltage-gated, ligand-gated or

mechanically gated (stretch-activated). The vast majority of plasma membrane Ca^{2+}-channels in animal cells are voltage-gated (opened by membrane depolarisation). Many of these channels are also regulated by phosphorylation or GTP-binding proteins. Ligand-gated channels are activated by the binding of extracellular agonists such as glutamate and ATP. Stretch-activated Ca^{2+}-channels are activated by tension on the plasma membrane (Johannes et al. 1991). The plasma membrane of animal cells also contains Ca^{2+}-channels which are activated by Ca^{2+}. The mode of action of these channels is still unclear but the suggestion is that empty Ca^{2+} stores release a messenger which diffuses to the membrane and opens these channels (Berridge and Bottman 1996; Gelli and Blumwald 1993).

Ca^{2+} release from internal stores can occur either via voltage-dependent or ligand-gated channels. In animal cells two families of receptors are responsible for releasing Ca^{2+}: inositol 1,4,5-triphosphate receptors (IP_3) and ryanodine receptors (RyRs). The information which controls the opening of these channels is transferred from cell surface either through a direct protein-protein interaction or through diffusible Ca^{2+}-mobilizing intracellular messenger such as IP_3 or cyclic adenosine diphosphate ribose (cADP ribose) (Berridge and Bottman 1996). In animal cells IP_3 gated channels are thought to be localized mainly in ER. In plants these channels are responsible for Ca^{2+} release from tonoplast vesicles and intact vacuoles (Johannes et al. 1991).

In plants two types of plasma membrane Ca^{2+}-channels have been defined on the basis of their pharmacological properties. The first type is dihydropyridine (DHP) sensitive; the other type is phenylakylamine sensitive. Endomembranes Ca^{2+} -channels are similar to ones in animals (Gelli and Blumwald 1993).

In fungi there is evidence for Ca^{2+} entering the cytosol through ligand-, voltage- and mechanically-gated channels (Gadd 1995).

Stretch -activated channels have been suggested as mechanotransducers in response to a variety of mechanical perturbations and hypo-osmotic shock (Batiza et al. 1996).

Recently in yeast two genes possess a Ca^{2+}-mediating role have been identified: CCH1 and MID1. MID1 is a transmembrane protein with some homology to cyclic nucleotide-gated cation channels. CCH1 shows high homology with animal Ca^{2+}-channel α1-subunit genes. It seems that both proteins are parts of the same pathway for Ca^{2+} uptake (Fischer et al. 1997).

1.3.3 Ca^{2+}-ATPases

In animal cells two major classes of Ca^{2+}-ATPases have been identified. The first one termed the ER-type named after its localization in the ER, transports two Ca^{2+} for each ATP hydrolysed. ER Ca^{2+}-ATPase is not stimulated by Calmodulin (CaM). The second type originally found in the plasma membrane and called the PM type transports one Ca^{2+} per ATP hydrolysed and is stimulated but CaM. In plant cells there is increasing evidence that ATPases are divided into roughly similar groups (Bush 1995).

During the pumping cycle a phosphate group is transferred to an aspartate residue on the Ca^{2+}-ATPase. This phosphorylation of the protein results in the conformational change needed to transport Ca^{2+} across the membrane. Dephosphorylation restores protein to its former state ready for the transport of another Ca^{2+} ion. The energy released from ATP hydrolysis drives the Ca^{2+} pumping activity of the ATPase (Hancock 1997).

The importance of Ca^{2+}-ATPases has been demonstrated in yeast by mutation of the *pms1* gene, which encodes a PM-type ATPase that is found in the yeast tonoplast membrane (Cunningham and Fink 1994b). A possible ER Ca^{2+}-ATPase has been found in *Schizosaccharomyces pombe* (Ghislain et al. 1990). This is encoded by the *cta*3 gene, which most closely resembles mammalian ER Ca^{2+}-ATPase genes. By inhibiting vacuolar Ca^{2+} uptake (using a protonophore to uncouple the proton gradient) and

permeabilizing the plasma membrane (using nystatin), the *cta*3 gene product was shown to be a non-vacuolar, internal ATP-dependent Ca^{2+}-channel. Residual ATP-dependent Ca^{2+} uptake was observed in the *cta*3 null mutant, suggesting that another non-vacuolar Ca^{2+}-ATPase exists (Halachmi and Eilam 1996).

In filamentous fungi Ca^{2+} transporting ATPase was found in plasma membrane. Ca^{2+} transport is not strongly dependent on the existence of a proton gradient across the plasma membrane. The operation of this Ca^{2+} pump depends on MgATP although it can use MgGTP with lesser efficiency. Inhibitory data suggest that it resembles P-type Ca^{2+}-ATPases of plant plasma membrane (Hernandez et al. 1994).

1.3.4 Antiporters

The second major class of efflux transporters are Ca^{2+}/nH^{+} antiporters. The antiporters are secondary transporters that do not directly require ATP for transport. They are driven by a proton gradient which is generated by H^{+} -ATPases (Bush 1995; Johannes et al. 1991).

Ca^{2+}/H^{+} antiport transporters in the plasma membrane pump Ca^{2+} out of the cytosol in exchange for H^{+} (Stroobant and Scarborough 1979). It is thought that these transporters are ATP-dependent pumps with a stoichiometric ratio of 2 H^{+} ions per Ca^{2+} ion (Miller et al. 1990).

In the vacuole, Ca^{2+}/H^{+} antiport systems transport Ca^{2+} across the vacuolar membrane, and the proton gradient across the vacuole is maintained by H^{+}-ATPase pumps (Anraku et al. 1991; Klionsky et al. 1990), which also help to control cytosolic pH. Several stoichiometries have been suggested for fungal vacuolar Ca^{2+}/H^{+} antiports, with stoichiometric ratio H^{+}/Ca^{2+} being the most likely (Gadd 1995). Mutants of *S. cerevisiae* lacking a functional gene for a vacuolar H^{+}-ATPase are not able to control $[Ca^{2+}]_c$ (Ohya

et al. 1991), showing the importance of maintaining the proton gradient and the importance of the vacuole in Ca^{2+} storage. The H^+/Ca^{2+} antiport protein VCX1 which is inactivated by calcineurin, a Ca^{2+}/calmodulin-dependent protein phosphatase has been identified in yeasts (Cunningham and Fink 1996). Conservation of vacuolar Ca^{2+} transporters between species appears to be very high, as H^+/Ca^{2+} antiports from *A. thaliana* are operable in *S. cerevisiae* (Hirschi et al. 1996), as are putative ER Ca^{2+}-ATPase pumps of *A. thaliana* (Liang et al. 1997). The importance of the vacuole for Ca^{2+} homeostasis is highlighted, as it allows fungal cells to grow in media containing $CaCl_2$ with a concentration as high as 100 mM $CaCl_2$ (Ohya et al. 1986).

1.3.5 Ca^{2+} binding proteins

Cells possess a great variety of Ca^{2+}-binding proteins that contribute to Ca^{2+}-mediated signalling, either by buffering free Ca^{2+} ions and thus shaping the cellular response or by acting as sensors that mediate the messenger role of Ca^{2+} (Berridge and Bottman 1996).

Most of Ca^{2+}-binding proteins bind Ca^{2+} through six or seven oxygen atoms, provided by glutamate or aspartate amino residues. Another common feature of Ca^{2+}-binding proteins is the presence of a structure called EF-hand. This is a secondary structure that comprises two α-helices positioned in such a way as to point like the forefinger and thumb of a right hand. A Ca^{2+}-binding loop containing active Ca^{2+}-binding glutamate and aspartate residues lies between the α-helices (Hancock 1997).

Ca^{2+}-binding proteins can be divided into two groups: soluble (nonmembranous) proteins and the intrinsic membrane proteins (Carafoli 1987). Intrinsic membrane proteins bind Ca^{2+} on one side of the membrane (plasma membrane or membrane of an organelle), transport them across, return back and then the cycle starts again. Soluble proteins can be also subdivided into two categories. The first group works like a buffer only. Proteins of this group bind Ca^{2+}, to maintain its low concentration in cytosol. The

second group not only buffers Ca^{2+} but these proteins also change their conformation allowing them to interact with enzyme targets and thus transduce signals. Thus these proteins are also called "Ca^{2+} modulated proteins".

1.3.5.1 Calmodulin

One of the most important proteins of this group is the primary intracellular Ca^{2+}-binding protein calmodulin (CaM). CaM is involved in mediating a vast number of signalling pathways. Sometimes it is an integral part of enzyme complex. With cAMP, CaM can both activate adenylyl cyclase which is responsible for cAMP synthesis and Ca^{2+}/CaM phosphodiesterase, which causes cAMP breakdown.

CaM is a small, relatively acidic protein. In most cells it can bind 4 Ca^{2+} molecules although in the budding yeast it can only bind 3 (Luan et al. 1987). Its affinity to Ca^{2+} is approximately 10^{-6} mol/l. The shape of the protein molecule resembles a dumb-bell, with two globular regions connected by a long, flexible and very mobile α-helix. Each of the globular domains contains two EF hand regions, with their characteristic helix-loop-helix topology, each of which can bind to one molecule of Ca^{2+}. The two EF hands within each globular region are connected by a short antiparallel β-sheet region. Despite the similarity in two regions, their affinity to Ca^{2+} differs. The C terminal domain has the higher affinity and binds Ca^{2+} first leading to major conformational changes within the molecule. These conformational changes reveal two hydrophobic patches, one in each half of the protein. This patches then interact with the CaM target proteins such as protein kinases, phosphatases, adenylate cyclases, phosphodiesterases and Ca^{2+}-ATPases (Gadd 1995; Hancock 1997). The affinity of Ca^{2+}-CaM complex to the target proteins is 4 orders of magnitude higher then of Ca^{2+} on its own (Pietrobon et al. 1990).

CaM is involved in important cell functions in yeast and filamentous fungi including: cell proliferation, cell cycle control and nuclear division (Anraku et al. 1991). CaM has

been identified in many fungal species including: *S. cerevisiae*, *S. pombe*, *Aspergillus nidulans*, *N. crassa*, *Candida albicans* (Cox et al. 1982; Davis et al. 1986; Gadd 1995; Saporito and Sypherd 1991 and Takeda and Yamamoto 1987). The filamentous fungal CaM of *Neurospora crassa* is indistinguishable from the vertebrate CaM by its Ca^{2+}-binding properties. It is slightly less acidic then it vertebrate counterpart. Its amino acid composition resembles one of the plant CaM (Cox et al. 1982). CaM-targeted proteins include protein kinases, phosphatases, adenylate cyclases, phosphodiesterases and Ca^{2+}-ATPases.

1.3.6 Intracellular Ca^{2+} stores

Because Ca^{2+} in high concentrations is toxic to the cell, an effective system is required for regulating $[Ca^{2+}]_c$. This system consists of a number of pumps located in the plasma membrane or on the membranes of intracellular organelles such as the vacuoles, mitochondria, endoplasmic reticulum (ER), membrane vesicles and Golgi. These organelles serve as compartments for the storage of Ca^{2+}, and are able to take up and release Ca^{2+} ions (Cornelius and Nakashima 1987).

The release of Ca^{2+} from internal stores is mediated by voltage or ligand-gated channels. The later are activated by the ligand binding to the receptor on the plasma membrane, which leads to the activation of phospholipase C (PLC) which catalyses the hydrolysis of phosphotidylinositol 4,5-biphosphate (IP_3) and diacylglycerol. IP_3 is highly mobile in the cytoplasm and diffuses into the cell interior where it binds to IP_3 receptors. This causes a conformational change in the receptor, allowing it to interact with the integral channel which is opened and allowing Ca^{2+} to enter cytoplasm (Bootman et al. 2001).

IP_3 has been identified in animal, plant and fungal cells. In animal cells IP_3 causes the release of Ca^{2+} from the ER which acts as the major Ca^{2+} store. In Cornelius et al (1989) *Neurospora crassa* to stimulate Ca^{2+} efflux from vacuoles. Based on the inhibitor data,

some similarities between the vacuolar IP_3 receptor in filamentous fungi and ER IP3 receptor in animal cells has been suggested. Furthermore there is a suggestion that the vacuole in fungal hyphae serves a similar role as a Ca^{2+} store as the ER does in animal cells.

Vacuoles. Vacuoles appear to be the main Ca^{2+} storage organelle in fungi (Cornelius and Nakashima 1987) (Miller et al. 1990) with the estimated concentration of free Ca^{2+} approximately 30 μM (Strayle et al. 1999). Ca^{2+} flux across vacuolar membranes occurs via the Ca^{2+}/nH^{+} antiport system driven by proton gradient generated by the vacuolar membrane H^{+}-ATPase (Klionsky et al. 1990), (Anraku et al. 1991). In vacuoles Ca^{2+} is stored mainly as Ca-polyphosphates (Ohsumi and Anraku 1981). Ca^{2+} release from isolated vacuoles of *Neurospora* has been found to occur after the addition of IP_3, indicating the presence of IP_3 receptors and associated Ca^{2+}-channels in the vacuolar membrane (Cornelius and Nakashima 1987). The yeast vacuole membrane also contains putative high-affinity Ca^{2+} pump, PMC1p, which is a product of the *pmc1* gene. Pmc1p is approximately 40% similar to plasma membrane Ca^{2+}-ATPases (PMCAs). It is expected to catalyse the high affinity and ATP-dependent transport of Ca^{2+} into the vacuole (Cunningham and Fink 1994a).

Mitochondria. Mitochondria in animal cells can be considered as a Ca^{2+} store under some circumstances. Theses organelles have a substantial capacity for Ca^{2+} uptake and can significantly buffer cytosolic Ca^{2+} rises. Mitochondria sequester Ca^{2+} via a low-affinity, high speed uniporter driven by the mitochondria membrane potential (Bootman et al. 2001).

In *Penicillium notatum* mitochondria were reported to be a primary store of free Ca^{2+} with lower concentrations of Ca^{2+} associated with the ER, Golgi, vacuoles and plasma membrane components (Pitt and Barnes 1993)

Golgi. In yeasts a Ca^{2+} pump has been found associated with the Golgi complex. It is encoded by *pmr1* gene. PMR1p is approximately 30% similar to members of the SERCA family, which are Ca^{2+}-ATPases found in the sarcoplamic/ER of animal cells. Genetical evidence suggests that the primary function of PMR1p is Ca^{2+} transport supplying Ca^{2+} to Golgi for specific secretory functions (Cunningham and Fink 1994a).

Endoplasmic reticulum. Ca^{2+} is generally thought to play important roles in protein trafficking in the ER and related secretory compartments. To date there is no evidence in fungi for the existence of SERCA-type Ca^{2+} pumps (Cunningham and Fink 1994a). *Schizosaccharomyces pombe* contains a P-type ATPase gene, *cta3* distinct from the *pma1* gene encoding the plasma membrane H^{+}-ATPase. Deduced amino acid sequence of the CTA3 protein is closely related to that of mammalian endo(sarco)plasmic reticulum Ca^{2+}-ATPases and it is proposed that the CTA3 protein is involved in Ca^{2+} transport and homeostasis (Gadd 1995). Whether this protein is involved in Ca^{2+} transport into the ER is not known but unidentified Ca^{2+} transporters have been measured in some membrane preparations (Okorokov et al. 1997).

In *Saccharomyces cerevisiae* the steady-state concentration of ER Ca^{2+} was shown to be 10 μM. The mutants lacking the *pmr1* gene known to encode the "Golgi" Pmr1 pump showed severely reduced levels of ER Ca^{2+} demonstrating that this pump controls at least in part, the Ca^{2+} concentration in the yeast ER (Strayle et al. 1999).

1.4 CRITERIA FOR CALCIUM INVOLVEMENT IN SIGNAL TRANSDUCTION

As indicated earlier (Sections 1.2 and 1.3) Ca^{2+} plays an important role in mediating signal-response coupling within cells, and acts in both signal propagation and amplification. In order to experimentally demonstrate a clear relationship between

changes in $[Ca^{2+}]_c$ and a cellular response to a specific stimulus, there are several criteria which one should aim to establish (Parton and Read 1999):

- A positive correlation between the response to a specific stimulus and the change in Ca^{2+} concentration.
- The change in $[Ca^{2+}]_c$ concentration should precede the response.
- Prevention of the change in $[Ca^{2+}]_c$ concentration using inhibitors or chelators should inhibit the response to a stimulus.
- Artificial changes in the ion concentration (e.g. by using ionophores), mimicking the changes which occur upon stimulation, should evoke a comparable cellular response.

1.5 CALCIUM MEASUREMENT IN LIVING CELLS

The direct measurement of $[Ca^{2+}]_c$ dynamics in living cells is an extremely important experimental tool for analysing $[Ca^{2+}]_c$-mediated signal transduction.

Ideally the technique for Ca^{2+} measurement should have the following attributes (Carafoli 1987):

- be able to measure Ca^{2+} in the 10 nM-10 mM Ca^{2+} range.
- be able to reveal transient changes in Ca^{2+} that occur within milliseconds.
- not damage morphology and functional properties of the cells (Ca^{2+} buffering capacity).

- not diffuse into the medium across plasma membrane or redistribute across intracellular membrane boundaries.

Currently there are several techniques available for measuring $[Ca^{2+}]_c$ in living cells. $[Ca^{2+}]_c$ can be measured with Ca^{2+}-sensitive microelectrodes (Miller et al. 1994), fluorescent dyes (e.g. fluo-3, fura-2 and indo-1(Parton and Read 1999) or luminescent proteins (Miller et al. 1994). Each of these techniques has its advantages and disadvantages (Table 1.2).

The measurement of $[Ca^{2+}]_c$ with calcium-sensitive microelectrodes involves inserting two microelectrodes, the Ca^{2+}-sensitive microelectrode and a reference electrode (they can be incorporated in to a double-barrelled microelectrode) into the cytoplasm of a single cell (Read et al. 1993). This technique has been used to analyse $[Ca^{2+}]_c$ homeostasis in hyphae of *Neurospora crassa* (Miller et al. 1990) but the technique has not been widely used for fungi because of technical difficulties.

The use of fluorescent dyes for $[Ca^{2+}]_c$ measurement in hyphae of higher fungi has been fraught with problems associated with dye loading and dye sequestration within organelles (Knight et al. 1993a; Read et al. 1992; Knight et al. 1993b). The other problems known are photobleaching selectivity between other divalent cations such as Mn^{2+}, Fe^{2+}, Zn^{2+}, Co^{2+}, Ni^{2+} and Mg^{2+} and loading, which sometimes occurs very slowly (Cobbold and Rink 1987).

Feature	Fluorescent dye	Recombinant aequorin	Micro electrode	Cameleon
Concentrations of free Ca^{2+} which can be easily measured	50 nM- 5 μM	200 nM- 300 μM	10 nM-> 1mM	10nM-10 mM
Quantum yield of light emitting probe	high	low at present	na	high
Spatial resolution	subcellular	single cells	single cells	subcellular
Period over which $[Ca^{2+}]_c$ measurements can be obtained	few min -many hours	lifetime of the organism	few min-1 h	lifetime of the organism
$[Ca^{2+}]_c$ quantification	can be good with ratio dyes	reasonable	good	good
Cytotoxicity	not usual	none	na	not usual
$[Ca^{2+}]_c$ buffering	can be a problem	no	na	no
possible radiation damage	with UV exited dyes	na	na	sometimes
photobleaching of probes	yes	na	na	yes
microinjection	sometimes	na	essential	na
organelle compartmentation or leakage of probes	sometimes required	no	na	no
binding of probe to cell components (e.g. proteins, cell walls or organelles)	can be a problem	apparently not	na	no

Table 1.2 Comparison of different Ca^{2+} reporters adapted from Read et al. 1993.

The third approach, involving the use of Ca^{2+}-sensitive photoproteins (e.g. aequorin, obelin) (Cobbold and Rink 1987). Aequorin has been extensively used in animal cells and plant cells (Knight et al. 1992), but has only recently been applied to filamentous fungi (Collis 1996; Nelson 1999).

Aequorin has several advantages compared with other molecules used to measure and image Ca^{2+}.

1. It is non-disturbing to cells and has not been found to interfere with Ca^{2+}-mediated functions in any of the cells in which it has been studied (Blinks 1982).

2. Over the physiological pH range (6.6-7.4) pH has no significant influence on calcium sensitivity (Cobbold and Rink 1987)

3. It has a very large dynamic range facilitating the measurements of free Ca^{2+} over a thousand-fold range of concentrations from 0.1 to 100 μM in fresh water and 0.3 to 300 μM in marine cells. The wide dynamic range of aequorin is very important since a lot of Ca^{2+} shifts and gradient *in vivo* are very large.

4. It exhibits an ultralow background signal because autoluminescence is practically absent from cells and tissues, so the only background signals to overcome are purely instrumental (Miller et al. 1994).

5. Aequorin genes has been cloned and genetically engineered which allowed its expression in different organisms (Inouye et al. 1985; Prasher et al. 1985a). Depending on which promoter is used to drive the aequorin gene, aequorin can be expressed n all or selective cells of an organism.

6. Recombinant aequorin can be targeted to different organelles by fusing apoaequorin to organelle targeting signals or to the coding sequence of normally resident protein (Rizzuto et al. 1992). Aequorin has been used to measure $[Ca^{2+}]_c$ in the nucleus, ER, mitochondria, vacuole, and chloroplasts.

The main limitation of aequorin is probably that because its quantum yield of light is low (compared with fluorescent dyes), imaging and measuring of intracellular Ca^{2+} at the subcellular level is not usually possible.

1.5.1 Ca^{2+} measurements in living cells using recombinant aequorin

1.5.1.1 Background on aequorin

Aequorin is a Ca^{2+}-sensitive photoprotein of the jellyfish *Aequorea victoria* (Mr = 21,400) (Nakajima - Shimada et al. 1991a). The protein consists of a single polypeptide chain, apoaequorin, a hydrophobic luminophore, coelenterazine and bound oxygen (Knight et al. 1991a). Once Ca^{2+} ions are bound to two of the three Ca^{2+}-binding sites in aequorin, the protein is converted into an oxygenase. The oxygenase catalyses the oxidation of the substrate coelenterazine by the bound oxygen and this results in blue light emission (λ_{max} 470 nm). The amount of luminescence emitted by aequorin is dependent upon the free Ca^{2+} concentration and thus aequorin can be used to measure $[Ca^{2+}]_c$ after it has been introduced into a cell.

Aequorin is composed of 189 amino acid residues and has three EF hand structures that are characteristic for Ca^{2+}-binding sites. The protein has hydrophobic regions at which the protein may interact with coelenterazine (Inouye et al. 1985).

Native aequorin is not homogenous, and it consists of eight different molecular forms, isoaequorins, which are designated aequorin A-H. The Mr, luminescence activity and first-order reaction rate constants of these isoforms are slightly different. As regards to Ca^{2+} sensitivity, aequorin D is known to be the most sensitive (Shimomura 1986).

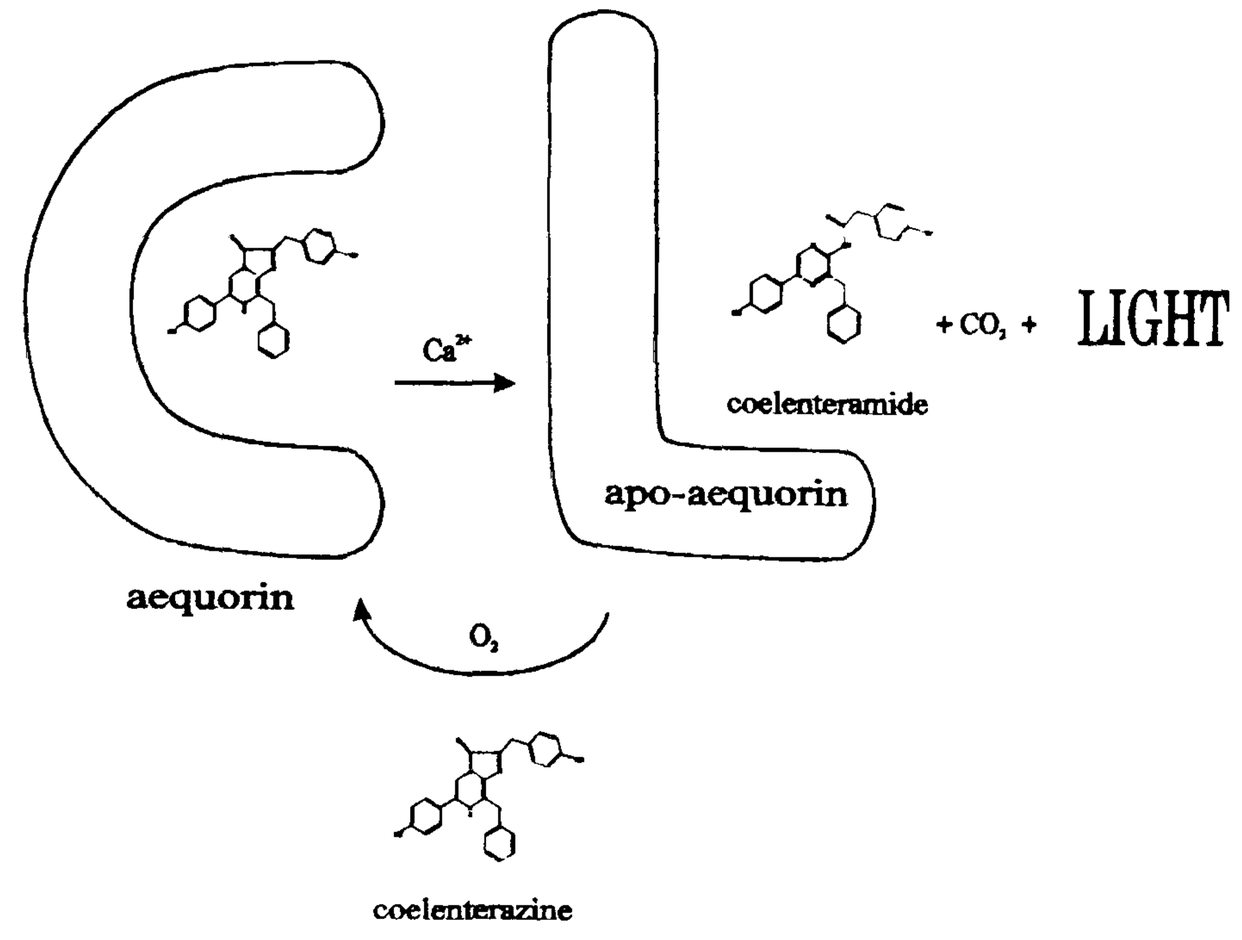

Figure 1.3 Schematic illustration of the aequorin luminescence and regeneration (adapted from Shimomura et al 1988).

The properties of aequorin can be also altered by using different chemically synthesized analogues of coelenterazine. This aequorin is called semi-synthetic aequorin. For example the use of *cp*, *f* or *h*-coelenterazine results in aequorin reporter 10-20 times more sensitive to Ca^{2+} than the apoaequorin reconstituted with native coelenterazine. The *hcp*-coelenterazine exhibits very favourable characteristics such as a fast response upon binding Ca^{2+} and the highest luminescence quantum yield among the all available analogues. The low sensitivity to Ca^{2+} of *n*-coelenterazine allow it to be used to measure very high Ca^{2+} concentrations. Reconstitution of aequorin with *e*-coelenterazine produces semi-synthetic aequorin with a bimodal spectrum of luminescence emission. It provides a simpler method for quantification of $[Ca^{2+}]_c$ *in vivo* using the ratio luminescence at two wavelengths. For this approach there is no information needed on the amount of expression (recombinant aequorin), reconstitution or consumption of

aequorin which is normally required for calibration with aequorin (Knight et al. 1993b; Shimomura et al. 1993).

Aequorin has been widely used to measure $[Ca^{2+}]_c$ in large animal (Campbell et al. 1996) and plant cells (Callaham and Hepler 1991) after introduction into these cells by microinjection. This method requires using expensive, purified aequorin and may injure cells.

The cloning and characterisation of two apoaequorin genes (AQ440, Inouye et al. 1985; and AEQ1, Prasher et al 1985) led to the new technology of using recombinant aequorin for Ca^{2+} measurement. This approach has now been used for Ca^{2+} measurements in plants (Knight et al. 1991b; Prasher et al. 1985), yeast cells (Nakajima - Shimada et al. 1991b), bacteria (Knight et al. 1991a), mammalian cell lines (Kendall et al. 1996; Rizzuto et al. 1995) and slime moulds (Saran et al. 1994). Treatments of the transgenic organisms with coelenterazine allows the formation of functional aequorin within the cytosol of their cells, thereby producing luminous transgenic organisms whose light emission directly reports Ca^{2+} (Knight et al. 1993b). Since the early 1990s a number of studies of Ca^{2+} signalling in plants and animals have involved the use of recombinant aequorin (Table 1.6 and 1.7). The works on fungi has been mainly done on yeasts and are not as numerous as animal and plant research (Table 1.5).

Subject of study	Organisms	System	Reference
Anoxia	*Arabidopsis thaliana*	seedlings	Baum et al. 1999
Blue light	*A. thaliana*	pollen tubes	Malho et al. 1998
Circadian rhythm	*Nicotiania plumbaginifolia*	seedlings	Wood et al. 2001
Cold shock	*A. thaliana*, *Anabaena sp*	roots	Plieth et al. 1999, Torrecilla et al. 2000
Fungal elicitors	*N. plumbaginifolia* *Glycine max L*	callus cultures	Knight et al. 1991b, Mithofer et al. 1999
Heat	*N. plumbaginifolia* *Anabaena sp*	seedlings	Gong et al. 1998, Torrecilla et al. 2000
Hypo-osmotic shock	*N. tabacum*	guard cells	Takahashi et al. 1997
Oxidative stress	*N. plumbaginifolia*	seedlings	Price et al. 1994
Salinity	*A. thaliana*	seedlings	Knight et al. 1997
Touch	*N. plumbaginifolia*	callus cultures	Knight et al. 1991b
Wind	*N. plumbaginifolia*	seedlings	Knight et al. 1992

Table 1.3 Key studies on calcium signalling in plants involving Ca^{2+} measurement using recombinant aequorin and various physico-chemical treatments.

Subject of study	Organisms	System	Reference
Calcium transients	humans	heart muscle strips	Hasenfuss et al. 1998
	mice	skeletal miotubes	Robert et al. 2001
Vertebrate development	zebrafish	eggs	Creton et al. 1998
Ooplasmic segregation	zebrafish	embryos	Leung et al. 1998
Intracellular Ca^{2+} elevations	Xenopus laevis	oocytes	Grygorczyk et al. 1996
Ca^{2+} transients	dogs	cardiac Purkinje-fibers	Stowe et a. 1994
Early development	medaka fish	zygotes	Fluck et al. 1992
Ca^{2+} transients	guinea-pigs	venticular papillary muscles	Bosnjak et al. 1992
Cytokinesis	medaka fish	eggs	Foyouzi-Youssefi et al. 2000
Aterosclerosis	rats	platelets	Saladino et al. 1996
Effect of polyunsaturated fatty acids	rats	cardiac myocytes	Podszasy et al. 1995
Cell injury	rat	hepatocytes	Gasbarrini et al.1993
Heart contractions	human	heart muscles	Meuse et al. 1992

Table 1.4 Key studies on calcium signalling in animals involving Ca^{2+} measurement using recombinant aequorin.

Subject of study	Organisms	Reference
Aequorin expression in yeast	*Saccharomyces cerevisiae*	Nakajima-Shimada et al. 1991a
Intracellular Ca^{2+}	*S. cerevisiae*	Nakajima-Shimada et al. 1991b
Hypotonic shock	*S. cerevisiae*	Batiza et al. 1996
ER Ca^{2+}	*S. cerevisiae*	Strayle et al. 1999

Table 1.5 Key studies on calcium signalling in yeasts involving Ca^{2+} measurement using recombinant aequorin.

1.5.1.2 Transformation of fungi with recombinant aequorin

In contrast to what has been done with plant and animal cells, little work has been done on filamentous fungi. The first attempt to transform fungi with the native apoaequorin gene was done in *Neurospora crassa.* The level of expression was very low, approximately 365 times less than in transgenic *Nicotiana plumbaginifolia.* It was also found that the ratio of mRNA production was much less extreme than with the protein level. It therefore seemed likely that the block at the apoaequorin expression was at or after translation stage. It was then found that native apoaequorin gene contains 44 codons that are rare in *N. crassa* but only 1 that is rare in *N. plumbaginifolia.* Therefore it was suggested that codon bias was the most likely cause of the low levels of aequorin expression (Collis 1996). Codon bias can occur for any amino acid because they can be encoded by several codons. The choice of codon correlates with the abundance of the corresponding tRNA. Highly expressed genes show the greatest bias, with little or no bias in low expression genes.

To overcome this problem, a synthetic apoaequorin gene (*aeqS*) with optimal codon usage for expression in *Aspergillus* and *Neurospora* was designed and synthesized. The synthetic gene produced $5 \cdot 10^5$ increase in level of apoaequorin expression in *N. crassa* than the native gene. Afterwards an expression vector (pAEQ1-15) containing this gene under the control of the constitutive glucose-6-phosphate dehydrogenase promoter (*gpdA*) was used to transform *A. niger* and *A. awamori.* A very high level of apoaequorin expression was obtained, and by incubation of the transgenic fungi in

the luminophore coelenterazine, active aequorin was formed (Table 1.6). Using this method, intracellular $[Ca^{2+}]_c$ transients have been shown in response to high extracellular Ca^{2+}, changes in extracellular pH, and to hypo-osmotic and touch stimuli (Nelson 1999).

Organism	Strain	Aequorin gene	Promoter	Expression vector	µg aequorin per g total protein
Neurospora crassa	1,2,1	*aeqA*	ms	pNCAEQ1	0.15
	3,5	*aeqD*	grg-1	pNCAEQ3	0.045
	2,3,1,1	*aeqS*	grg-1	pNCAEQ3	22.62
Nicotiana plumbaginifolia	2,4	*aeqA*	^{35}S	pDH51	4,74

Table 1.6 Comparison of level of aequorin expression.

Using the codon-optimised aequorin several other species were transformed. The most successful ones were *Aspergillus nidulans* (Table 2.1) and the plant pathogene *Phyllosticta ampelicida* (Shaw et al. 2001)

1.6 SPATIAL CHARACTERISTICS OF CALCIUM SIGNALING

Calcium is a ubiquitous intracellular signalling molecule controlling a wide range of cellular processes. During its life a cells has to respond to a wide range of often conflicting external stimuli, many of which use Ca^{2+} as a second messenger. This raises the question of how such a simple signal molecule can regulate so many diverse cellular processes. It is likely that a number of factors such as cell's developmental history, other signalling molecules present and the cellular localization of the elements that process the Ca^{2+} signal all contribute to the control and specificity (Berridge 1997b; McAinsh and Hetherington 1998).

In animal and plant cells, specificity in Ca^{2+} signalling is initially controlled by the fact of whether or not the cell is competent to respond to a certain stimulus. In cases when a cell is competent the second step in differentiating between Ca^{2+}-mobilizing stimuli is operated through different amplitude, spatial or temporal modes of the Ca^{2+} signal which are embodied in the so-called "Ca^{2+} signatures". First, the amplitude of Ca^{2+} increases varies in response to different stimuli. Second, different stimuli can cause localized increases in $[Ca^{2+}]_c$. Third the kinetics of the stimulus-induced $[Ca^{2+}]_c$ increases varies. These features have been shown in both plant and animal cells (McAinsh and Hetherington 1998).

Stimulus-induced increases in $[Ca^{2+}]_c$ can occur in the form of spikes (single transient responses to defined stimuli), oscillations (repetitive increases in $[Ca^{2+}]_c$), waves (spatial correlate of a Ca^{2+} spike in which Ca^{2+} is initially elevated in a defined location in the cell before spreading throughout the cell as a regenerative increase) (Sanders et al. 1999). It was also found that the mechanisms of generation and maintenance of these modes has the potential to encode signalling information.

1.6.1 Parameters of $[Ca^{2+}]_c$ transients

It has been known for some time that signalling information can be encoded in different characteristics of the "Ca^{2+} signature" of a $[Ca^{2+}]_c$ transient: amplitude, frequency and duration (McAinsh and Hetherington 1998). Malho et al (1998) distinguished four different parameters of a Ca^{2+} transient: the rise time, the peak concentration, the decay time and resting level after the transient. During the rise time Ca^{2+} release into the cytosol is greater than Ca^{2+} uptake from the cytosol. At the peak, release is equal to uptake. During the decay time, although Ca^{2+} release is still ongoing, Ca^{2+} uptake is dominant. The resting level of $[Ca^{2+}]_c$ after the transient can be significantly higher than the one before the $[Ca^{2+}]_c$ transient and can last for a considerable amount of time. The importance of these parameters has been shown in animal cells by Dolmetsch et al (1997). By mimicking parts of the $[Ca^{2+}]_c$ transient they showed that different components of the transient are responsible *in vivo* for protein translocation, protein phosphorylation and gene expression.

Another important parameter of a $[Ca^{2+}]_c$ transient is the presence of a secondary $[Ca^{2+}]_c$ increase. For example it was shown that the second ozone-induced $[Ca^{2+}]_c$ peak in the seedling of *A. thaliana* provides the necessary information to direct expression of gluthathione-S-transferase (Clayton et al. 1999).

1.7 PHYSICO-CHEMICAL TREATMENTS USED WITH FUNGI

Numerous physico-chemical stimuli have been studied in plants in connection with $[Ca^{2+}]_c$ changes measured using recombinant aequorin (Table 1.3). However very few studies of this type have been done with fungi. Nakajima-Shimada et al (1991a) showed that apoaequorin could be expressed in yeast *Saccharomyces cerevisiae* under the control of the GAL1 promoter and that cells accumulated high enough levels of aequorin to detect a $[Ca^{2+}]_c$ signal (Nakajima - Shimada et al. 1991a). Using this system it was shown that when a or α cells of *S. cerevisiae* were treated with a mating pheromone, α-factor, this generated extracellular Ca^{2+}-dependent luminescence only in the a mating type cells. The maximum $[Ca^{2+}]_c$ increase was estimated to be 590 ± 200 nM and occurred 45-50 min after addition of α-factor. Another stimulus used involved the addition of glucose to glucose starved cells. This treatment resulted in a $[Ca^{2+}]_c$ response with a maximal amplitude of 340 ± 40nM, which occurred 2 min after the addition of glucose (Nakajima - Shimada et al. 1991b).

Using recombinant aequorin it has been also demonstrated that hypo-osmotic shock caused an almost immediate transient increase in $[Ca^{2+}]_c$ in budding yeast from the base line of approximately 200 nM to a peak of 1100 nM. Both internal and external stores were shown to be involved in this $[Ca^{2+}]_c$ transient. Initially there was a release of Ca^{2+} from internal stores which was then sustained by the apparent activation of stretch-activated channels in the plasma membrane. Isotonic shock did not result in a $[Ca^{2+}]_c$ increase (Batiza et al. 1996).

1.8 PHARMACOLOGICAL TREATMENTS USED WITH FUNGI

There are numerous commercially available pharmacological inhibitors which are widely used, particularly in animal cell signalling studies. Some of these compounds are highly selective and are able to block the specific signalling pathways whilst other are not. Furthermore, virtually all of these compounds have been developed against targets in animal cells and thus they commonly show reduced selectivity for equivalent targets in plants and fungal cells.

One therefore needs to be very careful interpreting the results obtained using these pharmacological agents when they have been applied in studies on fungi. Key studies in which Ca^{2+}-modulating pharmacological agents have been used with fungi are shown in Table 1.8 and 1.9. Often the concentrations of these compounds used to obtain inhibitory effects were much higher than in animal cells which raises the question of the actual specificity of the inhibition observed. For example Corzo and Sanders (1992) showed that La^{3+} (a Ca^{2+}-channel blocker) also caused membrane depolarization through Ca^{2+}-independent events. Treating fungal cells with Ca^{2+} modulating agents whilst directly measuring $[Ca^{2+}]_c$ (e.g. with recombinant aequorin) can greatly aid the interpretation of results because different parameters of the Ca^{2+}-signature (e.g. the rates of $[Ca^{2+}]_c$ increase and decrease, and the $[Ca^{2+}]_c$ amplitude) which is commonly characteristic for different signalling pathways, can be readily analysed.

The only one known fungal specific Ca^{2+}-channel blocker is KP4. This inhibitor is a killer toxin of *Ustilago maydis* which in nature is primary effective against species in the family Ustilaginaceae (Koltin and Day 1975). In *U. maydis* Gage et al (2001) showed that KP4 acted in a manner analogous to calcium chelators (EGTA) and the Ca^{2+}-channel inhibitor Cd^{2+}. KP4 also inhibited ^{45}Ca uptake in *Ustilago*. It has therefore been proposed that KP4 blocks fungal Ca^{2+}-channels. Interestingly, it was shown that KP4 was effective at a concentration of 0.33 μM, whereas it takes millimolar concentration of EGTA to obtain the same levels of inhibition. This

difference in efficacy is probably the result of KP4 specifically targeting Ca^{2+}-channels, whereas EGTA needs to chelate all the Ca^{2+} in the medium (Gage et al. 2001). KP4 has also been found to be effective of blocking voltage-gated Ca^{2+}-channels in mammalian neurons (Gu et al. 1995).

Compound	Agonist selectivity	Organisms	Process affected	Reference
A23187	ionophore which is selective for Ca^{2+}	*Penicillium notatum*	release of Ca^{2+} from mitochondria	Pitt and Barnes 1993
		Neurospora crassa	enhanced stipe extension growth rate; hyphae branching	Fraser and Moore 1993, Reissig and Kinney 1983
		Ophiostoma ulmi	inhibition of germ tube formation	Gadd and Brunton 1992
		Fusariun oxysporium	stimulation of lipase production	Hoshino et al. 1991
Caffeine	causes release of Ca^{2+} from internal Ca^{2+} stores	wood- rotting fungi	inhibition of growth	Arora and Ohlan 1997
CPA	reverse inhibits Ca^{2+}- ATPases which fill internal Ca^{2+} stores	*Saccharomyces cerevisiae*	Ca^{2+}-ATPase in the ER	Okorokov et al. 1997
		N. crassa	hyphal widening, hyper branching	Silverman-Gavrila and Lew 2001

Table 1.7 Agonists of Ca^{2+} signalling used in studies on fungi. Abbreviations: CPA = cyclopiazonic acid.

Compound	Inhibitor selectivity	Organisms	Process inhibited	Reference
BAPTA	chelates Ca^{2+}	*Saccharomyces cerevisiae*	hypo-osmotic shock	Batiza et al. 1996
Cinnarizine	inhibits Ca^{2+}-channel activity	*Fusarium graminearum*	hyphal branching	Robson et al. 1991a
Co^{3+}	inhibits Ca^{2+}-channel activity	*F. graminearum*	hyphal branching	Robson et al. 1991a
Gd^{3+}	inhibits Ca^{2+}-channel activity	*S. cerevisiae*	hypo-osmotic shock	Batiza et al. 1996
La^{3+}	inhibits Ca^{2+}-channel activity	*Neurospora crassa*	Ca^{2+} influx	Corzo and Sanders 1992, Gibbon and Kropf 1994
Nd^{3+}	inhibits Ca^{2+}-channel activity	*Zoophthora radicans*	appressorium formation	Magalhaes et al. 1991
Nifedipine	inhibits L-type Ca^{2+}-channel activity	*F. graminearum* *Botrytis cinerea*	appressorium formation hyphal branching	Robson et al. 1999a, Hudecova et al. 1994
Ruthenium Red	inhibits CICR from ryanodine sensitive intracellular Ca^{2+} stores	*Candida albicans*, *N. crassa*	Ca^{2+} influx hyphal widening	Calvert and Sanders 1995, Silverman-Gavrila and Lew 2001
TFP	CaM antagonist, inhibits CaM-dependent phosphodiesterase	*Z. radicans*, *F. graminearum*	hyphal branching, appressorium formation	Magalhaes et al. 1991, Robson et al. 1991a
TMB-8	inhibits Ca^{2+} release from internal Ca^{2+} stores	*Z. radicans*	appresorium formation	Magalhaes et al. 1991
Verapamil	inhibits L-type Ca^{2+} - channel activity	*N. crassa* *B. cinerea*	hyphae branching, hyphal growth	Dicker and Turian 1990, Hudecova et al. 1994
W-5	CaM antagonist, inhibits CaM-dependent phosphodiesterase	*Z. radicans*,	appressorium formation	Magalhaes et al. 1991
W-7	CaM antagonist, inhibits CaM-dependent phosphodiesterase	*Z. radicans*, *F. graminearum*	hyphal branching, appressorium formation	Magalhaes et al. 1991, Robson et al. 1991a

Table 1.8 Antagonists of Ca^{2+} signalling used in studies on fungi. Abbreviations: CICR = calcium-induced calcium release. TFP-trifluroperazine. W-5 = N-(6- Aminohexyl)-1-naphthalenesulfonamide; W-7 = N-(6-Amino-hexyl)-5-chloro-1-naphthalenesulfonamide

1.9 INTRODUCTION TO THE RESEARCH CARRIED OUT IN THE THESIS

Up until recently there has not been a method for routinely measuring $[Ca^{2+}]_c$ in filamentous fungi. In addition, very little is known about Ca^{2+} signalling in filamentous fungi. Using the codon-optimised apo-aequorin gene expressed in *Aspergillus awamori* as a Ca^{2+}-reporter (Nelson 1999), the aims of this study were:

- To optimise the existing calibration method for converting aequorin luminescence into $[Ca^{2+}]_c$ concentration and evaluate the accuracy of this method for use in filamentous fungi. The existing calibration has been empirically derived for use in plant and animal cells. However, filamentous fungi transformed with recombinant aequorin synthesize much greater amounts of aequorin than plants and animals. Therefore it was necessary to assess how suitable the existing calibration method was for use in filamentous fungi.

- To analyse the effects of different physico-chemical treatments (mechanical perturbation, hypo-osmotic shock, hyper-osmotic shock, high external $CaCl_2$ and cold and heat shock) on $[Ca^{2+}]_c$ in filamentous fungi and to characterise different parameters of the $[Ca^{2+}]_c$ responses (i.e. their Ca^{2+} signatures). Previously it has been shown that these physico-chemical treatments cause a transient increase in $[Ca^{2+}]_c$ in *A. awamori* (Nelson 1999). However, no detailed analysis of the Ca^{2+} signature, within which signal transduction information is encoded has been made.

- To analyse the effects of different Ca^{2+} agonists and antagonists on the Ca^{2+} signatures associated with mechanical perturbation, hypo-osmotic shock and addition of external $CaCl_2$. Although the Ca^{2+} signal transduction network has been described in animal and plants cells in details little is known about which components of this network are present in filamentous fungi. Using

Ca^{2+} modulators with known targets in animal cells some of components of calcium signalling machinery which exists in filamentous fungi can be identified.

- To analyse the physiological responses which possibly occur as a consequences to changes in $[Ca^{2+}]_c$. After characterising different Ca^{2+} signatures associated with different external signals, it is important to analyse the resulting physiological responses.

- To analyse the novel potential of using the recombinant aequorin method in fungicide mode-of-action studies. The aequorin method allows not only the monitoring of changes in $[Ca^{2+}]_c$ but could also help in predicting which part of Ca^{2+} signal transduction network has been targeted by fungicide.

- To analyse the novel potential of using recombinant aequorin method as a toxicity test for environmental pollutants. At present, only bacteria are commonly used in luminescence-based biosensors for toxicity testing.

2 MATERIALS AND METHODS

2.1 CHEMICALS

Unless otherwise stated all the chemicals were obtained from Calbiochem-Novabiochem (UK) Ltd. (Nottingham, UK), Sigma (Dorset, UK) or Fischer Scientific Ltd (Loughborough, UK).

For pharmacological agents not soluble in water stock solutions were prepared in solvents as indicated. Water soluble pharmacological agents were dissolved in VS medium.

2.2 ORGANISMS AND MEDIA

Most of the experiments were carried out with the *Aspergillus awamori* 66a strain, which has been transformed with the recombinant aequorin gene. This gene was previously designed and synthesised with optimal codon usage for expression in *Aspergillus* and *Neurospora* (Nelson et al. 2001).

A. niger strains CDA1, RCA3, HDCA3 were obtained from Dr. Mojca Bencina (Ljubljana, Slovenia). *A. nidulans* strains 3.2, 3.3, 3.4 and av6 were supplied by Dr. Debora Bell-Pederson (Texas A & M University, College Station, USA). *A. nidulans* AXB4aeq11, AXB4aeq17, ΔsuAaeq17 and ΔsuAaeq18 were obtained from Prof. Axel Brakhage (Institut fur Mikrobiologie und Genetik, Darmstadt, Germany).

All media and salt solutions were made up in distilled H_2O (dH_2O) and sterilised by autoclaving at 121°C at 15 psi for 20 min prior to use.

A. awamori and *A. niger* cultures were grown: (a) on solid rich media with glucose (RMG) (section 2.2.1), (b) in liquid Vogel's media with sucrose (VS medium)

(section 2.2.2), or (c) on solid VS medium (section 2.2.2). *A. nidulans* cultures were grown on solid or liquid minimal media (MM) (section 2.2.3).

Species	Strain	Aequorin	Relevant phenotype	Plasmid	Selection marker	Medium
A. awamori	66a	Cyt	-	pAEQ 1-15	*amdS*	Vogel's (VS)
A.niger	15-21	Cyt	-	pAEQ 1-15	*amdS*	VS
	RCA3	Cyt	*nic⁻, leu⁻*	pAEQ 1-15	*amdS*	VS
	HDCA3	Cyt	*nic⁻, leu⁻*	pAEQ 1-15	*amdS*	VS
A.nidulans	3.2	Cyt	*bio⁻, met⁻*	pAEQ 1-15	*argB2*	Minimal (MM)
	3.3	Cyt	*bio⁻, met⁻*	pAEQ 1-15	*argB2*	MM
	3.4	Cyt	*bio⁻, met⁻*	pAEQ 1-15	*argB2*	MM
	av 6	Cyt	*bio⁻, met⁻*	pAEQ 1-15	*argB2*	MM
	AXB4 Aeq11	Mit	*bio⁻*	pSuAaeq	*ble*	MM
	AXB4 Aeq17	Mit	*bio⁻*	pSuAaeq	*ble*	MM
	△suA aeq17	Mit	*paba⁻*	pSuAaeq	*ble*	MM
	△suA aeq18	Mit	*paba⁻*	pSuAaeq	*ble*	MM

Table 2.1 Strain of *Aspergillus* used in the experiments.

For the toxicity analysis (section 2.4.6) cultures of well established bacterial biosensor *Vibrio fischeri* was used. The freeze -dried standard stock of the bacterium was obtained from Microtox Ltd (AZUR Environmental, Winnersh Triangle Wokingham, UK). Freeze-dried bacteria were resuspended in 2 % NaCl was used for subsequent use.

2.2.1 Rich liquid media with glucose (RMG)

RMG was used to obtain large numbers of spores for inoculating liquid media and for long term storage of strains on silica gel.

1 g neopeptone (DIFCO, Beston Bickinson, Sparks, USA) , 0.5 g yeast extract and 2% agar were added to 450 ml dH_2O) and sterilised by autoclaving. The following sterile autoclaved component were then added and the volume adjusted to 500 ml with sterile H_2O.

50x AspA solution (see Table 2.2)	10 ml
1 M $MgSO_4$	1 ml
1000x trace elements (see Table 2.3)	0.5 ml
50% glucose	10 ml
10% casein amino acids	5 ml

Compound	Amount
$NaNO_3$	150 g
KCl	13 g
KH_2PO_4	38 g
10 N KOH	<25 ml until pH 5.5
DH_20	To 500 ml

Table 2.2 Salt AspA solution for RMG media.

Compound	Amount
dH_20	80 ml
$ZnSO_4.7\ H_2O$	2.2 g
H_3BO_3	1.1 g
$MnCl_2.4\ H_20$	0.5 g
$FeSO_4.7\ H_20$	0.5 g
$CoCl_2.6\ H_20$	0.17 g
$CuSO_4.5\ H_20$	0.16 g
$Na_2MoO_4.2\ H_20$	0.15 g
ethylenediaminetetraacetic acid (EDTA)	5 g

Table 2.3 1000x Trace element solution for RMG media. Compounds were added and dissolved one by one in the order given in Table 2.3. The solution was then boiled and allowed to cool to 60°C. The pH was adjusted to 6.5 with concentrated KOH, then cooled down to room temperature and adjusted to 100 ml with dH_2O. The solution was sterilised by autoclaving at 121°C at 15 psi for 20 min. 5 ml of 1 M acetamide was added to the media for transformants possessing the acetamidase selection marker gene (*amdS*).

2.2.2 Vogel's media

In liquid culture *A.awamori* and *A.niger* was grown in Vogel's medium (Vogel 1956) using sucrose as the carbon source (Table 2.4).

Compound	Amount
Na_3 citrate·2 H_20	126.7 g
KH_2PO_4	250 g
NH_4NO_3	100 g
$MgSO_4·7H_20$	10 g
$CaCl_2·2H_2O$	5 g
D-Biotin solution	5 ml
Trace element solution (see Table 2.5)	5 ml
dH_2O	to 1 liter

Table 2.4 Vogel's medium N x50 stock solutions. Chloroform (3 ml) was added as a preservative and the solution stored at room temperature. 5 mg of D-biotin was dissolved in 100 ml of 50% v/v ethanol (EtOH). The solution was stored at $4^{O}C$.

Compound	Amount
citric acid·1 H_2O	5.0 g
$ZnSO_4·7$ H_2O	5.0 g
$Fe(NH_4)_2(SO_4)_2·6H_2O$	1.0 g
$CuSO_4·5H_2O$	0.25 g
$MnSO_4·1H_2O$	0.05 g
H_3BO_3	0.05 g
$Na_2MoO_4·2H_2O$	0.05 g
dH_2O	to 100 ml

Table 2.5 Trace elements solution for Vogel's media. Chloroform (1 ml) was added as a preservative and the solution was stored at room temperature. For solid media 2 % agar was added.

2.2.3 Minimal media

In liquid cultures *A. nidulans* was grown in minimal media.

Compound	Amount
$NaNO_3$	120.0 g
KC1	10.4 g
$MgSO_4 \cdot 7H_20$	10.4 g
KH_2PO_4	30.4 g
dH_2O	1 liter

Table 2.6 Minimal medium N x20 stock solutions. The pH was adjusted to 6.5 with 1 N NaOH. Chloroform (3 ml) was added as a preservative and the solution stored at room temperature.

When needed the stock was diluted 20 times and the following components were added: 10 g glucose (dextrose) and 2 ml of salt solution (Table 2.3) per 1 liter of media. *A. nidulans* transformants 3.2, 3.3, 3.4 and av6 (see section 2.2) required methionine (0.125 g/liter) and biotin (250µl/liter) of a 0.01% biotin solution. *A. nidulans* transformants expressing aequorin targeted to mitochondria AXB4aeq11 and AXB4aeq17 (Table 2.1, Section 2.2) required biotin (250µl/liter) of a 0.01% biotin solution, deletion straines △suAaeq17 and △suAaeq18 required *p*-aminobenzoic acid (36 µl of 1 g/liter solution). For solid media 2 % agar were added.

2.2.4 Culturing *Aspergillus awamori*

Thick plates of solid RMG were poured (at least 25 ml of media per 9 cm plate), and allowed to solidify. Plates were either used immediately or stored at 4°C and used within 2 weeks. Inoculation was carried out using a meniscus of spore suspension in a sterile wire loop, and streaked over the whole plate. The spore suspension used was either from spores rehydrated by vortexing a small amount of a silica stock in a 0.5 ml 0.8% NaCl (PZ). Plates were grown in the dark at 30°C for 8 days and then harvested.

A spore plate was harvested by gently adding 10 ml PZ and disrupting the conidia from the conidiophores with a sterile glass rod. The conidial suspension was poured

into a sterile 14 ml round bottomed Falcon® tube (Becton Dickinson, New Jersey, USA), and the plate washed with a further 5 ml PZ which was added to the Falcon® tube. The suspension was vortexed for 1 min to separate the conidia, and then centrifuged for 5 min at 3000 rpm. The solution was decanted and the spore pellet resuspended in PZ by vortexing. The spores were pelleted as before, and the wash step repeated. Finally, the conidia were resuspended in 5 ml PZ and stored at 4°C. The spore concentration was determined in an haemocytometer after diluting the 10 fold. For silica stocks, the spores were pelleted once more and resuspended in 0.5 ml of a sterile solution of 5% skimmed milk (Premier Beverages, Edinburgh, UK) and 4% L-glutamic acid (freshly made up from separate stock solutions). Three vials containing approximately 0.5 g of sterile 1-3 mm silica grains (Fluka, Buchs, Switzerland) were each aliquoted in 0.2 ml of the spore suspension, mixed thoroughly by vortexing and stored at 4°C. Spore suspensions in PZ could be kept for up to six months, and silica stocks should be replaced every two years.

A method for growing *Aspergillus* cultures for *in vivo* luminometry was developed using still liquid culture in 96 well plates (EG & G Berthold, Bad Wildbad, Germany). Twelve ml of sterile Vogel's media with 1% sucrose was inoculated with 1×10^5 spores per ml. Coelenterazine (see section 3.2) was added in methanol (MeOH) to a final concentration of 2.5 μM. The final MeOH concentration was not more than 0.1%, which was found not to affect spore germination or hyphal growth (Nelson 1999). Using a 12-channel pipette (Anachem, Luton, UK), 100 ml of the inoculated media was added to each well, and the plate covered with a microplate lid (Labsystems, Helsinki, Finland). Cultures were incubated in a humidity chamber in the presence of free water at 30°C for 24 h, unless otherwise stated.

When growing *Aspergillus* cultures on solid media in 96 well plates 2% agar were added to the 12 ml of Vogels media and autoclaved. A 12-channel pipette was used to add 100 μl of the media to each well. After the media have solidified 20 μl of liquid VS media containing the spores and coelenterazine were added to each well. Subsequent incubation conditions of these plates were the same as for those containing liquid culture.

2.3 DETERMINATION OF AEQUORIN CONCENTRATION IN DIFFERENT STRAINS

2.3.1 Standard curve and quantification of aequorin luminescence

Purified recombinant aequorin D from Cambridge Bioscience (Cambridge, UK) was used to quantify the amount of aequorin luminescence obtained from transformed cells analysed in the luminometer used in this study. A dilution series, from 1 *p*moles to 0.01 *f*moles of aequorin was made for the protein sample, and each dilution incubated with 2.5 μM coelenterazine in reconstitution buffer (10 mM ethyleneglycol-bis-(β-aminoethyl)-N,N,N',N'-tetraacetic acid (EGTA), 50 mM Tris, 500 mM NaCl, 10 mM β–mercaptoethanol, H_2O, total volume 100 ml) at 4°C for 4 hours prior to stimulation. Wells were injected with 100 mM $CaCl_2$ and the luminescence monitored. The luminescence obtained over 20 s after stimulation was integrated and plotted against the aequorin concentration.

2.3.2 Protein assay

2.3.2.1 Preparation of whole cell extract from *Aspergillus* strains

Whole cell extracts were used to compare the expression levels of apoaequorin in different *Aspergillus* transformants. Cultures were grown in liquid media 100 ml media in 250 ml flasks for 24 h at 30°C in a shaking incubator (150 rpm/min). Mycelia were harvested by sieving the media containing fungus through filter paper (Whatman International Ltd, England) under negative pressure provided by a Buchner funnel. A mortar was filled with liquid nitrogen (one third full), the mycelia added and ground to a fine powder with a pestle. The mycelial powder was transferred to pre-weighed and cooled Eppendorf tubes and stored in liquid nitrogen until all samples had been ground. The samples were then weighed and suspended in extraction buffer (10 mM EGTA, 50 mM Tris.Cl, pH7.4, 500 mM NaCl, 10 mM β-

mercaptoethanol and H_2O). 1 ml of buffer was added to every 0.2 g of mycelia. Samples were vortexed for a minimum of 30 sec, and placed on ice until all samples were ready. Insoluble material then pelleted at 13,000 g for 5 min in a microcentrifuge. The supernatant was retained and stored at -70 °C.

2.3.2.2 Estimation of protein concentration

The concentration of a protein in a solution was estimated using the modified method of Bradford (1976) by following the standard procedure described in the protein kit of Bio-Rad (Bio-Rad Microscience, Hemel Hempstead, Herts, UK). BSA standards of 0, 200, 400, 600, 800, 1000 and 1200 µg/ml were prepared in the extraction buffer and 2 µl were added to microplate well followed by 100 µl of Biorad protein assay dye-reagent. Each sample was mixed by gentle inversion, taking care not to cause foaming, and after a period of 5 to 20 min the optical density of the solution was read at 595 nm (OD_{595}) in a spectrophotometer Dynatech MR5000 (Dynex Technologies Inc. Chantily, UK). For each BSA standard solution 6 wells were measured and the average reading was plotted against concentration to give a standard curve. The protein concentration of the solution of interest was then determined by appropriate dilution of the sample and addition of 2 µl of this solution to 100 µl of the dye-reagent. The optical density was then determined as outlined above. This reading was used in conjunction with the standard curve to determine the concentration of protein in the solution of interest.

2.4 MEASUREMENTS OF AEQUORIN LUMINESCENCE USING LUMINOMETRY

2.4.1 Plate luminometry

Luminometry was performed using an EG & G Berthold (Bad Wildbad, Germany) LB96P MicroLumat luminometer which was controlled by a dedicated PC. The

luminometer was designed to measure luminescence using 96 well microplates (black or white). Two 100 ml built-in injectors allowed liquid to be delivered to individual microplate wells. Adjustable delay times between injections and between the last injection and the start of measurement can be defined. The use of injectors specifically designed for this purpose guarantees instantaneous mixing of the samples as well as the highest precision of luminescence measurements. The MicroLumat LB 96P is equipped with a sample chamber heater, allowing heating of the microplate up to 42°C. The Windows software WinGlow, which was supplied with the luminometer allowed all measurements to be programmed. The 96 well plates used were obtained from EG&G Berthold or Dynex Technologies Inc. (Chantily, UK), and were white with flat-bottomed wells.

The luminometer provides three different kinds of measurements referred by EG & G Berthold as counting modes: *integrate*, *kinetics* and *repeated*.

For measurements in the *integrate* mode, the light detected is integrated over a freely selectable time from 0.1 s to 5000 s. The light output is printed as a single number which corresponds to the sum of all the luminescence obtained in the defined time. In the *kinetics* counting mode the light emission from each sample is plotted as a 20-point kinetics curve over a predefined period. This mode is used to analyse fast reaction kinetics. The *repeated* measurement mode allows long-term measurement of light from samples by periodically repeated measurements of the samples. The maximal number of samples which can be measured is limited to 60. The data is output in the respective printout of the relative light unit (RLU) values of all samples for each time point. In this study single measurement was always 1 s, however, the cycle time (time between measurements) varied.

The parameters for a measurement (definition of counting mode, injectors, counting time, number and position of samples, etc.) are entered in a so-called counting protocol and stored. Based on the parameters you have entered the program calculates the best measurement procedure, so that the measurement can be run in the quickest way possible. Winglow automatically creates 2 different files, one which is

the natural Winglow file but also a text file which can be easily transformed into an Excel file.

2.4.2 Tube luminometry

The LB96P MicroLumat plate luminometer is not equipped with a cooling or heating stage to rapidly alter the temperature of samples. The cold and heat shock experiments were therefore carried out with different tube luminometer system designed by Dr. Christoph Plieth (University of Kiel, Kiel, Germany). A plastic 5 ml tube with fungal cultures and a heat exchanger was placed in a purpose-built light tight sample housing in front of Photomultiplier Tube (PMT) Model 9829A (Electron Tubes Ltd. Ruislip, Middlesex, UK).

Luminescence counts were integrated over 2 s periods. The temperature was measured in parallel by means of a NTC-resistor which was placed near the cultures. The A/D converter thermosensor voltage was fed into a second computer which simultaneously triggered the photon counter. This set-up allowed simultaneously measurements of the Ca^{2+}-dependent luminescence and temperature.

2.4.3 Coelenterazine

Coelenterazine was purchased from Cambridge Bioscience (Cambridge, UK) or Biosynth AG (Staad, Switzerland). Manipulation of coelenterazine was performed in near-darkness. 5 mg quantities were separated into 2.5 µM aliquots by dissolving them in cold 100% MeOH. Then solutions were dispensed into Eppendorf tubes and dried down under vacuum using a desiccator. Tubes were wrapped in aluminium foil and stored at -70°C. Coelenterazine was dissolved in 40 µl 100% MeOH prior to use.

2.4.4 Calibration of aequorin luminescence

The luminometer measures light emission in relative lights units (RLU). To convert RLU into $[Ca^{2+}]_c$ concentrations the following empirically derived equation was used:

$$pCa = 0.332588 (-\log K) + 5.5593,$$

where k = luminescence counts s^{-1} / total luminescence counts (Fricker et al. 1999).

The total amount of luminescence was measured as an integral of all luminescence up to complete aequorin discharge. Aequorin was discharged by adding 2 M $CaCl_2$ in 10% ethanol to the wells followed by the injection of 100 mM $CaCl_2$. Conversions of RLU into $[Ca^{2+}]_c$ concentration were made using the Excel 7.0 spreadsheet kindly provided by Dr. Mark Knight (Department of Plant Science, University of Oxford). Cold and heat shock experiments were performed using a different set-up (see Section 2.4.1). In the latter case the conversion of RLU into $[Ca^{2+}]_c$ was performed using a special program designed by Dr. Christoph Plieth (University of Kiel, Kiel, Germany).

2.4.5 Physico-chemical measurements and experimental treatments

2.4.5.1 Physico-chemical and pharmacological treatments

Several physico-chemical and pharmacological treatments were tested. With the exception of cold and heat shock, all the physico-chemical treatments (mechanical perturbation [iso-osmotic medium], hypo-osmotic shock [5% VS medium], hyper-osmotic shock [medium of a higher concentration than the medium in which the fungus was growing in] and high external $CaCl_2$) were applied through 100 µl injectors of the plate luminometer. Cold and heat shock were performed in the tube luminometer by cooling and heating the fungal colonies by drawing ice-cold or pre-

warmed water through a heat exchange coil. The rate of temperature changes was determined by the flux through the coil as described in (Plieth et al. 1999). All the pharmacological agents used were obtained commercially except KP4 which has was kindly supplied by Dr. Marc Fischer (University of York, York, UK). All pharmacological inhibitors were added 5 min before the application of the physico-chemical treatment in a total volume of 25 µl VS media. The Ca^{2+}-agonists were either applied through the 100 µl injectors (without extra further physico-chemical stimulation) or were pre-incubated with cultures for 5 min prior to stimulation with the physico-chemical treatment. Controls involved the addition of VS media, and an appropriate concentration of solvent where applicable, added in the same way as which the antagonist/agonist was applied. All the experiments were performed at least twice with 4-6 replicates each.

2.4.5.2 Treatment with cell permeabilizing agents

This part of the work was done in collaboration with the Dr. Charlotte Thrane and Dr. Stefan Olsson (Royal Veterinary and Agriculture University, Copenhagen, Denmark). Five chemicals were studied:

- Amphotericin B. This is a commercially available antifungal agent from *Streptomyces* spp. that forms channels by complexing with membrane sterols (Ghannoum and Rice 1999). A 1 mM stock solution was made up in water.
- Surfactin. This is a commercially available lipopeptide antibiotic from *Bacillus subtilis*. It is a powerful biosurfactant causing lysis of bacteria (Nakano et al. 1988). A 10 mM stock solution was made in DMSO.
- Tensin. This is a compound purified in Copenhagen from an antagonistic *Pseudomonas spp.* The compound is produced in low amounts *in vivo* (Nielsen et al. 2000). A 10 mM stock solution was made up in DMSO.
- Viscosinamide. This was also purified in Copenhagen from *Pseudomonas fluorescens* DR54, which is a cyclic depsipeptide antagonistic to *Pythium* and

Rhizoctonia (Nielsen et al. 1999). A 10 mM stock solution was made up in DMSO.

- Gramicidin S. This is a commercially available pentadecapeptide from *B. brevis* which forms ion channels. It also causes K^+/H^+ exchange in mitochondria in a non-voltage dependent manner (Koeppe et al. 1995). A 10 mM stock solution was made in DMSO.

All the compounds were added as 100 µl aliquots with an Anachem multichannel pipette except where indicated. 4-6 replicates were performed for each treatment. Dilutions of the antifungal compounds were made in VS medium prior to addition to the cultures. When using the luminometer injectors the number of washing cycles prior to conducting an experiment were > 12. All the compounds tested except amphotericin B were water insoluble.

The injection system of the luminometer comprised long plastic tubes of very small (1.5 mm) diameter. When water insoluble compounds were added in VS media using the injectors uneven distribution of the solution was observed. To avoid this problem all of the five chemicals were added by hand using the multichannel pippette. Because of this experimental set up there was a 5 s delay before luminescence measurements could be obtained.

2.4.5.3 Treatment with fungicides

This part of the work was done in collaboration with DuPont (Wilmington, USA). 13 chemicals were sent to Edinburgh by DuPont to be tested for their ability to alter $[Ca^{2+}]_c$. The identity of these compounds was not revealed until after the testing was completed. However, DuPont did make it clear that some of the compounds were fungicides which might influence $[Ca^{2+}]_c$ homeostasis. The stock solutions of all the compounds were prepared in DMSO. All compounds were initially tested at two concentrations (3 ppm and 100 ppm) for their agonistic activity as described in section 2.4.5.1. This involved applying the fungicides to the 24 h old cultures growing in the wells of the multiwell plate using the luminometer injector.

Measurements over 10 min period were performed at this stage of screening. Compounds which did not have a major agonistic effects on the primary $[Ca^{2+}]_c$ response or caused the final $[Ca^{2+}]_c$ resting level to be lowered were then tested for their antagonistic effect on $[Ca^{2+}]_c$ (section 2.4.5). Compounds (Manzate, methyl 2-benzimidazolecarbamate [MBC], Beam) which resulted in the most interesting $[Ca^{2+}]_c$ responses were analysed further for their long term effects on $[Ca^{2+}]_c$ and their dose-dependent effects on $[Ca^{2+}]_c$. Long term measurements were performed for 30 and 60 min after the addition of the compounds. For the analysis of the dose-dependent effects, 5 concentrations were chosen: 1 ppm, 3 ppm, 10 ppm, 30 ppm and 100 ppm. In all cases, controls contained media and appropriate concentration of the solvent.

2.4.6 Toxicity analysis

Three well known and well characterised toxicants were tested: $ZnSO_4 \cdot 7H_2O$, $K_2Cr_2O_7$ and 3,5- dichlorophenol (3,5-DCP). The concentrations used were chosen based on experience with *V. fischeri* bioassays, through range finding and interest in observing effects at high and low concentrations.

For toxicity analysis, stock solutions of each chemical were made in water in volumetric flasks and were stored at room temperature ($ZnSO_4$ and $K_2Cr_2O_7$) or at 4°C (3,5-DCP).

First, all three chemicals were tested for their agonistic effects by injecting them directly into the microwells containing the fungus. The second approach was to study the effect of preincubation of the toxicant on the Ca^{2+}-signature resulting from the response to the addition of external $CaCl_2$. All three toxicants were added 5 min and 30 min before treatment with 5 mM $CaCl_2$ in a total volume of 25 µl H_2O. The preincubation time periods chosen were those routinely used in bacterial biosensors experiments (Ribo 1997). Control experiments involved preincubation with water only.

Vibrio fischeri bioassays utilised cultures of the organism grown in *Photobacterium* Broth (PB) at 25°C for 20 h when optimum light output was achieved (Prof. Nick Christofi, personal communication). A 100 µl volume of *V. fischeri* suspension was added to each of the 96 wells in a microtitre plate to which was then added a 100 µl volume of solution (2% NaCl) containing the test substance at the appropriate concentration. The control for each measurement consisted of 6 wells containing *V. fischeri* to which a 2% NaCl solution was added. Chemicals were tested in five different concentrations and each concentration was tested in three replicates. Plates were measured in an Anthos Lucy 1 luminometer (Anthos Labtec Instruments, Salzburg, Austria). Measurements were made over a period of 30 min. IC_{50} values were calculated for 5 and 30 min incubations. Recording of data started immediately after addition of the test solutions to the wells containing the cultures. The standard proprietary Microtox bioassay was also carried out (Azur 1997).

2.5 IMAGING AEQUORIN LUMINESCENCE

Imaging was performed with a low light camera (EG&G Berthold LB96P Microlumat Luminograph LB980). The camera gain was set at 100%. Images were integrated over 2 s periods with 6 s intervals. Cultures were grown on solid VS media for 48 h in 5 cm Petri dishes. Plates were inoculated with 20 ml of cell suspension (1.06×10^8 cells/ml). Prior to inoculation 20 µl drop of 0.95 µM coelenterazine was spread over the surface of the media using a sterile glass rod.

All treatments (except mechanical perturbation) were applied by spraying them on the surface of the growing culture using a Humbrol power pack (Humbrol Ltd, Hull, UK). Mechanical perturbation involved touching cultures with a sterile glass rod.

2.6 METHODS FOR ASSAYING EFFECTS OF PHARMACOLOGICAL AGENTS ON FUNGAL GROWTH AND SPORULATION

Analysis of the growth rate and of sporulation was performed with the cultures of *A. awamori* growing on solid VS medium in 9 cm Petri dishes. 30 ml of VS medium was poured into the plates and allowed to solidify. 8.5 cm circles of filter paper (Whatman International Ltd, England) were then placed aseptically on the surface of the media. Inoculation was done using 6 mm diameter assay discs (Schleicher& Schuell, Dassel, Germany). At first they were soaked in the spore suspension $5 \cdot 10^5$ spores/ml and then one assay disc was carefully place on top of the filter paper circles in the centre of the Petri dish. Cultures were grown at 30°C for 24 h and then the filter paper together with the spore- soaked assay disc were removed and placed onto VS medium (Section 2.2.2) containing the pharmacological agent of interest. Stock solutions of $LaCl_3$ was made in dH_2O and sterilised using 0.2 µm syringe filter (Nalgene) to avoid changing their activity during autoclaving. Due to difficulties in dissolving the required concentrations of BAPTA and caffeine in water, these compounds were added to VS medium and autoclaved. $CaCl_2$ was also added prior to the autoclaving. For KP4, A23187 and CPA the appropriate amount of stock solution was added to the medium after autoclaving. Control contained the appropriate concentration of the solvent. The measurements of colony diameter and observation on the level sporulation were made every 24 h for 8 days. Experiments was performed three times with 6 replicates each.

2.7 LIGHT MICROSCOPY

To analyse hyphal branch formation *A. awamori* was grown in liquid VS medium on coverslips. The spore concentration in 50 µl drops of the media varied from 500 and 500000 spores/ml. The cultures were grown for 24 h at 30°C. The number of branches forming from the single germ tube emerging from each spore were counted in 75 fields of view. The treatment involved (a) stimulation by the addition of 50 µl

10 mM $CaCl_2$ (5 mM final concentration), 5% VS medium or 100% VS medium; (b) addition of A23187 in two concentrations 10 μM and 50 μM (final); (c) untreated control. The analysis of branching frequency was carried out 1h, 3h, 5h and 7 h after each treatment.

The second analysis of branch formation involved growing *A. awamori* on cellophane on solid VS medium. 8.5 cm diameter pieces of cellophane were cut, soaked in distilled water, covered with aluminium foil and autoclaved. Each piece of cellophane was then aseptically placed on top of solid VS medium in a Petri dish. A spore suspension of *A. awamori* was spread in strips over the surface of cellophane using sterile loop. The plates were incubated at 30°C for 24 h after which the cellophane was aseptically lifted and transferred to the VS medium containing the drug of interest. Every hour part of the cultures were cut out using a sterile scalpel and placed with the cellophane down on the coverslip for inspection with the light inverted microscope.

Light microscopy of the macrocolonies formed in the wells of microplates containing agar (see section 2.2.4) were carried out by scooping the solid agar block from the well using a sterile disposable scalpel (Swann Morton Ltd, Sheffield, UK) and carefully placing the agar on the coverslip. Observations were carried out using inverted microscope (Nikon Corporation, Tokyo, Japan).

2.8 CONFOCAL MICROSCOPY

Solid VS medium with 2% agar was poured into the Petri dishes and allowed to solidify. A spore suspension of *A. awamori* was spread in strips over the surface of agar plate using sterile loop. The cultures were grown at 30°C for 24 h. Medium containing 2.5% agar and pharmacological agent of interest was prepared as described in Section 2.6. After 24 h the blocks of agar (approximately 1cm to 0.8 cm) containing mycelia were cut out of the media and transferred upside down on the media containing the pharmacological agent. For the control agar blocks were placed on the VS medium containing solvent.

After 30 min and then every hour one of the blocks was removed and placed on a drop of dye on the coverslip in order to analyse culture morphology. The dye used was FM4-64 (Molecular Probes Inc, Eugene, Oregon, USA).

After loading with dye, cells were imaged using a confocal laser scanning microscopy (CLSM). Confocal microscopy provides significantly better resolution and contrast than conventional light microscopy by rejecting out-of focus blur and allowing thin optical sectioning (Czymmek et al. 1994).

For confocal microscopy a Bio-Rad MRC600 confocal system, using a 25 mW Argon ion laser (with laser lines at 488 and 514 nm) and mounted on a Nikon Diaphot TMD inverted microscope with epifluorescence equipment, was employed (all supplied by Bio-Rad Microscience, Hemel Hempstead, Herts., UK). Image capture and processing were performed with a dedicated PC running COMOS software supplied by Bio-Rad. The intensity of the laser beam was regulated via neutral density filters to 1, 3 and 10% of the full intensity. The MRC600 was equipped with two protomultipliers, PMT 1 (channel 1) and PMT 2 (channel 2), for fluorescence imaging. Channel 2 was also used to collect brightfield images via an optical fibre which collects light from a transmitted light detector located behind the condensor. For confocal imaging x20 dry (NA 0.7), x40 dry (NA 0.95) and x60 oil (NA 1.4) plan apo objectives were used.

2.9 LIVE-DEAD ASSAY

Live-dead staining was performed as described in (Oparka and Read 1994). The assay is based on the ability of some fluorescence probes (e.g. propidium iodide) to test the integrity of the plasma membrane and the ability of other probes (e.g. fluorescein diacetate [FDA]) to detect specific enzyme reactions within the cytosol. In present study both propidium iodide and FDA were used.

Stock solutions of propidium iodide and FDA were prepared separately at concentrations of 3 mg/ml for propidium iodide in dH_2O and 3 mg/ml for FDA in acetone. The stocks were store in the dark at 4°C. One drop of the FDA stock was

placed in 10 ml VS medium. Propidium iodide was diluted to a concentration of 100 µg/ml with distilled water. Just before addition to the cells, the FDA and propidium iodide were mixed together in equal volumes.

For the live-dead assays, cultures were grown as described in Section 2.8. After 3 h of incubation on the media containing drug agar blocks were placed on the microscopic slide and treated with the combined solution of propidium iodide and FDA. After 5 min the stained cultures were examined using a x25 (NA,) objective and a B1 filter block (excitation filter = 450-495 nm, dichromic mirror = 510 nm; long pens filter = 520 nm) with Reichert-Jung Polyvar fluorescence microscope (Leica UKLtd., Milton Keynes, UK). Dead or damaged cells fluoresce red, living cells fluoresce green.

3 DEVELOPMENT OF THE RECOMBINANT AEQUORIN METHOD FOR CALCIUM MEASUREMENT IN FILAMENTOUS FUNGI

3.1 INTRODUCTION

With the cloning of apoaequorin cDNA, it has become possible to express the apoaequorin gene in a wide range of different organisms, and to target aequorin to different cell compartments, in order to measure changes in intracellular Ca^{2+} under different physiological conditions (see Section 1.5.1). The crucial requirement for these measurements is that the level of apoaequorin expression is sufficient to allow measurements of Ca^{2+} changes of different magnitude. Recently an apoaequorin gene, codon optimised for expression in *Aspergillus* and *Neurospora* has been produced (see Section 1.5.1.2). This recombinant aequorin gene has been used in the present study.

The way in which aequorin luminescence is converted into free Ca^{2+} concentrations is fundamentally different from the calibration required to convert the fluorescence of Ca^{2+}-sensitive dyes into free Ca^{2+} concentrations. This is because aequorin is consumed during an experiment. The method used to convert aequorin luminescence values recorded into $[Ca^{2+}]$ concentrations in plants expressing aequorin is based on the empirically derived equation:

$$pCa = 0.332588\ (-\log k) + 5.5593$$

where $k = L/ L_{max}$; 0.332588 and 5.5593 are calibration coefficients (Fricker et al. 1999).

This formula relies on the relationship between $[Ca^{2+}]$ and the ratio between the light intensity recorded per second (L) and that which is recorded when all of the aequorin

in the cell had been exposed to the saturating concentrations of Ca^{2+} (L_{max}) (Allen et al. 1977). L_{max} can be obtained from the total aequorin light output recorded from cells after discharging all of the aequorin. This usually requires the addition of excess Ca^{2+} in the presence of a cell permeabilizing agent (Brini et al. 1995). The most commonly used permeabilizing agent is 10% or 20% ethanol although detergents such as Triton-X and 10% igepal (old name Nonidet P-40) have been also used (Cessna et al. 1998; Cobbold and Rink 1987; Fricker et al. 1999).

The drawbacks of this equation are that calibration coefficients were determined at one particular temperature (25°C) which causes difficulties when attempting to determine free Ca^{2+} concentration at other temperatures or during cold or heat shock (Fricker et al. 1999). Also the equation is based on an intracellular aequorin concentration of $5 \cdot 10^{-8}$ M (Allen et al. 1977) which raises questions about applicability of this equation when dealing with different aequorin concentrations.

The aims of the research described in this chapter were:

- To estimate the aequorin concentration in a range of aequorin expressing transformants of *Aspergillus awamori*, *A. niger* and *A. nidulans*.
- To improve calibration methods for converting aequorin light emission into $[Ca^{2+}]_c$ concentration in filamentous fungi.

3.2 RESULTS

3.2.1 Determination of amount of aequorin in different transformants

To obtain values for the amount of aequorin present in different transformants protein was extracted from 24 h old cultures. After total discharge of the aequorin present in the protein extract by adding 100 mM $CaCl_2$, the concentration of aequorin (in µg aequorin per g of total protein) was determined. The concentration of protein

in a cell extract was estimated using the standard procedure described in the protein kit of Bio-Rad (Bio-Rad Microscience, Hemel Hempstead, Herts, UK). The method used was based on using purified aequorin D for building a standard curve of aequorin light emission by adding 100 mM $CaCl_2$ to different concentrations of aequorin (Figure 3.1) ranging from 10^{-17} M to 10^{-8} M. Using the standard curve obtained from purified protein, the total amount of aequorin present in soluble cell extract was determined from the luminescence obtained from the sample. The curve of aequorin light emission has a sigmoid shape. At aequorin concentrations below 10^{-14} M the light emission does not change significantly. At aequorin concentration from 10^{-13} M to 10^{-10} M light emissions increases exponentially and at concentration above 10^{-10} M light emission approaches its peak.

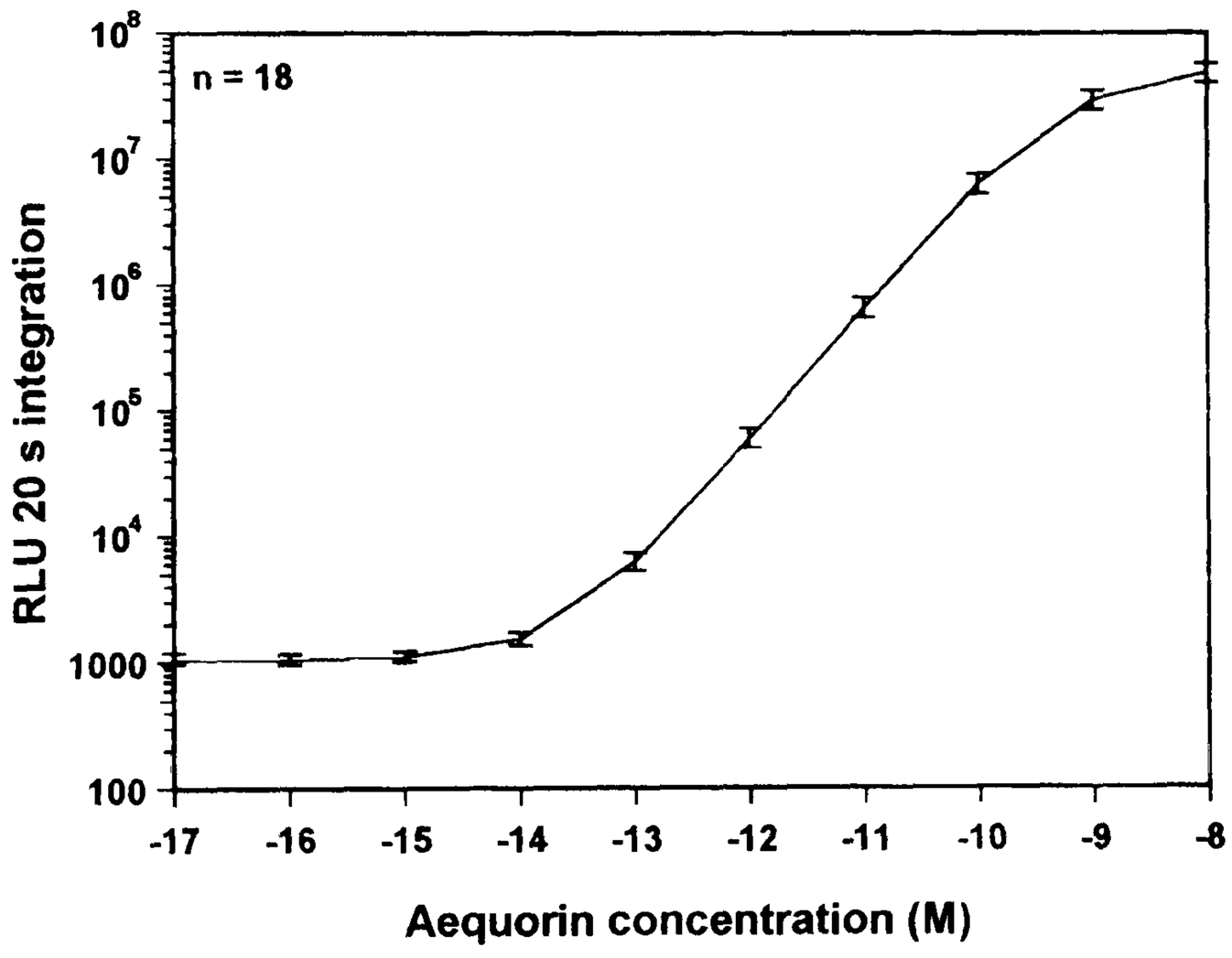

Figure 3.1 Standard curve of aequorin light emission. Results represent mean ± SE. The volume of each sample was 100 µl.

Using the aequorin light emission curve and data from the luminescence values obtained after aequorin discharge in protein extracts, the aequorin concentration in different transformants was determined. These values were related to the amount of total protein present. Table 3.1 shows that among all the transformants tested, *A.*

awamori 66a and *A. niger* 15-21 gave the highest values of 21.8 µg and 13.4 µg aequorin per g of total protein, respectively. This was respectively 484 and 300 times higher than the expression of the native aequorin gene in *N. crassa* (Table 3.1).

Species	**Strain**	**µg aequorin per g of total protein**				
		Exp 1	Exp 2	Exp 3	Exp 4	Mean ± SD
Aspergillus awamori	66a	33.85	19.20	6.41	21.8 27.9 21.6	$21.8_{total} \pm 9.2$ $23.8_{exp4} \pm 3.6$
A. niger	15-21	14.61	22.64	3.06		13.4 ± 9.8
A. nidulans	3.2	8.758	3.534	1.889		4.7 ± 3.6
	3.3	11.3	1.052	3.537		5.3 ± 5.3
	3.4	4.337	1.545	0.376		2.1 ± 2.0
	av6	3.498	0.682	0.408		1.5 ± 1.7
	AXB4Aeq11*	3.646	0.779	0.967		1.8 ± 1.6
	AXB4Aeq17*	0.662	0.094	0.214		0.3 ± 0.3
	△suAaaeq17*	0.046	0.017	0.032		0.03 ± 0.01
	△suAaaeq18*	0.102	0.695	0.333		0.4 ± 0.3
Neurospora crassa	3,5					0.045
Nicotiana plumbaginifolia	2,4					4.7

Table 3.1 Comparison of levels of aequorin expression in different strains. The data for *N. plumbaginifolia* and *N. crassa* were obtained by Collis (1996). Abbreviations: Exp = experiment, $mean_{total}$ = mean of all 4 experiments, $mean_{exp4}$ = mean of experiment 4. * = strains in which aequorin is expressed in mitochondria.

Aspergillus nidulans strains 3.2, 3.3, 3.4 and av6 have approximately 10 times less aequorin than *A. awamori* 66a and *A. niger* 15-21 transformants. *Aspergillus nidulans* strains AXB4Aeq11, AXB4Aeq17, △suAaaeq17 and △suAaaeq18, in which aequorin had been targeted to mitochondria, have approximately 10 times less aequorin then cytosolic transformants of *A. nidulans*. When compared with the amount of aequorin produced by the plant *Nicotiana plumbaginifolia* the value was

similar to the strain of *A. nidulans*, in which aequorin was produced in the cytoplasm.

Data from the separate experiments (exp 1, exp 2, exp 3 and exp 4) showed high variability in the protein estimates, which resulted in very high SD values. However when aequorin amount was determined in three separate flasks on the same day with *A. awamori* 66a it was found that variation between them was much smaller. This suggested that the amount of aequorin differs from day to day rather than the variations in the amount of aequorin measured in individual transformants being primarily due to experimental error (Table 3.1).

3.2.2 Methods for discharging aequorin inside hyphae

The luminometer measures aequorin light emission in relative lights units (RLU). The calibration of the aequorin signal requires discharging all of the remaining aequorin present within the fungal cells at the end of the experiment and then determining the amount of aequorin present at each point during the experiment. For plants cells the most widely used method of aequorin discharge involves the use of 10-20% ethanol in the presence of high concentration of external $CaCl_2$. When this method was tested in fungi rapid and complete discharge of aequorin was achieved. Different concentrations of ethanol were tested using the higher aequorin expressing strain, *A. awamori* 66a. With 20% ethanol and 1 M $CaCl_2$ the luminescence went down below the original resting level within 5-7 min (Fig. 3.2).

However, the total luminescence (i.e. the integrated luminescence) after addition of 10% ethanol (Fig. 3.3) was 2.6 times higher than after addition of 20% ethanol in the presence of 1 M $CaCl_2$ (Table 3.2), which suggested that ethanol caused quenching of aequorin luminescence. The use of 1 M $CaCl_2$ and 10% ethanol did not completely discharge the aequorin within 20 min (Fig. 3.3) so a higher concentration of $CaCl_2$ was tested. 1.5 M $CaCl_2$ in the presence of 10% ethanol was found to completely discharge the intracellular aequorin within 20 min (Figure 3.4). If one compares the amplitudes of $[Ca^{2+}]_c$ responses to 50 mM external $CaCl_2$ in Figs. 3.3 and 3.4 the

amplitude on Fig. 3.3 was 10^4 RLU/s whereas the amplitude on Fig. 3.4 was an order of magnitude lower.

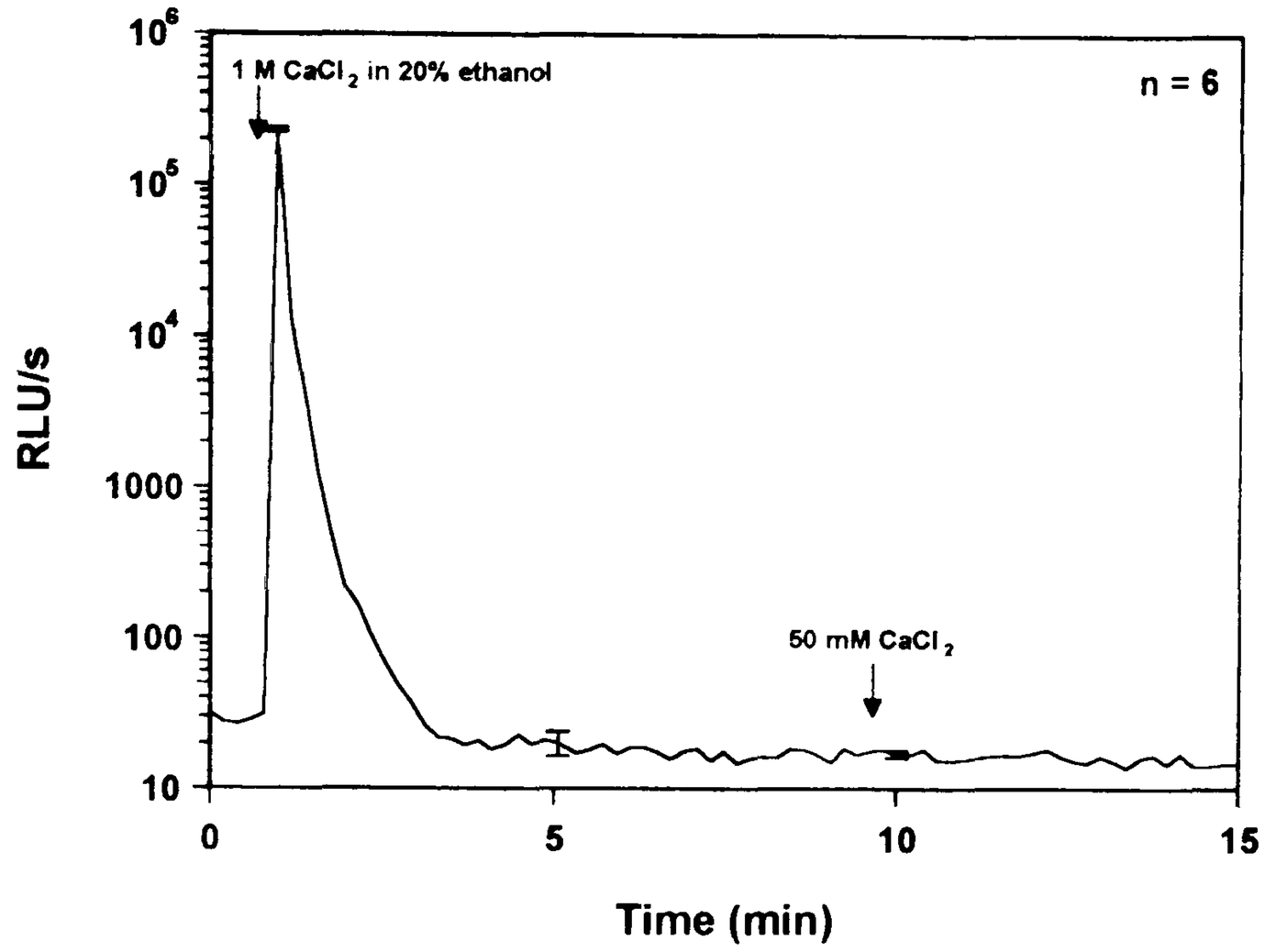

Figure 3.2 Aequorin discharge with 20% EtOH in the presence of 1 M $CaCl_2$. Results represent mean ± SE.

	Amphotericin B + 1.5 M $CaCl_2$	**10% ethanol + 1.5 M $CaCl_2$**	**10% ethanol + 1 M $CaCl_2$**	**20% ethanol + 1.5 M $CaCl_2$**
Total amount of counts	$12 \cdot 10^6$	$8 \cdot 10^6$	$4 \cdot 10^6$	$3 \cdot 10^6$

Table 3.2 Comparison of total amount of light detected (RLU) during aequorin discharge after adding different permeabilizing agents in the presence of high external $CaCl_2$. Results represent the integrated luminescence during 25 min discharge. The values are representative numbers from one experiment. n = 6

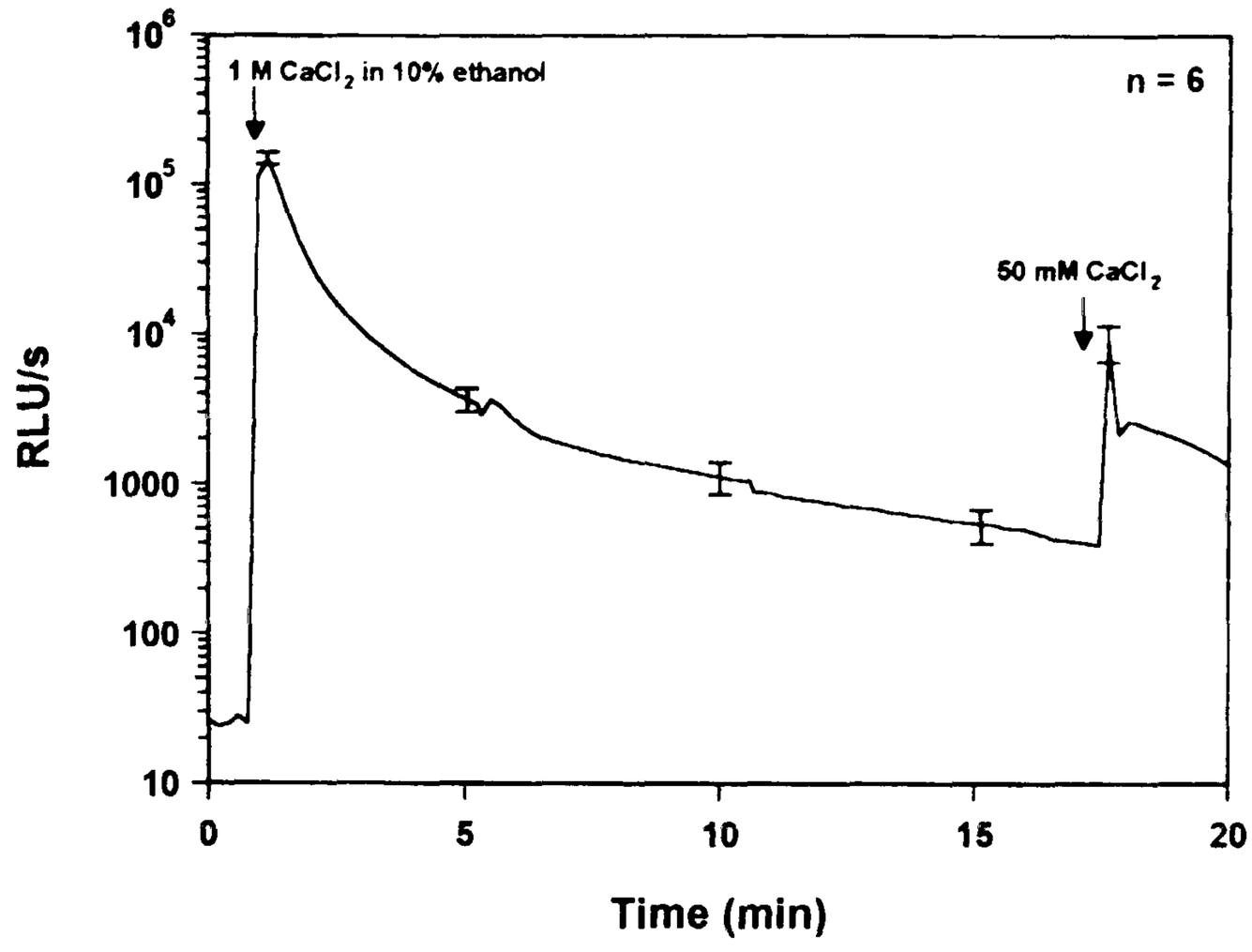

Figure 3.3 Aequorin discharge in hyphae by adding 10% EtOH in the presence of 1 M $CaCl_2$. Results represent mean ± SE.

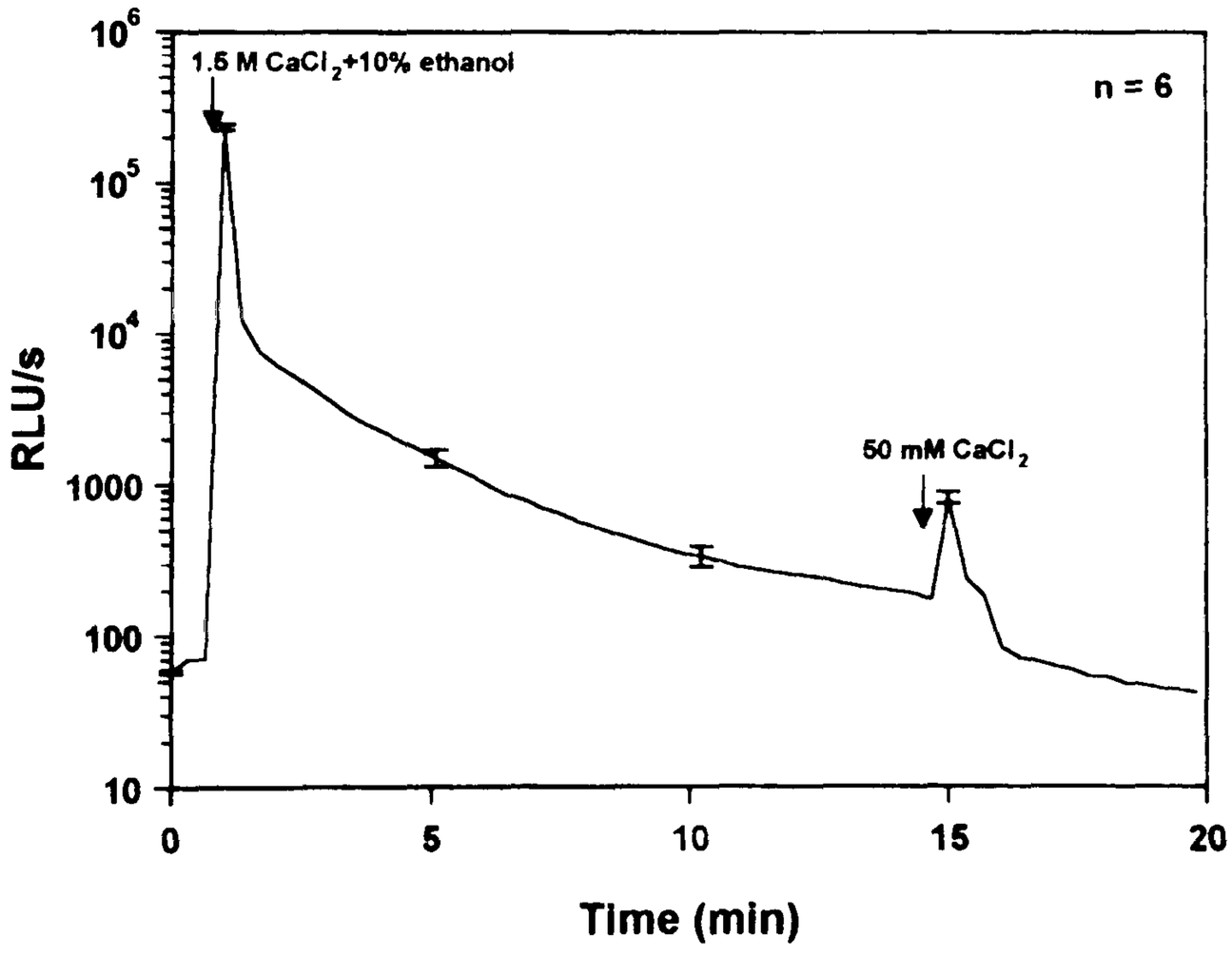

Figure 3.4 Aequorin discharge in hyphae by adding 10% EtOH in the presence of 1.5 M $CaCl_2$. Results represent mean ± SE.

To determine the amount of aequorin quenching by EtOH, pure aequorin D was purchased from Cambridge Bioscience (Cambridge, UK). Aequorin was diluted to a concentration of $1 \cdot 10^{-10}$ M and was then discharged using: (a) 1.5 M $CaCl_2$ and (b) 1.5 M $CaCl_2$ in 10% ethanol. The results from this experiment showed that 10% ethanol caused 24% ± 3.6 (SE, n = 12) quenching of aequorin. Therefore, in all subsequent experiments in which aequorin in hyphae was discharged by 10% ethanol in the presence of 1.5 M $CaCl_2$, the total luminescence detected was multiplied by a correction factor of 1.24. Though the introduction of the correction factor allowed the use of 10% ethanol as a permeabilizing agent another agent was tested. The detergent igepal (also known as Nonidet P-40) has been used at a 10% concentration for this purpose in tobacco cells (Cessna et al. 1998) and so was used here. 10% igepal was a very viscous liquid which was impossible to inject through the luminometer injectors. If injected by hand 30 s delay occurred from the moment of injection to the moment when the measurements started. This made calculations of the total amount of aequorin in hyphae impossible to obtain.

In studies on the mode-of-action of fungicides (see section 6.2.1) it was observed that amphotericin B caused a very high $[Ca^{2+}]_c$ increase in treated cells. When amphotericin B was tested as permeabilizing agents with 1.5 M $CaCl_2$ the complete discharge of aequorin was achieved within 25 min (Fig. 3.5). The total number of counts obtained using amphotericin B was 1.5 times higher than when 10% ethanol was used. This value is close to the value of 1.24 used to correct for aequorin quenching by 10% ethanol.

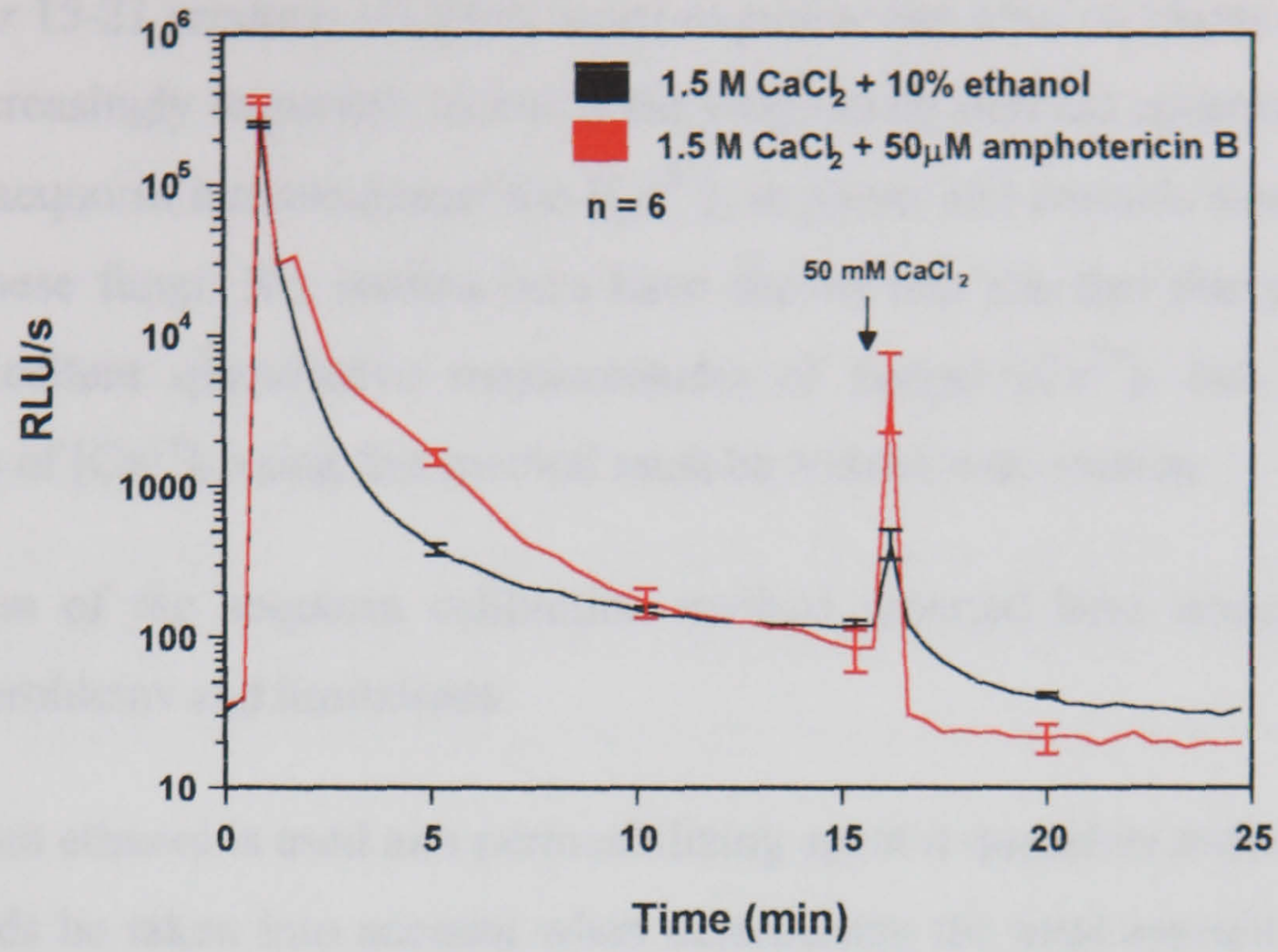

Figure 3.5 Aequorin discharge with 50 μM amphotericin B in the presence of 1.5 M $CaCl_2$. Arrow indicates when 10% EtOH+1.5 M $CaCl_2$ was injected. Results represent mean ± SE.

3.3 DISCUSSION

The first transformation of a filamentous fungus (*N. crassa*) with the native apoaequorin A gene resulted in very low expression making it difficult to observe changes in $[Ca^{2+}]_c$ (Collis 1996). The results suggested that codon bias might have been a cause of the low level of expression. This was shown to be the case when a synthetic codon optimised aequorin was used to transform a range of filamentous fungi (*A. awamori, A. niger* and *N. crassa*) (Nelson 1999). In the present study the concentrations of aequorin in transformants of these fungi and in a number of other recently transformed fungi have been carefully analysed. The data presented in Table 3.1 showed that the amount of aequorin present in the *Aspergillus* strains 66a and 15-21 transformed with the synthetic aequorin is respectively ≈ 500 and 300 times higher than that of *N. crassa* transformed with the native apoaequorin A.

When compared with the amount of aequorin in plants it was shown that *A. awamori* and *A. niger* 15-21 produce 3-4 times more aequorin than tobacco plants. Therefore it became increasingly important to test if the empirically derived equation developed to convert aequorin luminescence into $[Ca^{2+}]_c$ in plants and animals was suitable for use with these fungi. My studies here have shown that the that this equation can provide excellent quantitative measurements of fungal $[Ca^{2+}]_c$ but that precise estimations of $[Ca^{2+}]_c$ using this method must be treated with caution.

Optimisation of the aequorin calibration method reported here demonstrated the following problems and limitations:

- When ethanol is used as a permeabilizing agent it quenches aequorin, and this needs be taken into account when determining the total amount of aequorin discharged.

- Using the Berthold luminometer employed in this study only two injections of ethanol were possible because the automatic injectors of this luminometer are only set up to dispense 100 µl volume and the total volume of each well in a multiwell plate is 350 µl of which 100 µl is media containing the culture.

- Complete aequorin discharge should be achieved within 1 h because the amount of aequorin present in the mycelium of each microplate well will change as the fungus grows. Growing mycelia constantly produces apoaequorin and active aequorin will continue to form inside hyphae because coelenterazine is present in the culture medium.

- Because of variations in the biomass of cultures grown in the multiwell plates it is essential to determine the amount of aequorin present at the end of each experiment in order to convert aequorin luminescence into $[Ca^{2+}]_c$.

Ethanol proved to be a very effective permeabilizing agent and the cheapest and easiest to handle. However, ethanol caused significant quenching of aequorin. A correction factor was determined which compensated for the loss of light due to this

quenching. However, a new permeabilizing agent (amphotericin B) was found which can permeabilize the plasma membrane without damaging the protein. Amphotericin B is an antibiotic derived from strains of the actinomycete *Streptomyces nodosus*. It is believed to form pores in the fungal plasma membrane by interacting with ergosterols (Ghannoum and Rice 1999). The concentration of amphotericin B necessary to obtain complete aequorin discharge was low (50 μM) and the agent itself is relatively cheap. The applicability of amphotericin B to fungi other than *A. awamori* still needs to be tested. Because the permeabilizing properties of amphotericin B were only found at a late stage in my experiments it was decided to carry on using ethanol in order that the results from all experiments were directly comparable.

Existing empirically derived formula for calibrating aequorin luminescence was determined at 25°C and using an aequorin concentration of $5 \cdot 10^{-8}$ M (Allen et al. 1977; Fricker et al. 1999). Ideally the equation has to be derived at every temperature used and for every new transformant which has a different aequorin concentration. This, however, would be too laborious and costly to be done routinely. Furthermore, due to the fact that the aequorin concentration seems to vary between cultures on a day-to-day basis it would be very impractical to change the equation every time. Most of the experiment in the current research were performed using *A. awamori* 66a strain with the aequorin concentration varying between $4.9 \cdot 10^{-8}$ M and $26 \cdot 10^{-8}$ M, which is within one order of magnitude of $5 \cdot 10^{-8}$ M, on which the calibration equation has been based. In the literature the equation has been used with different concentrations of aequorin which greatly exceed the concentrations observed in our studies (eg. $2 \cdot 10^{-5}$ M aequorin, Allen and Blinks, 1978).

In summary the main conclusions from the research described in this chapter were:

- All of the fungal transformants tested possessed levels of aequorin expression high enough for monitoring $[Ca^{2+}]_c$ changes under the different conditions

used. The highest levels of expression were observed in *A. awamori* 66a and *A. niger* 15-21 strains.

- The existing methods for aequorin calibration can be used in fungi to convert RLU into $[Ca^{2+}]_c$ concentration, although precise estimations of $[Ca^{2+}]_c$ concentrations using this method need to be treated with caution.

- Amphotericin B showed great potential as a permeabilizing agents in fungi for converting aequorin luminescence into $[Ca^{2+}]_c$ concentrations.

4 ANALYSIS OF CALCIUM SIGNALLING AND HOMEOSTASIS IN LIVING FUNGAL HYPHAE IN RESPONSE TO DIFFERENT TREATMENTS

4.1 INTRODUCTION

Calcium is a well-known second messenger involved in the transduction of different external stimuli and hormonal signals in eukaryotic cells. To demonstrate a signalling role for Ca^{2+} it is essential to measure resting $[Ca^{2+}]_c$ as well as $[Ca^{2+}]_c$ changes arising in response to stimuli or environmental signals (Torrecilla et al. 2000). A great number of studies describing changes in $[Ca^{2+}]_c$ have been done on animal and plant cells subjected to different treatments. However, very little work in this area has been done on filamentous fungi. The reason for this has been the lack of both routine and reliable methods for monitoring intracellular free Ca^{2+} in living fungal cells. Imaging Ca^{2+} using fluorescent dyes has been shown to be technically very demanding and often not very reliable (see Section 1.5). The use of fungi transformed with the aequorin gene provides the possibility for monitoring Ca^{2+} changes in living fungal cells in response to diverse environmental stimuli.

For a long time researchers have been interested in how cells distinguish between different external stimuli when often many of them elevate $[Ca^{2+}]_c$. One hypothesis proposed is that the spatial and temporal characteristics of the $[Ca^{2+}]_c$ transients encode signal transduction information. Several parameters which may encode this information and which can be readily quantified are: amplitude, length of the transient, lag-time and rise-time of the Ca^{2+} signature (Malho et al. 1998) (for more details see section 1.6).

A wide range of physico-chemical treatments have been found to elicit changes in $[Ca^{2+}]_c$ in plant, animal and yeast cells expressing recombinant aequorin (see Tables 1.3, 1.4 and 1.5). In contrast, no similar published studies have been done on filamentous fungi. However, several treatments (mechanical perturbation, hypo-

osmotic shock and high external $CaCl_2$) had been shown to induce $[Ca^{2+}]_c$ increases in filamentous fungi (Collis 1996; Nelson et al. 1998)

The aims of the research described in this chapter were:

- To develop a routine method for measuring time-dependent changes in $[Ca^{2+}]_c$ in hyphae subjected to different physico-chemical and pharmacological treatments.
- To characterise and quantify the specific Ca^{2+} signatures associated with a range of treatments which have been shown to increase $[Ca^{2+}]_c$.
- To analyse the sources of $[Ca^{2+}]_c$ increases using appropriate pharmacological inhibitors.
- To identify different components of the Ca^{2+} signalling machinery using appropriate Ca^{2+} modulators

4.2 RESULTS

4.2.1 Physico-chemical treatments

4.2.1.1 $[Ca^{2+}]_c$ responses to mechanical perturbation, hypo-osmotic shock, hyper-osmotic shock and external $CaCl_2$

The effect of four treatments on $[Ca^{2+}]_c$ were analysed: mechanical perturbation, hypo-osmotic shock, hyper-osmotic shock and high external Ca^{2+} (0.05 and 5 mM $CaCl_2$).

All the measurements were carried out in a similar manner, which allowed direct comparison of the results (see Section 2.4.1). $[Ca^{2+}]_c$ was measured both before, during and after stimulation. The resting level of $[Ca^{2+}]_c$ measured was on average 60 ± 15 nM (± SE). Each of the treatments, except hyper-osmotic shock, which

caused a $[Ca^{2+}]_c$ transient indistinguishable from the one caused by mechanical perturbation, resulted in a distinct $[Ca^{2+}]_c$ transient with a characteristic Ca^{2+} signature. The following features of these Ca^{2+} signatures were quantified (Table 4.1):

- *lag time*, which characterises the time from the application of the stimulus to the moment when the $[Ca^{2+}]_c$ began to rise.
- *rise time*, which characterises the time from the application of the stimulus to the maximum amplitude of the response
- *amplitude*, which is the maximum $[Ca^{2+}]_c$ concentration achieved during the $[Ca^{2+}]_c$ transient.
- *full width half maximum (FWHM)*, which characterises the length of the transient at the point where the amplitude equals half of the maximum amplitude of the $[Ca^{2+}]_c$ transient.

Treatment		**Features of $[Ca^{2+}]_C$ signatures**			
		lag time (s)	rise time (s)	amplitude (Ca^{2+} concentration)	FWHM (s)
External Ca^{2+}	**0.05 mM**	0	3-10	0.3 ± 0.03 μM	49-51
	5 mM	0	3	1.2 ± 0.16 μM	24-26
Hypo-osmotic shock		0	3-5	0.2 ± 0.02 μM	38-40
Mechanical perturbation		0	3	0.13 ± 0.01 μM	48-50

Table 4.1 Effects of different physico-chemical treatments which increase $[Ca^{2+}]_c$. Abbreviations: FWHM = full width half maximum. Results represent the mean ± SE. n = 24 for each treatment. Mean and SE were calculated from 4 separate experiments with 6 replicates in each experiment performed within a 2 week period.

All the treatments analysed had an undetectable (i.e. 0 s) lag time. The rise time varied from 3-10 s between treatments, especially after application of 0.05 mM

$CaCl_2$. After mechanical perturbation, hypo-osmotic shock and 0.05 mM $CaCl_2$ $[Ca^{2+}]_c$ reached the final resting level after ~2 min, and after treatment with 5 mM external $CaCl_2$ the final resting level was reached after 1 min. Such short recovery times indicate that the physico-chemical treatments do not affect cells ability to recover to normal $[Ca^{2+}]_c$ levels, and thus to do not perturb the Ca^{2+} homeostatic mechanism of the hyphae.

Compared with mechanical perturbation, hypo-osmotic shock resulted in a $[Ca^{2+}]_c$ transient with a greater amplitude but a similar FWHM (Fig. 4.1). Addition of 0.05 $CaCl_2$ induced a $[Ca^{2+}]_c$ transient with a higher amplitude compared to that resulting from hypo-osmotic shock (cf Figs. 4.1 and 4.2). 5 mM $CaCl_2$ resulted in a $[Ca^{2+}]_c$ response which had a much greater amplitude yet much shorter FWHM than caused by 0.05 mM $CaCl_2$. These unique Ca^{2+} signatures resulting from each of the 4 treatments suggested that different Ca^{2+} signalling pathways may be involved.

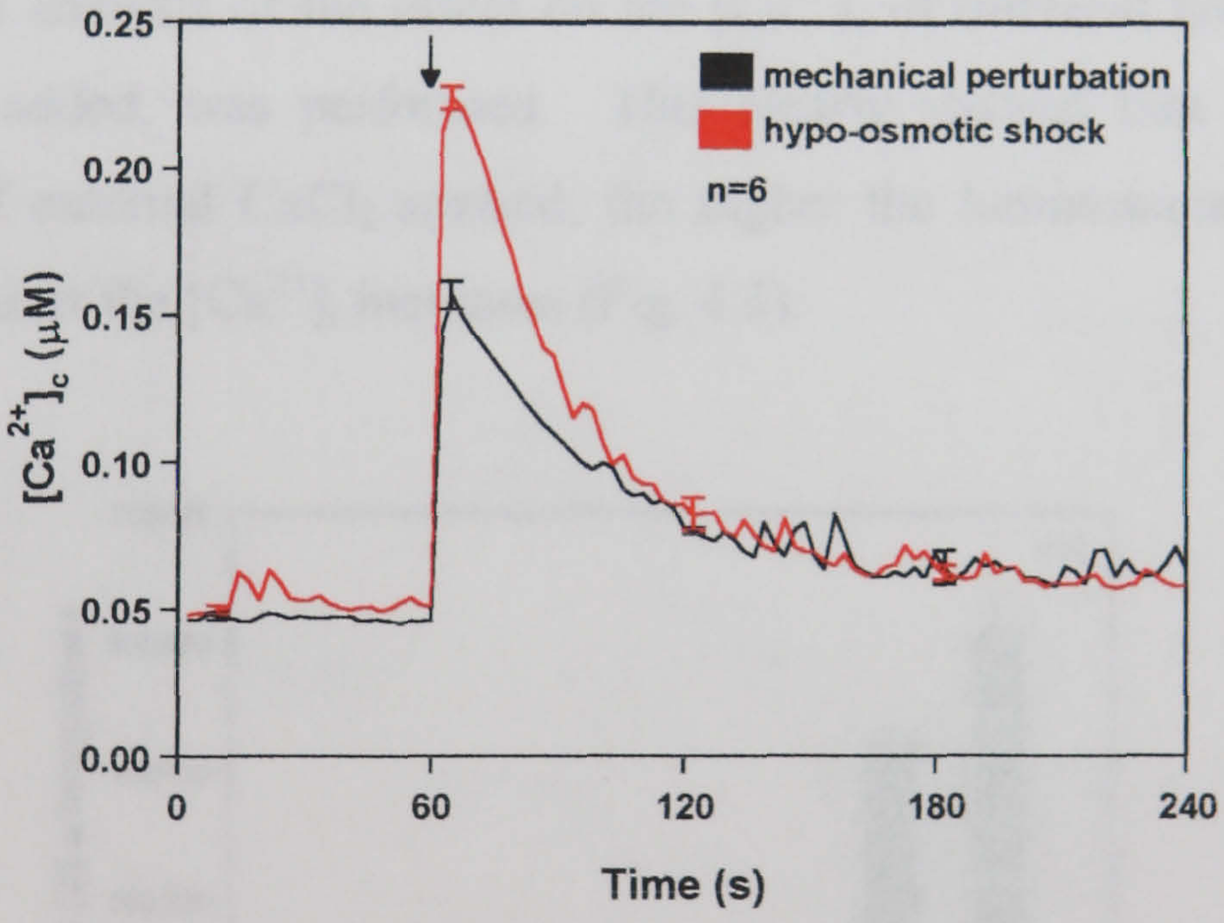

Figure 4.1 Effect of mechanical perturbation and hypo-osmotic shock on $[Ca^{2+}]_c$. The arrow indicated the point when the treatment was applied. Results represent mean ± SE. Measurements were performed using the kinetic measuring protocol.

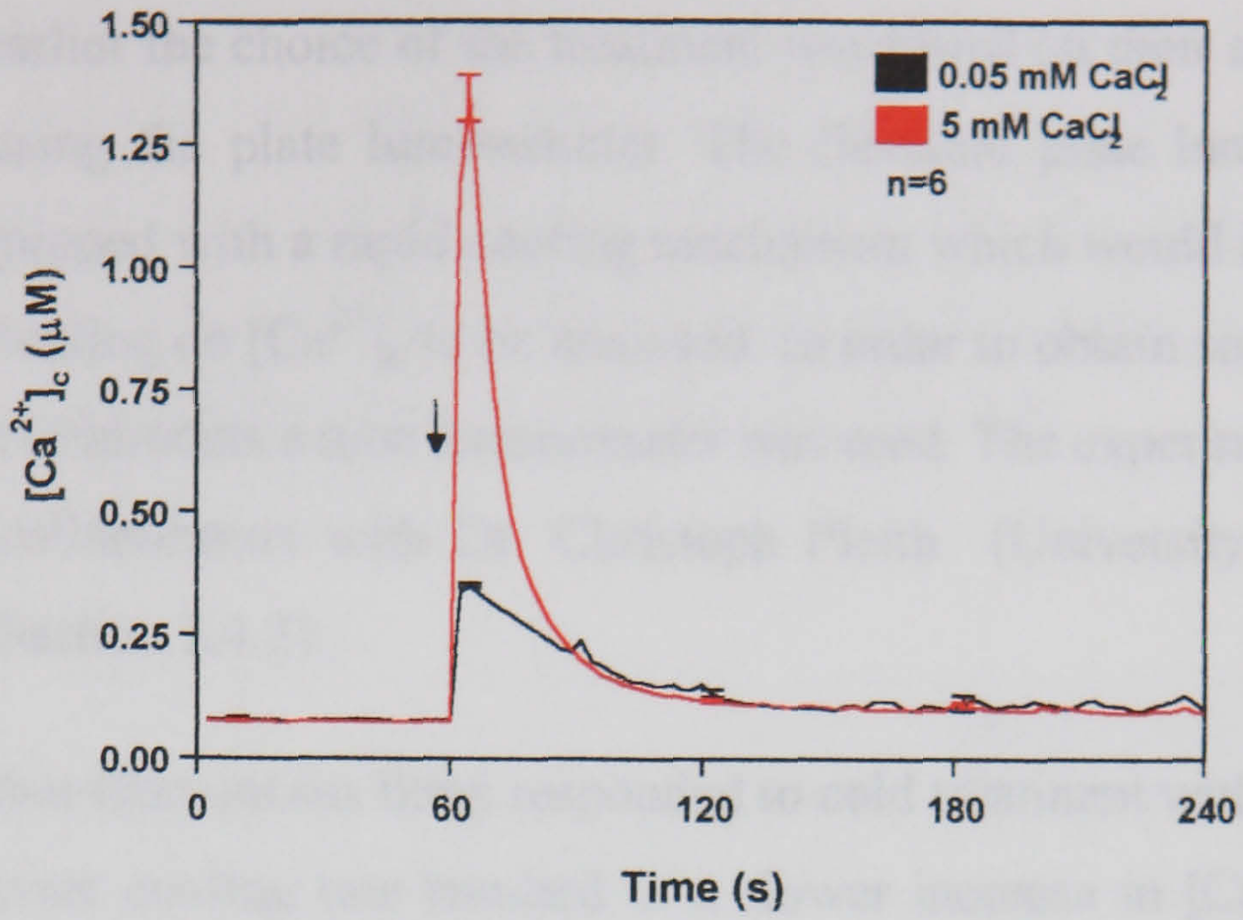

Figure 4.2 Effect of external $CaCl_2$ on $[Ca^{2+}]_c$. The arrow indicated the point when the treatment was applied. Results represent mean ± SE. Measurements were performed using the kinetic measuring protocol.

A dose-response analysis of the effect on the $[Ca^{2+}]_c$ of different concentrations of external $CaCl_2$ added, was performed. This clearly showed that the higher the concentration of external $CaCl_2$ applied, the higher the luminescence emitted and therefore the greater the $[Ca^{2+}]_c$ increases (Fig. 4.3).

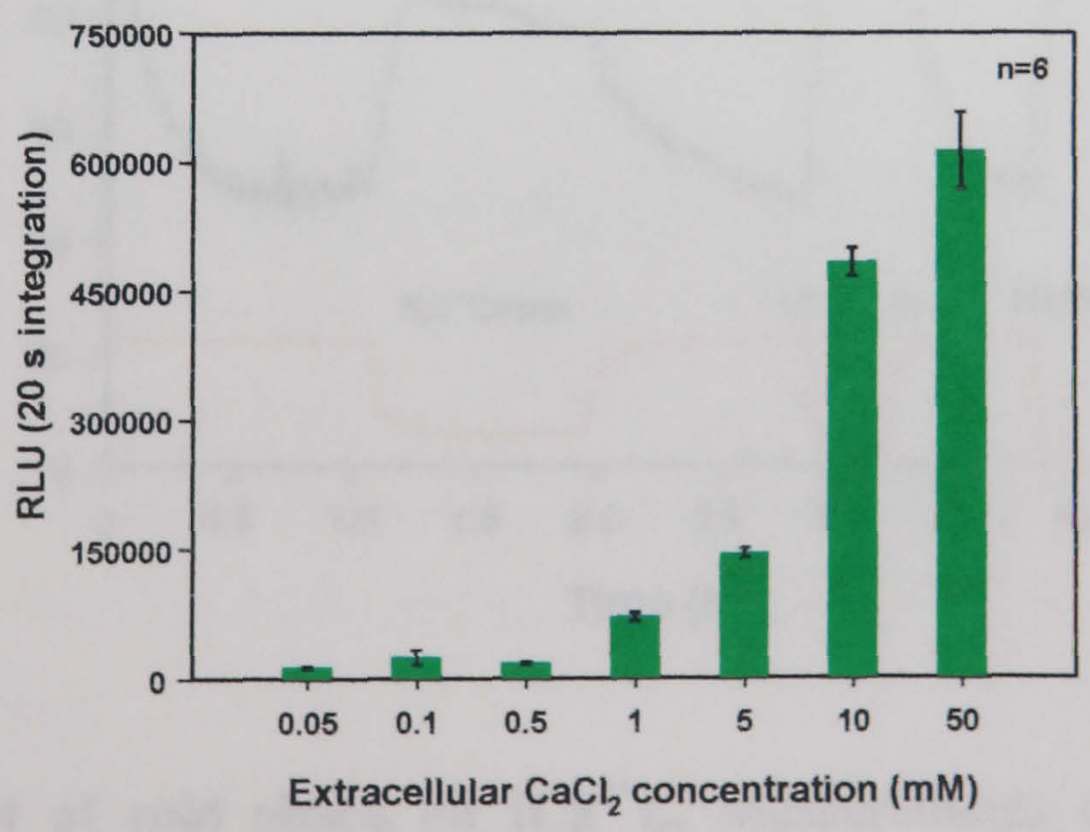

Figure 4.3 Effect of different concentrations of external $CaCl_2$ on $[Ca^{2+}]_c$. Results represent mean ± SE.

4.2.1.2 $[Ca^{2+}]_c$ responses to cold and heat shock

As mentioned earlier the choice of the treatment was based on their applicability for being applied using the plate luminometer. The Berthold plate luminometer used here was not equipped with a rapid cooling mechanism which would allow the effect of cooling and heating on $[Ca^{2+}]_c$ to be analysed. In order to obtain some preliminary data about these treatments a tube luminometer was used. The experiments have been carried out in collaboration with Dr. Christoph Pleith (University of Kiel, Kiel, Germany) (see Section 2.4.2).

Fig. 4.4 shows that filamentous fungi responded to cold treatment with an increase of $[Ca^{2+}]_c$. The slower cooling rate resulted in a slower increase in $[Ca^{2+}]_c$ whilst the faster cooling rates resulted in faster $[Ca^{2+}]_c$ increases. When temperatures returned to normal, $[Ca^{2+}]_c$ recovered its normal resting level. With the repeated cooling stimulation the $[Ca^{2+}]_c$ increase was successively lower which suggested that some sort of adaptation occurred (Fig. 4.4).

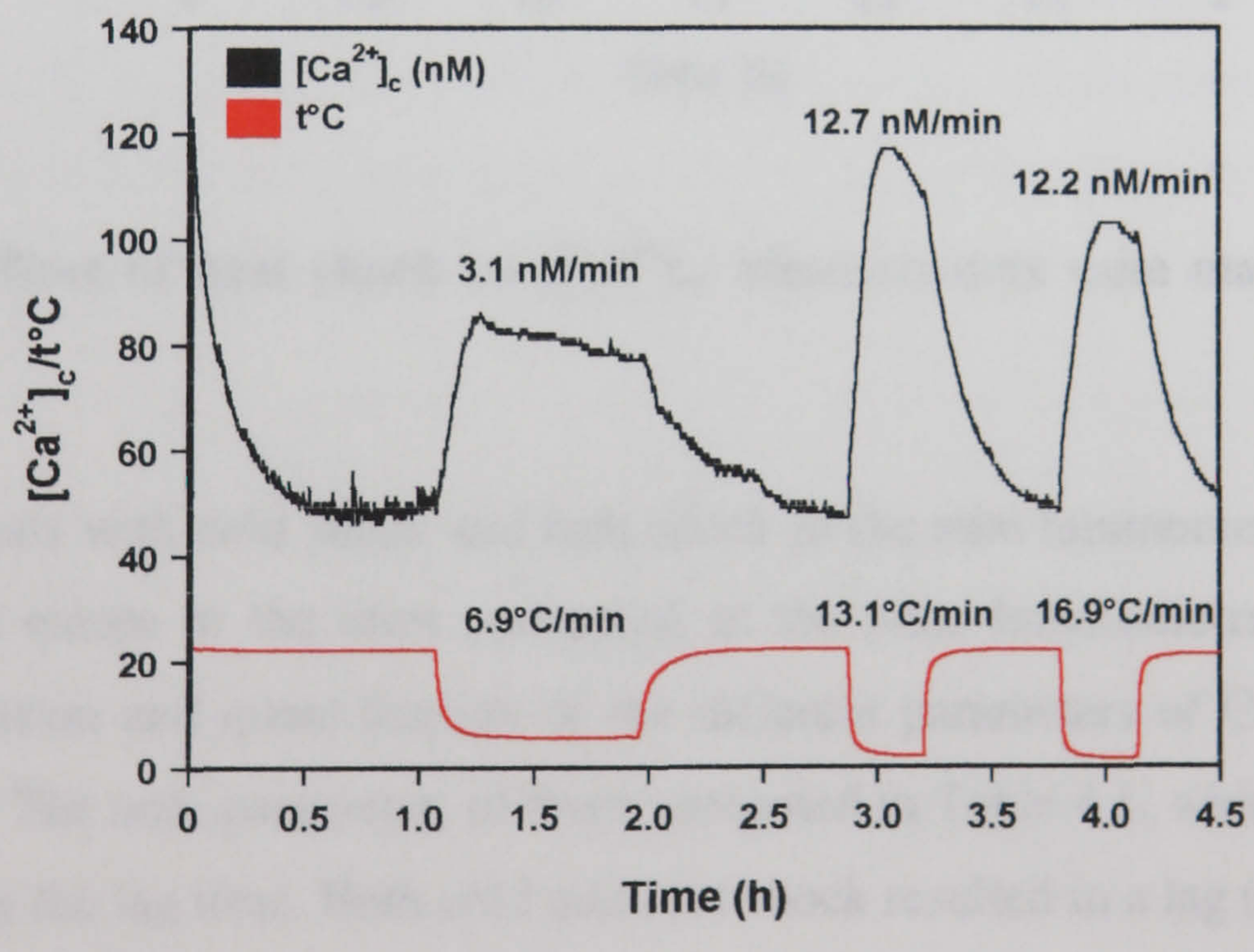

Figure 4.4 Effect of cold shock on $[Ca^{2+}]_c$. Measurements were made in tube luminometer. 6.9°C/min, 13.1°C/min and 16.9°C/min = cooling rates during the period when the temperature decreased linearly. 3.1 nM/min, 12.7 nM/min, 12.2 nM/min = rates of $[Ca^{2+}]_c$ increase during the period corresponding to when these cooling rates were measured.

Heat shock also resulted in a $[Ca^{2+}]_c$ increase. With repeated cycles of heating applied no decrease in the amplitude of the $[Ca^{2+}]_c$ response was observed but the recovery from repeated heat shock stimulation was slower (Fig. 4.5). When the temperature returned to normal following heat shock, the $[Ca^{2+}]_c$ did not return to resting level after 20 min and the final $[Ca^{2+}]_c$ resting level became higher and higher after repeated heat shock stimuli at 40 min intervals (Fig. 4.5).

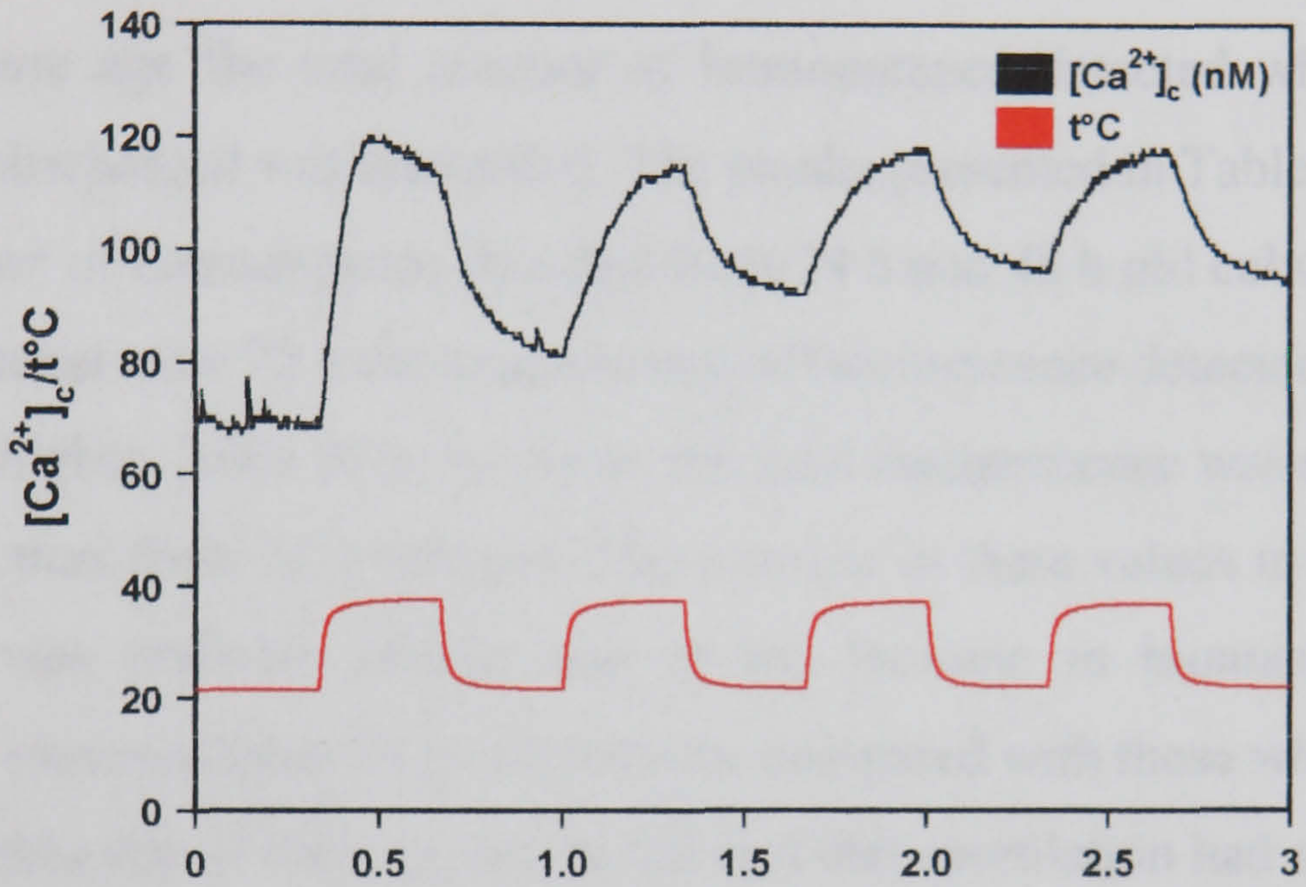

Figure 4.5 Effect of heat shock on $[Ca^{2+}]_c$. Measurements were made in a tube luminometer.

The experiments with cold shock and heat shock in the tube luminometer were of a very different nature to the ones performed in the plate luminometer. This made $[Ca^{2+}]_c$ calibration and quantification of the different parameters of Ca^{2+} signature very difficult. The only parameter, of those presented in Table 4.1, which was easily quantified was the lag time. Both cold and heat shock resulted in a lag time of 0 (i.e. it was not detectable).

4.2.1.3 $[Ca^{2+}]_c$ responses in cultures of different age

All the experiments described above were carried out using 24 h old cultures. However it was decided to next analyse the $[Ca^{2+}]_c$ responses of older cultures because they may possess some advantages for plate luminometry (i.e. higher signal to background ratio, more aequorin present in the cells, more consistent biomass). Therefore, the effects of different physico-chemical treatments on cultures of different age were studied.

For each culture age the total amount of luminescence detected when all of the aequorin was discharged was quantified. The results presented in Table 4.2 show that the total amount of luminescence detected from 24 h and 48 h old cultures was fairly similar. In contrast after 72 h the total amount of luminescence detected was an order of magnitude higher. After 96 h, however, the total luminescence was approximately 5 times lower than from 72 h cultures. The increase in these values in older cultures up to 72 h was probably mostly due to the increase in biomass. The lower luminescence observed from 96 h old cultures, compared with those which were 72 h old, was probably due at least in part, to the fact that sporulation had started. Spores of *A. awamori* are pigmented dark brown which will result in light absorbed and thus remained undetected by the photomultiplier detector of the luminometer.

Culture age	**24 h**	**48 h**	**72 h**	**96 h**
Total amount of luminescence (RLU)	$1.2 \cdot 10^7$	$1.3 \cdot 10^7$	$1.3 \cdot 10^8$	$5.6 \cdot 10^7$
$[Ca^{2+}]_c$ resting level (μM)	0.057 ± 0.006	0.088 ± 0.01	0.093 ± 0.017	0.128 ± 0.007

Table 4.2 Estimation of total amount of luminescence and $[Ca^{2+}]_c$ resting levels in cultures of different age. The total number of RLU for each culture age are representative. The total number of RLU differed significantly between experiments but the difference between cultures of different age in a single experiment was consistently the same. Results for the $[Ca^{2+}]_c$ resting levels represent mean ± SE. n = 48.

Measurements were made on changes in the $[Ca^{2+}]_c$ resting level of cultures of different age (Table 4.2). The $[Ca^{2+}]_c$ resting level of 48 h old fungal cultures was 1.8 times greater than that of 24 h old cultures. Only a very small difference was observed in the $[Ca^{2+}]_c$ resting level between 48 h and 72 h old cultures. However 96 h old cultures had a 1.4 times higher $[Ca^{2+}]_c$ resting level than younger cultures. This increase in $[Ca^{2+}]_c$ resting level was significant ($P < 0.05$) but it is important to note that even the value observed for 96 h old cultures did not exceed the $[Ca^{2+}]_c$ resting levels of < 200 nM which have been reported for other eukaryotic cells (Bush 1995).

The $[Ca^{2+}]_c$ response of cultures of different age to different physico-chemical treatments was analysed. As mentioned before, the luminometer measures light emission in RLU which are then manually converted into $[Ca^{2+}]_c$ (see Section 2.4.4). Initially the $[Ca^{2+}]_c$ responses of cultures of different ages were analysed in terms of RLU. The data presented in Figs 4.6 and 4.8 show that the aequorin luminescence detected increased in response to all treatments with culture age up to 72 h, followed by a decrease in luminescence detected at 96 h. Interestingly, when 72 h old cultures were stimulated with 50 mM $CaCl_2$ the luminescence approached $1.2 \cdot 10^6$ RLU (Fig. 4.8). It was found that this level of luminescence could be observed with the naked eye in a darkroom.

However when the RLU were converted into $[Ca^{2+}]_c$ concentrations (Figs. 4.7 and 4.9) all the differences became much less significant. In particular, at 72 h when the massive increase in light emission was observed (Figs. 4.6 and 4.8) the $[Ca^{2+}]_c$ response was not significantly different ($P < 0.05$) compared with 48 h old cultures (cf. Figs. 4.6 with 4.7 and 4.8 with 4.9) and with mechanical perturbation even a decrease was observed (Fig. 4.7). In 96 h old cultures when a significant reduction in light emission was observed, there was no significant difference in the $[Ca^{2+}]_c$ response compared with the $[Ca^{2+}]_c$ response at 76 h ($P < 0.05$).

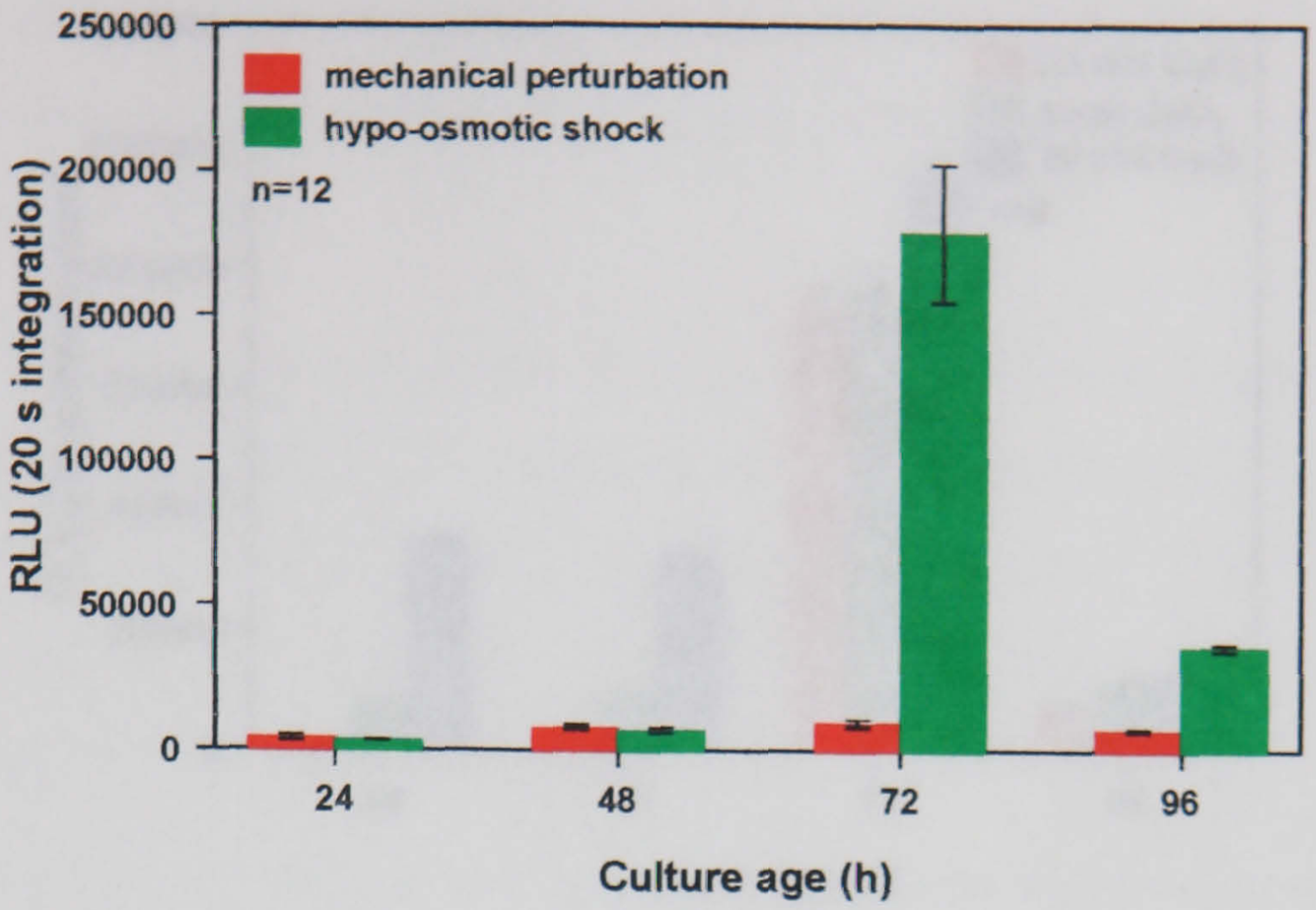

Figure 4.6 Effects of mechanical perturbation and hypo-osmotic shock on aequorin luminescence in cultures of different age. Results represent the mean ± SE.

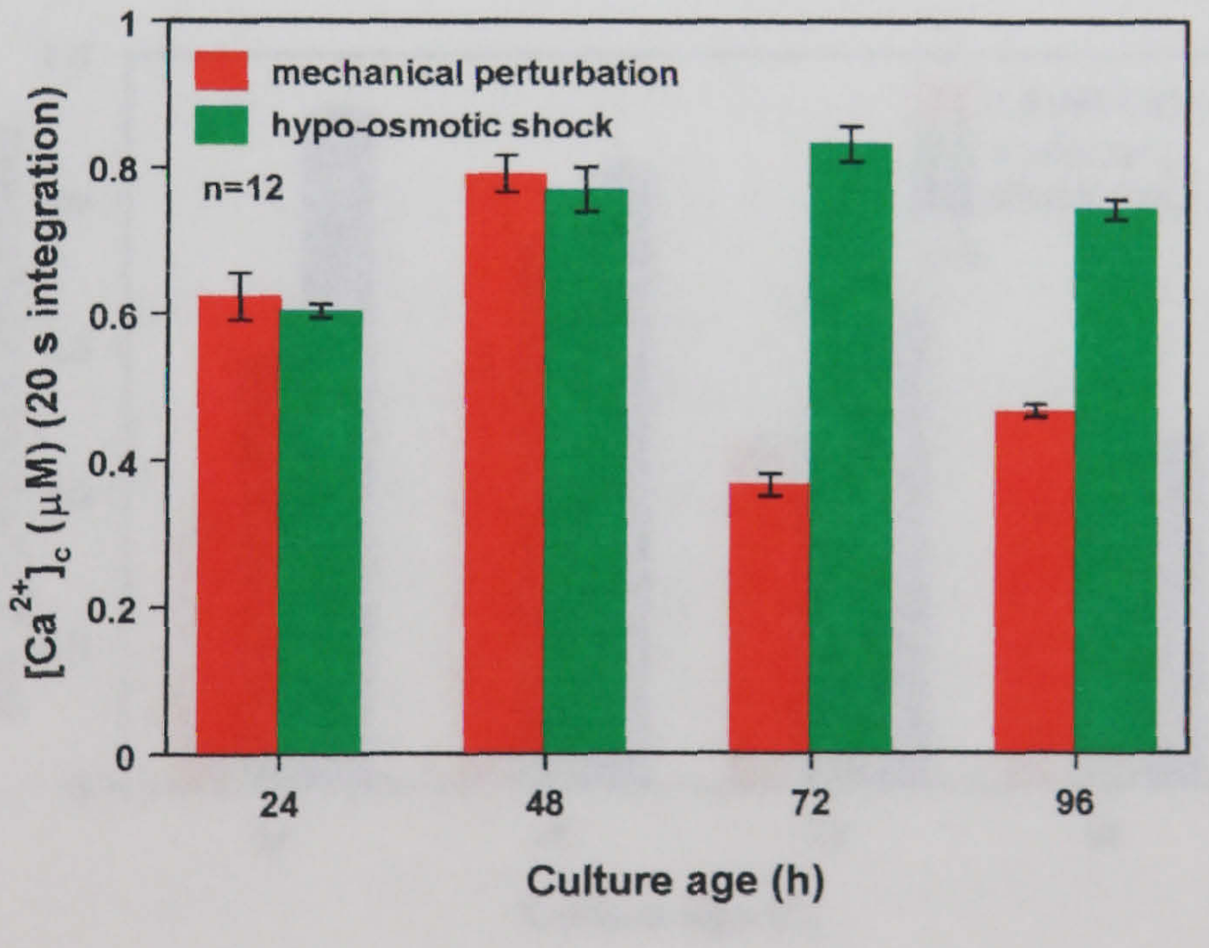

Figure 4.7 Effects of mechanical perturbation and hypo-osmotic shock on $[Ca^{2+}]_c$ in cultures of different age. Results represent the mean ± SE.

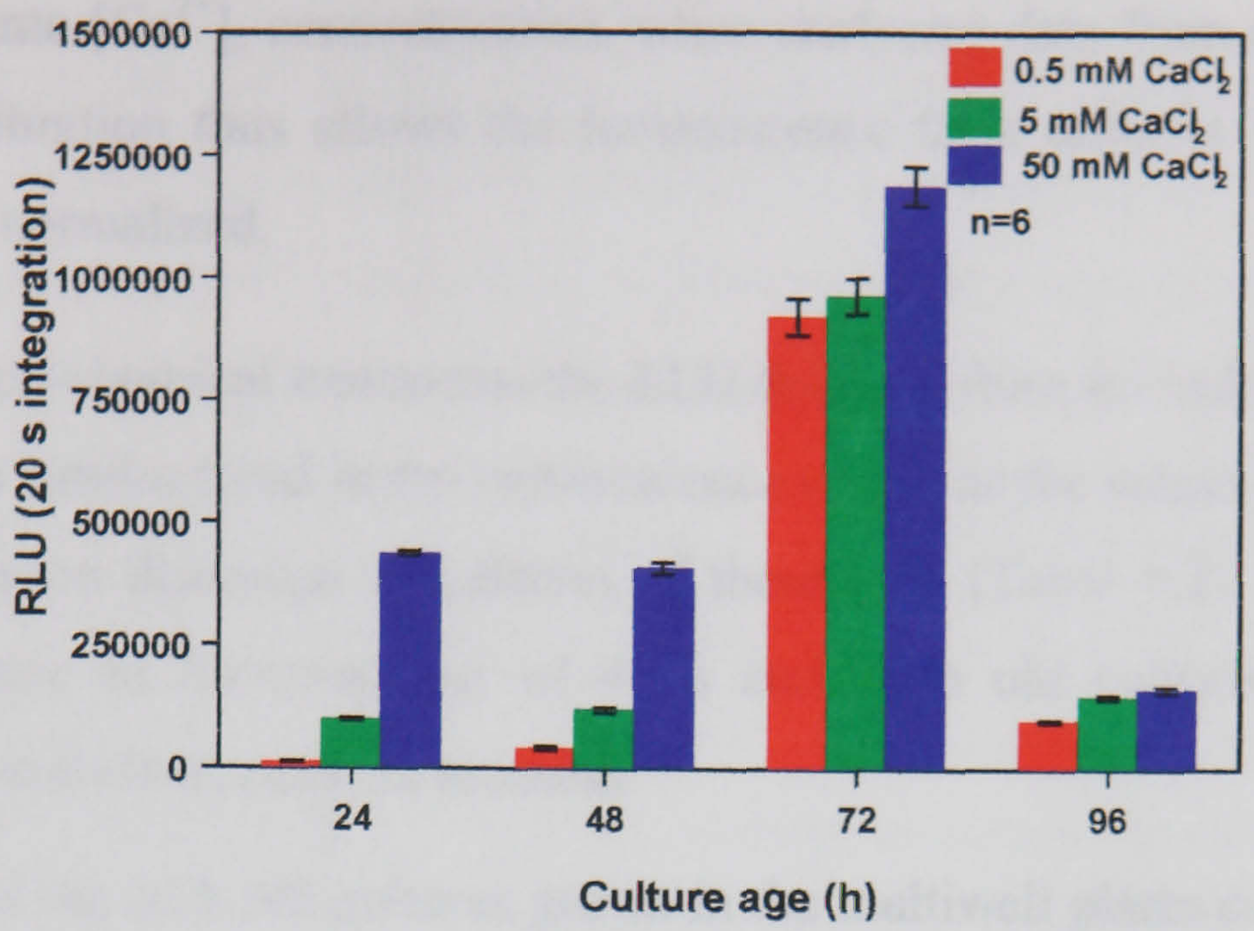

Figure 4.8 Effects of different concentrations of external $CaCl_2$ (0.5, 5 and 50 mM) on aequorin luminescence in cultures of different age. Results represent mean ± SE.

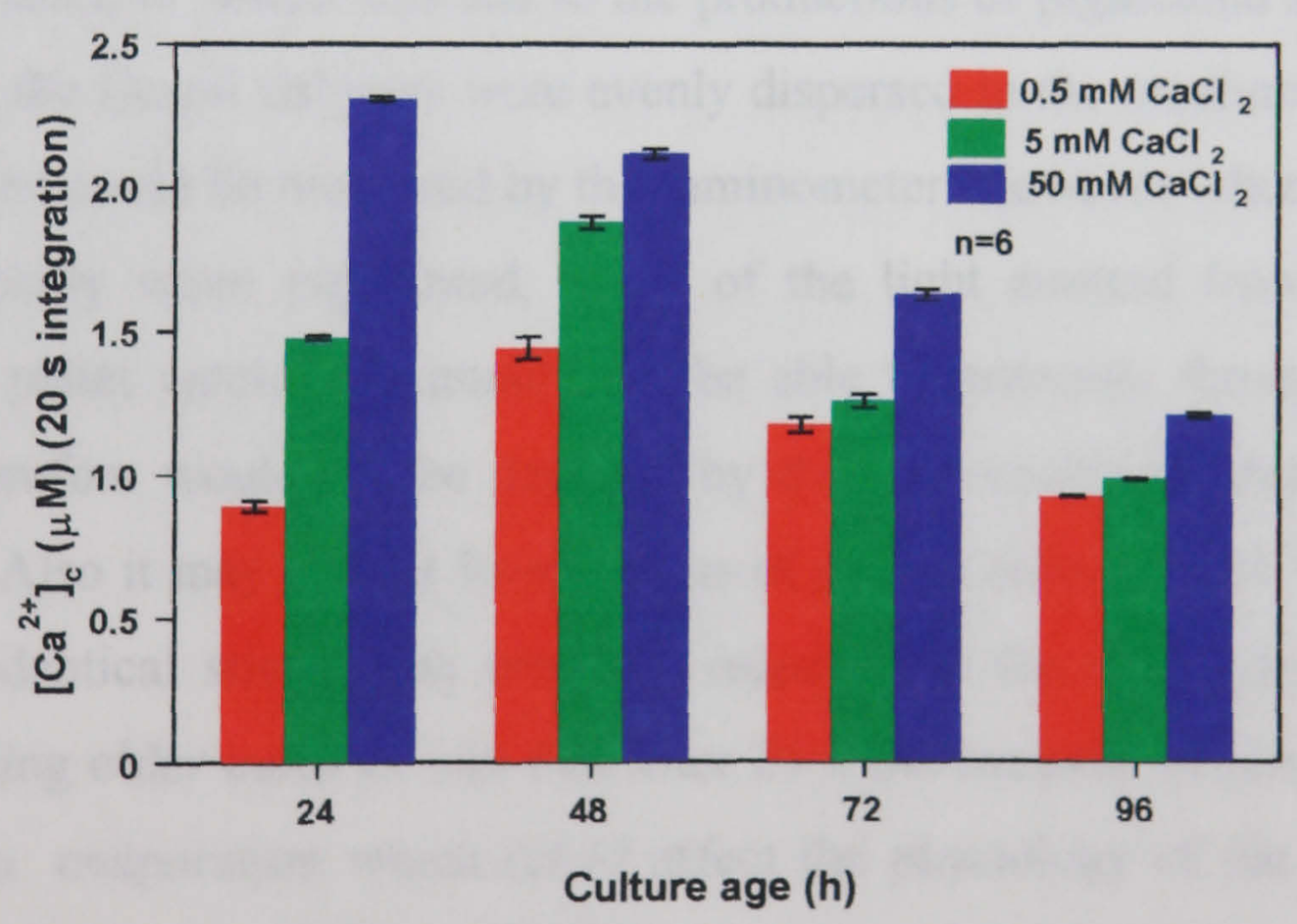

Figure 4.9 Effects of different concentrations of external $CaCl_2$ (0.5, 5 and 50 mM) on $[Ca^{2+}]_c$ in cultures of different age. Results represent mean ± SE.

The above data emphasise the importance of calibrating aequorin luminescence, and converting it into $[Ca^{2+}]_c$ concentrations, when analysing data from different culture ages. The calibration thus allows the luminescence from cultures with a different biomass to be normalized.

With all physico-chemical treatments the RLU detected from the cultures of different age followed a similar trend in the luminescence values as the values obtained from a complete aequorin discharge of cultures of these ages (Table 4.2). This confirmed that the increase in luminescence of 48 h and 72 h old cultures was probably primarily due to their increase in biomass.

The mycelia of the 24 h old cultures grown in the multiwell plates could not be seen with the naked eye, the media containing cultures appeared completely transparent. However, with 48 h old cultures a thick mycelial pellet could be observed on the surface of the media and, with 72 h old cultures this pellet was so thick that it could be easily scooped out of the well using a sterile loop. After 72 h the pellet started changing from white to light brown, and by 96 h the whole colony was dark brown/black (much of which was due to the productions of pigmented spores). In 24 h old cultures the fungal colonies were evenly dispersed in the medium and most of the light emitted could be measured by the luminometer. However when a pellet was formed, especially when pigmented, much of the light emitted from the bottom layers of this pellet would presumably not be able to penetrate through the upper layers and therefore would not be detected by the photomultiplier detectors of the luminometer. Also it may be that lower layers of a thick colony pellet would not be subjected to identical stimulation from the injectors as the upper layers. Another issue when using older cultures was that after 24 h the medium became reduced in amount due to evaporation which could affect the physiology of the cultures and hence potentially result in different $[Ca^{2+}]_c$ responses. Therefore it was decided that all subsequent experiments would be routinely carried out with 24 h old cultures.

4.2.1.4 Imaging aequorin luminescence

As mentioned in the last section, the luminescence after treatment of 72 h old cultures with 50 mM $CaCl_2$ could be observed with the naked eye. It was therefore decided to image the $[Ca^{2+}]_c$ response to different physico-chemical stimuli using a low light camera.

The influence of the following four treatments, imaged in whole colonies grown on solid medium in 5 cm Petri dishes (see Section 2.5) was analysed: mechanical perturbation (touch), hypo-osmotic shock, and high external $CaCl_2$ (0.05 [data not shown] and 5 mM) (Figs 4.10-4.12). All of these treatments resulted in increased aequorin luminescence which could be readily imaged. Quantitative data obtained by imaging were extracted from the images to determine the amplitude and length of each $[Ca^{2+}]_c$ response (Table 4.3). In accordance with the results obtained from luminometry (see Section 4.2.1.1), the highest level of luminescence was detected after treatment with 5 mM $CaCl_2$, less light was detected after treatment with 0.05 mM $CaCl_2$, which in turn resulted in greater light being emitted than after mechanical perturbation or hypo-osmotic shock in which the light emission was approximately the same (Table 4.3). With mechanical perturbation (by carefully applying a sterile glass rod to the culture surface), the length of the $[Ca^{2+}]_c$ transient was 22 s which was longer than the transient length for both hypo-osmotic shock and 0.05 $CaCl_2$ (12 sec) which in turn was longer than for 5 M $CaCl_2$ (6 sec) (Figs. 4.10-4.12; Table 4.3). Again these results followed a similar trend to the results for similar treatments measured by luminometry (cf. Tables 4.1 and 4.3).

Treatment	Amplitude (photons)	Length of $[Ca^{2+}]_c$ response (s)
Mechanical perturbation	283,200	22
Hypo-osmotic	285,300	12
0.05 mM $CaCl_2$	323,000	12
5 mM $CaCl_2$	516,800	6

Table 4.3 Image analysis. Amplitude (in photons) per relative unit area over 2 s period of integration.

4.2.2 Pharmacological treatments

4.2.2.1 Antagonists

To analyse the source of the $[Ca^{2+}]_c$ increase resulting from each physico-chemical treatment different Ca^{2+} antagonists were tested: $LaCl_3$, KP4, ryanodine, nifedipine, TMB-8, verapamil and BAPTA (Table 4.4). All of these antagonists have been used effectively on mammalian and plant cells (Johannes et al. 1991; Li et al. 1997) except KP4. In fungi ryanodine has not been so far used successfully (Silverman-Gavrila and Lew 2001), verapamil has often given contradictory results, being effective in some cases and not effective in another (Hernandez et al. 1994) and nifedipine and TMB-8 were found to inhibit processes thought to be Ca^{2+}-mediated (see Table 1.8).

The concentrations of antagonists used in my experiments were initially based on concentrations reported to be effective in animal cells. If no inhibition was observed higher concentrations were used. All the antagonists were tested in a similar manner (see section 2.4.5.1). Cells were preincubated with the antagonists for 5 min. After this preincubation the $[Ca^{2+}]_c$ resting level was monitored for 40 s after which a stimulatory treatment (mechanical perturbation, hypo-osmotic shock or high external $CaCl_2$) was applied.

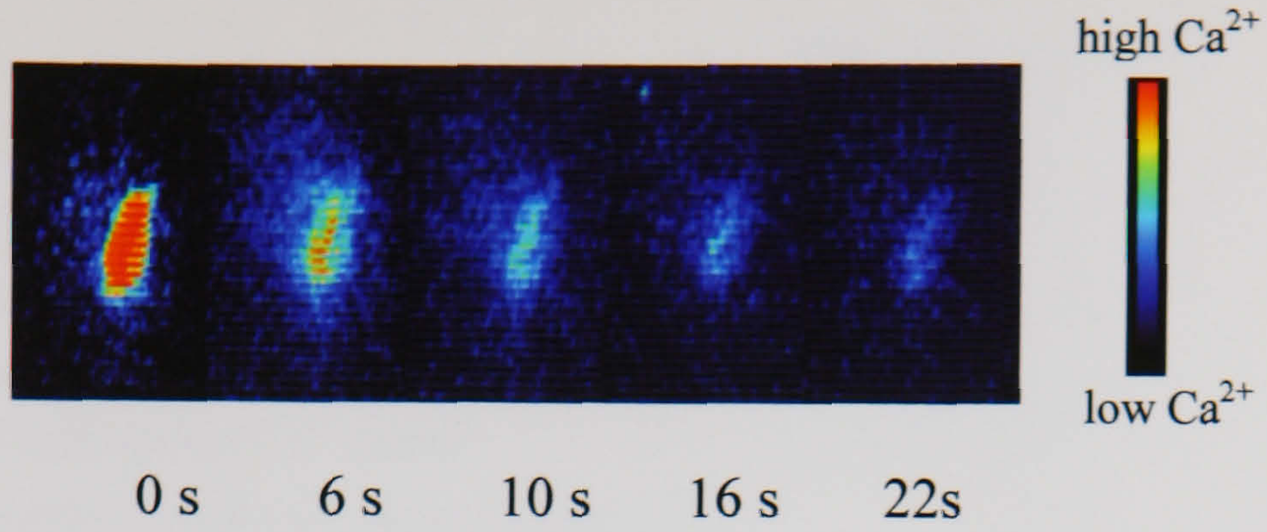

Figure 4.10 Luminescence imaging of a fungal colony subjected to mechanical perturbation by applying sterile glass rod to culture surface.

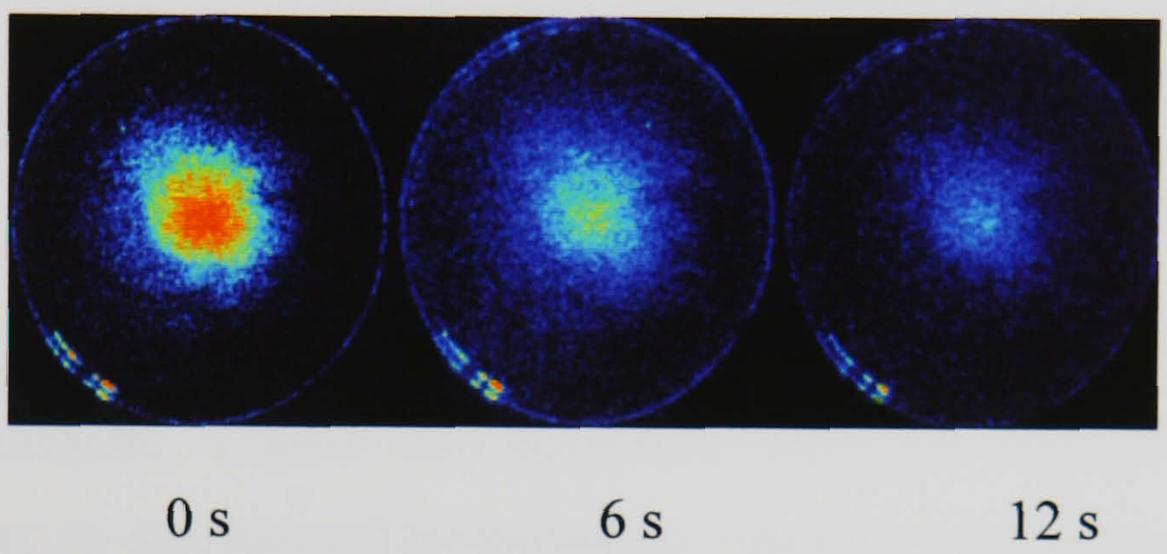

Figure 4.11 Luminescence imaging of a fungal colony subjected to hypo-osmotic shock by treatment with water.

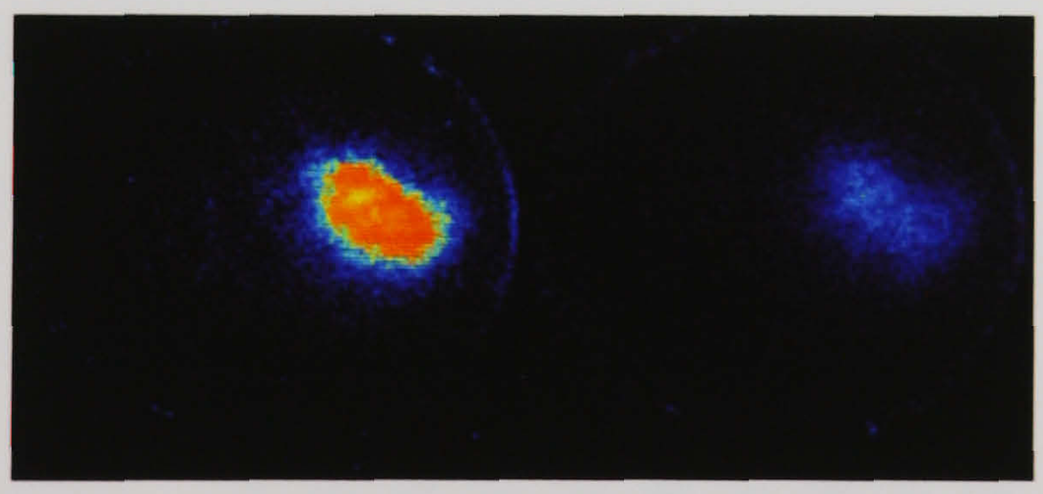

Figure 4.12 Luminescence imaging of a fungal colony subjected to 5 mM $CaCl_2$.

Inhibitor	Mode of action	Concentration range tested	Inhibitory effect
La^{3+}	inhibits Ca^{2+} - channel activity	0.1-20 mM	yes
KP4	inhibits fungal Ca^{2+}-channel activity	0.5-5.4 µM	yes
Ryanodine	inhibits Ca^{2+} release from internal IP_3-dependent Ca^{2+} stores	0.001-300 µM	no
Nifedipine	inhibits L-type Ca^{2+}-channel activity	1-200 µM	no
TMB-8	inhibits Ca^{2+} release from internal Ca^{2+} stores	10-200 µM	no
Verapamil	inhibits L-type Ca^{2+}-channel activity	1-200 µM	no
BAPTA	chelates Ca^{2+}	0.5-10 mM	yes

Table 4.4 Summary of inhibitory effects of different Ca^{2+} antagonists on $[Ca^{2+}]_c$ in *A. awamori* subjected to mechanical perturbation, hypo-osmotic shock and high external $CaCl_2$.

Ryanodine, nifedipine, TMB-8 and verapamil were not effective in inhibiting the $[Ca^{2+}]_c$ responses to mechanical perturbation, hypo-osmotic shock or external $CaCl_2$ under the conditions applied. No clear dose dependent inhibition was observed with any of these agents (e.g. as shown for nifedipine in Fig. 4.13).

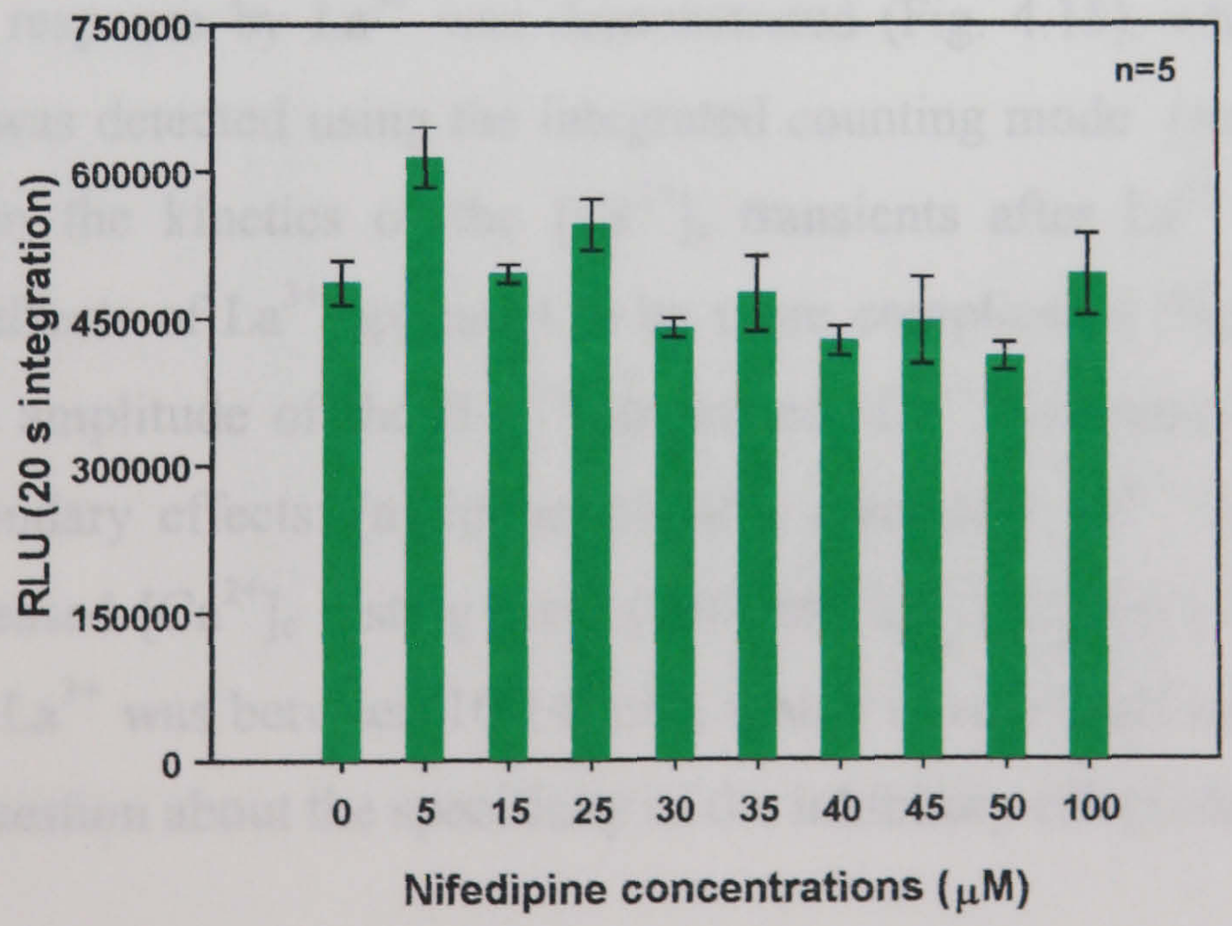

Figure 4.13 Effect of nifedipine on the $[Ca^{2+}]_c$ response to external $CaCl_2$. Results represent mean ± SE.

La^{3+} was found to inhibit the $[Ca^{2+}]_c$ response to hypo-osmotic shock and high external $CaCl_2$, but not to mechanical perturbation (Table 4.5).

Inhibitor	**Treatment**		
	Mechanical perturbation	**Hypo-osmotic shock**	**External Ca^{2+}**
La^{3+}	-	10-14 mM	10-14 mM
KP4	-	0.4-1.2 μM	0.4-1.2 μM
BAPTA	0.5-5 mM	0.5-5 mM	n.a.

Table 4.5 Effects of different pharmacological inhibitors on Ca^{2+}-mediated responses. The concentrations refer to the IC_{50} for each pharmacological agent (i.e. approximate concentrations of pharmacological agents which result in 50% inhibition of the $[Ca^{2+}]_c$ increase). - = no inhibition. n.a. = not appropriate. n = 6 for each treatment.

La^{3+} inhibition of the $[Ca^{2+}]_c$ response to external $CaCl_2$ was dependent on the concentration of external $CaCl_2$. At low concentrations of external $CaCl_2$ (0.1 and 0.5 mM), 5 mM La^{3+} caused an increase in the $[Ca^{2+}]_c$ response (Fig. 4.14). When hyphae were stimulated with 5 mM external $CaCl_2$ a clear dose-dependent inhibition of the $[Ca^{2+}]_c$ response by La^{3+} was demonstrated (Fig. 4.15), when the aequorin luminescence was detected using the integrated counting mode (see section 2.4.1). However, when the kinetics of the $[Ca^{2+}]_c$ transients after La^{3+} treatment were analysed, the effects of La^{3+} appeared to be more complicated (Fig. 4.16). Besides decreasing the amplitude of the $[Ca^{2+}]_c$ transients, La^{3+} also appeared to have the following secondary effects: (a) induction of a secondary Ca^{2+} transient (20 mM La^{3+}); (b) increased $[Ca^{2+}]_c$ resting level (>10 mM La^{3+}). Table 4.5 shows that the IC_{50} value for La^{3+} was between 10-14 mM, which is very high concentration, and this rises the question about the specificity of the inhibitory effect observed.

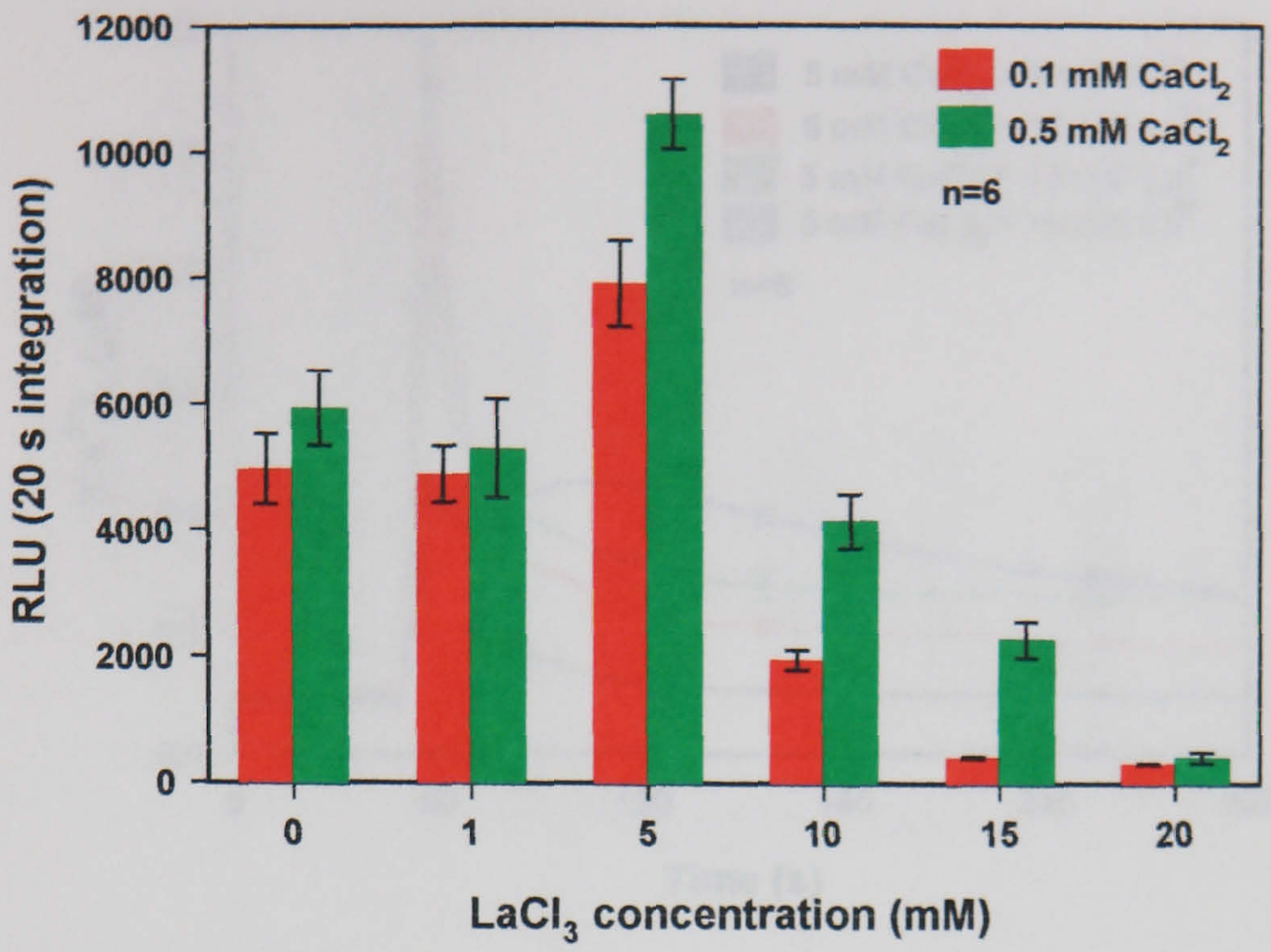

Figure 4.14 Effect of La^{3+} on the $[Ca^{2+}]_c$ response to low concentrations of external $CaCl_2$ (0.1 and 0.5 mM). Results represent mean ± SE.

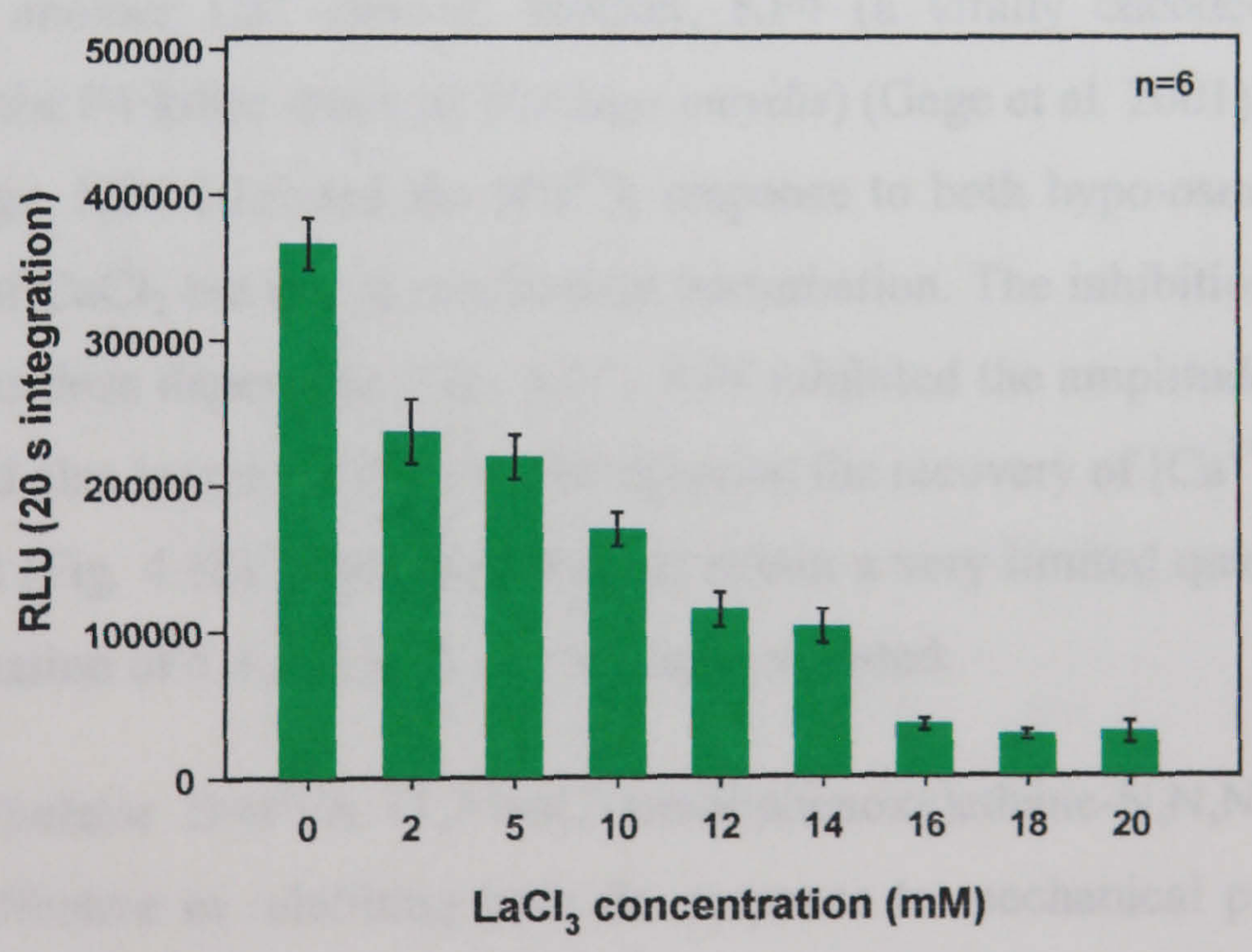

Figure 4.15 Dose-dependent effects of La^{3+} on the $[Ca^{2+}]_c$ response to 5 mM external $CaCl_2$. Results represent mean ± SE.

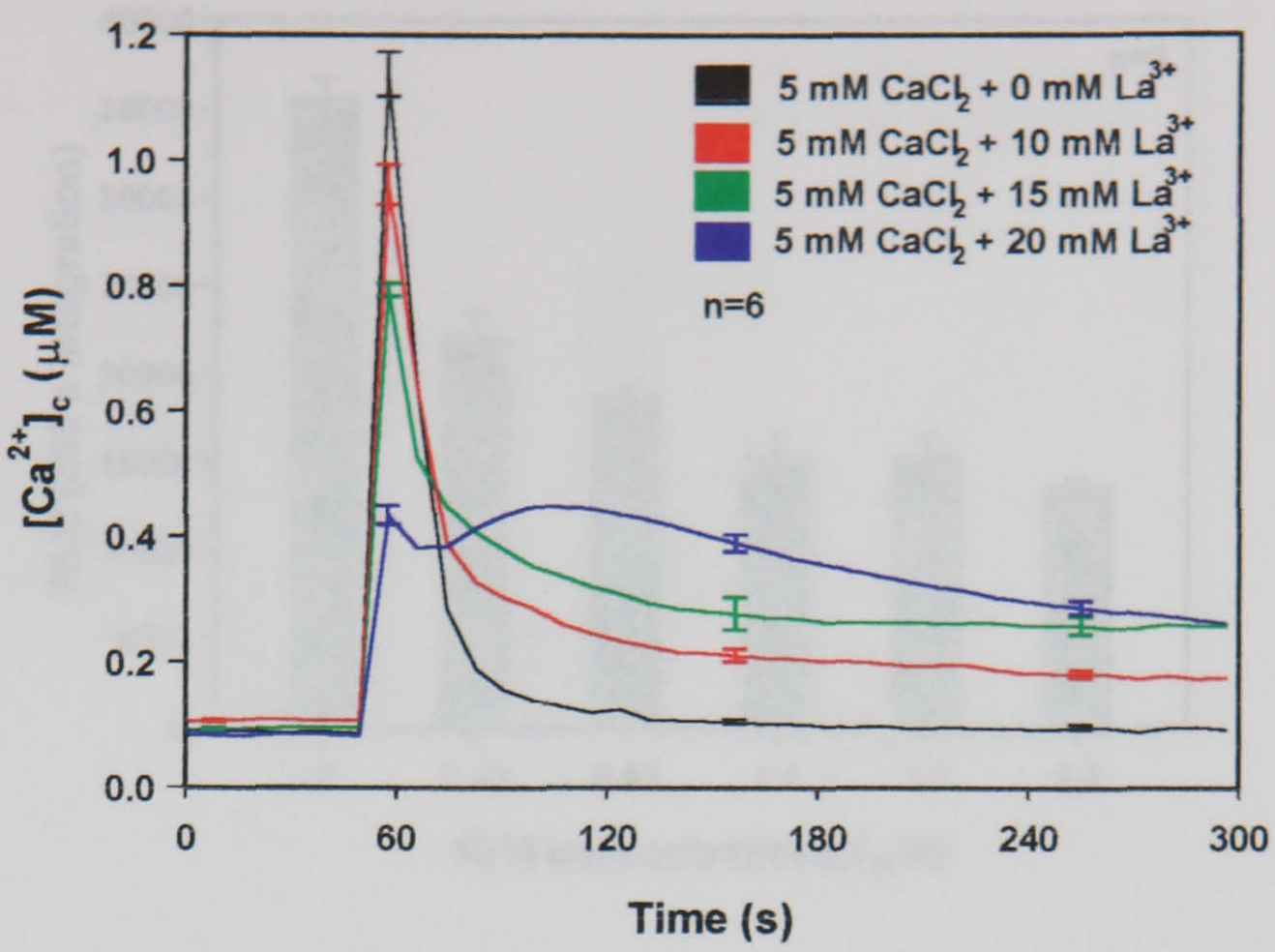

Figure 4.16 Effect of La^{3+} on the $[Ca^{2+}]_c$ response to 5 mM external $CaCl_2$. Results represent mean ± SE. Measurements were performed using the repeated measuring protocol. Cycle time 11.6 s.

In contrast another Ca^{2+}-channel blocker, KP4 (a virally encoded fungal toxin secreted by the P4 killer strain of *Ustilago maydis*) (Gage et al. 2001), had an IC_{50} in the μM range. KP4 inhibited the $[Ca^{2+}]_c$ response to both hypo-osmotic shock and high external $CaCl_2$ but not to mechanical perturbation. The inhibition of the $[Ca^{2+}]_c$ response was dose dependent (Fig. 4.17). KP4 inhibited the amplitude of the $[Ca^{2+}]_c$ transient and also increased the FWHM delaying the recovery of $[Ca^{2+}]_c$ to its normal resting level (Fig. 4.18). I was only able to obtain a very limited quantity of KP4 so the concentration of 5.4 μM KP4 was the highest tested.

The Ca^{2+} chelator BAPTA (1,2-bis(2-aminophenoxy)ethane-N,N,N',N'-tetraacetic acid) was effective in inhibiting both the response to mechanical perturbation and hypo-osmotic shock (Fig. 4.19). Almost complete inhibition was observed with 5 mM BAPTA. It was not appropriate to apply the high external $CaCl_2$ treatment because BAPTA would chelate the Ca^{2+} added.

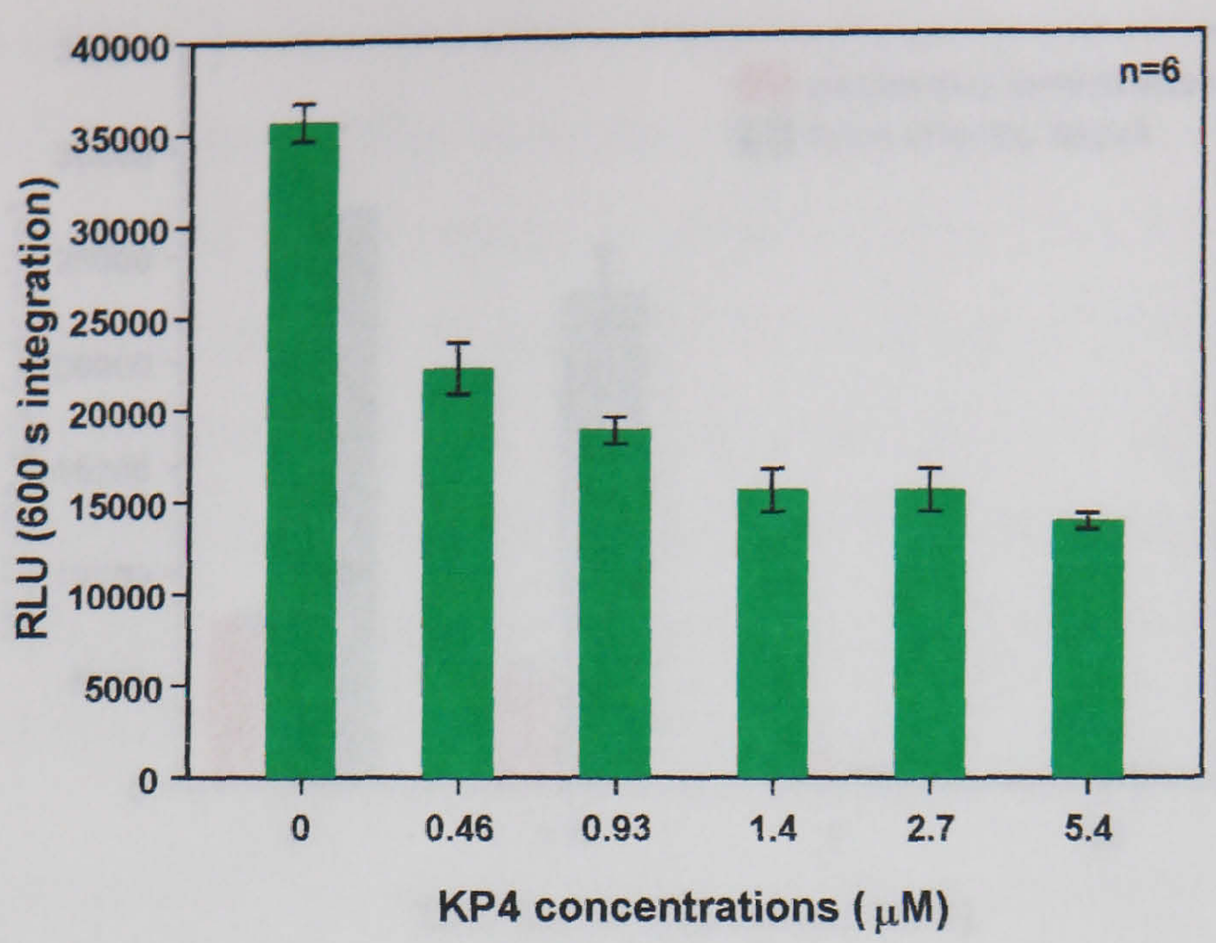

Figure 4.17 Dose-dependent effect of KP4 on the $[Ca^{2+}]_c$ response to 5 mM external $CaCl_2$. Results represent mean ± SE.

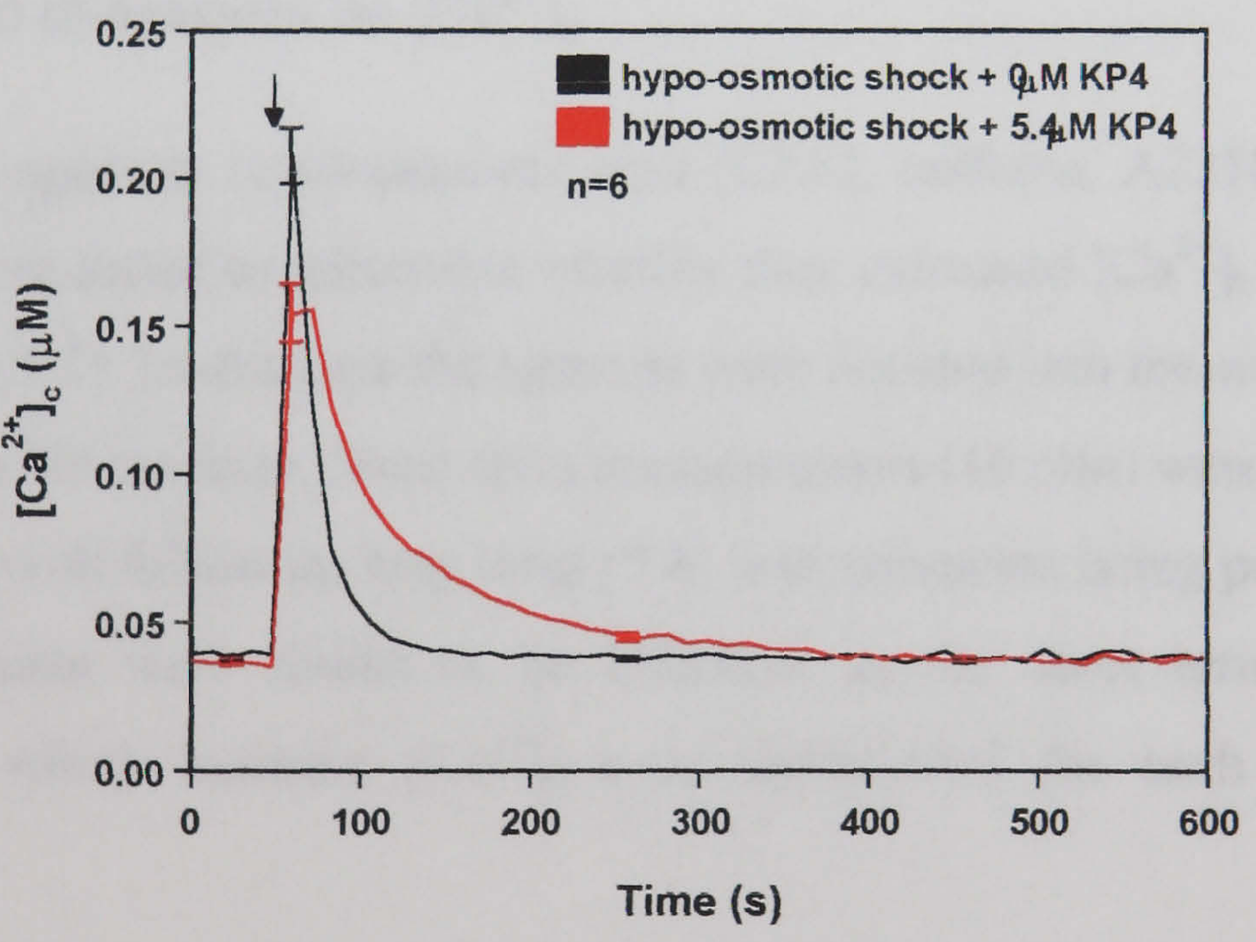

Figure 4.18 Effect of KP4 on the $[Ca^{2+}]_c$ response to hypo-osmotic shock. The arrow indicated the point when the treatment was applied. Results represent mean ± SE. Measurements were performed using the repeated measuring protocol. Cycle time 11.6 s.

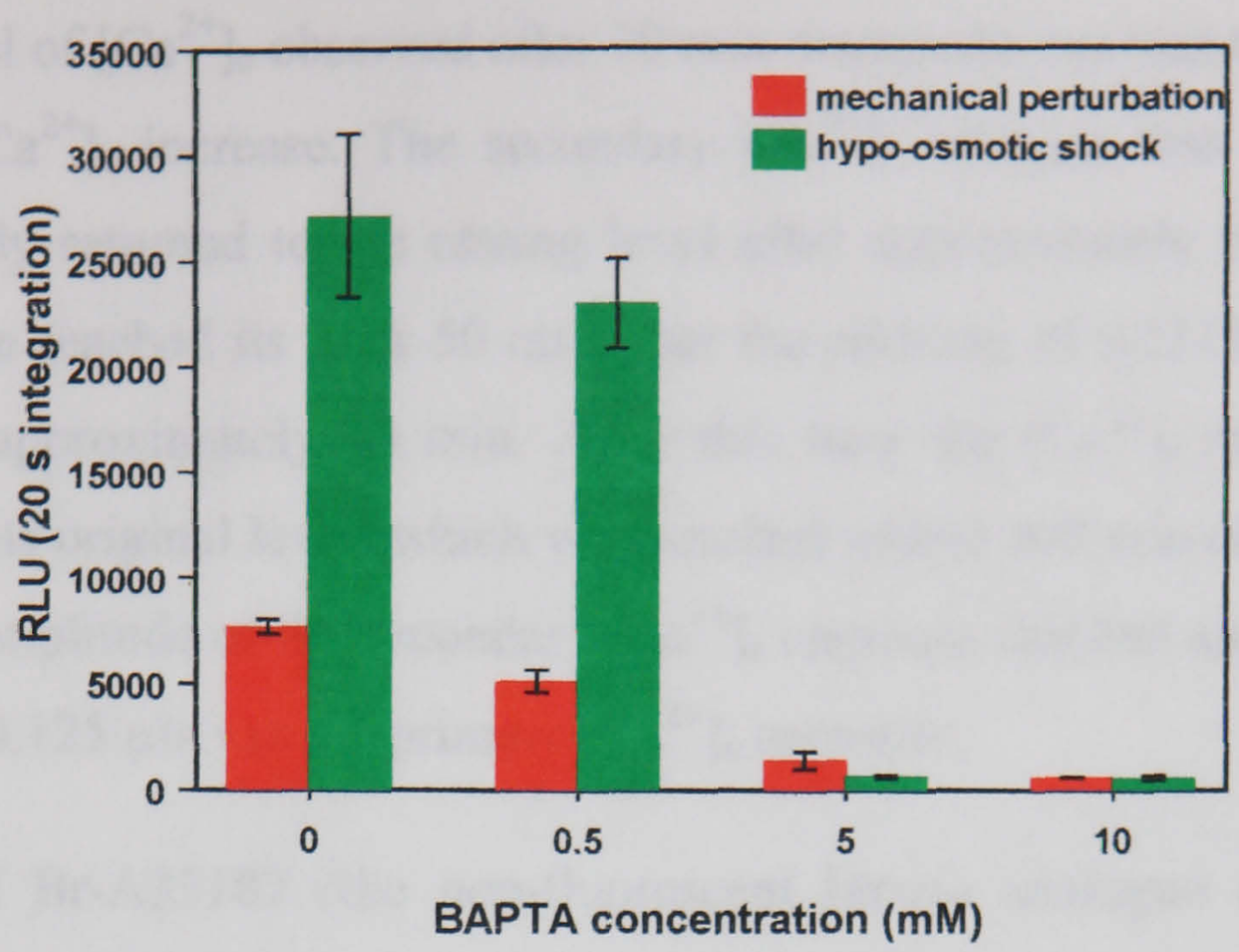

Figure 4.19 Dose-dependent effect of BAPTA on the $[Ca^{2+}]_c$ response to mechanical perturbation and hypo-osmotic shock. Results represent mean ± SE.

4.2.2.2 Agonists

4.2.2.2.1 Effect of agonists on $[Ca^{2+}]_c$

Various known agonists (cyclopiazonic acid [CPA], caffeine, A23187, Br-A23187 and BAY(-)) were tested to determine whether they increased $[Ca^{2+}]_c$ in *A. awamori* (see Section 2.4.5.1). In this case the agonists were injected into the wells at a known concentration in VS medium. Short term measurements (10 min) were performed for all the agonists with follow up long term (5 h) measurements being performed when individual agonists were found to be effective in the short term. The lowest concentrations which increase $[Ca^{2+}]_c$ were determined for each of the active agonists.

The lowest effective concentration of A23187 was 10 μM (Fig. 4.20, Table 4.6). At this concentration the initial amplitude of $[Ca^{2+}]_c$ increase was not significantly affected ($P < 0.05$) but a higher final $[Ca^{2+}]_c$ resting level was observed. The initial $[Ca^{2+}]_c$ increase was due to mechanical perturbation and the subsequent increase in $[Ca^{2+}]_c$ resting level was probably caused by the ionophore. When long term

measurements were performed (Fig. 4.21) it was shown that this gradual increase in the resting level of $[Ca^{2+}]_c$ observed after 10 min measurements was the beginning of a secondary $[Ca^{2+}]_c$ increase. The secondary $[Ca^{2+}]_c$ increase was very prolonged $[Ca^{2+}]_c$ and only returned to the resting level after approximately 5 h. The second $[Ca^{2+}]_c$ increase reached its peak 50 min after the addition of A23187 and stayed at that level for approximately 90 min. After this time the $[Ca^{2+}]_c$ started to slowly return back to its original level, which was reached within 300 min of the addition of A23187. The amplitude of the secondary $[Ca^{2+}]_c$ response reached approximately the same level (c. 0.125 μM) as the primary $[Ca^{2+}]_c$ response.

The effects of Br-A23187 (the non-fluorescent bromo analogue of A23187) on $[Ca^{2+}]_c$ were very similar to the effects caused by A23187. However, Br-A23187 is twice as expensive as its non-bromo analogue, and therefore A23187 was used in all subsequent experiments.

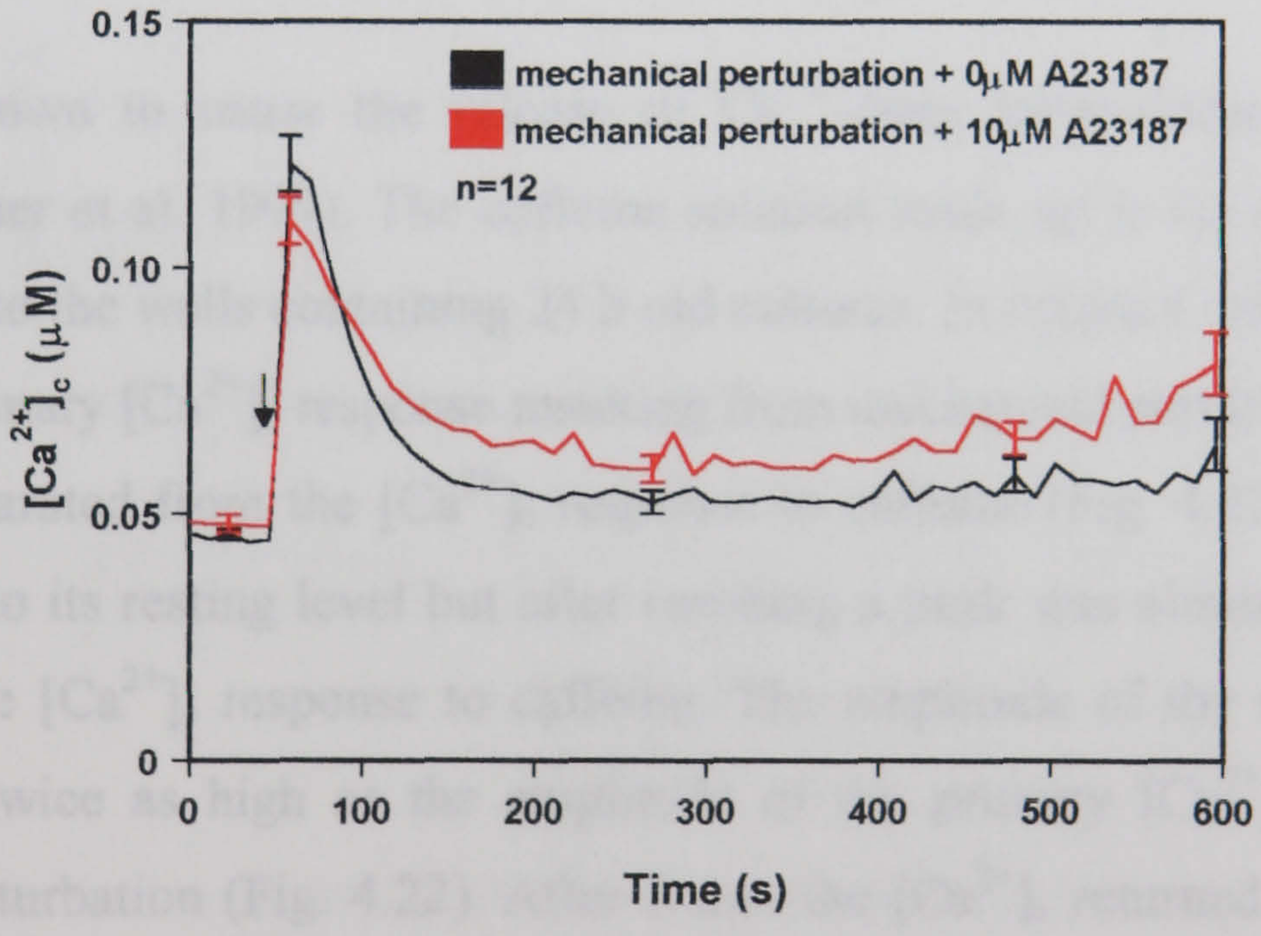

Figure 4.20 Effect of 10 μM A23187 on $[Ca^{2+}]_c$ over a short time period (10 min). The arrow indicates the point when the treatment was applied. Results represent mean ± SE. Measurements were performed using the repeated measuring protocol. Cycle time 11.6 s.

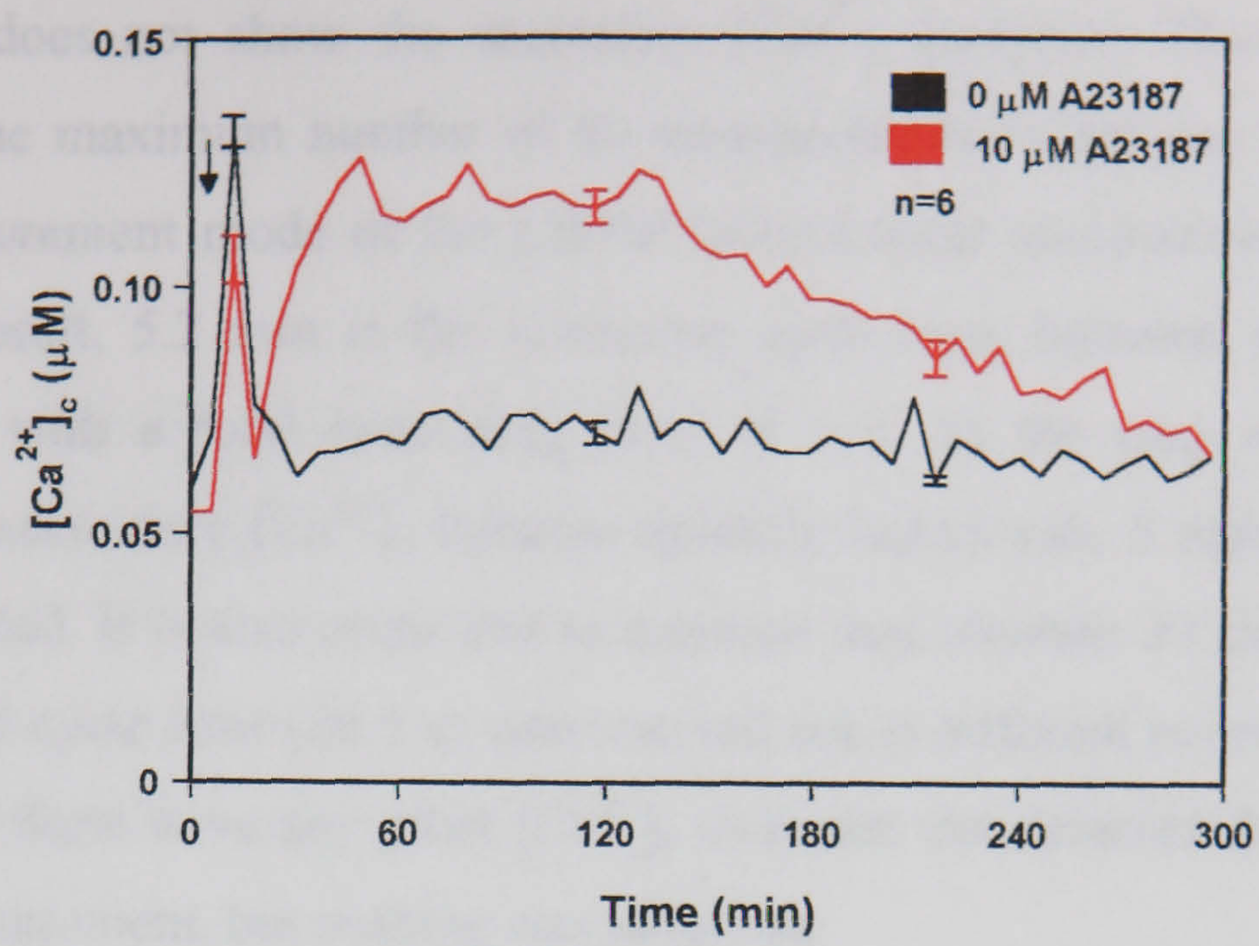

Figure 4.21 Effect of 10 μM A23187 on $[Ca^{2+}]_c$ over a long time period (300 min). The arrow indicates the point when the treatment was applied. Results represent mean ± SE. Measurements were performed using the repeated measuring protocol. Cycle time 5.2 min.

Caffeine is known to cause the release of Ca^{2+} from intracellular Ca^{2+} storage organelles (Bauer et al. 1999). The caffeine solution made up in iso-osmotic media was injected into the wells containing 24 h old cultures. In contrast with the effect of A23187 the primary $[Ca^{2+}]_c$ response resulting from mechanical perturbation was not completely separated from the $[Ca^{2+}]_c$ response to caffeine (Fig. 4.22). The $[Ca^{2+}]_c$ did not return to its resting level but after reaching a peak was almost immediately followed by the $[Ca^{2+}]_c$ response to caffeine. The amplitude of the second $[Ca^{2+}]_c$ transient was twice as high as the amplitude of the primary $[Ca^{2+}]_c$ response to mechanical perturbation (Fig. 4.22). After 5 min the $[Ca^{2+}]_c$ returned to its original resting level. However, long term measurements indicated that the second $[Ca^{2+}]_c$ transient was followed by a third $[Ca^{2+}]_c$ increase approximately 30 min after the addition of caffeine (Fig. 4.23). The third $[Ca^{2+}]_c$ response was not as prolonged as with A23187. The peak of the response was reached 1 h after the addition of caffeine and the $[Ca^{2+}]_c$ returned to its resting level after approximately 1.5 h. Figures 4.22 and 4.23 are complementary to each other. Figure 4.22 shows the primary and

secondary $[Ca^{2+}]_c$ increases. Figure 4.23 shows the first and the third $[Ca^{2+}]_c$ increases but does not show the secondary $[Ca^{2+}]_c$ transient. This is due to the limitation of the maximum number of 60 measurements which can be made using *repeated* measurement mode of the LB96P MicroLumat luminometer (see Section 2.4.1). As a result, 5.2 min is the minimum cycle time between two successive measurements with a total measuring time of 5 h. In the case of the caffeine treatment, the secondary $[Ca^{2+}]_c$ increase actually lasted only 5 min and therefore was not recorded. It is also important to mention that separate 30 min experiments with the shorter cycle time (30.5 s) were carried out at different points of 5 h period to test whether there were any other $[Ca^{2+}]_c$ increases not detected during the a 5 h periods of measurement, but nothing was observed.

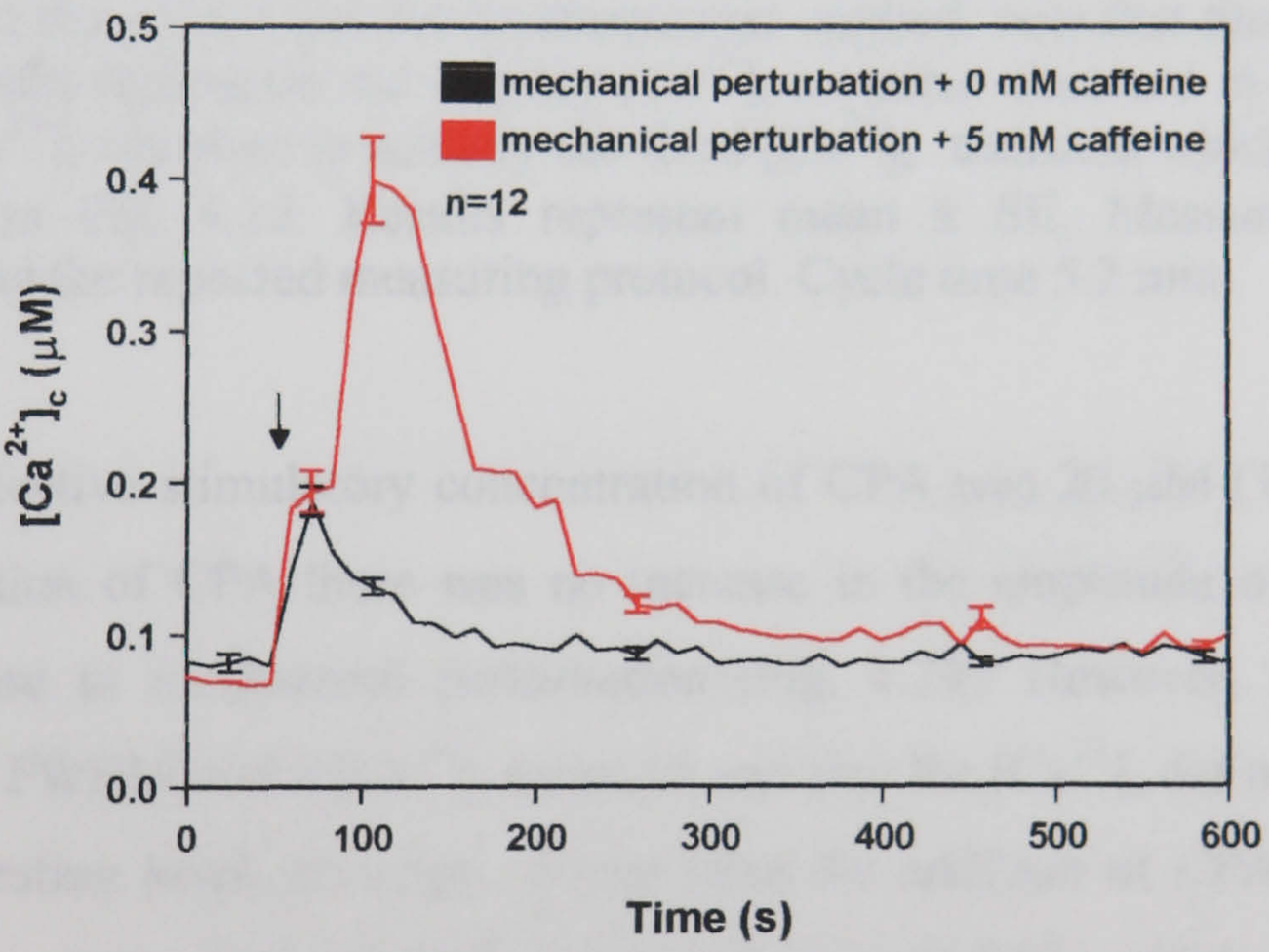

Figure 4.22 Effect of caffeine on $[Ca^{2+}]_c$ over a short time period (10 min). The arrow indicated the point when the treatment was applied. Results represent mean ± SE. Measurements were performed using the repeated measuring protocol. Cycle time 11.6 s.

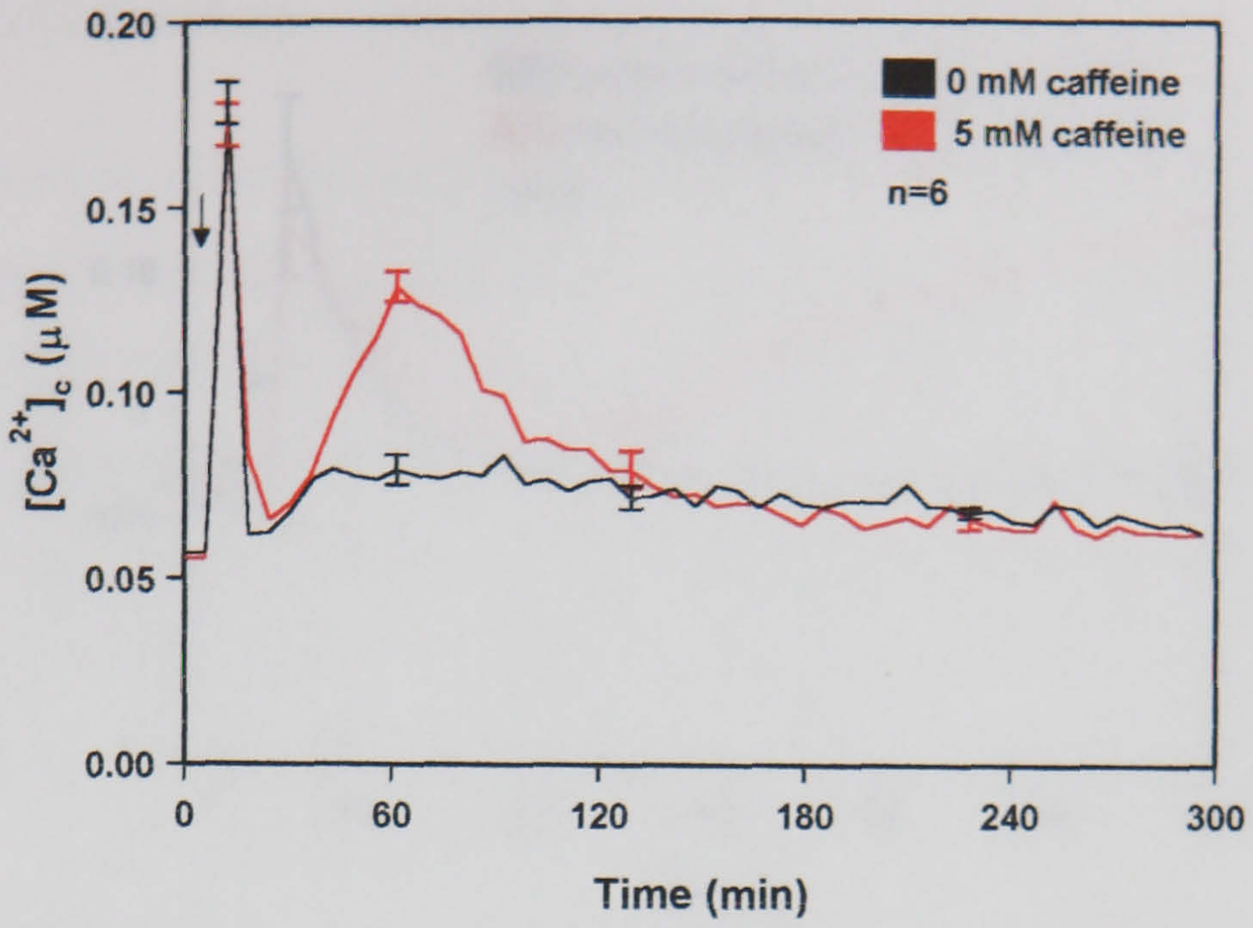

Figures 4.23 Effect of caffeine on $[Ca^{2+}]_c$ over a long time period (300 min). The arrow indicated the point when the treatment was applied. note that the first increase in $[Ca^{2+}]_c$ actually represents the primary $[Ca^{2+}]_c$ transient observed in Fig. 4.22 and the second $[Ca^{2+}]_c$ transient is actually the third $[Ca^{2+}]_c$ transient which occurs after those shown in Fig. 4.22. Results represent mean ± SE. Measurements were performed using the repeated measuring protocol. Cycle time 5.2 min.

The lowest effective stimulatory concentration of CPA was 20 μM (Table 4.6). At this concentration of CPA there was no increase in the amplitude of the primary $[Ca^{2+}]_c$ response to mechanical perturbation (Fig. 4.24). However, there was an increase in the FWHM of the $[Ca^{2+}]_c$ transient and also the $[Ca^{2+}]_c$ did not completely return to its resting level. However, 3 min after the addition of CPA a secondary $[Ca^{2+}]_c$ increase was observed (Fig. 4.24) and this reached a peak concentration within 1 h after the addition of CPA. The secondary $[Ca^{2+}]_c$ increase was very prolonged and the $[Ca^{2+}]_c$ returned close to its resting level only after 5 h (Fig. 4.25).

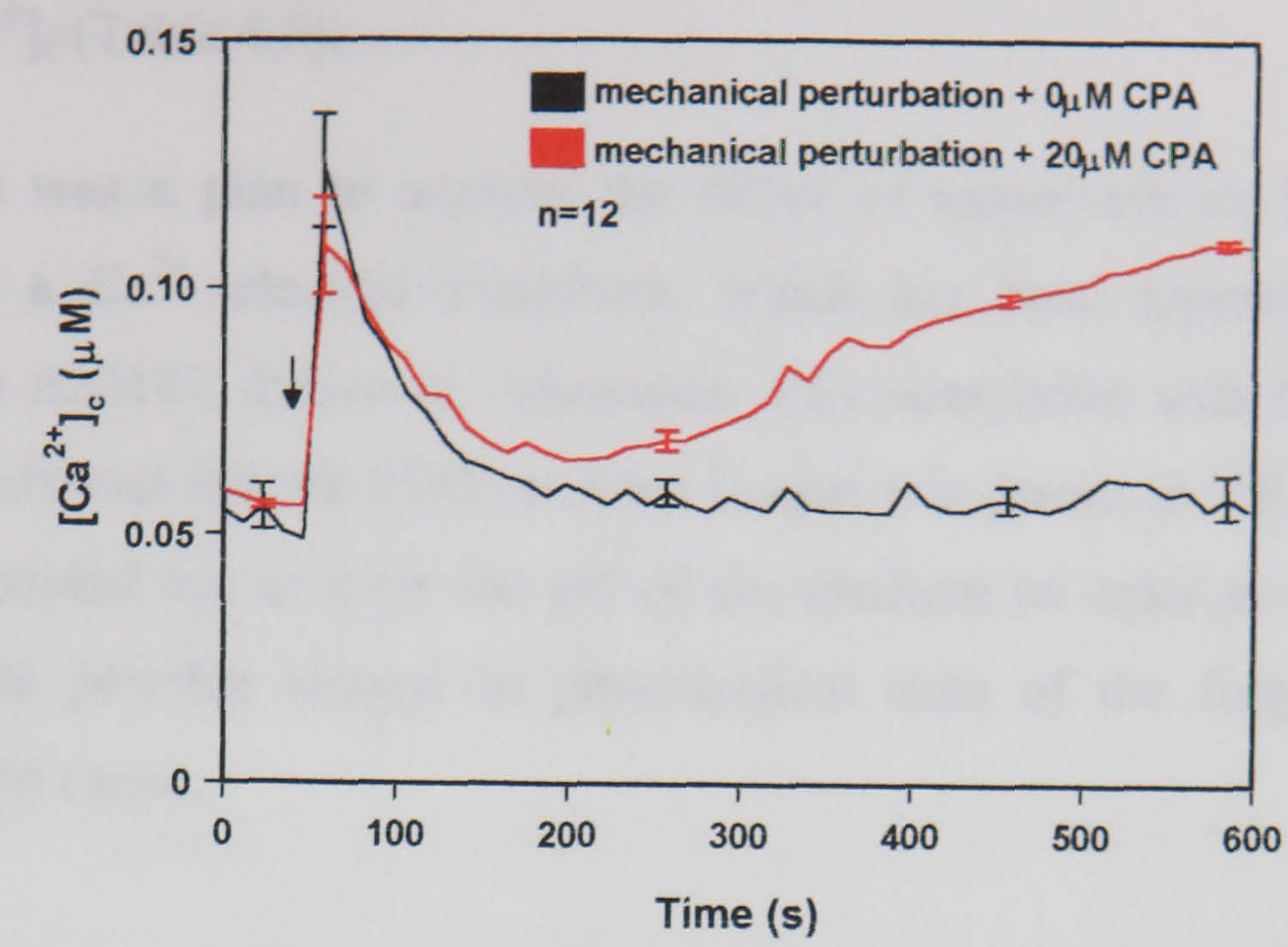

Figure 4.24 Effect of CPA on $[Ca^{2+}]_c$ over a short period of time (10 min). The arrow indicates the point when the treatment was applied. Results represent mean ± SE. Measurements were performed using the repeated measuring protocol. Cycle time 11.6 s.

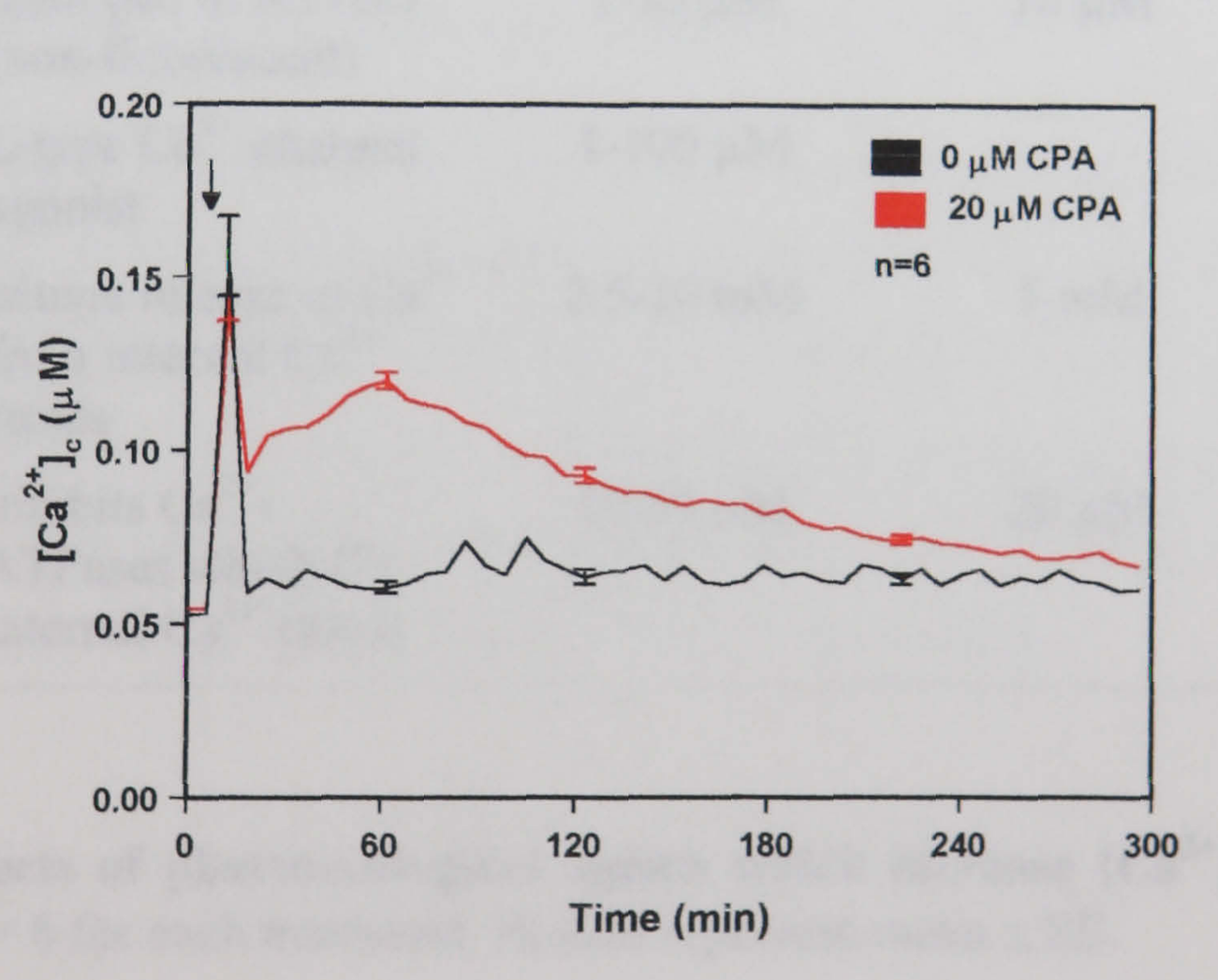

Figure 4.25 Effect of CPA on $[Ca^{2+}]_c$ over long period of time (300 min). The arrow indicates the point when the treatment was applied. Results represent mean ± SE. Measurements were performed using the repeated measuring protocol. Cycle time 5.2 min.

Another Ca^{2+} agonist which was tested was BAY(-), but this was found to have no effect on $[Ca^{2+}]_c$ (Table 4.6).

Initially there was a plan to analyse the effect of ionomycin on hyphal $[Ca^{2+}]_c$. Ionomycin is a Ca^{2+}-selective ionophore, which has been reported to be more effective than A23187. However, ionomycin only complexes with Ca^{2+} at pH 7-9 (Aagaard-Tillery and Jelinek 1995) and the fungus was grown in VS medium at pH 5.8. It was decided not to alter the pH of the medium in order to use ionomycin because of the possible change in physiological state of the fungus which this treatment might cause.

Ca^{2+} agonist	**Mode of action**	**Concentration range tested**	**Lowest effective concentration**	**$[Ca^{2+}]_c$ increase**
A23187	ionophore which is selective for Ca^{2+}	1-50 μM	10 μM	+
Br-A23187	analogue of A23187 (non-fluorescent)	1-50 μM	10 μM	+
BAY (-)	L-type Ca^{2+}-channel agonist	1-100 μM	-	-
Caffeine	causes release of Ca^{2+} from internal Ca^{2+} stores	2.5-20 mM	5 mM	+
CPA	inhibits Ca^{2+}-ATPases which fill internal Ca^{2+} stores	10-50 μM	20 μM	+

Table 4.6 Effects of pharmacological agents which increase $[Ca^{2+}]_c$. n.a. = not appropriate, n = 6 for each treatment. Results represent mean ± SE.

4.2.2.2.2 Effect of Ca^{2+} agonists on the $[Ca^{2+}]_c$ responses to physico-chemical treatments

In order to investigate whether internal Ca^{2+} reserves might play a role in generating the $[Ca^{2+}]_c$ transient resulting from mechanical perturbation, hypo-osmotic shock and high external $CaCl_2$ treatments, the effects of caffeine and CPA on the $[Ca^{2+}]_c$ responses to these three physico-chemical treatments were analysed. For this purpose hyphae were pretreated with either caffeine or CPA for 5 min prior to applying the physico-chemical treatment.

Five min after applying 5 mM caffeine the resting level of $[Ca^{2+}]_c$ prior to the physico-chemical treatment was increased from 64 nM ± 2 (SE) to 72 nM ± 1 (SE) (Figs. 4.26-4.28). Caffeine did not affect the amplitude of the $[Ca^{2+}]_c$ response to hypo-osmotic shock (Fig. 4.27) or high external $CaCl_2$ (Fig. 4.28), but did significantly reduce the amplitude of the $[Ca^{2+}]_c$ response to mechanical perturbation (Fig. 4.26). With all three treatments caffeine caused a delay of 10 min for the $[Ca^{2+}]_c$ to return to its resting level. The delay in the recovery to resting level was more pronounced with the higher concentration of caffeine (10 mM).

CPA also caused an increase in the initial $[Ca^{2+}]_c$ resting level but to a much greater magnitude (Figs. 4.29-4.31). Cells treated with 50 µM CPA had a $[Ca^{2+}]_c$ resting level 2-3 times (119 nM ± 10 [SE]) higher than cells treated with the control solution (63 nM ± 2 [SE]). In spite of this when each of the three physico-chemical treatments were applied, the resulting $[Ca^{2+}]_c$ increase had the similar trend as in the control, although the initial and end concentration of $[Ca^{2+}]_c$ were higher.

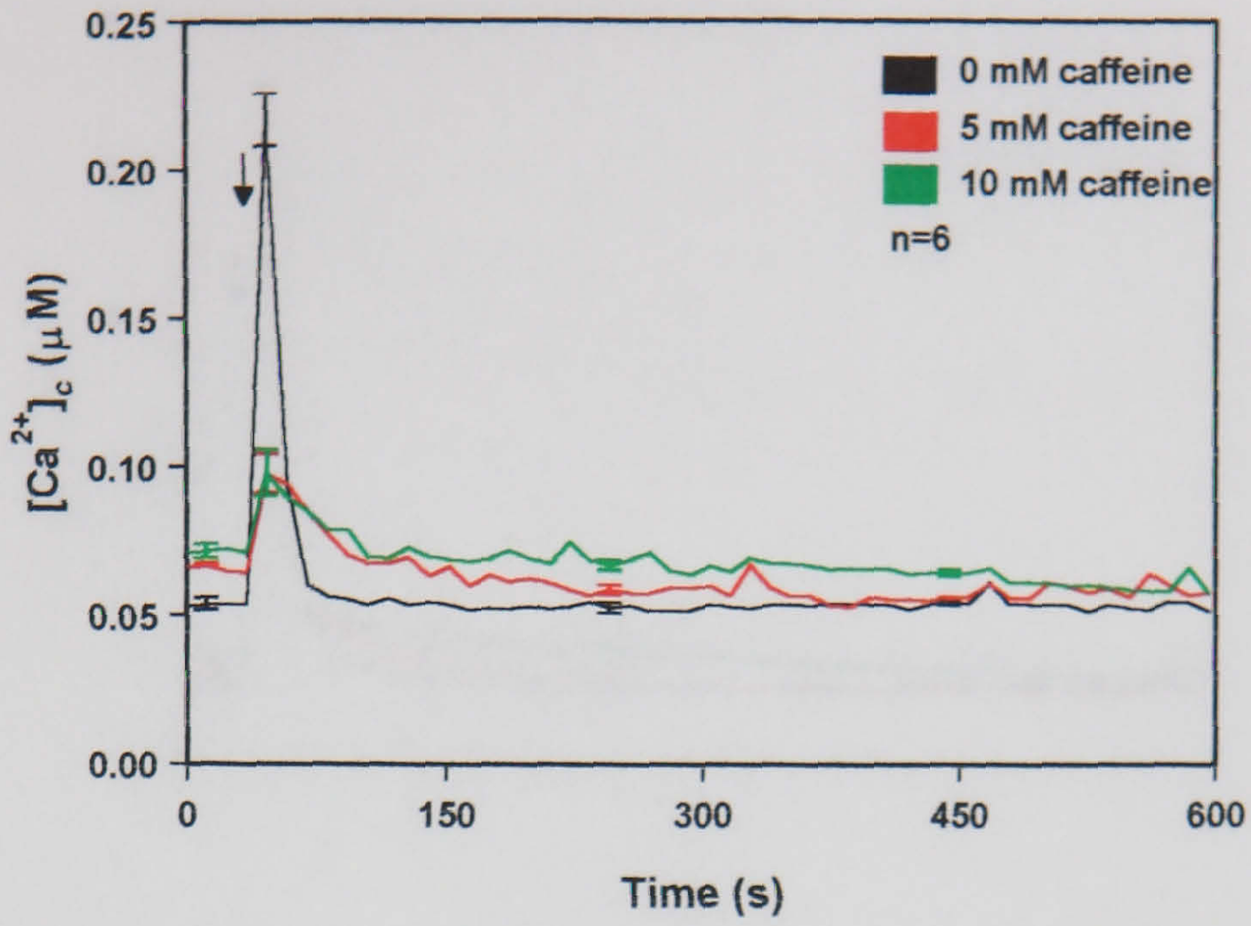

Figure 4.26 Effect of caffeine on the $[Ca^{2+}]_c$ response to mechanical perturbation. Caffeine was added 5 min before mechanical perturbation was applied (shown by the arrow). Results represent mean ± SE. Measurements were performed using the repeated measuring protocol. Cycle time 11.6 s.

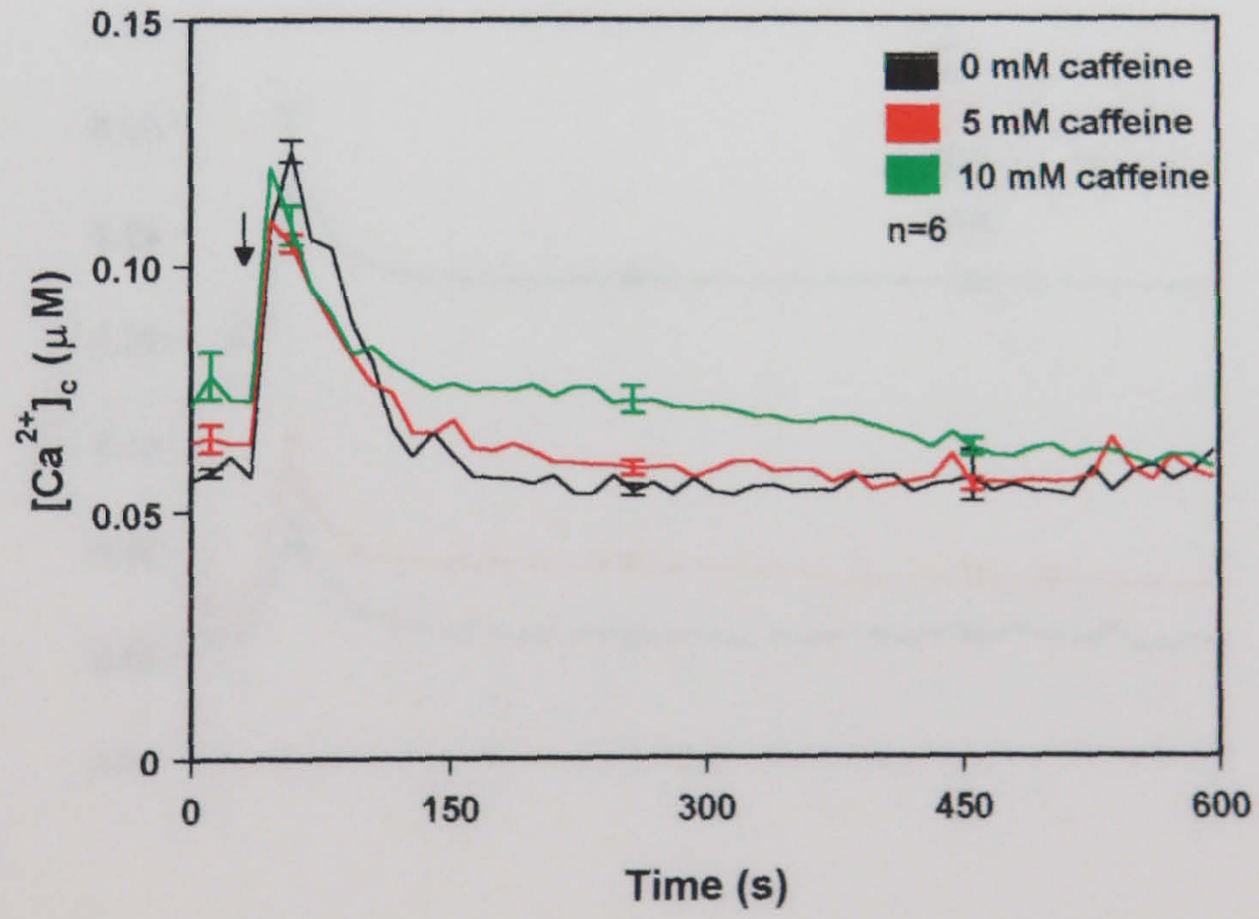

Figure 4.27 Effect of caffeine on the $[Ca^{2+}]_c$ response to hypo-osmotic shock. Caffeine was added 5 min before hypo-osmotic shock was applied (shown by the arrow). Results represent mean ± SE. Measurements were performed using the repeated measuring protocol. Cycle time 11.6 s.

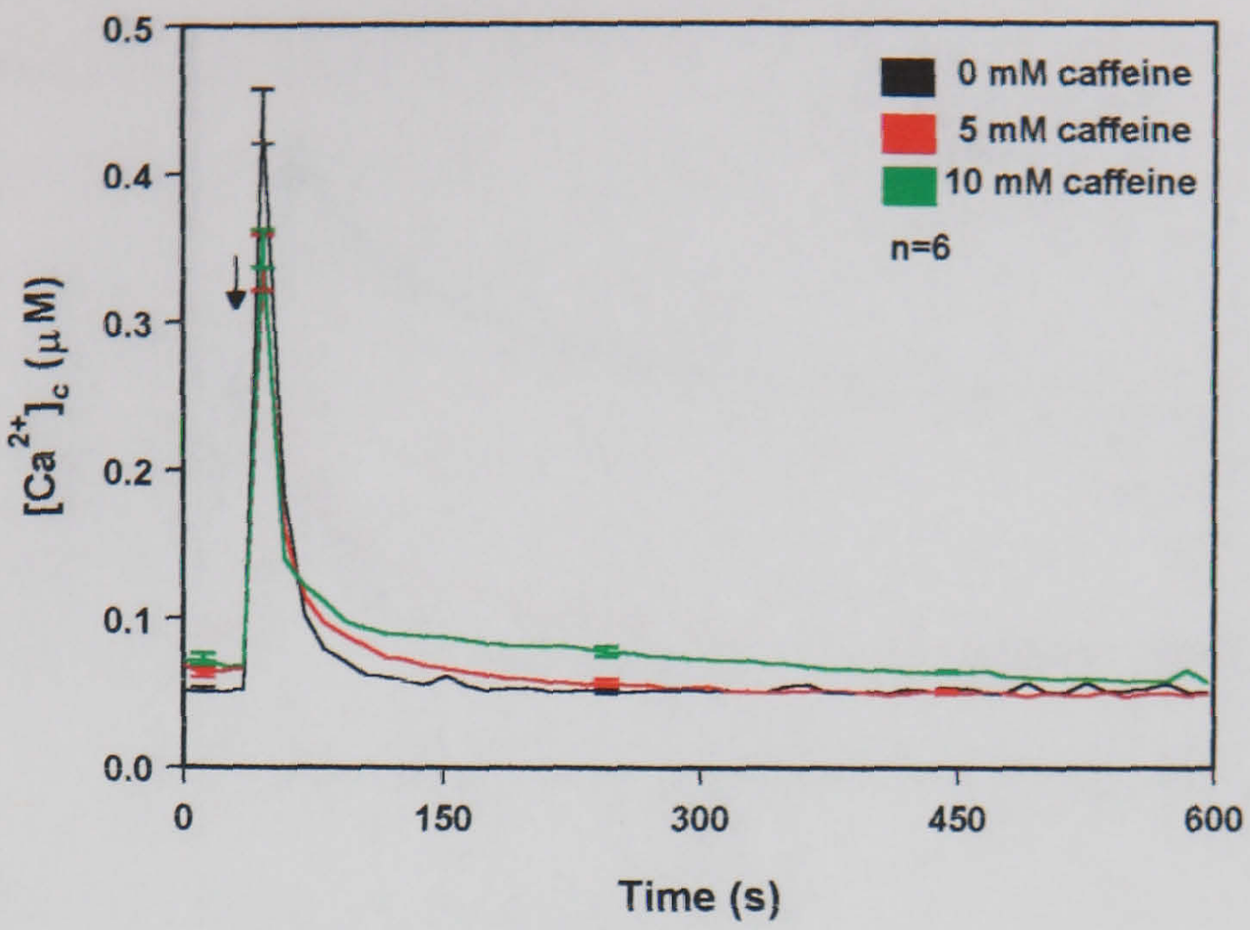

Figure 4.28 Effect of caffeine on the $[Ca^{2+}]_c$ response to 5 mM external $CaCl_2$. Caffeine was added 5 min before external $CaCl_2$ was applied (shown by the arrow). Results represent mean ± SE. Measurements were performed using repeated measuring protocol. Cycle time 11.6 s.

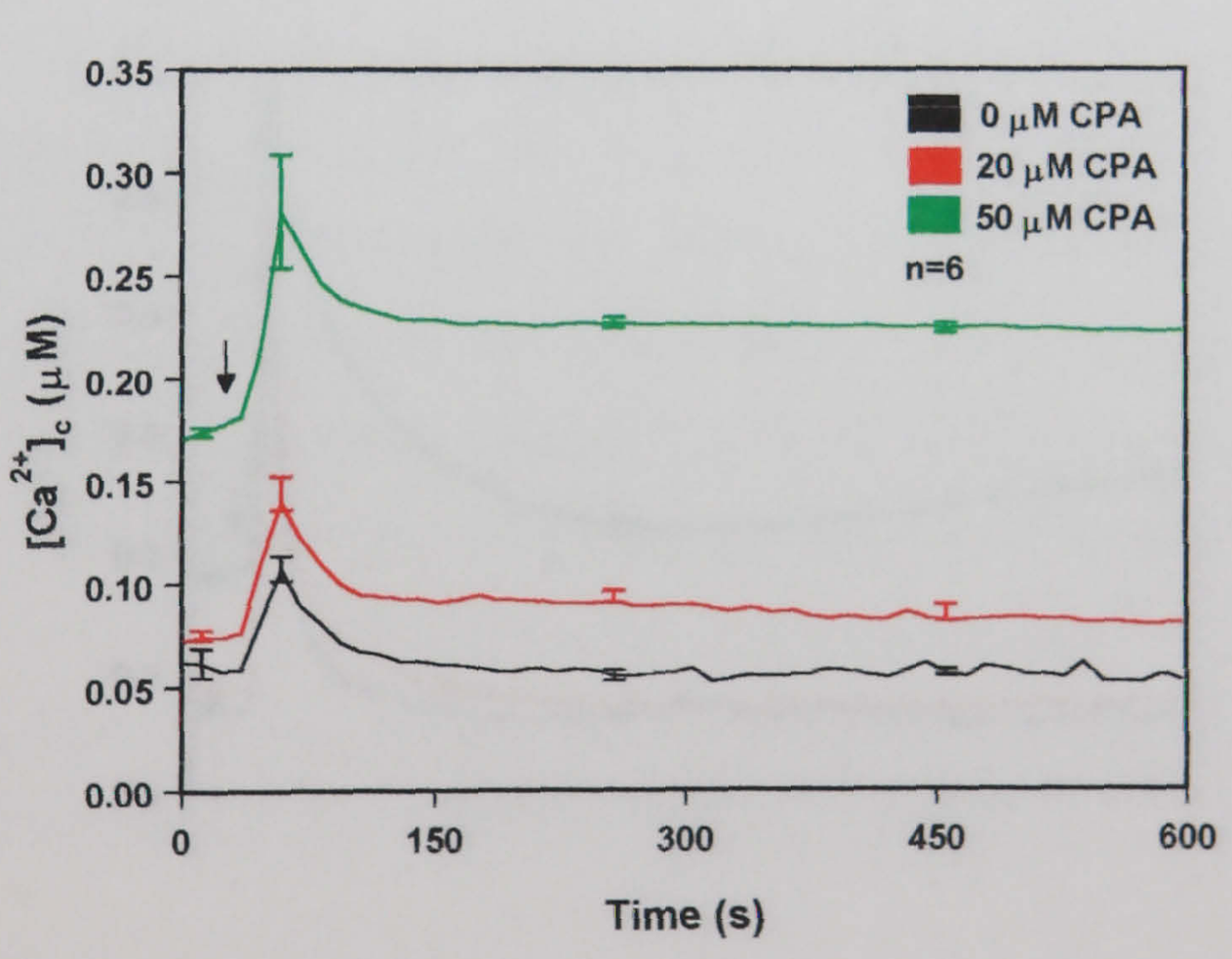

Figure 4.29 Effect of CPA on the $[Ca^{2+}]_c$ response to mechanical perturbation. CPA was added 5 min before mechanical perturbation was applied (shown by the arrow). Results represent mean ± SE. Measurements were performed using the repeated measuring protocol. Cycle time 11.6 s.

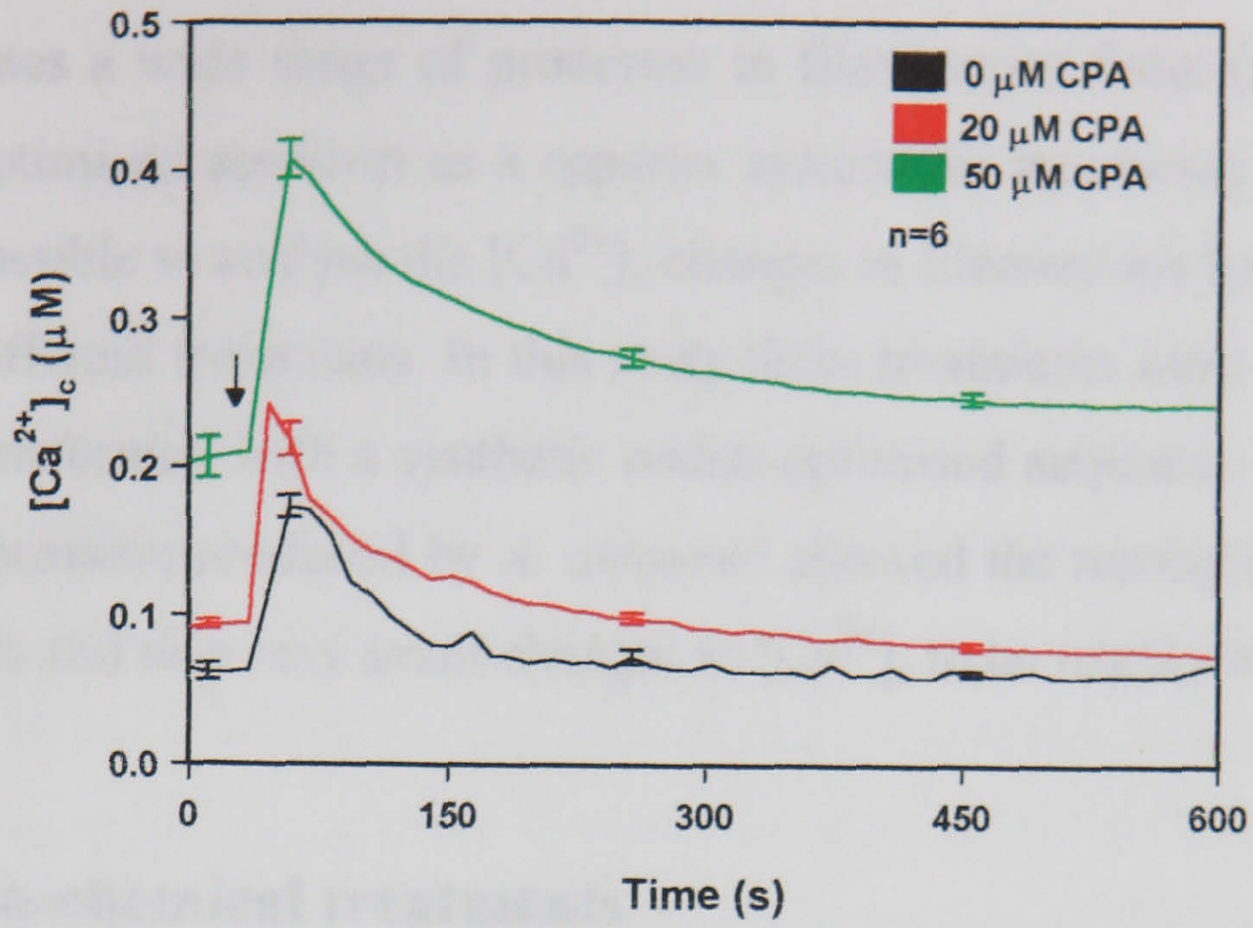

Figure 4.30 Effect of CPA on the $[Ca^{2+}]_c$ response to hypo-osmotic shock. CPA was added 5 min before hypo-osmotic shock was applied (shown by the arrow). Results represent mean ± SE. Measurements were performed using the repeated measuring protocol. Cycle time 11.6 s.

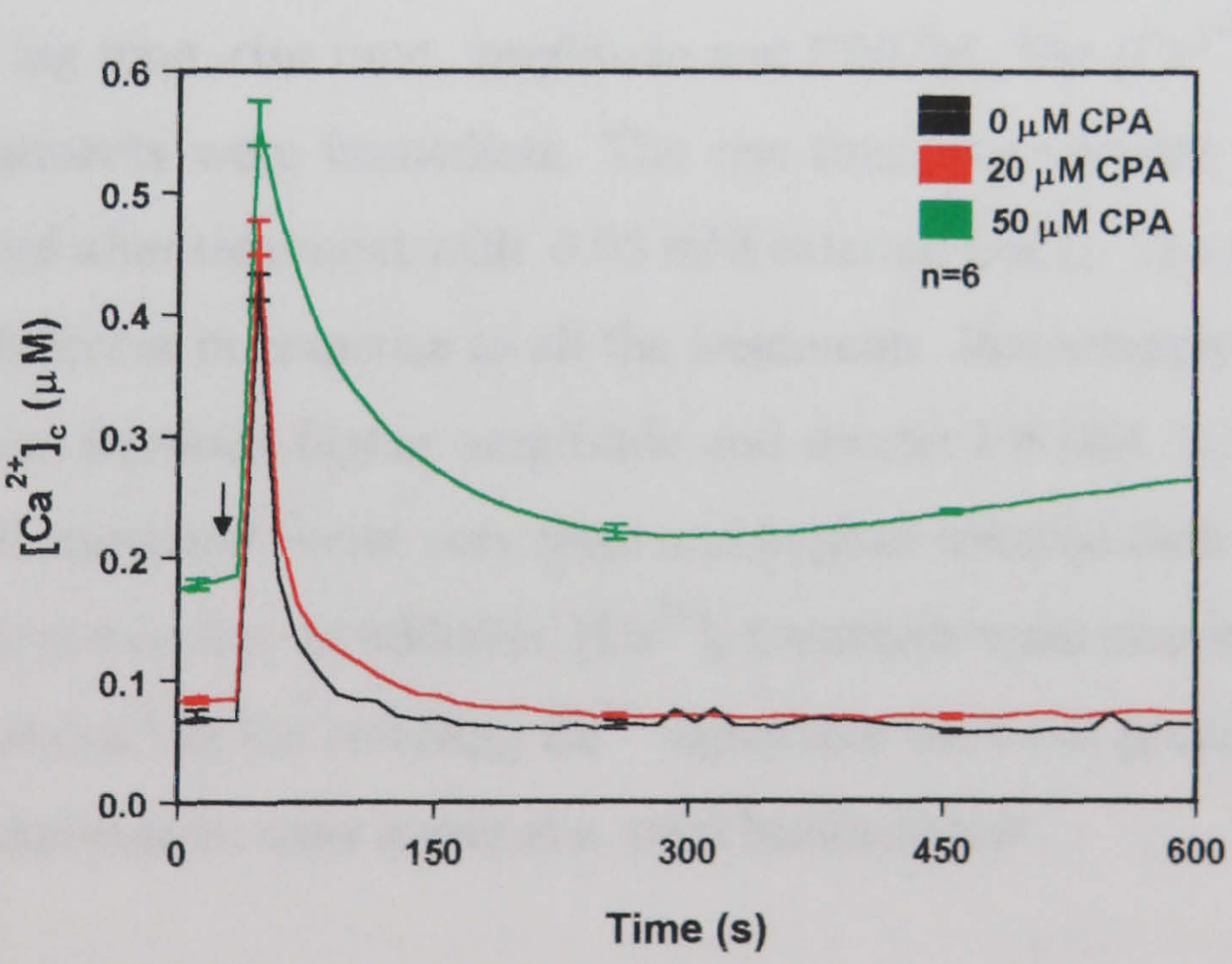

Figure 4.31 Effect of CPA on the $[Ca^{2+}]_c$ response to 5 mM $CaCl_2$. CPA was added 5 min before external $CaCl_2$ was applied (shown by the arrow). Results represent mean ± SE. Measurements were performed using the repeated measuring protocol. Cycle time 11.6 s.

4.3 DISCUSSION

Calcium regulates a wide range of processes in filamentous fungi (see Table 1.1). Using codon-optimised aequorin as a reporter system for measuring $[Ca^{2+}]_c$ it has now become possible to analyse the $[Ca^{2+}]_c$ changes in filamentous fungi in response to a range of different treatments. In this study these treatments were analysed using *A. awamori* transformed with a synthetic codon-optimised aequorin. The high level of aequorin expression produced by *A. awamori* allowed the resting $[Ca^{2+}]_c$ level in growing cultures and also very small changes in $[Ca^{2+}]_c$ to be readily measured.

4.3.1 Physico-chemical treatments

A number of physico-chemical treatments have been analysed in plants using recombinant aequorin (Table 1.3). In this study *A. awamori* was subjected to the following treatments in the plate luminometer: mechanical perturbation (touch), hypo-osmotic shock and high external $CaCl_2$. The $[Ca^{2+}]_c$ responses to these treatments each had a unique Ca^{2+} signature which was characterised by unique combination of lag time, rise time, amplitude and FWHM. The $[Ca^{2+}]_c$ responses to each of the treatments were immediate. The rise time was variable with the most variation observed after treatment with 0.05 mM external $CaCl_2$. The amplitudes and FWHMs were different in response to all the treatments. Interestingly, there seemed to be a correlation between higher amplitude and shorter FWHM. $[Ca^{2+}]_c$ transients in response to all treatments were very short and hyphae restored their resting $[Ca^{2+}]_c$ levels within a few minutes. In addition, $[Ca^{2+}]_c$ transients were also induced by cold shock and heat shock but the resulting Ca^{2+} signatures were not precisely quantified because the measurements were made in a tube luminometer.

4.3.2 Pharmacological treatments

4.3.2.1 Ca^{2+} antagonists

The next step in the investigation was to analyse the source of Ca^{2+} which was involved in each of the $[Ca^{2+}]_c$ responses. This analysis was done using commercially available pharmacological inhibitors with known selectivity and with one fungus derived inhibitor KP4. It is important to emphasize that the mode-of-action for nearly all pharmacological inhibitors has been determined on animal cells. Many of these inhibitors have also been used on plant cells (Johannes et al. 1991) but typically the effective inhibitory concentrations were much higher in plant than in animal cells. Similarly with fungal cells the effective inhibitory concentrations were also higher than used for plant cells which raises questions about the actual selectivity of these inhibitors in fungal and plant cells. One should be also aware that the intracellular targets of these inhibitors might not be present in fungal or plant cells at all or they may be significantly different in their structure thus preventing the efficient binding of the Ca^{2+} antagonist to them. The data presented in Table 4.4 show that of six commercially available inhibitors tested only two (La^{3+} and BAPTA) had an inhibitory effect on the $[Ca^{2+}]_c$ responses to the physico-chemical treatments used. Therefore it was particular interesting to analyse the effects of KP4 on Ca^{2+} signature. KP4 is so far the only one available fungus derived Ca^{2+}-channel blocker (Gu et al. 1995). Interestingly, the IC_{50} for KP4 was in the µM range whereas the IC_{50} for $LaCl_3$ was in the mM range. It is therefore seems likely that KP4 is more selective for Ca^{2+}-channels than $LaCl_3$.

The results above suggest that Ca^{2+} transport across the plasma membrane from the external medium is a significant source of the $[Ca^{2+}]_c$ increase in response to the mechanical perturbation, hypo-osmotic shock and high external $CaCl_2$ because La^{3+} is a competitive inhibitor of plasma membrane located L-type Ca^{2+}-channels and BAPTA will reduce the extracellular Ca^{2+} concentration by chelating it. The exact specificity of KP4 is not yet known but it has been shown that KP4 acted in a manner analogous to calcium chelators (EGTA) and the Ca^{2+}-channel inhibitor Cd^{2+} (Gage et

al. 2001): i.e. it inhibits the uptake of external Ca^{2+}. No data using inhibitors provided evidence that internal Ca^{2+} stores play a major role in causing the $[Ca^{2+}]_c$ increase in each treatment because ryanodine and TMB-8 did not inhibit the different $[Ca^{2+}]_c$ responses. However, these results need to be treated with caution because ryanodine, TMB-8, nifedipine and verapamil may not be effective Ca^{2+} modulators in *A. awamori* or their targets may not be involved in increasing $[Ca^{2+}]_c$ in response to mechanical perturbation, hypo-osmotic shock and high external $CaCl_2$. Interestingly of the Ca^{2+}-channel blockers tested nifedipine was found to be ineffective in inhibiting the $[Ca^{2+}]_c$ response in fungi and this was supported by the finding that BAY(-), its ortho-CF_3 analogue was the only agonist which was ineffective in increasing $[Ca^{2+}]_c$.

Another very interesting point is that both La^{3+} and KP4 inhibited both the $[Ca^{2+}]_c$ response to hypo-osmotic shock and high external Ca^{2+}, but not to mechanical perturbation. This indicates that the Ca^{2+} sources involved in mechanical perturbation may be different from these involved in the $[Ca^{2+}]_c$ response to hypo-osmotic shock and high external $CaCl_2$. This suggestion was supported by the data obtained using the Ca^{2+} agonists. Caffeine, which is known to cause the release of Ca^{2+} from internal stores (see Table 4.6), caused a decrease in the amplitude of the $[Ca^{2+}]_c$ response to mechanical perturbation but not to hypo-osmotic shock and external $CaCl_2$. This suggests that the $[Ca^{2+}]_c$ transient resulting from mechanical perturbation may be partially derived from Ca^{2+} released from a caffeine-sensitive internal store.

Furthermore the selectivity of La^{3+}, which did have an inhibitory effect, also needs to be questioned. Corzo and Sanders (1992) showed that La^{3+} causes depolarisation of the plasma membrane in *Neurospora crassa*, which may have an influence on the influx of Ca^{2+} into the cytoplasm. In the present study the effect of La^{3+} on $[Ca^{2+}]_c$ was firstly analysed using the so-called integrated protocol (see section 2.4.1). The dose-dependent inhibition observed (see Figs. 4.14 and 4.15) was consistent with the known mode of action of La^{3+} in blocking Ca^{2+}-channels. Interestingly Fig. 4.14 shows that with low concentrations of external $CaCl_2$ (0.1 and 0.5 mM) as a stimulus there was an increase in the amplitude of the $[Ca^{2+}]_c$ response observed with 5 mm

$LaCl_3$. With a higher concentration of external $CaCl_2$ (5 mM) the same 5 mM concentration of $LaCl_3$ caused an inhibition of the amplitude of the $[Ca^{2+}]_c$ response. The possible reason for this is that at low concentrations of external $CaCl_2$ the side-effects of La^{3+} caused by depolarisation of the membrane are more significant than when the concentration of external $CaCl_2$ is 10-50 times higher.

When the kinetics protocol (see section 2.4.1) was used the data obtained showed more complicated effects of La^{3+}. It appeared that La^{3+} not only inhibited the amplitude of the $[Ca^{2+}]_c$ response but at a concentration of 20 mM it also caused a secondary increase in $[Ca^{2+}]_c$ (consistent with Ca^{2+} release from the internal stores) and at all concentrations above 5 mM an increase in the $[Ca^{2+}]_c$ final resting level. The last effect is consistent with La^{3+} inhibiting the activity of a Ca^{2+}-ATPase or Ca^{2+} transporter responsible for pumping Ca^{2+} out of the cytosol. In animal cells La^{3+} is known to prevent the formation of a phosphorylated intermediate of the ER type Ca^{2+}-ATPase (Bush 1995). Interestingly, the side effects of $LaCl_3$ (i.e. increased $[Ca^{2+}]_c$ resting level and secondary Ca^{2+} increase) were observed after mechanical perturbation indicating that these effects are not correlated with La^{3+} activity as a Ca^{2+}-channel blocker.

When using IC_{50} as a parameter characterizing the inhibitory effect of different Ca^{2+}-channel blockers, it is important to note that numbers presented in Table 4.5 were based on the amplitude of the $[Ca^{2+}]_c$ response measured in RLU. The IC_{50} value for La^{3+} was between 10 and 14 mM (Fig. 4.15; Table 4.5). However, when analysing the amplitudes in Fig. 4.16 the IC_{50} was between 15 and 20 mM. This difference is due to the fact that the RLU are not directly proportional to $[Ca^{2+}]_c$ concentration. The decision to determine IC_{50} values in RLU was based on fact that when screening different compounds, the integrated measuring mode proved to be the most convenient to use. The integrated mode produces a sum of the total luminescence obtained during the 20 s following stimulation (see Section 2.4.1).

4.3.2.2 Ca^{2+} agonists

Greater success was obtained with the Ca^{2+}-agonists. Addition of A23187, Br-A23187, caffeine and CPA all increased $[Ca^{2+}]_c$. The Ca^{2+}-signature after the addition of the agonists was characteristically biphasic (Figs. 4.20-4.25): the first rapid $[Ca^{2+}]_c$ increase was interpreted as resulting from mechanical perturbation and involved the uptake of $[Ca^{2+}]_c$ from the external medium and possibly internal stores as well. The secondary $[Ca^{2+}]_c$ response was much slower. With caffeine the secondary and the third $[Ca^{2+}]_c$ increases were interpreted as probably resulting from the release of Ca^{2+} from internal reservoirs. CPA is known to inhibit the activity of Ca^{2+}-ATPases. This prevents the uptake of Ca^{2+} into the internal stores resulting in them being emptied when $[Ca^{2+}]_c$ is increased. Caffeine by releasing Ca^{2+} from internal stores will also drain them of Ca^{2+}. Since caffeine and CPA are agonists which promote the release of Ca^{2+} from internal stores in hyphae of *A. awamori* this indicates that the necessary Ca^{2+} signalling machinery for this to occur is present.

A23187 is a mobile ion-carrier that forms stable complexes with divalent cations (Pfeiffer et al. 1974). In animal cells A23187 (at concentrations around 10 μM) is known to stimulate the passage of Ca^{2+} into cells from the external medium (Robson et al. 1991a). When fungal hyphae were treated with A23187 the long term elevations of $[Ca^{2+}]_c$ were observed. Afterwards, once the hyphae restored their $[Ca^{2+}]_c$ to their original resting level the A23187 may have been inactivated, or the Ca^{2+}-ATPases and Ca^{2+}/H^+ antiporter may have increased their activity in order to compensate for the higher $[Ca^{2+}]_c$ concentration.

The prolonged increase in $[Ca^{2+}]_c$ which resulted from treatment with A23187 shows that cells have difficulty in restoring their normal $[Ca^{2+}]_c$ resting levels. A23187 is known to aggregate over time in aqueous systems (Pfeiffer et al. 1974). This might lead to a localized very high concentration of the drug, which might be cytotoxic. The long term $[Ca^{2+}]_c$ increase observed might have been the results of dead cells releasing aequorin which in turn will interact with Ca^{2+} present in the media. The recovery of $[Ca^{2+}]_c$ to the resting level may indicate that cells adapted to the presence of A23187 in the medium. It is important to note that at the end of the $[Ca^{2+}]_c$

response to A23187 there was still plenty of active aequorin remaining in the cells. Therefore the recovery to resting level is not due to the reduction of active aequorin to very low levels. Caffeine also precipitates in liquid after a long period of time (typically 1-3 h). The third $[Ca^{2+}]_c$ increase observed following caffeine treatment may have been a result of cells death as was possibly the case for A23187. Another possible explanation is based on the fact that in plant cells caffeine is known to cause transient hyperpolarization of the plasma membrane (Bauer et al. 1999). This may occur in the same way in fungal cells. In the case of the application of CPA, hyphae had problems in restoring their $[Ca^{2+}]_c$ to normal levels due to the inhibition of Ca^{2+}-ATPase activity. When recovery did occur, approximately 5 h after addition of CPA, it was possibly due to the recovery of Ca^{2+}/H^+ antiporter or Ca^{2+}-ATPase activity. CPA does not precipitates in solution. The shape of the secondary $[Ca^{2+}]_c$ response to CPA was different from the one after treatment with A23187. The secondary $[Ca^{2+}]_c$ increase caused by CPA peaked 1 h after the addition of CPA. In the case of A23187 the peak luminescence was reached after approximately 50 min and $[Ca^{2+}]_c$ stayed at this level for over an 1 h. This again suggests that the long term increase might be due to cells death, possibly due to increasing A23187 aggregation over time.

4.3.2.3 Effect of Ca^{2+} agonists on Ca^{2+} response to physico-chemical treatments

The effects of agonists were also studied in combination with physico-chemical treatments. After 5 min incubation with caffeine an increase in the initial $[Ca^{2+}]_c$ resting level was observed. However, following mechanical perturbation the amplitude of the $[Ca^{2+}]_c$ response was greatly inhibited (see Fig. 4.26). In contrast, no changes in $[Ca^{2+}]_c$ amplitude were observed after applying hypo-osmotic shock or high external $CaCl_2$. This indicates that caffeine-sensitive internal stores of Ca^{2+} may play a role in the $[Ca^{2+}]_c$ response to mechanical perturbation, which would appear to be different to the sourced of Ca^{2+} responsible for the $[Ca^{2+}]_c$ increases resulting from the other two physico-chemical treatments. The recovery of $[Ca^{2+}]_c$ to its resting level was delayed following all three stimuli. The secondary $[Ca^{2+}]_c$ increase which was observed when hyphae were treated with caffeine alone was not present when

caffeine was combined with the physico-chemical treatments (cf. Figs. 4.22 and 4.26).

In the case of CPA the increase in the initial $[Ca^{2+}]_c$ resting level was very significant (Figs. 4.29-4.31). However, in spite of this the $[Ca^{2+}]_c$ response to physico-chemical treatments was normal with approximately the same rise times, amplitudes and lengths of transients as with just the physico-chemical treatments on their own. Although CPA-dependent internal stores of Ca^{2+} were depleted by the presence of CPA, the $[Ca^{2+}]_c$ response to the physico-chemical treatments was still normal. These results confirm that in response to these physico-chemical treatments (with possible exception of mechanical perturbation) the main source of Ca^{2+} for the $[Ca^{2+}]_c$ increase comes from external Ca^{2+}.

The main conclusions from the research described in this chapter are:

- Three physico-chemical treatments (mechanical perturbation, hypo-osmotic shock, high external $CaCl_2$) resulted in transient $[Ca^{2+}]_c$ increases and each of these $[Ca^{2+}]_c$ responses had a unique Ca^{2+} signature which was characterised by a unique combination of rise time, lag time, amplitude and FWHM. Heat and cold shock treatments also resulted in transient $[Ca^{2+}]_c$ increases.

- The sources of Ca^{2+} for the $[Ca^{2+}]_c$ increases resulting from hypo-osmotic shock, high external $CaCl_2$ and possibly mechanical perturbation were mainly external. Internal Ca^{2+} stores may also play a role in the $[Ca^{2+}]_c$ response to mechanical perturbation.

- Of six commercially available Ca^{2+} inhibitors studied only two (La^{3+} and BAPTA) were effective in inhibiting $[Ca^{2+}]_c$ increases. The IC_{50} values were both in the millimolar range, whereas the IC_{50} for fungal derived inhibitor KP4 was in the micromolar range.

- Treatments with the Ca^{2+} agonists A23187, caffeine and CPA resulted in biphasic $[Ca^{2+}]_c$ responses: the primary $[Ca^{2+}]_c$ increase was due to mechanical perturbation and the secondary $[Ca^{2+}]_c$ increase was due to the treatment with the agonists.

5 CHARACTERISATION OF CALCIUM-MEDIATED RESPONSES

5.1 INTRODUCTION

It is well known that Ca^{2+} is involved in regulating many physiological processes in filamentous fungi (see Table 1.1). One of the most studied of these processes is polarized tip growth. In plants it has been shown that Ca^{2+} plays an important role maintaining polarized growth of pollen tubes and algal filaments (Hepler and Waye 1985). In fungi the role of Ca^{2+} is less understood. However, there is evidence that Ca^{2+} plays an active role in regulating tip growth and also hyphal branching in fungi (Schmid and Harold 1988; Jackson and Heath 1989). Most of the studies of the role of Ca^{2+} in fungal morphogenesis have involved the use of Ca^{2+} modulators such as the ionophore A23187, calmodulin antagonists, Ca^{2+}-channel blockers, Ca^{2+} chelators and varying the concentration of external Ca^{2+} (Dicker and Turian 1990; Reissig and Kinney 1983; Robson et al. 1991a) (see Tables 1.7-1.9). For example, it was shown that low external Ca^{2+} caused an increase in branching and decrease in hyphal extension rate and an increase in hyphal diameter (Robson et al. 1991b). The mechanism by which Ca^{2+} affects hyphal extension is not known but could be the result of an interaction with the cytoskeleton at the apex, an effect on vesicle distribution, or an effect on wall assembly (Jackson and Heath 1989; Dicker and Turian 1990).

As discussed in Chapter 4 a lot of data obtained using filamentous fungi and pharmacological Ca^{2+} modulators have to be treated with caution (see Section 4.3). In particular if the concentrations of the Ca^{2+} modulators used are very high the response observed can be a side-effect which might not be related to the mode-of-action of the compound.

Using *A. awamori* the aims of the research described in this chapter were:

- To analyse the effects of different physico-chemical and pharmacological treatments, which were shown to influence $[Ca^{2+}]_c$ levels (see Chapter 4) on various aspects of hyphal morphology and physiology.

- To analyse the possible toxic side-effects of the pharmacological compounds used on hyphal growth and sporulation.

5.2 RESULTS

5.2.1 Growth characteristics of *A. awamori* in liquid medium

Before analysing the effects of different physico-chemical and pharmacological treatments which increase $[Ca^{2+}]_c$ on hyphal morphology, it was necessary to characterize the growth of *A. awamori* in liquid medium, as found in the individual wells of the microplate.

It was not possible to scoop out the 24 h old fungal cultures grown in liquid medium from the wells because the microcolonies tended to adhere themselves to the walls of the wells. It was therefore decided to grow *A. awamori* on coverslips in 50 µl droplets of VS medium in the humidity chamber. Four spore concentrations of the inoculum were tested: $5 \cdot 10^5$, $5 \cdot 10^4$, $5 \cdot 10^3$, $5 \cdot 10^2$ spores/ml. The growth of cultures resulting from the highest concentration of the inoculum ($5 \cdot 10^5$ spores/ml) could be seen with the naked eye after 24 h and was too dense for the analysis of separate hyphae on the coverslip. The optimum concentration of inoculum for analysing the effects on individual microcolony morphology was $5 \cdot 10^4$ spores/ml. However, even at this concentration, the analysis of branch formation was often extremely difficult. Figures 5.1 and 5.2 show that spores often stuck together and after germination formed a complex 3D network of interlinked and interwoven hyphae. At the same time occasionally small microcolonies, usually formed from late germinated spores, were observed (Fig. 5.3). After 24 h these microcolonies usually had one very long

germ tube which usually was out of the field of view of individual confocal images, and 1 or 2 other germ tubes which were much shorter.

Spores of *A. awamori* stuck to the surface of the coverslip but the hyphae themselves floated in the medium and even when flattened with a coverslip most of the hyphae in a single microcolony would be out-of-focus in different focal planes. Confocal microscope is highly suitable for 3D imaging (Czymmek et al. 1994). However, repeated scanning damaged the living hyphae. 70-100 optical sections were required to generate a 3D projection (Figs. 5.1-5.3) and even with this many scans, some parts of the microcolony were still out-of-focus. Even when using a x20 objective some of the hyphae still grew out of the field-of-view (Figs. 5.1 and 5.2). The x20 objective proved to have too low a magnification to analyse the hyphal morphology in detail, for which the x60 objective was used (Fig. 5.3).

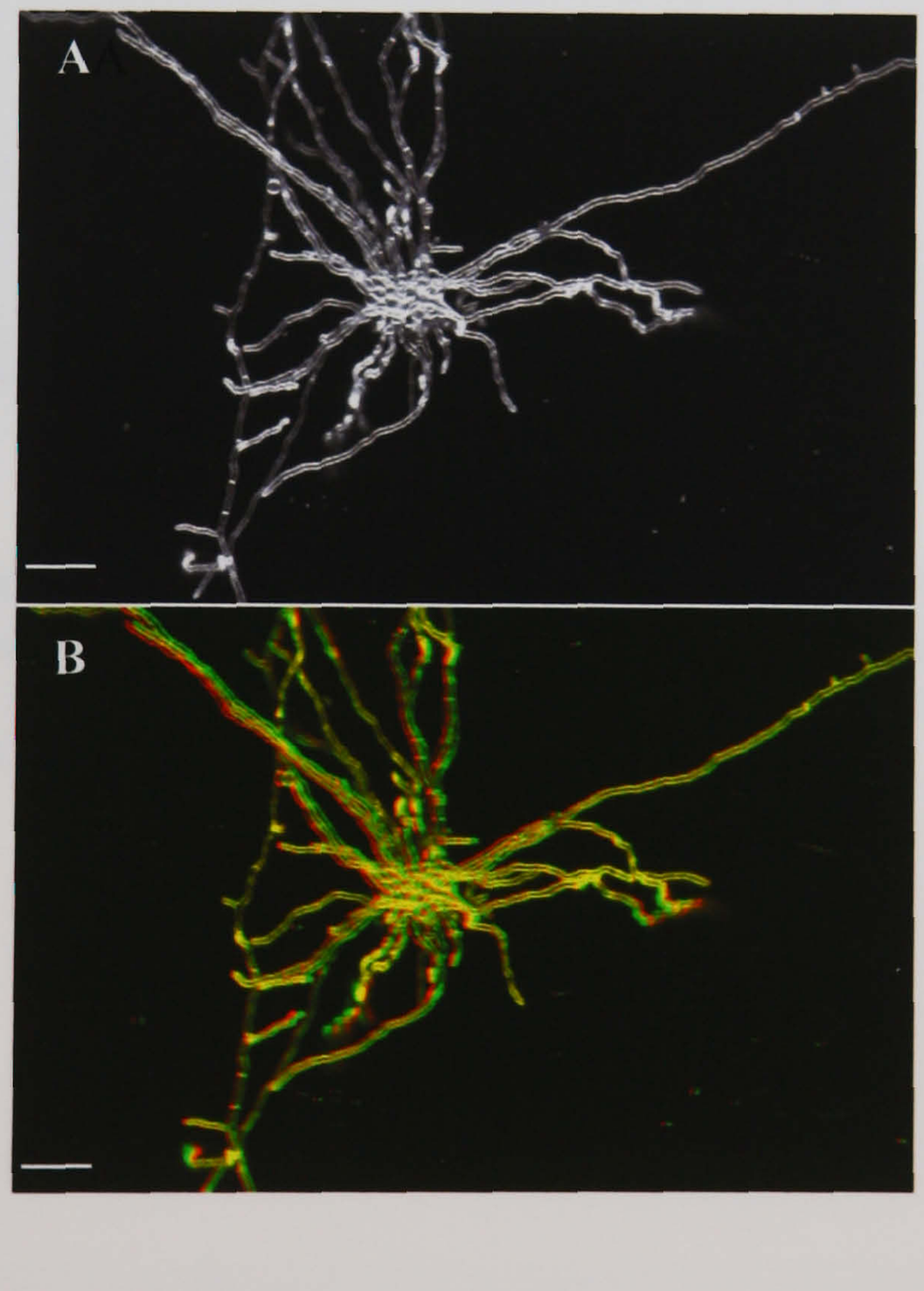

Figure 5.1 24 h old microcolonies of *A. awamori* germinated from a group of spores in a liquid droplet on a coverslip. Confocal images after staining with FM4-64 and images with a x20 dry objective. Bars = 10 μm. **A**. Single image of projection of confocal images. **B**. Pseudocoloured 3D projection of same confocal image.

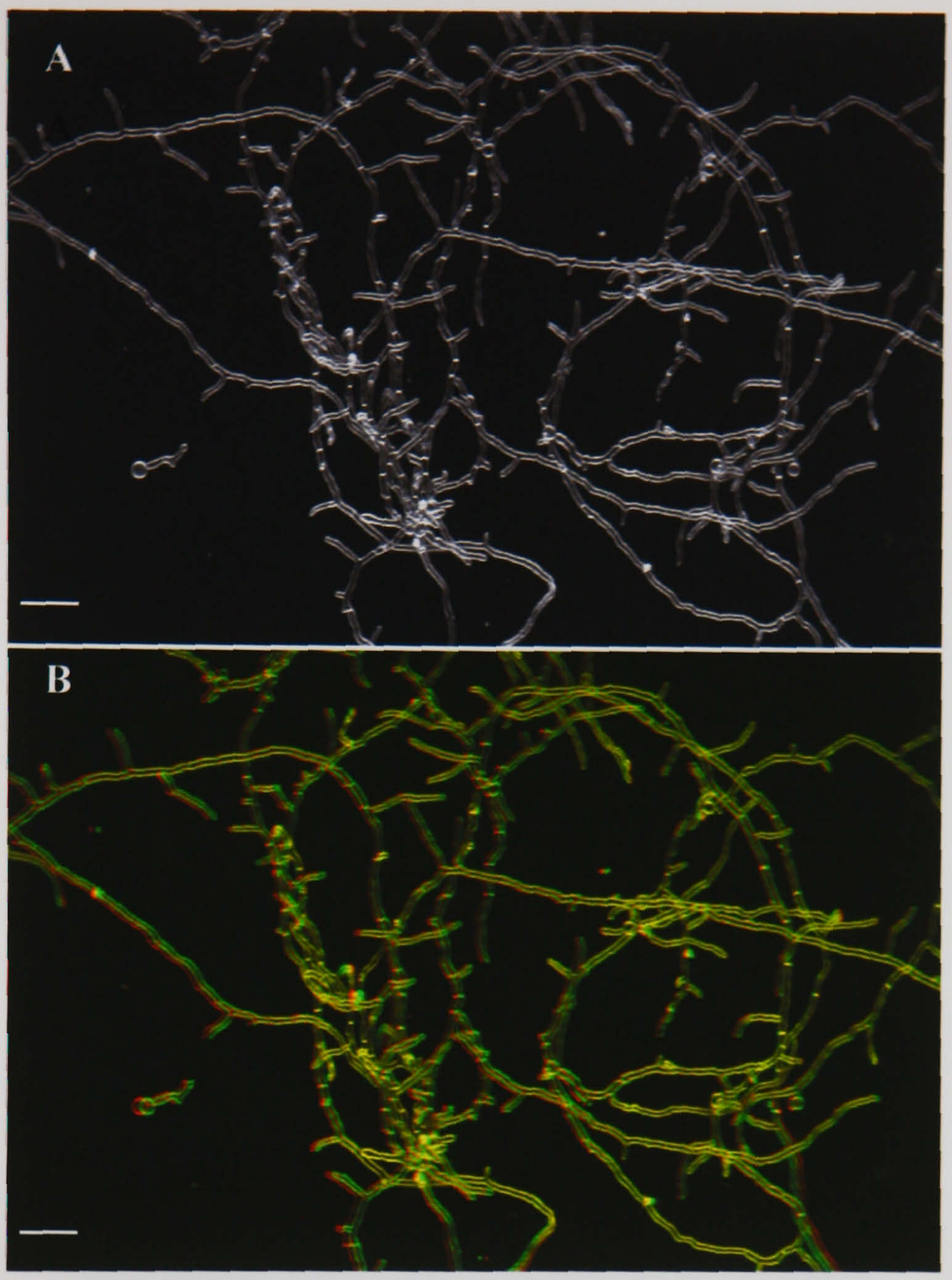

Figure 5.2 24 h old microcolonies of *A. awamori* grown in a liquid droplet on a coverslip. Confocal images after staining with FM4-64 and images with a x20 dry objective. Bars = 10 μm. **A**. Single image of projection of confocal images. **B**. Pseudocoloured 3D stereoprojection of confocal image.

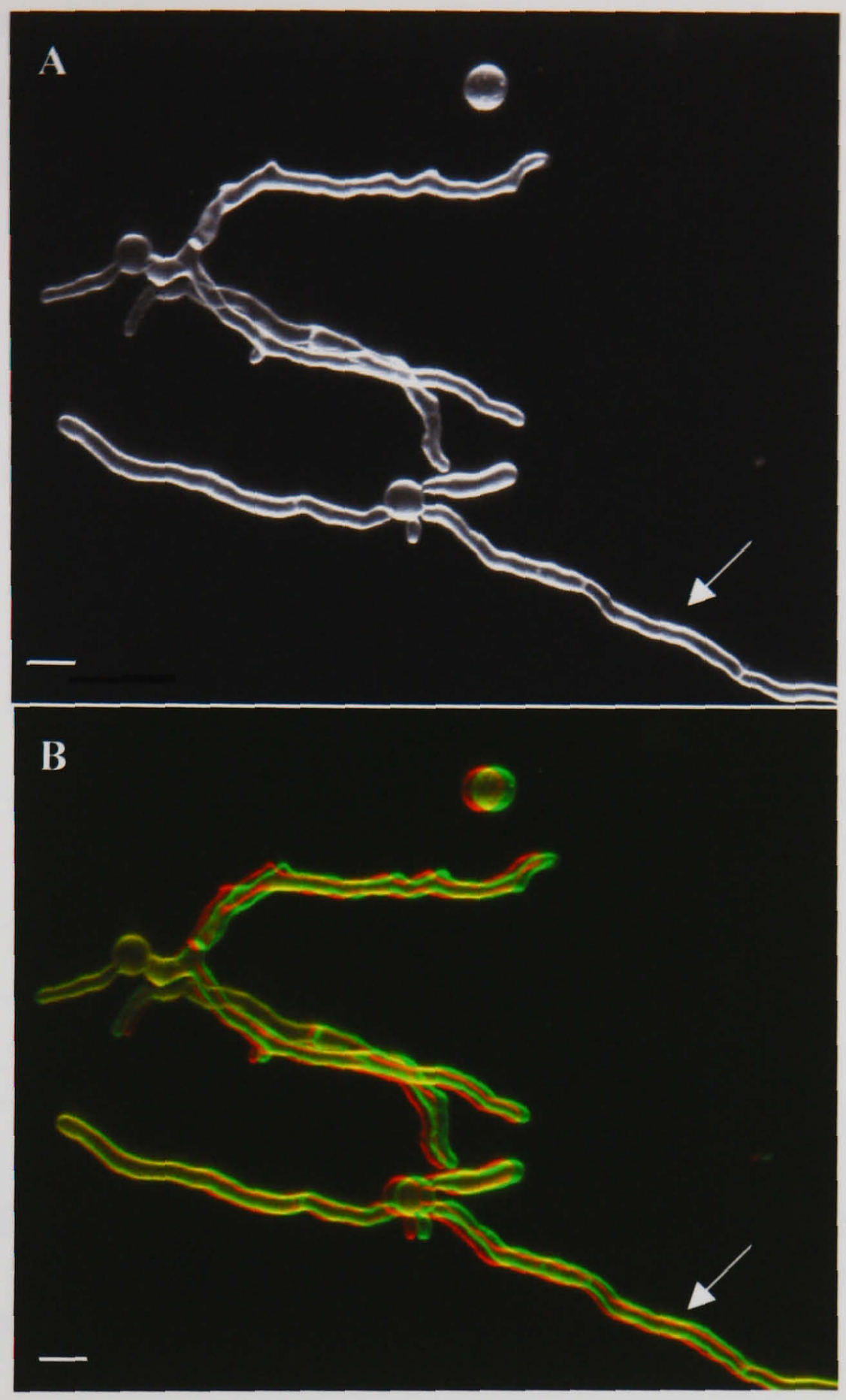

Figure 5.3 24 h old microcolonies of *A. awamori* grown in a liquid droplet on a coverslip. Confocal images after staining with FM4-64 and image with a x60 oil objective. Bars = 10 µm. **A.** Single image of projection of confocal images. **B.** Pseudocoloured 3D projection of confocal image. Arrow indicates the main germ tube.

5.2.2 Analysis of the effects of physico-chemical treatments on hyphal branching

In spite of the difficulties in obtaining the images of growing hyphae in liquid culture (see last Section) the decision was made to quantify the number of branches formed in 24 h old microcolonies at different times after the following physico-chemical treatments: mechanical perturbation, hypo-osmotic shock and 5 mM $CaCl_2$. For this

analysis it was found convenient to quantify the number of branches emerging from the main (longest) germ tube (see last Section). For each treatment 75 microcolonies were analysed (25 per coverslip). The number of branches was measured every 2 h for the period of 1-7 h following treatment of the 24 h old microcolonies (for details see Section 2.7). Table 5.1 shows that the number of branches increased with time. However, there was no significant difference between the three treatments and the control ($P < 0.05$).

Incubation time	Control	Mechanical perturbation	Hypo-osmotic shock	5 mM $CaCl_2$
1 h	1.13 ± 0.05	1.16 ± 0.05	1.16 ± 0.05	1.16 ± 0.05
3 h	1.46 ± 0.08	1.44 ± 0.07	1.37 ± 0.08	1.47 ± 0.16
5 h	1.59 ± 0.10	1.59 ± 0.08	1.49 ± 0.14	1.48 ± 0.08
7 h	1.96 ± 0.12	1.92 ± 0.14	1.72 ± 0.09	1.6 ± 0.08

Table 5.1 Effect of different physico-chemical treatments on hyphal branching in *A. awamori*. The control represents untreated cultures. Results represent mean ± SE. n = 75. The statistical analysis showed that there was no significant difference (5% LSD) between treatments at each time point.

5.2.3 Analysis of the effects of Ca^{2+} agonists on growth and hyphal morphology

5.2.3.1 Effects of Ca^{2+} agonists in liquid medium

The next experimental step was to analyse the effects of Ca^{2+} agonists, which had previously been shown to increase $[Ca^{2+}]_c$ over extended periods (2-5 h) on hyphal branching and morphology (see Section 4.2.2.2).

The first compound to be tested was the Ca^{2+}-selective ionophore A23187. A 50 µl droplet of medium inoculated with the fungus was grown for 24 h, at which time 50 µl of 20 µM or 100 µM A23187 were added. However, it was found that A23187

aggregated in liquid medium over extended period of time and these aggregates tended to concentrate around hyphae (Fig. 5.4). Compared with the control, branching was very suppressed (Table 5.2). The variation in the concentration of A23187 may have had damaging effects on hyphal growth and branching which might not have been the same if A23187 had been evenly distributed around the hyphae.

Incubation time	Control	10 µM A23187	50 µM A23187
1 h	1.27 ± 0.05	1.08 ± 0.05	1.06 ± 0.05
3 h	*1.45 ± 0.09*	*1.09 ± 0.03*	*1.09 ± 0.03*
5 h	*1.50 ± 0.07*	*1.09 ± 0.03*	*1.09 ± 0.03*
7 h	*1.90 ± 0.12*	*1.09 ± 0.03*	*1.09 ± 0.03*

Table 5.2 Effect of A23187 on hyphal branching. Results represent mean ± SE. n = 75. Numbers in italics represent data which are significantly different from the control at each time point (5% LSD). Note that the 10 and 50 µM treatment represent the final concentration of the compounds in 100 µl droplet on the coverslip.

Figure 5.4 Aggregation of A23187 around hyphae after incubation with 10 µM A23187 in 24 h old cultures. Brightfield image obtained using a x60 dry objective. Bar = 5 µm.

When cells were treated with caffeine a similar situation was observed. With time caffeine formed crystal-like structures around hyphae, which raised similar concerns,

as to how the results with A23187 should be interpreted. To try and overcome these problems of agonists aggregating, similar experiments were repeated using solid VS medium.

5.2.3.2 Effects of Ca^{2+} agonists in solid medium

Imaging hyphae growing on solid medium (Fig. 5.5) had several advantages over imaging hyphae growing in liquid medium, including:

- Hyphae could be kept in a single plane of focus
- There was no aggregation of agonists around hyphae
- Microscope objectives with higher magnifications (x40 and x60) and short working distance could be easily used.

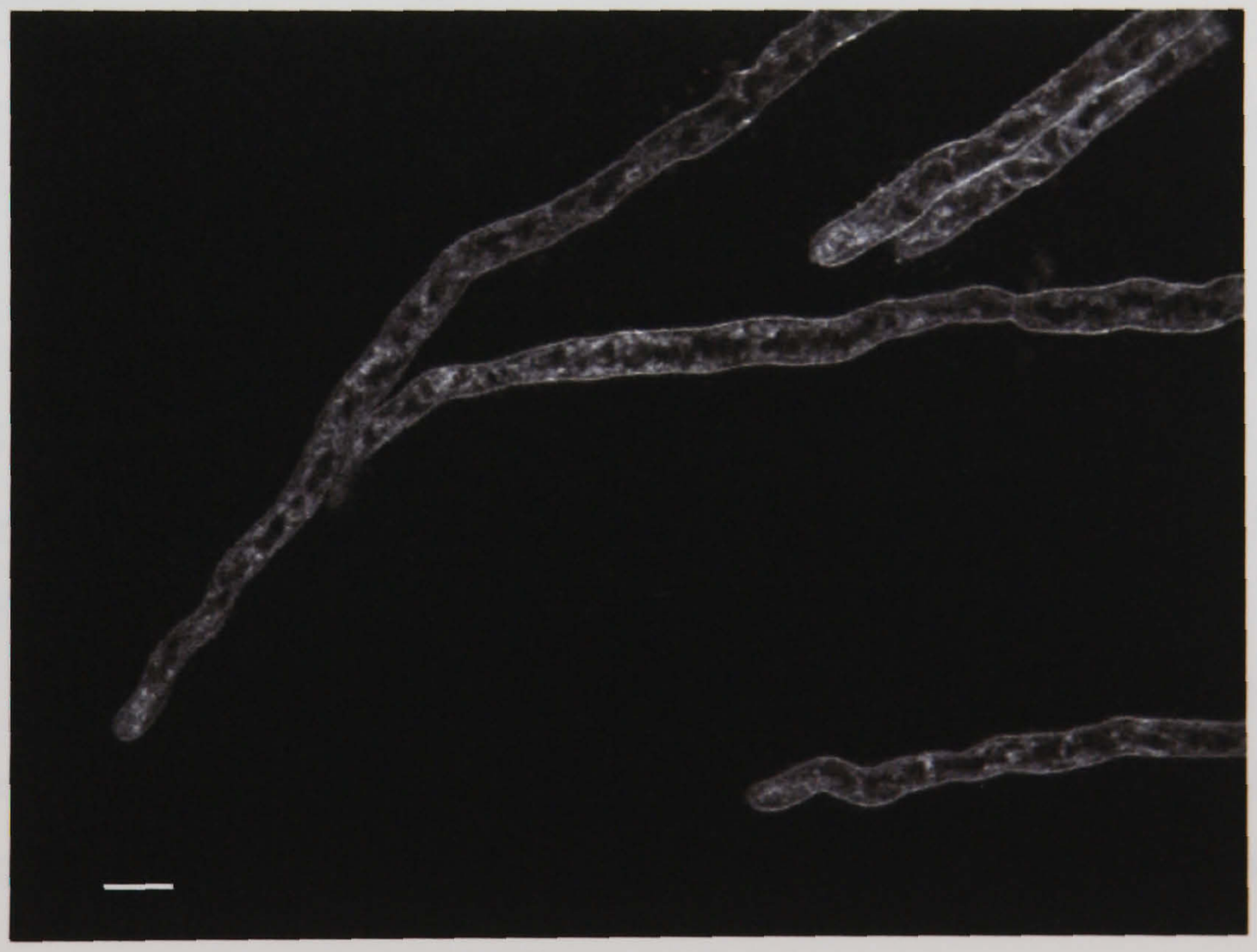

Figure 5.5 Confocal image of growing hyphae on solid medium after staining with FM4-64. Imaged using a x60 oil objective. Bar = 10 μM.

Analysis of the effects of Ca^{2+}-agonists on hyphal morphology and branching were conducted as described in Sections 2.7 and 2.8. It is important to note that only

lowest effective concentrations of agonists (see Section 4.2.2.2.1) were used in order to reduce non-specific side-effects caused by higher concentrations of the Ca^{2+} modulators.

Results presented in Table 5.3 show that A23187 caused a complete inhibition of the growth of individual hyphae 2.5 h after the cultures had been transferred on to the drug containing medium. Caffeine caused an initial inhibition of hyphal tip growth. However, after 2.5 h on the medium containing caffeine, tip growth was resumed. CPA was found not to stop the hyphal tip growth during the period of the experimentation (4.5 h).

Ca^{2+} agonist	**0.5 h**	**1.5 h**	**2.5 h**	**3.5 h**	**4.5 h**
10 µM A23187	yes	yes	no	no	no
20 µM CPA	yes	yes	yes	yes	yes
5 mM Caffeine	no	no	yes	yes	yes

Table 5.3 Effect of Ca^{2+} agonists on hyphal tip growth. Minimum of 5 hyphal tips were analysed at each time point. yes = growth evident, no = no growth.

When studying the effect of Ca^{2+} agonists on hyphal morphology it was found that 10 µM A23187 caused a significant change in hyphal morphology (Fig. 5.6). The first changes were observed 1 h after continuous incubation with A23187. Treatment with A23187 resulted in the form of swollen tips and multiple short branches particularly in the apical hyphal region. Two hours after treatment with A23187 some hyphae started to form bulbous hyphae tips which commonly lysed (Fig. 5.7). These data confirmed the suggestion (Section 4.3) that A23187 causes hyphal death.

control 10 μM A23187 (1 h) 10 μM A23187 (3 h)

Figure 5.6 Effects of A23187 on hyphal morphology and branching of *A. awamori* grown on solid medium for 24 h. Confocal images after staining with FM4-64 and images with a x60 oil objective. Bar = 10 μm.

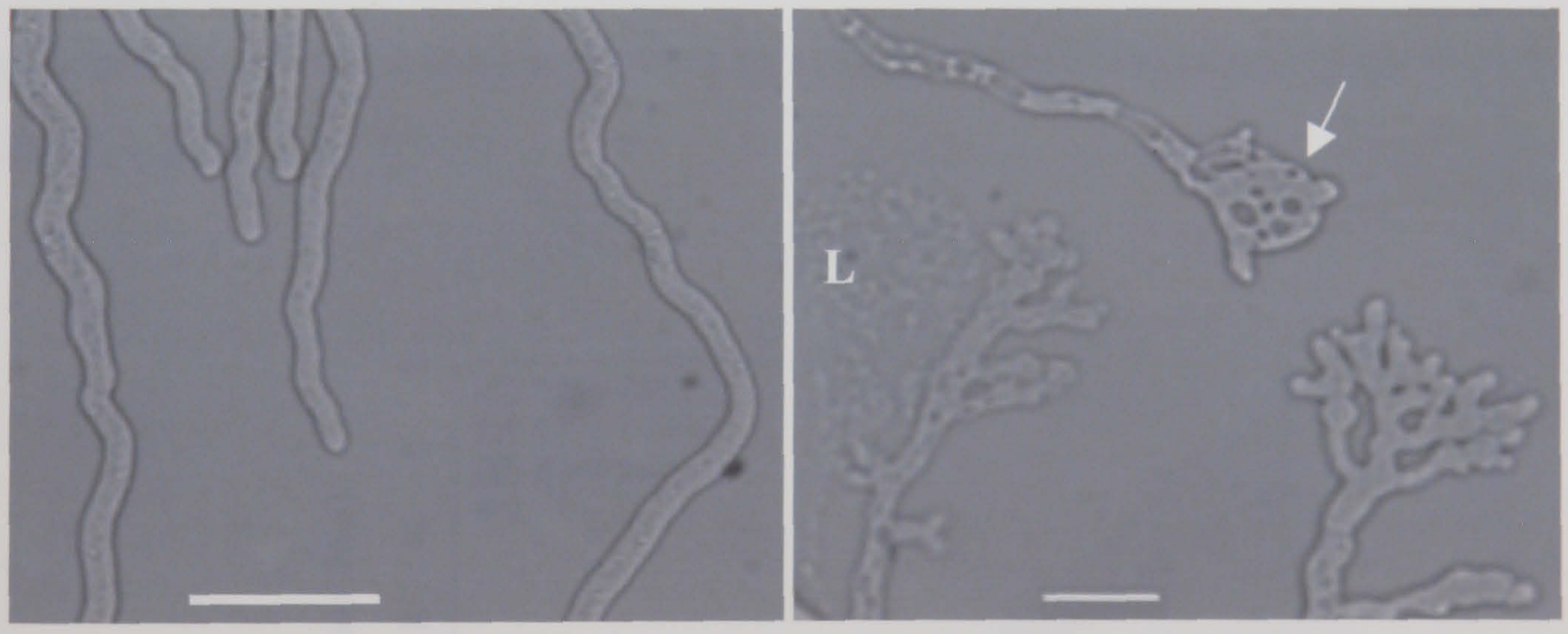

control 10 μM A23187 (3 h)

Figure 5.7 Effects of A23187 on hyphal morphology and branching of *A. awamori* grown on cellophane on solid medium for 24 h. Brightfield images obtained using x40 dry objective. Arrow indicates bulbous cell. L = lysis of hyphae. Bar = 10 μm.

Five mM caffeine and 20 μM CPA did not have a significant effect on hyphal morphology.

5.2.4 Analysis of the effects of Ca^{2+} modulators on growth rate and sporulation

5.2.4.1 Physico-chemical treatments (high external $CaCl_2$)

Due to the experimental set up (see Section 2.6), only one physico-chemical treatment was studied: addition of high external $CaCl_2$ (0.5 mM and 5 mM). Following the treatment of 24 h old cultures with $CaCl_2$ the radii of the fungal colonies were measured at 24 h intervals and the presence and intensity of sporulation were assessed visually by comparing the colour of the colonies with the appropriate controls .

It was found that 0.5 mM $CaCl_2$ did not affect colony growth or sporulation. 5 mM $CaCl_2$ had no effect on the sporulation but caused a slight increase in the growth rate after 72 h (Fig. 5.8).

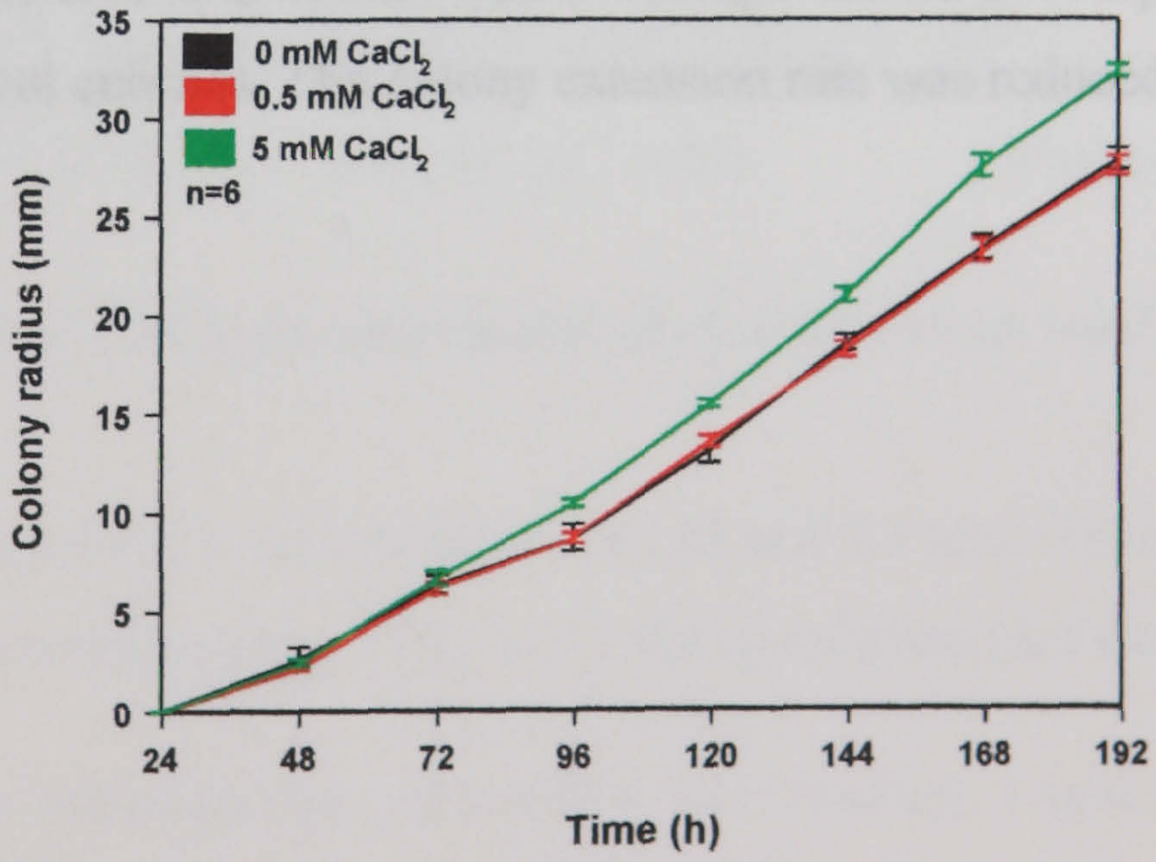

Figure 5.8 Effect of external $CaCl_2$ on colony growth. Results represent mean ± SE.

5.2.4.2 Pharmacological treatments

All pharmacological agents previously found to influence $[Ca^{2+}]_c$ (Section 4.2.2) were tested on their ability to affect growth and sporulation of *A. awamori*.

With the Ca^{2+} antagonists two concentrations were chosen: the IC_{50} concentration and the highest concentration which was applied during the luminometry experiments. With KP4 the highest concentration used was 5.4 μM due to the limited quantity of the compound available. The highest concentration of BAPTA tested was 5 mM due to its limited solubility.

With most agonists only the lowest effective concentrations determined in the luminometry assay (see Section 4.2.2.2) were studied due to the high cost of these chemicals, with the exception of caffeine where 2 concentrations were used.

5.2.4.2.1 Ca^{2+} antagonists

Two concentrations of $LaCl_3$ were tested: 10 mM and 20 mM. 10 mM $LaCl_3$ did not affect sporulation (not shown) but did cause a significant increase in the growth rate after 120 h ($P < 0.05$) (Fig. 5.9). 20 mM of $LaCl_3$ caused inhibition of both the growth rate and sporulation starting at 72 h (Figs. 5.9 and 5.10). The sporulation observed after treatment with 20 mM $LaCl_3$ was light brown in comparison with dark brown of the control cultures. The colony extension rate was reduced by ~30%.

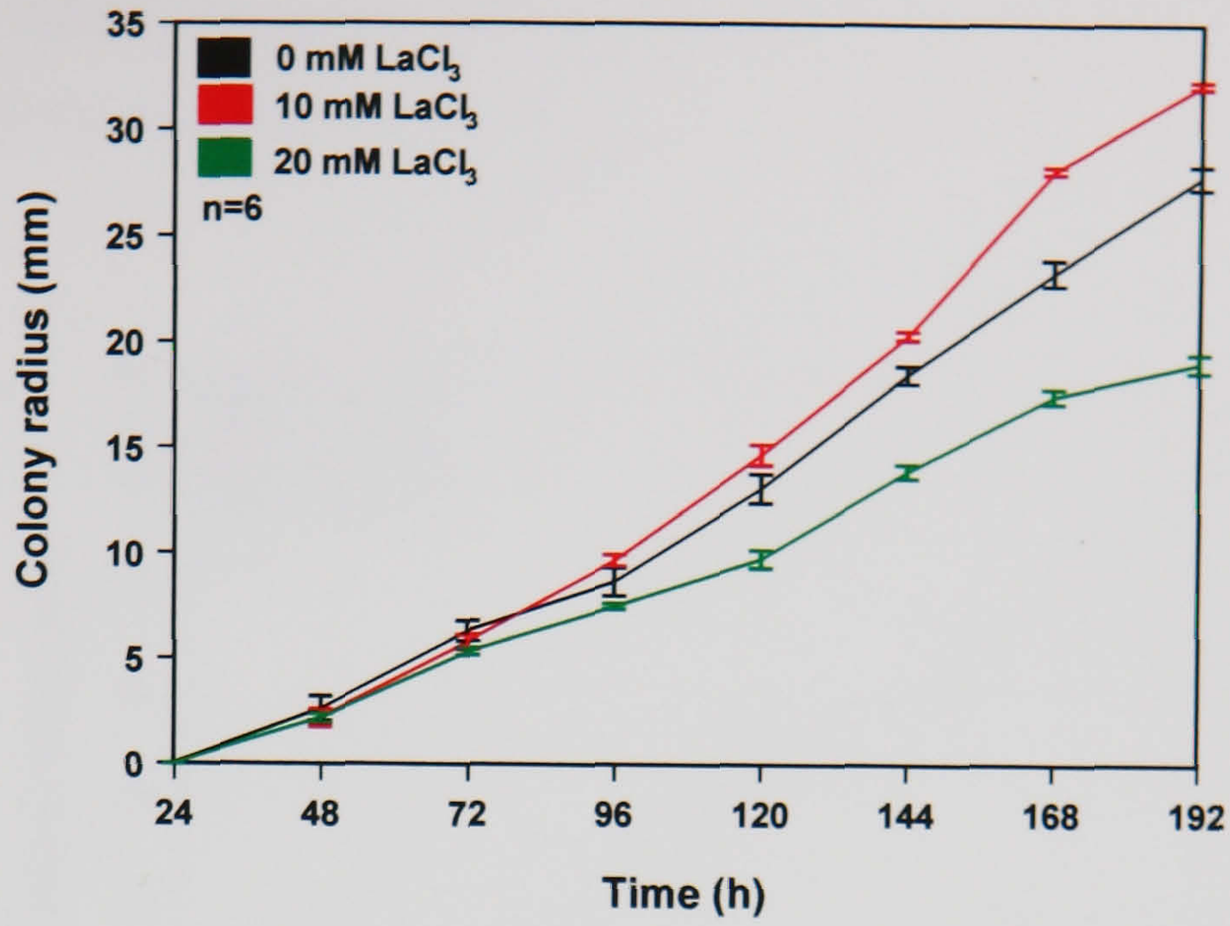

Figure 5.9 Effect of $LaCl_3$ on colony extension rate of *A. awamori* on solid medium. Results represent mean ± SE.

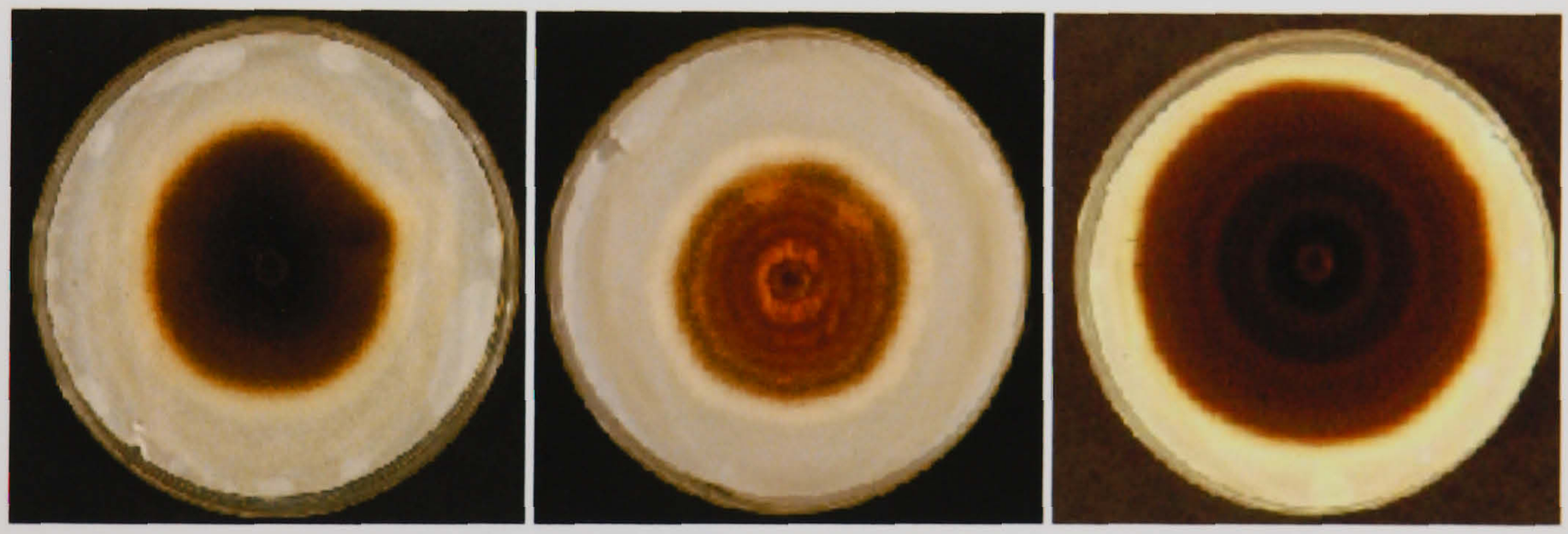

0 mM La^{3+} 120 h 20 mM La^{3+} 168 h 0 mM La^{3+} 168 h

Figure 5.10 Effect of $LaCl_3$ on sporulation of *A. awamori* on solid medium

Two concentrations of KP4 were studied: 0.4 μM and 5.4 μM. Neither concentration affected the colony extension rate (Fig. 5.11) and sporulation (not shown).

The effects of two concentrations of BAPTA were studied: 1 mM and 5 mM (Fig. 5.12). 1 mM BAPTA did not have a significant effect on the colony extension or sporulation. The extension rate was 97-98% of the control. 5 mM BAPTA strongly inhibited the colony extension rate of the fungus. The growth inhibition was

observed immediately after transfer onto the medium containing the drug. During the experiment the colony extension rate was 25-30% after 24 h and 18-20% of the extension rate of the control after 192 h.

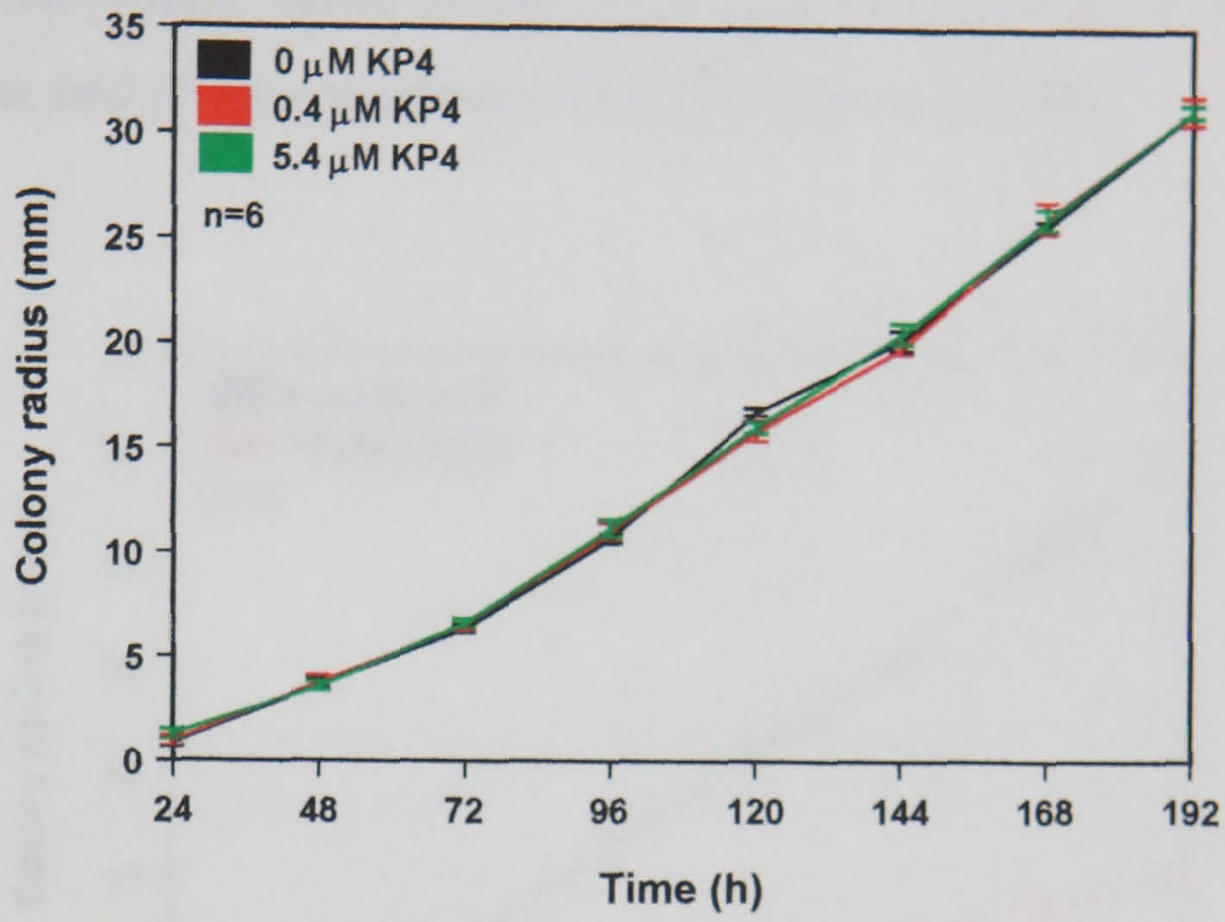

Figure 5.11 Effect of KP4 on the colony extension rate of *A. awamori* on solid medium . Results represent mean ± SE.

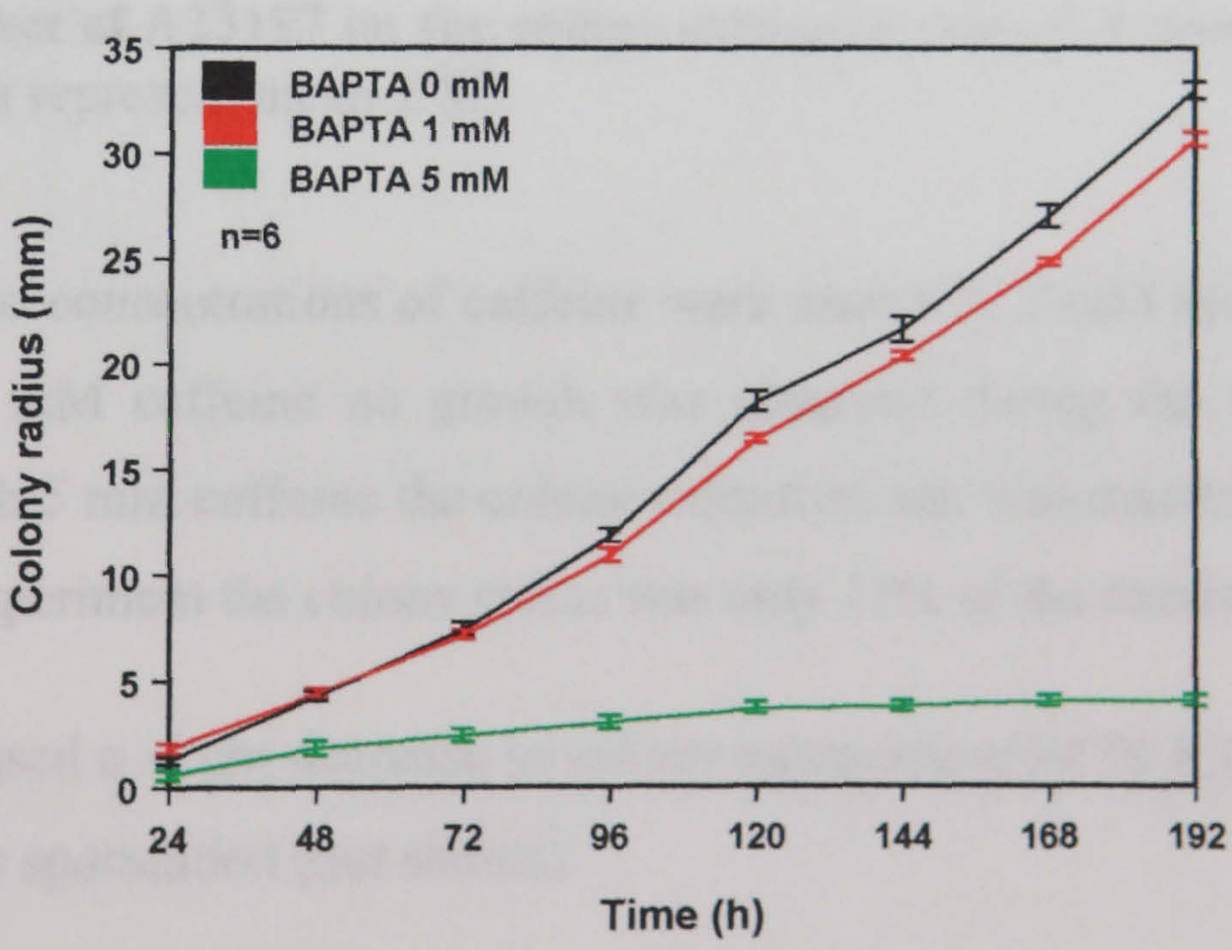

Figure 5.12 Effect of BAPTA on the colony extension rate of *A. awamori* on solid medium. Results represent mean ± SE.

5.2.4.2.2 Ca^{2+} agonists

10 μM A23187 caused a large decrease in the colony extension rate (Fig. 5.13) but had little effect on sporulation (data not shown). The decrease in the growth rate was observed immediately after cultures were transferred onto the medium containing the drug. After 48 h the colony radius on the medium containing A23187 was 54% of the control and by the end of the experiment (192 h) it was only 38%.

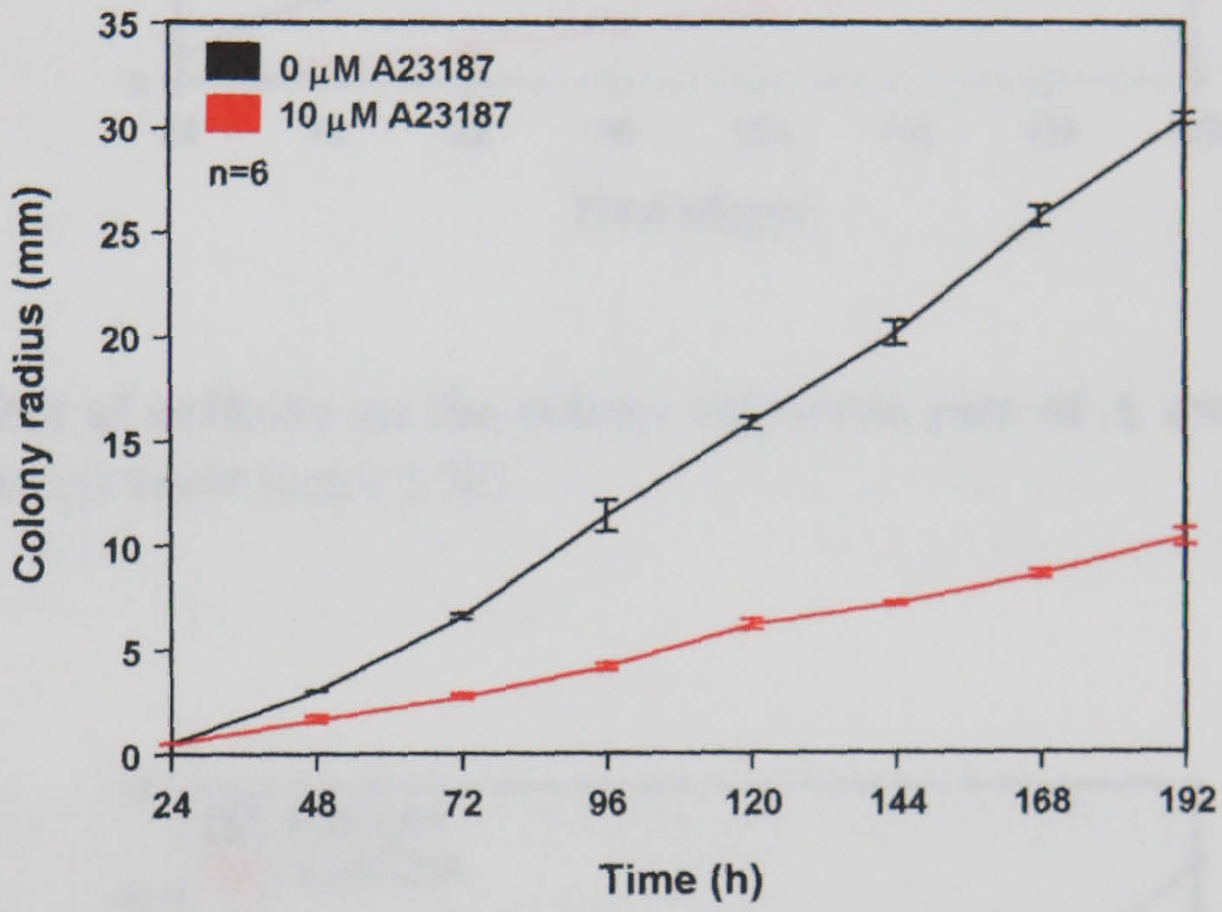

Figure 5.13 Effect of A23187 on the colony extension rate of *A. awamori* on solid medium. Results represent mean ± SE.

The effect of two concentrations of caffeine were analysed: 5 mM and 10 mM (Fig. 5.14). With 10 mM caffeine no growth was observed during the 8 days of the experiment. With 5 mM caffeine the colony extension rate was much reduced and at the end of the experiment the colony radius was only 11% of the control.

20 μM CPA caused a slight decrease in colony extension after 96 h (Fig. 5.15) and did not affect the sporulation (not shown).

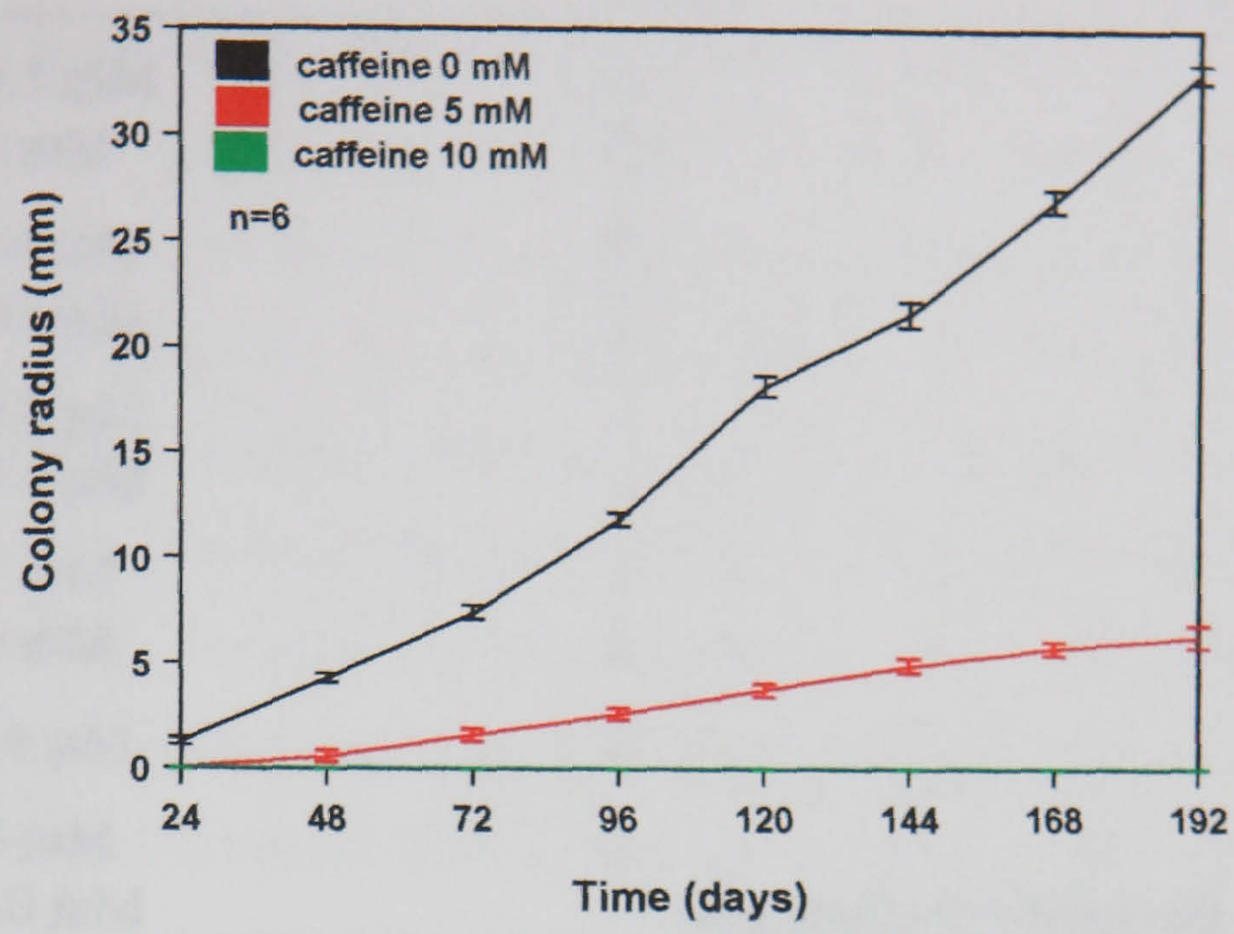

Figure 5.14 Effect of caffeine on the colony extension rate of *A. awamori* on solid medium. Results represent mean ± SE.

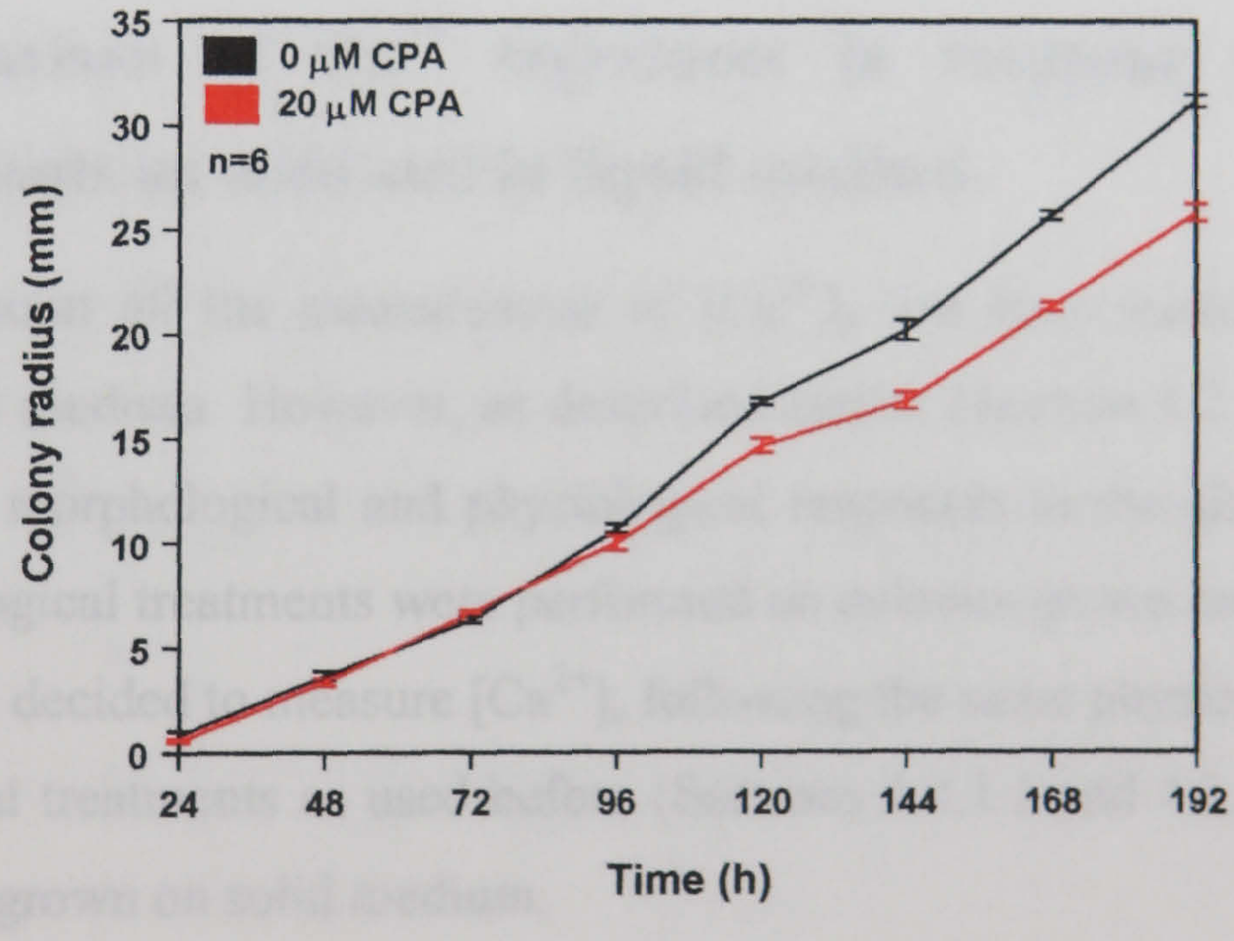

Figure 5.15 Effect of CPA on the colony extension rate of *A. awamori* on solid medium. Results represent mean ± SE.

Treatment		Extension rate	Sporulation
$CaCl_2$	0.5 mM	-	-
	5 mM	↑	-
La^{3+}	10 mM	↑	-
	20 mM	↓	↓
KP4	0.4 µM	-	-
	5.4 µM	-	-
BAPTA	1 mM	-	-
	5 mM	↓	↓
A23187	10 µM	↓	-
Caffeine	5 mM	↓	↓
	10 mM	no growth was observed	
CPA	20 µM	↓	-

Table 5.4 Effect of the different Ca^{2+} modulating treatments on colony extension rate and sporulation. n = 6. Abbreviations: ↑ = increase in parameter, ↓ = decrease in parameter, - = no change in parameter.

5.2.5 Comparison of Ca^{2+} signatures in response to different treatments on solid and in liquid medium

Up until this point all the measurement of $[Ca^{2+}]_c$ had been made from cultures grown in liquid medium. However, as described earlier (Section 5.2.3) much of the analysis of the morphological and physiological responses to the physico-chemical and pharmacological treatments were performed on cultures grown on solid medium. It was therefore decided to measure $[Ca^{2+}]_c$ following the same physico-chemical and pharmacological treatments as used before (Sections 4.2.1.1 and 4.2.2.2) but on the fungal cultures grown on solid medium.

In order to obtain $[Ca^{2+}]_c$ measurements with fungus grown on solid medium a new method of growing *A. awamori* in 96-well microplates using solid VS medium was developed (see Section 2.2.4). 100 µl of solid medium within individual wells were inoculated with spores and 24 h old cultures were then subjected to the different treatments.

5.2.5.1 Physico-chemical treatments

Initially three physico-chemical treatments were analysed: mechanical perturbation, hypo-osmotic shock and high external $CaCl_2$ (5 mM). The general trend of the $[Ca^{2+}]_c$ responses of cultures grown on solid or in liquid media were similar (Figs. 5.16-5.18). On solid medium the amplitudes of the $[Ca^{2+}]_c$ response to mechanical perturbation was the smallest and highest with 5 mM $CaCl_2$, and all of these responses were significantly higher than the $[Ca^{2+}]_c$ amplitudes achieved by cultures in response to those treatments in liquid culture. The FWHM of each $[Ca^{2+}]_c$ response on solid medium was also significantly greater than in liquid medium. Following all three treatments $[Ca^{2+}]_c$ returned to resting level within 5 min, no secondary $[Ca^{2+}]_c$ responses were observed and rise times and lag times were the same as when the fungi were grown in liquid medium. It is important to note that the increase in $[Ca^{2+}]_c$ amplitude was very different from experiment to experiment and therefore no quantitative data for statistical analyses were obtained.

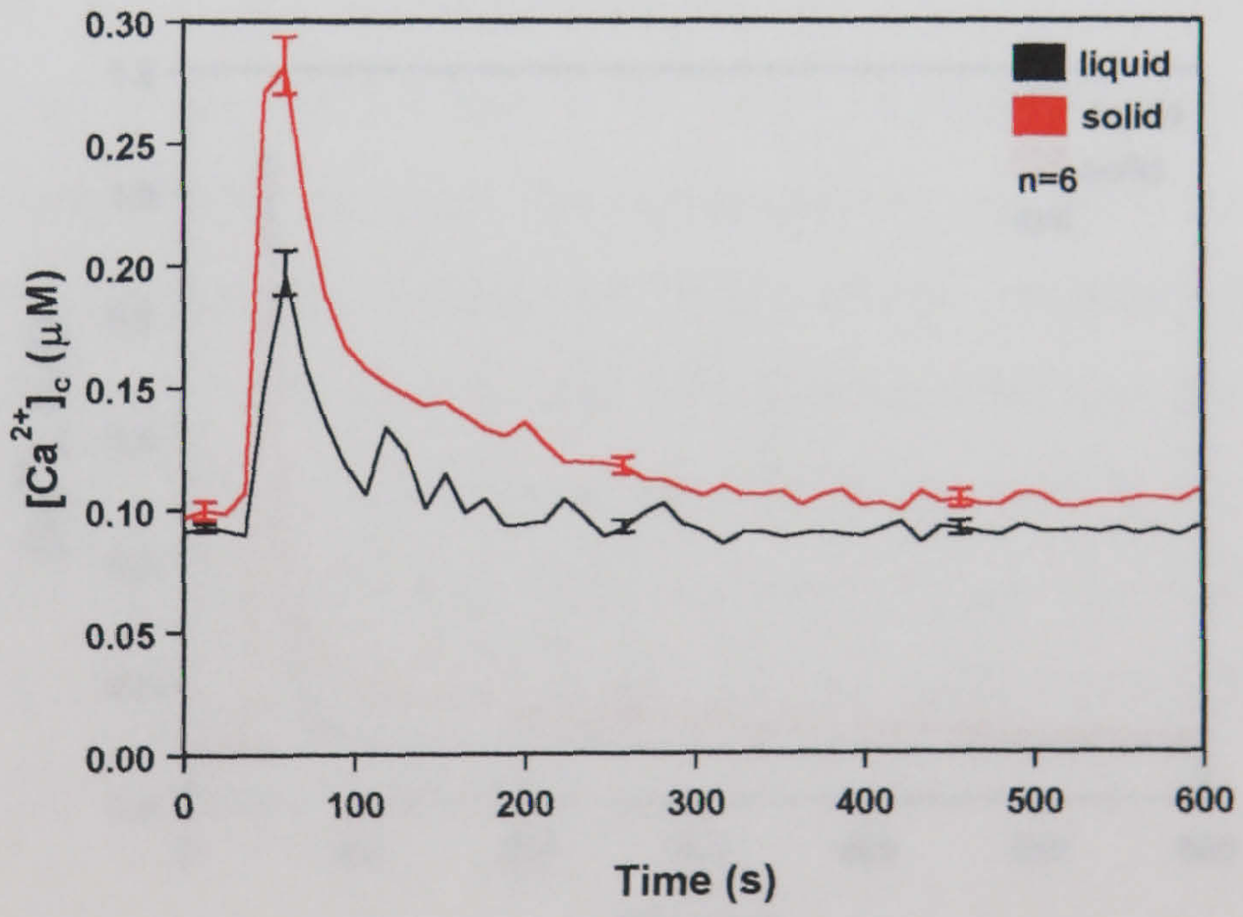

Figure 5.16 Effect of mechanical perturbation on $[Ca^{2+}]_c$ in cultures grown on solid and in liquid media. Results represent mean ± SE. Measurements were performed using the repeated measuring protocol. Cycle time 11.6 s.

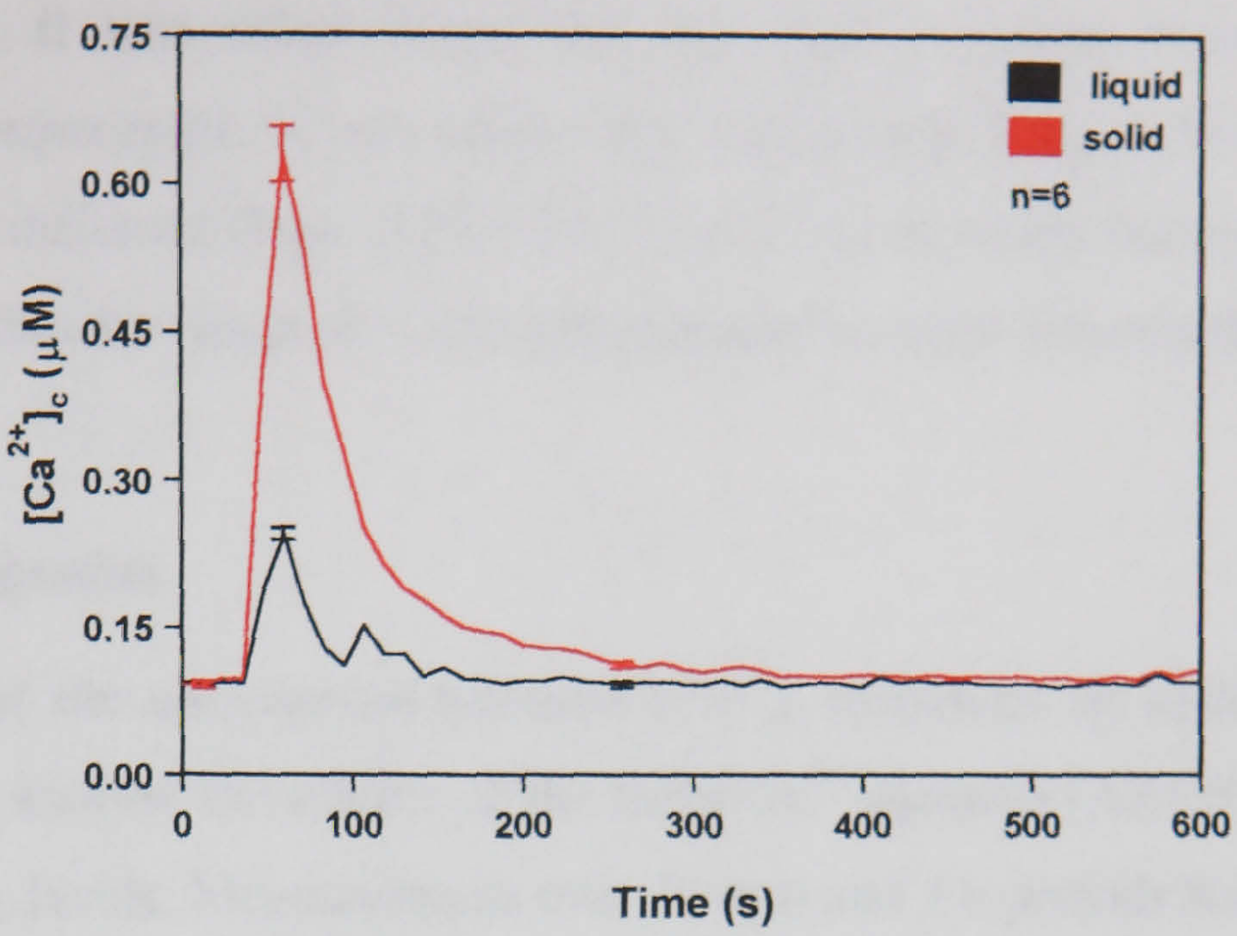

Figure 5.17 Effect of hypo-osmotic shock on $[Ca^{2+}]_c$ in cultures grown on solid and in liquid media. Results represent mean ± SE. Measurements were performed using the repeated measuring protocol. Cycle time 11.6 s.

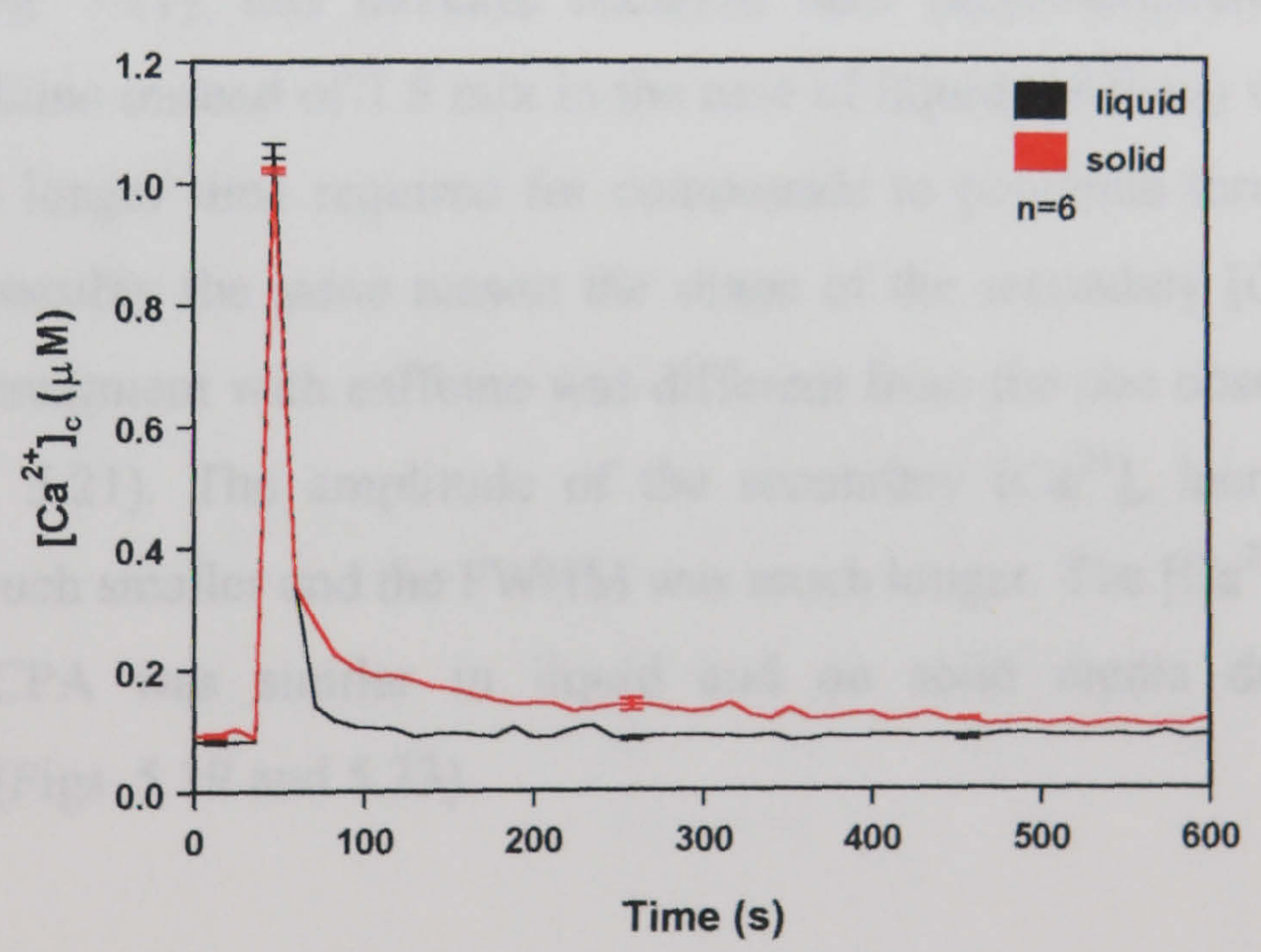

Figure 5.18 Effect of external $CaCl_2$ (5 mM) on $[Ca^{2+}]_c$ in cultures grown on solid and in liquid media. Results represent mean ± SE. Measurements were performed using the repeated measuring protocol. Cycle time 11.6 s.

In comparing $[Ca^{2+}]_c$ levels in cultures grown on solid medium with those grown in liquid medium, it was often found that the $[Ca^{2+}]_c$ resting level varied from experiment to experiment. It was often very similar (e.g. Figs. 5.16-5.18, 5.22) but also commonly different (Figs. 5.19-5.21, 5.23-5.24). It varied between 0.45 μM to 1.2 μM well within the range of < 200 nM recorded in other systems (Bush 1995).

5.2.5.2 Ca^{2+} agonists

The next part of the comparison between $[Ca^{2+}]_c$ responses on solid and in liquid medium was to analyse the effects of the three Ca^{2+} agonists (A23187, caffeine and CPA) on $[Ca^{2+}]_c$ levels. Measurements over 10 min and 5 h periods following agonist treatment were performed. Interestingly, the results of short term measurements (10 min) on solid medium were more similar to the ones obtained with cultures grown in liquid medium. The primary $[Ca^{2+}]_c$ increase in each case was probably a response to mechanical perturbation when the agonist was added. This increase was followed by a secondary $[Ca^{2+}]_c$ increase, which was the specific effect of the agonist. In the case of caffeine (Fig. 5.21), this increase occurred later (approximately 5 min after addition of caffeine instead of 1.5 min in the case of liquid medium) which possibly was due to the longer time required for compounds to penetrate through the solid medium. For possibly the same reason the shape of the secondary $[Ca^{2+}]_c$ increase observed after treatment with caffeine was different from the one observed in liquid medium (Figs. 5.21). The amplitude of the secondary $[Ca^{2+}]_c$ increase on solid medium was much smaller and the FWHM was much longer. The $[Ca^{2+}]_c$ response to A23187 and CPA was similar in liquid and on solid media during 10 min measurements (Figs. 5.19 and 5.23).

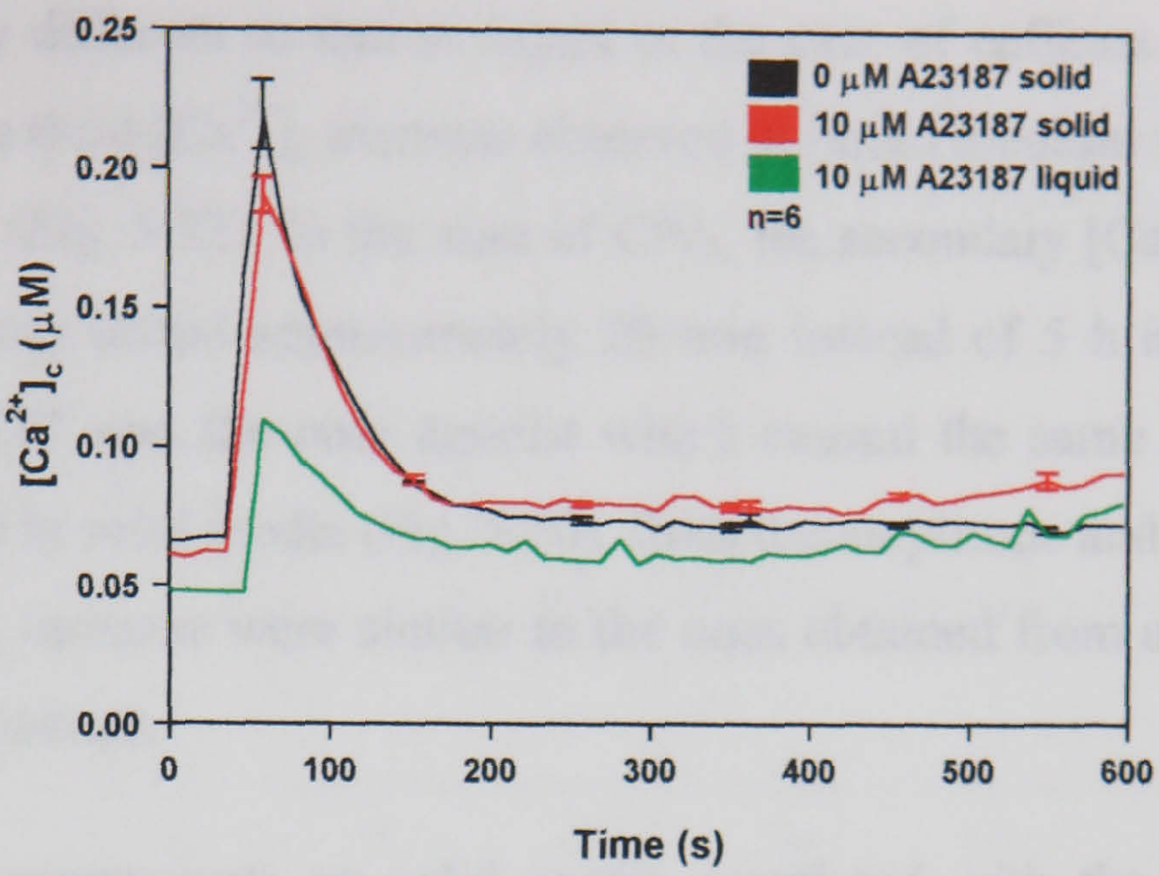

Figure 5.19 Effect of A23187 on $[Ca^{2+}]_c$ in cultures grown on solid and liquid VS medium (measurements over 10 min). Results represent mean ± SE. The data for $[Ca^{2+}]_c$ measurements from liquid medium is taken from Fig. 4.20. Measurements were performed using the repeated measuring protocol. Cycle time 11.6 s.

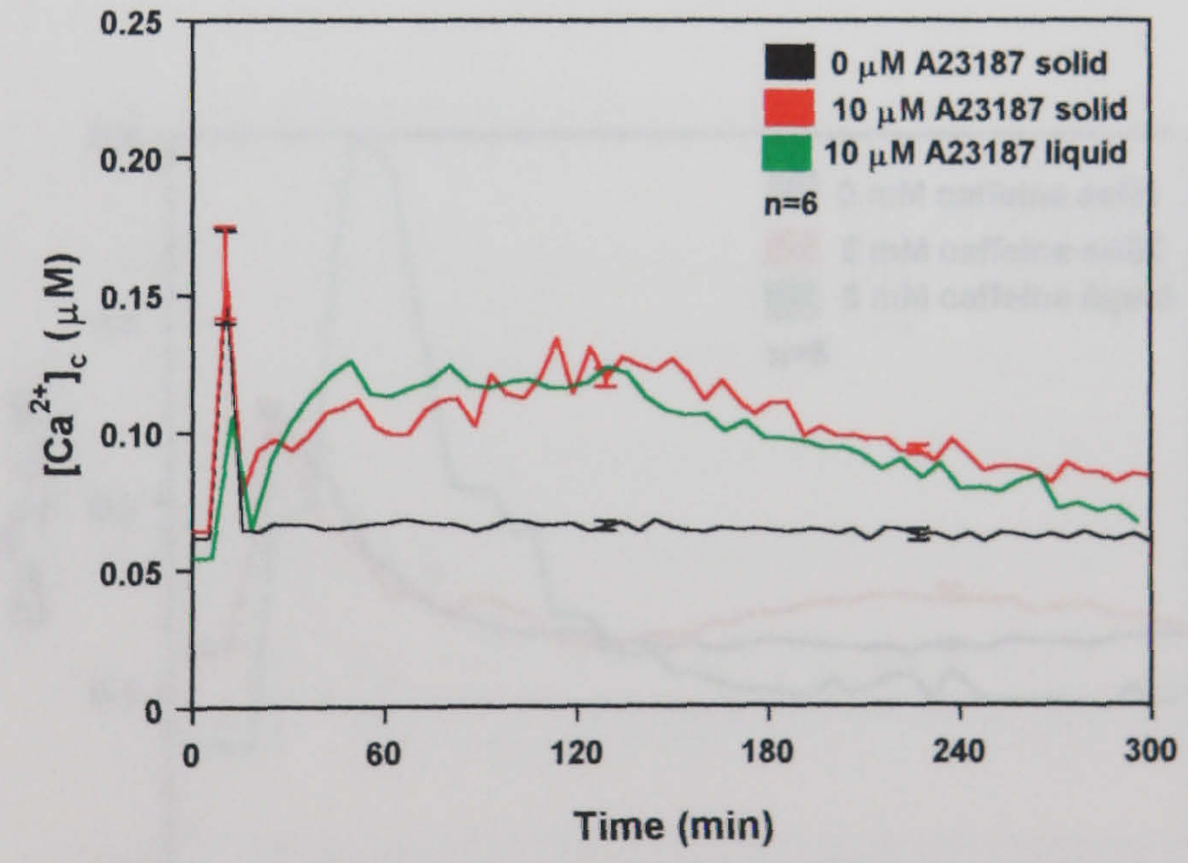

Figure 5.20 Effect of A23187 on $[Ca^{2+}]_c$ in cultures grown on solid and in liquid VS medium (measurements over 5 h). Results represent mean ± SE. The data for $[Ca^{2+}]_c$ measurements from liquid medium is taken from Fig. 4.21. Measurements were performed using the repeated measuring protocol. Cycle time 5.2 min.

The long term measurements performed showed that the $[Ca^{2+}]_c$ response on solid medium was very different to that in liquid in the case of caffeine and CPA. In the case of caffeine, a third $[Ca^{2+}]_c$ increase observed in liquid medium was not observed on solid medium (Fig. 5.22). In the case of CPA, the secondary $[Ca^{2+}]_c$ increase was very small and only lasted approximately 20 min instead of 5 h in liquid medium (Fig. 5.24). A23187 was the only agonist which caused the same $[Ca^{2+}]_c$ response both in liquid and in solid media (Fig. 5.20). Both the amplitude and the length of the secondary $[Ca^{2+}]_c$ increase were similar to the ones obtained from using the cultures grown in liquid medium.

These $[Ca^{2+}]_c$ measurements on solid media correlated with the observations on hyphal morphology described in Section 5.2.3.2. Caffeine and CPA at the concentrations tested did not results in long term increases in $[Ca^{2+}]_c$ and did not affect hyphal morphology whereas A23187 resulted in long term $[Ca^{2+}]_c$ increases and caused hyperbranching with the formation of the bulbous cells.

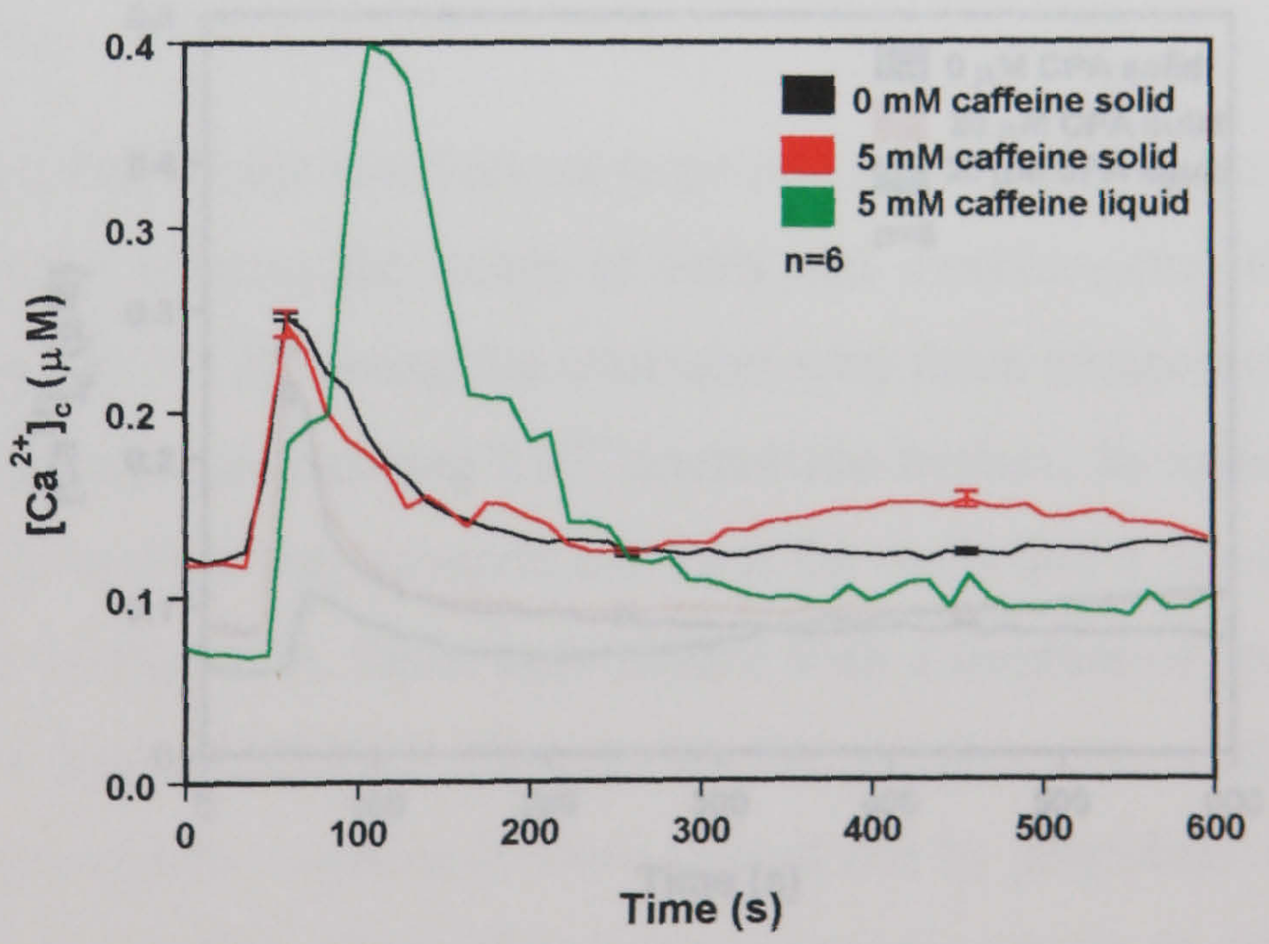

Figure 5.21 Effect of caffeine on $[Ca^{2+}]_c$ in cultures grown on solid and in liquid VS medium (measurements over 10 min). Results represent mean ± SE. The data for $[Ca^{2+}]_c$ measurements from liquid medium is taken from Fig. 4.22. Measurements were performed using the repeated measuring protocol. Cycle time 11.6 s.

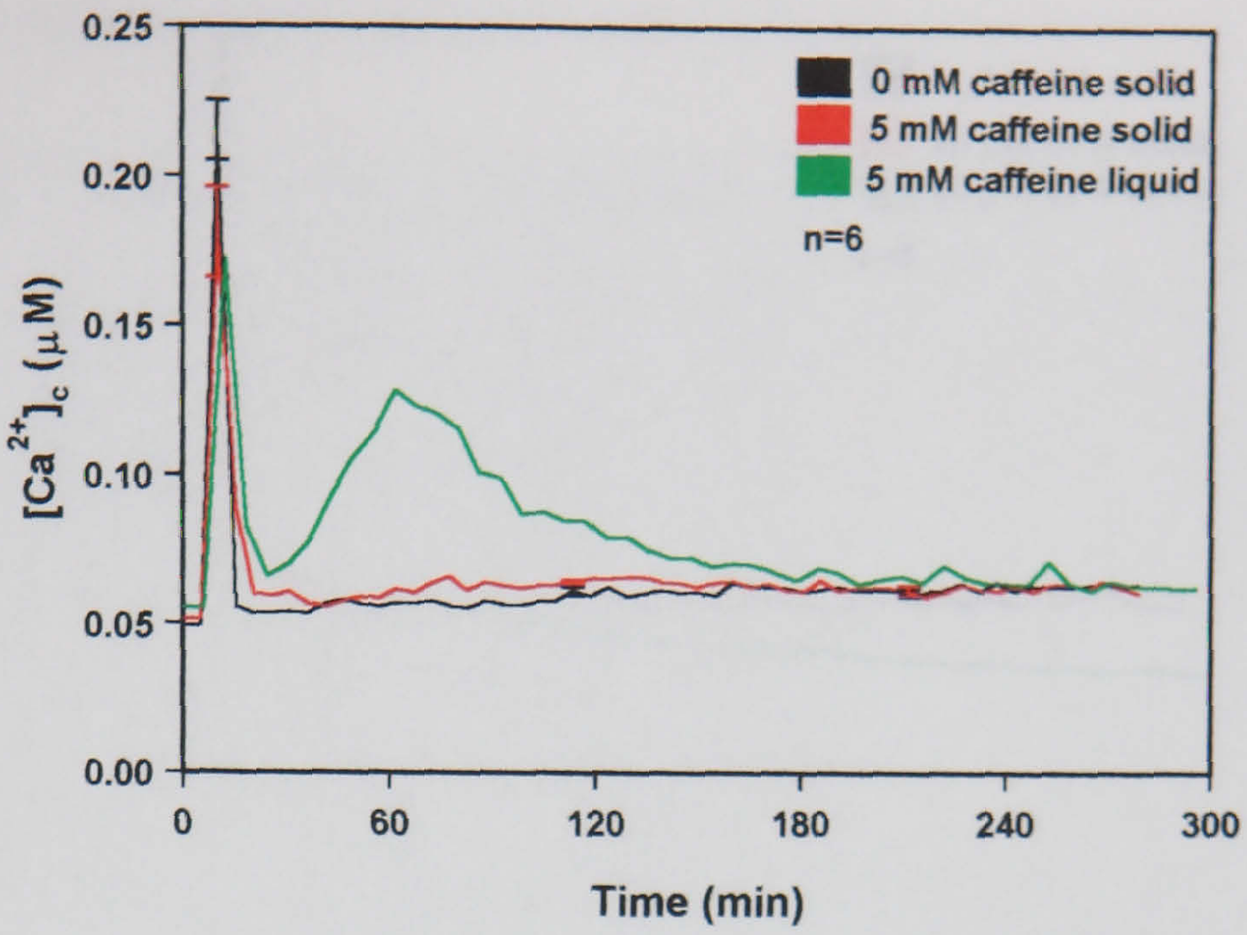

Figure 5.22 Effect of caffeine on $[Ca^{2+}]_c$ in cultures grown on solid and in liquid VS medium (measurements over 5 h). Results represent mean ± SE. The data for $[Ca^{2+}]_c$ measurements from liquid medium is taken from Fig. 4.21. Measurements were performed using the repeated measuring protocol. Cycle time 5.2 min.

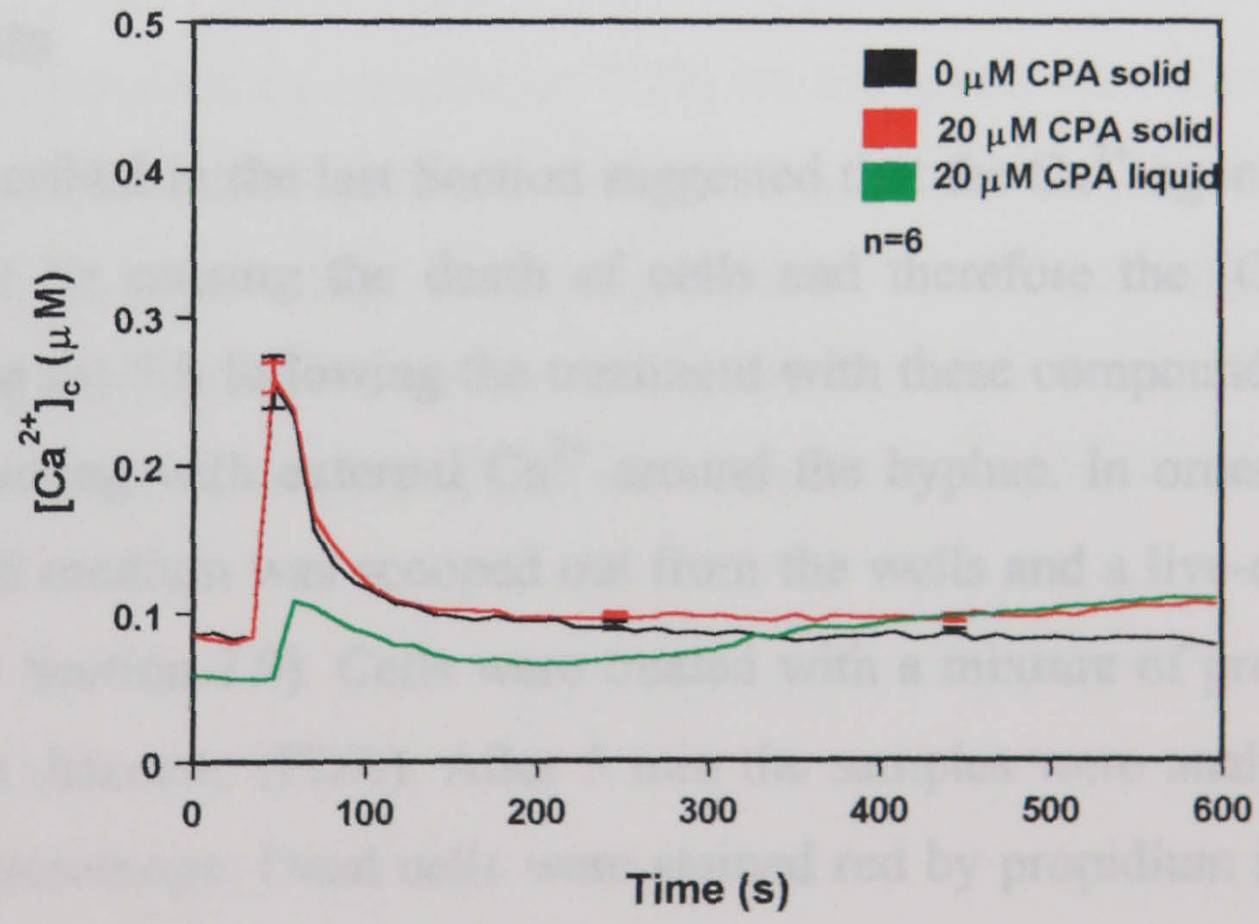

Figure 5.23 Effect of CPA on $[Ca^{2+}]$ in cultures grown on solid and in liquid VS medium (measurements over 10 min). Results represent mean ± SE. The data for $[Ca^{2+}]_c$ measurements from liquid medium is taken from Fig. 4.24. Measurements were performed using the repeated measuring protocol. Cycle time 11.6 s.

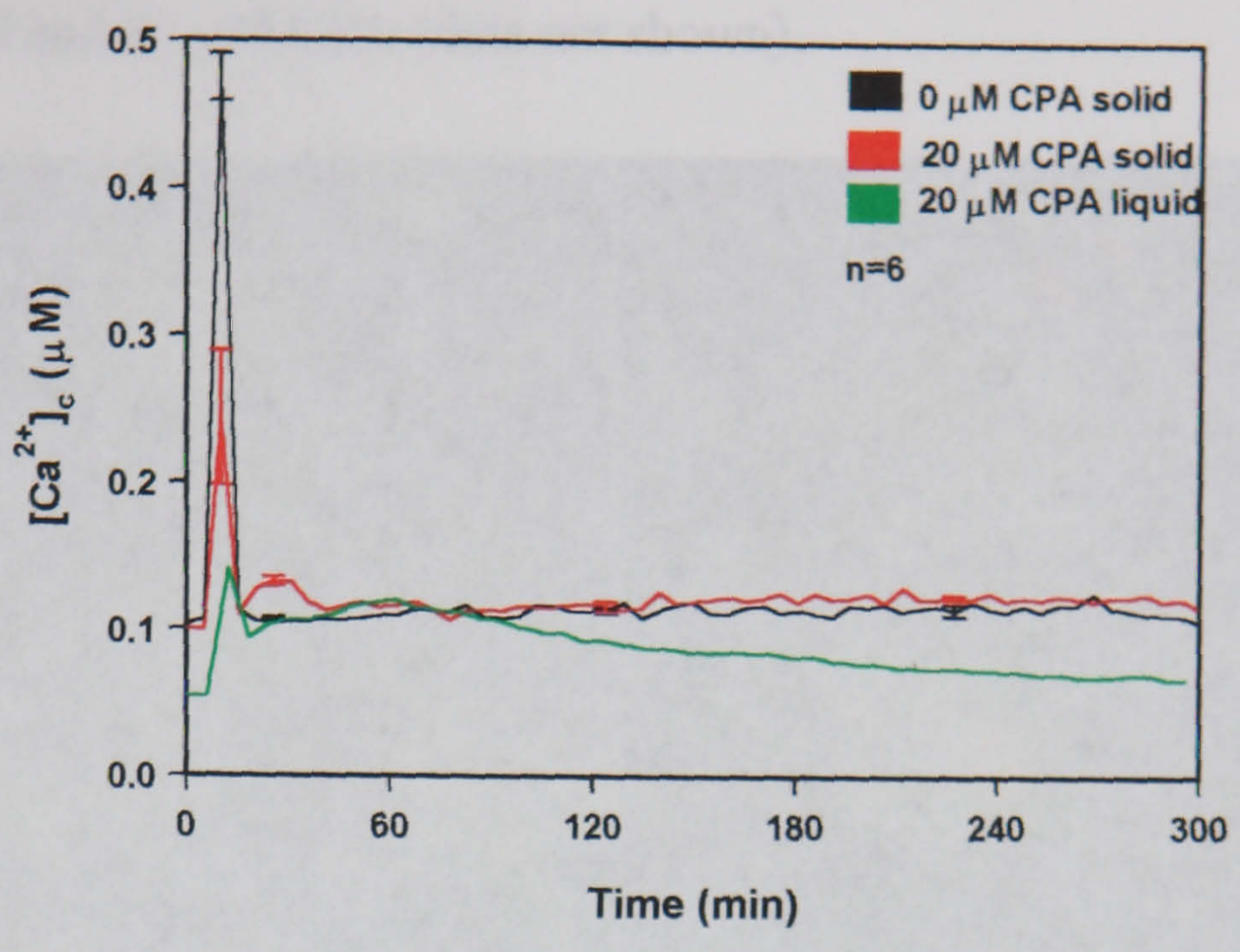

Figure 5.24 Effect of CPA on $[Ca^{2+}]_c$ in cultures grown on solid and in liquid VS medium (measurements over 5 h). Results represent mean ± SE. The data for $[Ca^{2+}]_c$ measurements from liquid medium is taken from Fig. 4.21. Measurements were performed using the repeated measuring protocol. Cycle time 5.2 min.

5.2.6 Live-dead analysis of cultures treated with different Ca^{2+} agonists

The results described in the last Section suggested that the Ca^{2+}-agonists (especially A23187) might be causing the death of cells and therefore the $[Ca^{2+}]_c$ response observed during the 5 h following the treatment with these compounds, was a result of aequorin reacting with external Ca^{2+} around the hyphae. In order to check this hypothesis solid medium was scooped out from the wells and a live-dead assay was performed (see Section 2.9). Cells were treated with a mixture of propidium iodide and fluorescein diacetate (FDA). After 5 min the samples were analysed under the fluorescence microscope. Dead cells were stained red by propidium iodide and live cells were stained green by FDA. The observations were made in 10 fields of view before a final assessment was made of the ratio of live/dead hyphae. After 3 h incubation with 5 mM caffeine approximately 5% cell death was observed. The amount of green hyphae both in the control and in the experimental treatment was similar (Fig. 5.25). This probably represented the natural death of hyphae, possibly

due to the mechanical perturbation during slide preparation. Similar results were obtained with 0 and 20 μM CPA (data not shown).

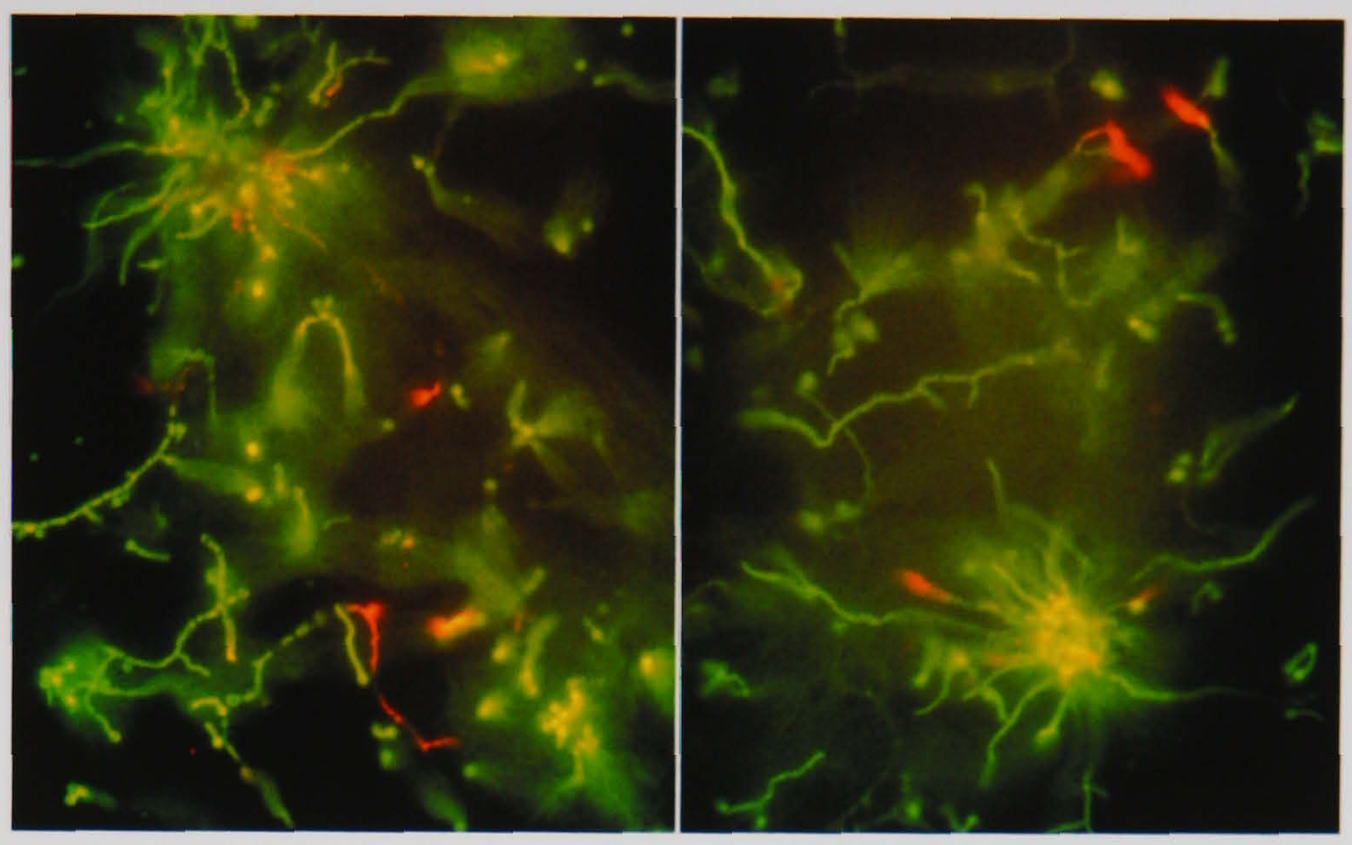

Control Caffeine 5 mM

Figure 5.25 Representative images of cultures grown for 3 h on media containing 5 mM caffeine or in the absence of the Ca^{2+} agonist (control). Stained with propidium iodide and FDA.

With 10 μM A23187 approximately 50% of hyphae were estimated to be dead whereas the control cultures containing 0.5% EtOH, which was similar to the EtOH concentration in the A23187 cultures, 95% of the hyphae were green (Fig. 5.26). It is important to also mention that in the top layer of the fungal colony most of the hyphae were dead, whilst in the lower layers more of the hyphae were alive. However, when imaging deep into the agar the optics were poor making fluorescence imaging difficult.

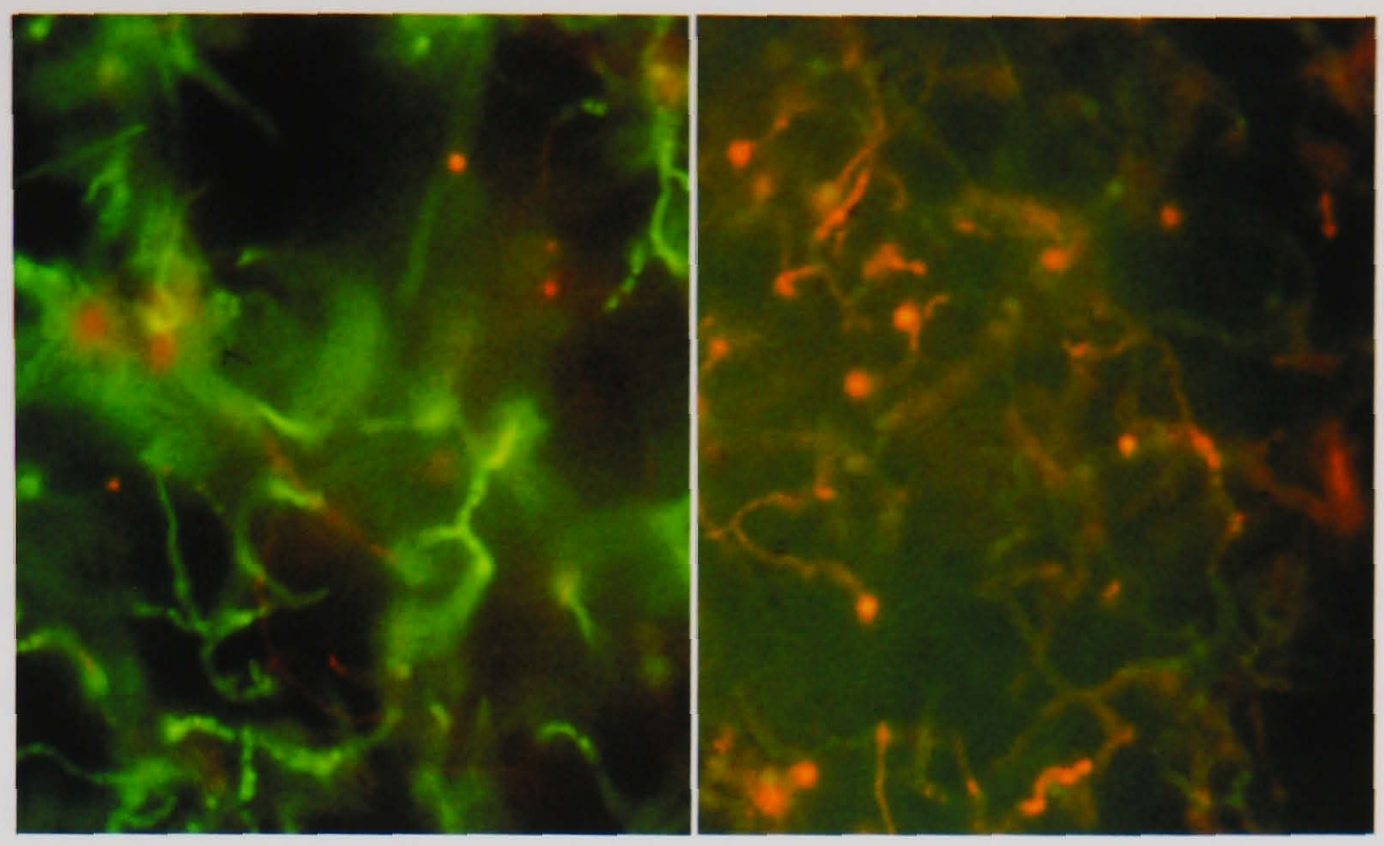

Control A23187 10 μM

Figure 5.26 Representative images of the cultures grown for 3 h on media containing 10 μM A23187 or in the absence of the Ca^{2+} agonist. Stained with propidium iodide and FDA.

5.3 DISCUSSION

One aim of the work described in this chapter was to attempt to identify morphological or physiological responses (colony extension rate, sporulation, hyphal tip morphology and hyphal branching) which resulted from physico-chemical treatments (mechanical perturbation, hypo-osmotic shock and high external $CaCl_2$) which had previously been shown to transiently increase $[Ca^{2+}]_c$ (see Section 4.2.1.1). Unfortunately growth rate, sporulation and hyphal branching were unaffected by these treatments.

The second aim was to try to determine whether the colony extension rate, sporulation and hyphal branching were Ca^{2+}-regulated by perturbing Ca^{2+} signalling and/or homeostasis within hyphae by using various pharmacological agents. It was shown that high concentrations of Ca^{2+} antagonists (5 mM BAPTA and 20 mM La^{3+}) inhibited both the colony extension rate and sporulation. On the contrary KP4 affected neither parameter. All Ca^{2+} agonists inhibited the extension rate of *A.*

awamori and with 10 mM caffeine no growth was observed during the 8 day experiment.

The Ca^{2+}-selective ionophore A23187 at a concentration of 10 μM was found to result in increased abnormal branching in *A. awamori* when grown on solid medium. Previously at this concentration A23187 was shown to cause an increase in branching in *Neurospora crassa* and *Fusarium graminearum* grown on solid medium (Reissig and Kinney 1983; Robson et al. 1991a). CPA and caffeine were shown not to affect hyphal branching.

The difficulties in conducting and analysing experiments in liquid medium (e.g. due to the precipitation of some pharmacological agents and 3D growth) made it necessary to perform experiments on solid VS medium. Therefore, luminometry on cultures grown on solid medium was performed. The most interesting observation made was that the $[Ca^{2+}]_c$ responses to physico-chemical treatments (mechanical perturbation, hypo-osmotic shock and high external $CaCl_2$) exhibited similar patterns both in liquid and on solid media. However, with mechanical perturbation and hypo-osmotic shock higher $[Ca^{2+}]_c$ amplitudes were observed. One possible explanation for these findings was that hyphae do not experience the same stimulation in air and on solid medium compared with in liquid medium, and this may result in different $[Ca^{2+}]_c$ responses.

On the contrary, experiments performed using Ca^{2+}-agonists showed that the $[Ca^{2+}]_c$ response was very different on solid and in liquid media with the exception of the results obtained after treatment with A23187. The different responses may have been because compounds have different diffusion rates and possible different behaviour in liquid compared with solid media. The most interesting observation was that no changes in hyphal branching after treatment with caffeine or CPA (two chemicals which did not cause a long term increase in $[Ca^{2+}]_c$ in hyphae growing on solid medium [Figs. 5.21 and 5.23]) was observed, whereas the hyphal branching was severally perturbed when cultures were treated with A23187 (which caused a long term $[Ca^{2+}]_c$ increase [Fig. 5.19]).

A particularly important question in the present study was whether A23187 was toxic to cells, and if so, whether this was due to it perturbing the $[Ca^{2+}]_c$ balance or whether the cytotoxicity resulted from some other side-effect. I found that 10 μM A23187 caused the following:

- A secondary long term (5 h) increase in $[Ca^{2+}]_c$, which started 20 min after agonist treatment (Fig. 5.20).
- A decrease in the colony extension rate 2.5 h after adding the agonist (Table 5.3, Fig. 5.12)
- Hyperbranching and formation of the bulbous cells 1h after agonist treatment (Fig. 5.7)
- Death of approximately 50% of cells 3 h after treatment (Fig. 5.26).

The perturbation of $[Ca^{2+}]_c$ homeostasis with 10 μM A23187 for such a long time (5 h) seemed to result in changes in hyphal morphology, increased branching and formation of the bulbous cells 2 h after treatment. Many of the hyphae after this period of time lysed and died, which in its turn sustained the long term $[Ca^{2+}]_c$ increase. However, not all hyphae died as colony growth on solid medium in the presence of 10 μM A23187 was found to continue, although at a much slower colony extension rate even after 8 days (see Section 5.2.4.2.2).

In summary the main conclusions from the research described in this chapter were:

- Physico-chemical treatments (mechanical perturbation, hypo-osmotic shock and external $CaCl_2$) which caused a short term increases in $[Ca^{2+}]_c$ did not affect colony extension rate, sporulation or hyphal morphology.
- Ca^{2+} antagonists La^{3+}, BAPTA at high concentrations inhibited sporulation and colony extension rate.
- Ca^{2+} agonists caffeine and CPA, which did not cause the long-term increase in $[Ca^{2+}]_c$ when cultures were grown in solid medium did not affect hyphal

branching but inhibited colony extension rate, and in the case of caffeine. sporulation. A23187 which caused long term increases in $[Ca^{2+}]_c$ significantly perturb hyphal branching and growth and caused hyphal death.

- The $[Ca^{2+}]_c$ responses to physico-chemical stimuli (mechanical perturbation, hypo-osmotic shock and high external $CaCl_2$) in fungi grown in liquid medium compared with those grown on solid medium were similar except the $[Ca^{2+}]_c$ amplitudes in the solid medium grown fungi were greater.

- The effects of Ca^{2+} agonists (caffeine and CPA) were different in solid and liquid media.

6 USE OF THE AEQUORIN METHOD FOR STUDYING THE MODE-OF-ACTION OF ANTIFUNGAL AGENTS

6.1 INTRODUCTION

Filamentous fungi constitute an economically important group of plant and human pathogens. One of the biggest challenges in modern biology is to provide more efficient methods for disease control. By analysing the basic cell biology of fungi it should be possible to identify specific molecular targets for novel antifungal agents which can be used to perturb spore germination, growth and/or development of fungal pathogens (Deacon 1997).

A wider range of antifungal agents are used in plant disease control than are used to treat humans and animals. In the context of plant diseases antifungal agents are commonly referred as fungicides. Fungicides are mainly chemically synthesized and can be subdivided into three groups (Deacon 1997):

- Inorganic fungicides (e.g. sulphur or copper), which have very general mode-of-action.

- Organic contact or protectant fungicides (e.g. dithiocarbamates, dicarboximides) which act only near a site of application. They are used to protect the plant surface or control an established infection.

- Systemic fungicides (e.g benzimidazoles, sterol synthesis inhibitors) which are absorbed by plants and then distributed internally. They can treat even deep-seated infections.

Another group of antifungal agents are used to treat diseases in animals and man. In clinical practice three major groups of antifungal agents are known: azoles, polyenes and allylamine/thiocarbamates. All of these compounds owe their antifungal

activities to inhibition of synthesis of or direct interaction with ergosterols (a predominant component of the fungal cell membrane) (Ghannoum and Rice 1999).

As mentioned above, up until now fungicides have been chemically synthesized. However, the use of antagonistic microorganisms to control plant pathogenic fungi is receiving increasing attention due to current legislation restricting the use of chemically synthesized fungicides. This method is usually referred to as biological control (Carlile and Watkinson 1996). Antagonistic activity of microorganisms is attributed to them releasing antibiotics (Nielsen et al. 2000).

Using *A. awamori*, the aims of the research described in this chapter were:

- To analyse the effects on $[Ca^{2+}]_c$ of various cell permeabilizing antifungal compounds produced by antagonistic microorganisms which could be potentially used as biocontrol agents.

- To test a range of commercially available fungicides on their ability to influence $[Ca^{2+}]_c$ and use this information to a better understanding of their modes-of-action.

6.2 RESULTS

6.2.1 Analysis of cell permeabilizing antifungal agents

Most of the compounds analysed in this study were water insoluble (except amphotericin B). The stock solutions were prepared either in MeOH or DMSO. It was therefore first decided to test the effects of these solvents on $[Ca^{2+}]_c$ in *A. awamori*. For this purpose the light output (in RLU) from 24 h old cultures treated with iso-osmotic media, either in the absence or in the presence of each of the solvents at different concentrations, was measured. It was shown that both MeOH and DMSO at concentrations up to 5% did not cause significant changes in aequorin

luminescence (Table 6.1). Concentrations above 5% had a significant effect in increasing aequorin luminescence and were avoided in all subsequent work.

Concentration of solvent (%)		**0**	**0.5**	**1**	**5**	**50**
Response (RLU 70 s integration)	**MeOH**	1347	1107	1111	*1337*	*4618*
	DMSO	1347	1170	1152	*1918*	*26675*

Table 6.1 Effect of methanol and DMSO on aequorin luminescence. Numbers in italics represent data which are significantly different between concentrations of the solvent (5% LSD).

Five chemicals were studied: amphotericin B, surfactin, tensin, viscosinamide, gramicidin S (for details see Section 2.4.5.2).

Compound	**Source**	**Mode-of-action**	**Minimum concentration effective at increasing $[Ca^{2+}]_c$**
Tensin	*Pseudomonas spp.*	not known	> 80 µM
Gramicidin	*Bacillus brevis*	forms ion channels	2.5 µM
Amphotericin B	*Streptomyces spp.*	forms channels by complexing with membrane sterols	2 µM
Surfactin	*B. subtilis*	biosurfactant, which causes lyses of bacteria	1.5 µM
Viscosinamide	*P. fluorescens*	antibiotic with biosurfactant properties	5 µM

Table 6.2 Summary of effects of cell permeabilizing agents on $[Ca^{2+}]_c$.

Compared with the untreated control, which just represented the tail end of mechanical perturbation resulting from the addition of medium with appropriate solvent, it was shown that all of the compounds tested caused a significant increase in $[Ca^{2+}]_c$ at very low concentrations. The effects of the five compounds on three

parameters of the $[Ca^{2+}]_c$ transient induced by the cell permeabilizing agents were assessed: amplitude, length of the transient, and final resting level (Table 6.3).

Compound	Concentration (µM)	Amplitude	Length of transient	Final resting level
Tensin	80	-	-	↑
	160	↑	↑	↑
	240	↑	↑	↑
Gramicidin	2.5	↑	↑	↑
	5	↑	↑	↑
	10	↑	↑	↑
	20	↑	↑	↑
Amphotericin B	2	↑	↑	-
	2.5	↑	↑	↑
	5	↑	↑	↑
	10	↑	↑	↑
	20	↑	↑	↑
Surfactin	1.5	↑	↑	-
	2	↑	↑	-
	2.5	↑	↑	↑
	5	↑	↑	↑
	10	↑	↑	↑
	20	↑	↑	↑
Viscosinamide	5	↑	↑	↑
	10	↑	↑	↑
	20	↑	↑	↑
	40	↑	↑	↑

Table 6.3 Qualitative analysis of the agonistic effects on the $[Ca^{2+}]_c$ transients induced by the cell permeabilizing agents. - = no effect (compared with untreated control = medium in the presence of the solvent); ↑ = increase in parameter. Final resting level after 5 min.

As mentioned above most of the compounds were insoluble in water. To avoid uneven distribution of possible particulates in the solution they were applied to the

fungal cultures in the multiwell plates by hand outside the luminometer. Therefore a short delay of ~30 s at the start of the measurements was introduced which made it not possible to assess the absolute numbers in terms of changes in amplitude and the precise lengths of the $[Ca^{2+}]_c$ transients (for details see Section 2.4.5.2).

The $[Ca^{2+}]_c$ response to tensin was dose-dependent. All three parameters of the $[Ca^{2+}]_c$ response were affected compared with the untreated control (growth medium in the presence of the solvent). Increases in $[Ca^{2+}]_c$ only occurred in response to high concentrations of tensin (> 80 μM) (Figs. 6.1 and 6.2).

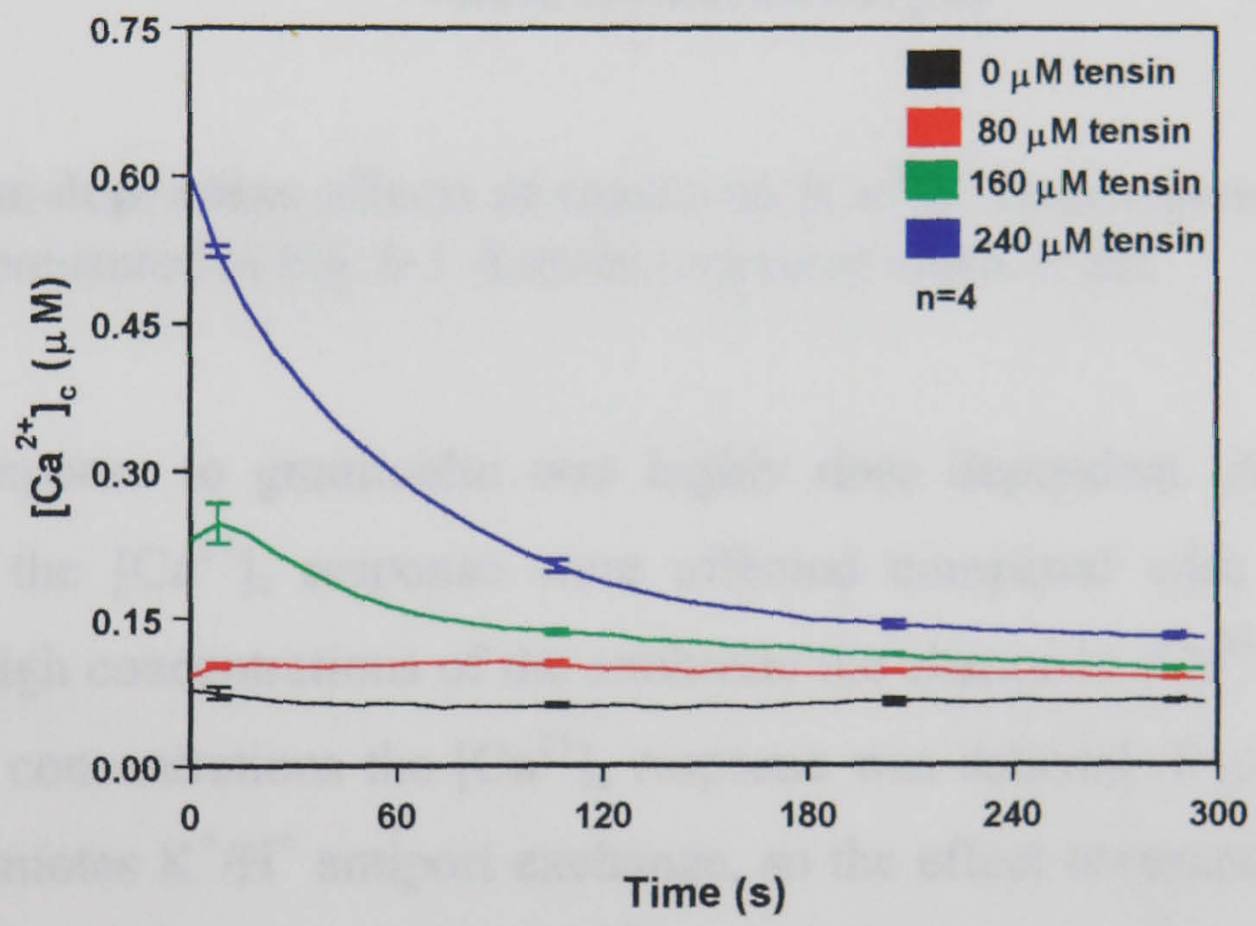

Figure 6.1 Effects of tensin on $[Ca^{2+}]_c$ kinetics. Results represent mean ± SE. Measurements were obtained using the repeated measuring protocol. Cycle time 11.6 s.

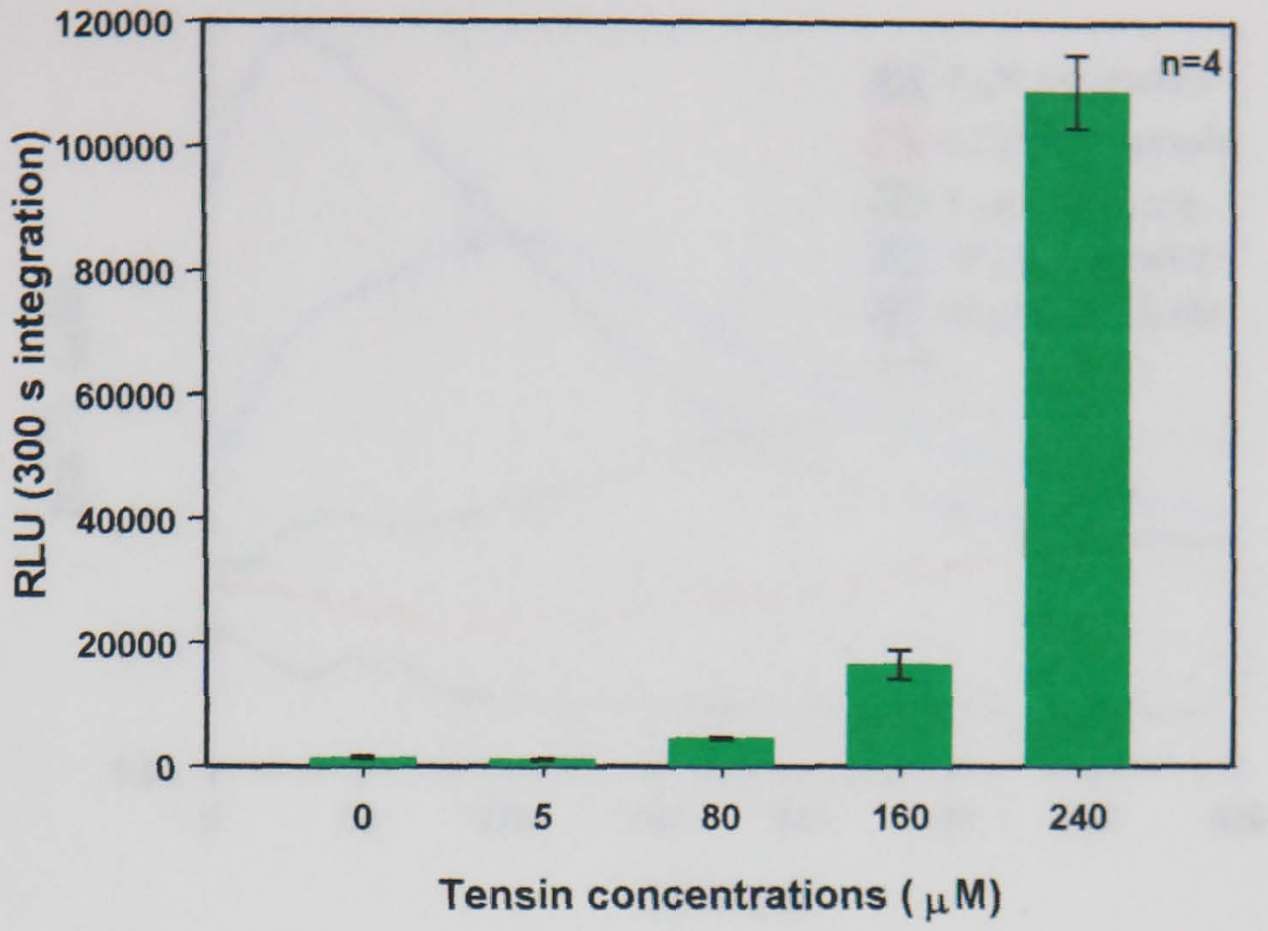

Figure 6.2 Dose-dependent effects of tensin on $[Ca^{2+}]_c$. Data represent integration of the kinetics presented in Fig. 6.1. Results represent mean ± SE.

The $[Ca^{2+}]_c$ response to gramicidin was highly dose dependent. Again all three parameters of the $[Ca^{2+}]_c$ response were affected compared with the untreated control. With high concentrations of the antibiotic the change in $[Ca^{2+}]_c$ was fast and great; at lower concentrations the $[Ca^{2+}]_c$ response was delayed (Figs. 6.3 and 6.4). Gramicidin promotes K^+/H^+ antiport exchange, so the effect observed was probably not a direct effect of the compounds on Ca^{2+} flux.

With amphotericin B the $[Ca^{2+}]_c$ response occurred immediately upon addition of the compound and was highly dose dependent. The lower the concentration of amphotericin B the later the $[Ca^{2+}]_c$ increase was initiated (Figs. 6.5 and 6.6). After a 1 h incubation with amphotericin B the resting levels of $[Ca^{2+}]_c$ were higher than in the control. All results obtained with this compound were highly reproducible probably due to the high solubility of amphotericin in water.

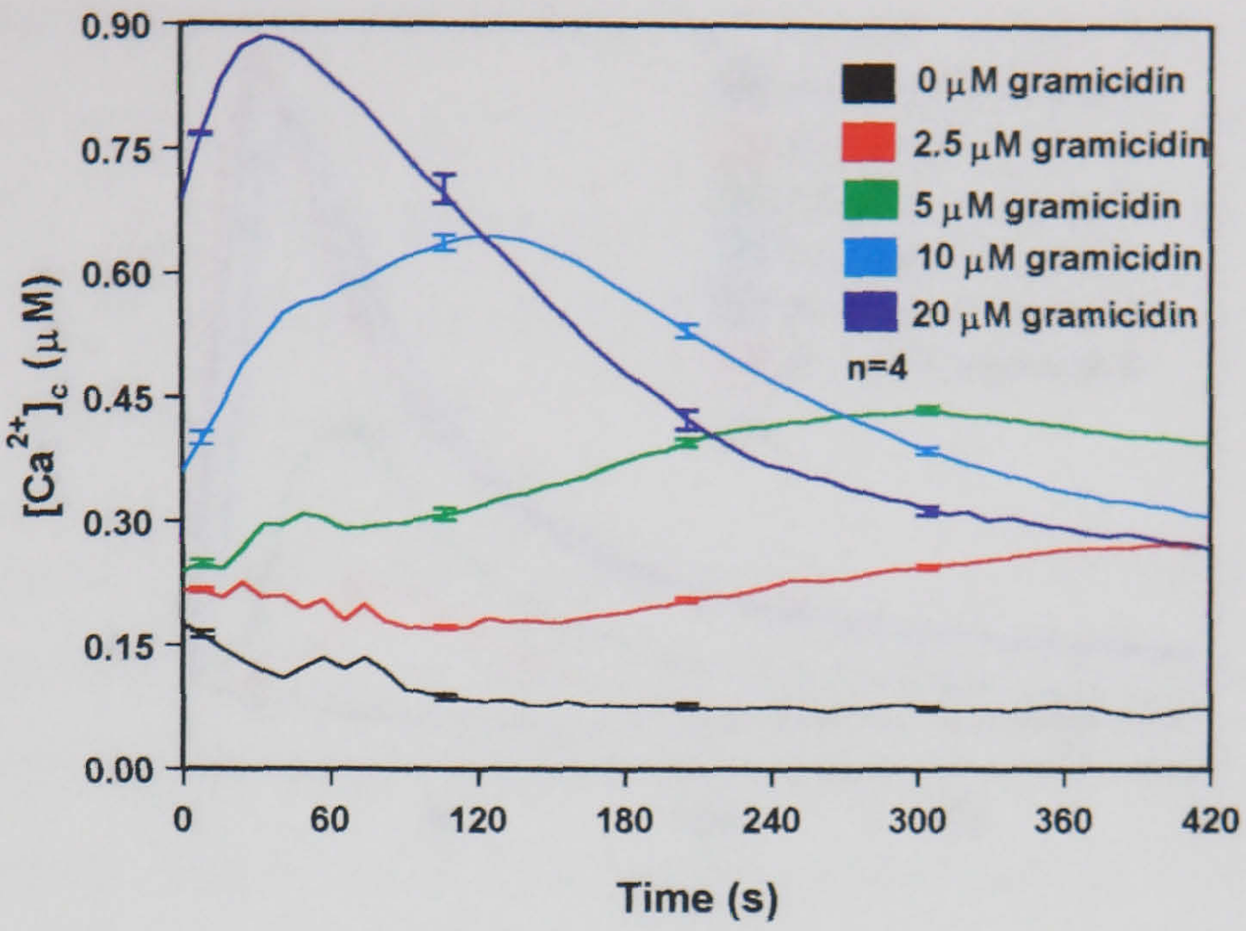

Figure 6.3 Effects of gramicidin on $[Ca^{2+}]_c$ kinetics. Results represent mean ± SE. Measurements were obtained using the repeated measuring protocol. Cycle time 11.6 s.

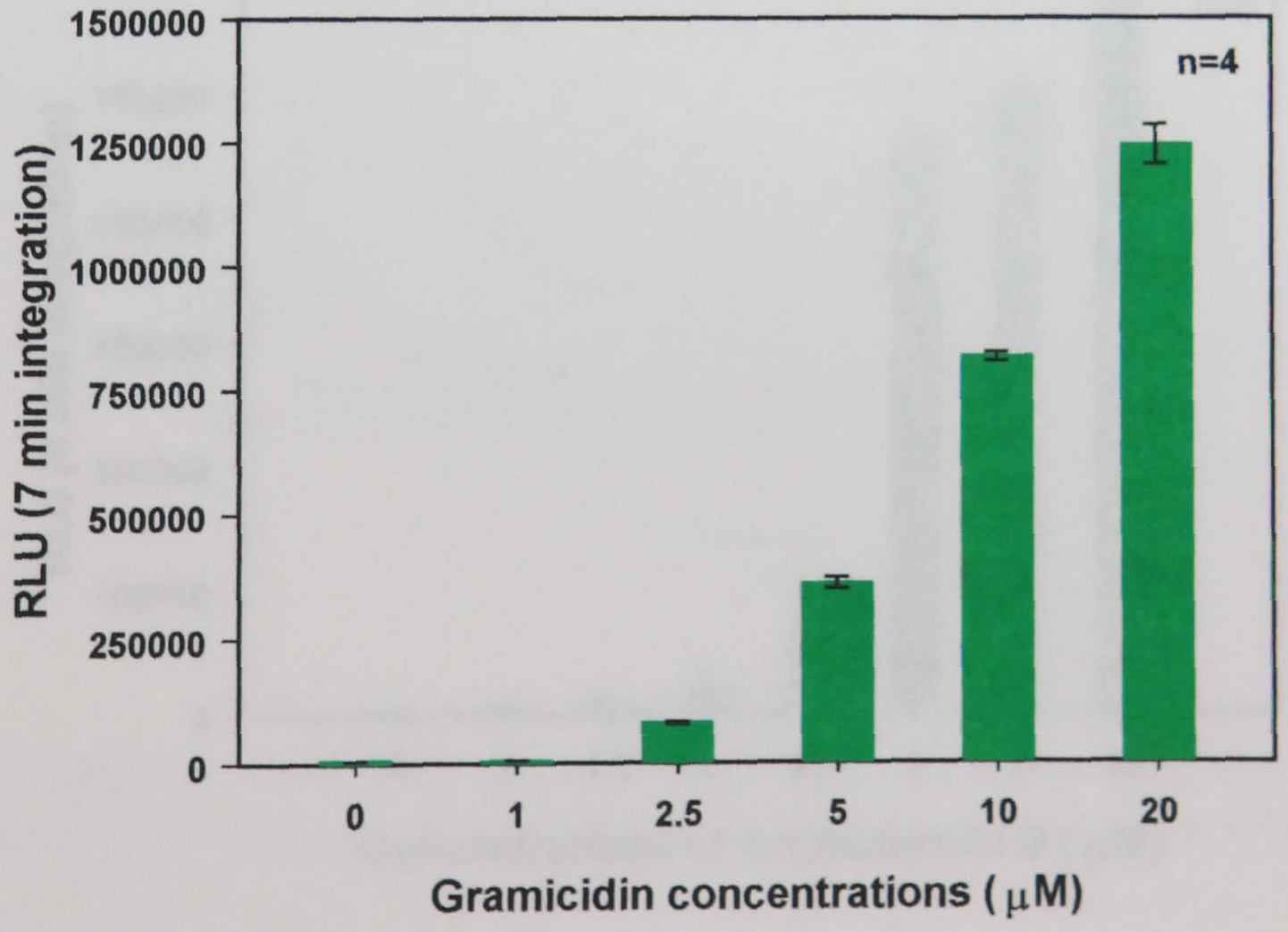

Figure 6.4 Dose-dependent effects of gramicidin on $[Ca^{2+}]_c$. Data represent integration of the kinetics presented in Fig. 6.3. Results represent mean ± SE.

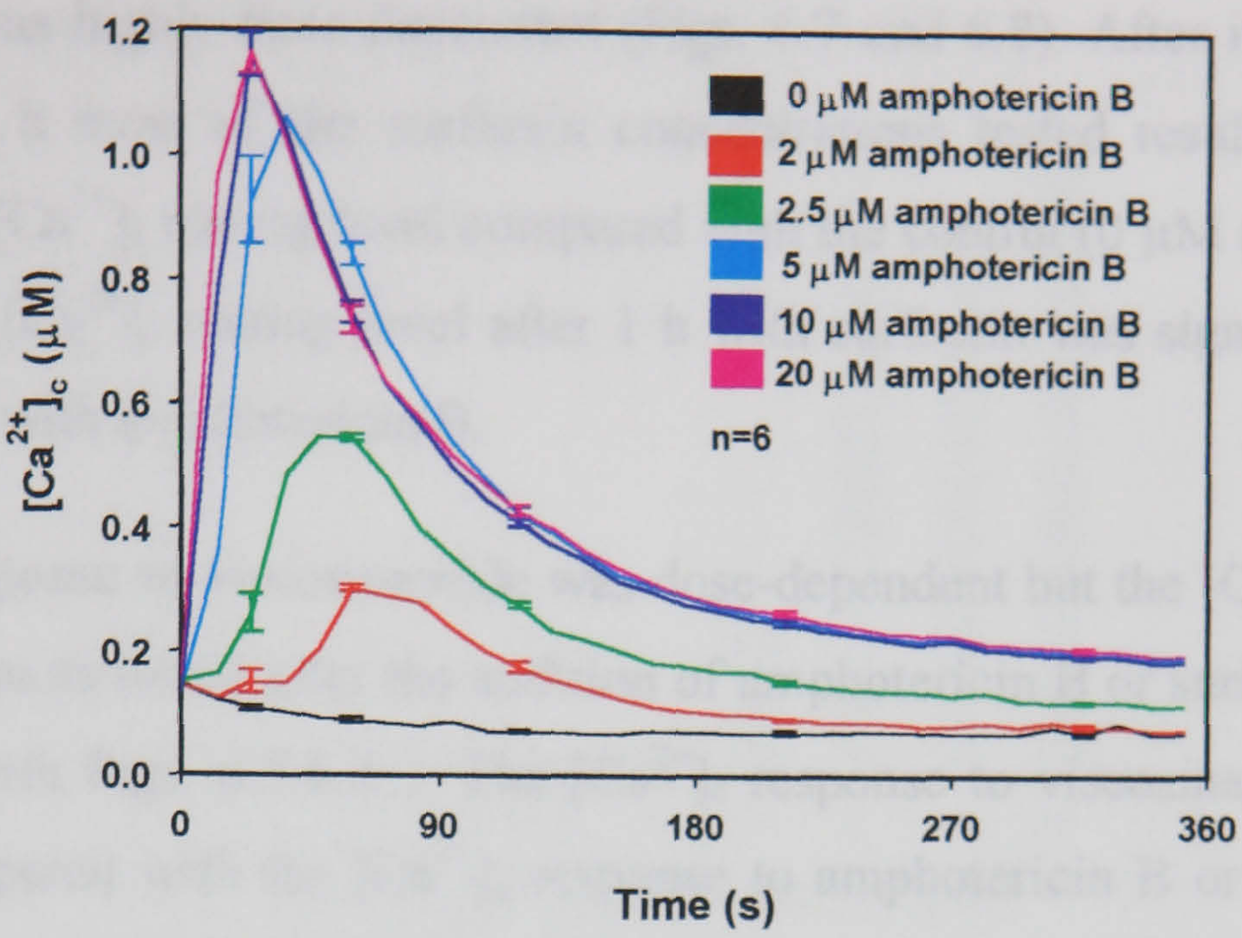

Figure 6.5 Effect of amphotericin B on $[Ca^{2+}]_c$. Results represent mean ± SE. Measurements were obtained using the repeated measuring protocol. Cycle time 11.6 s.

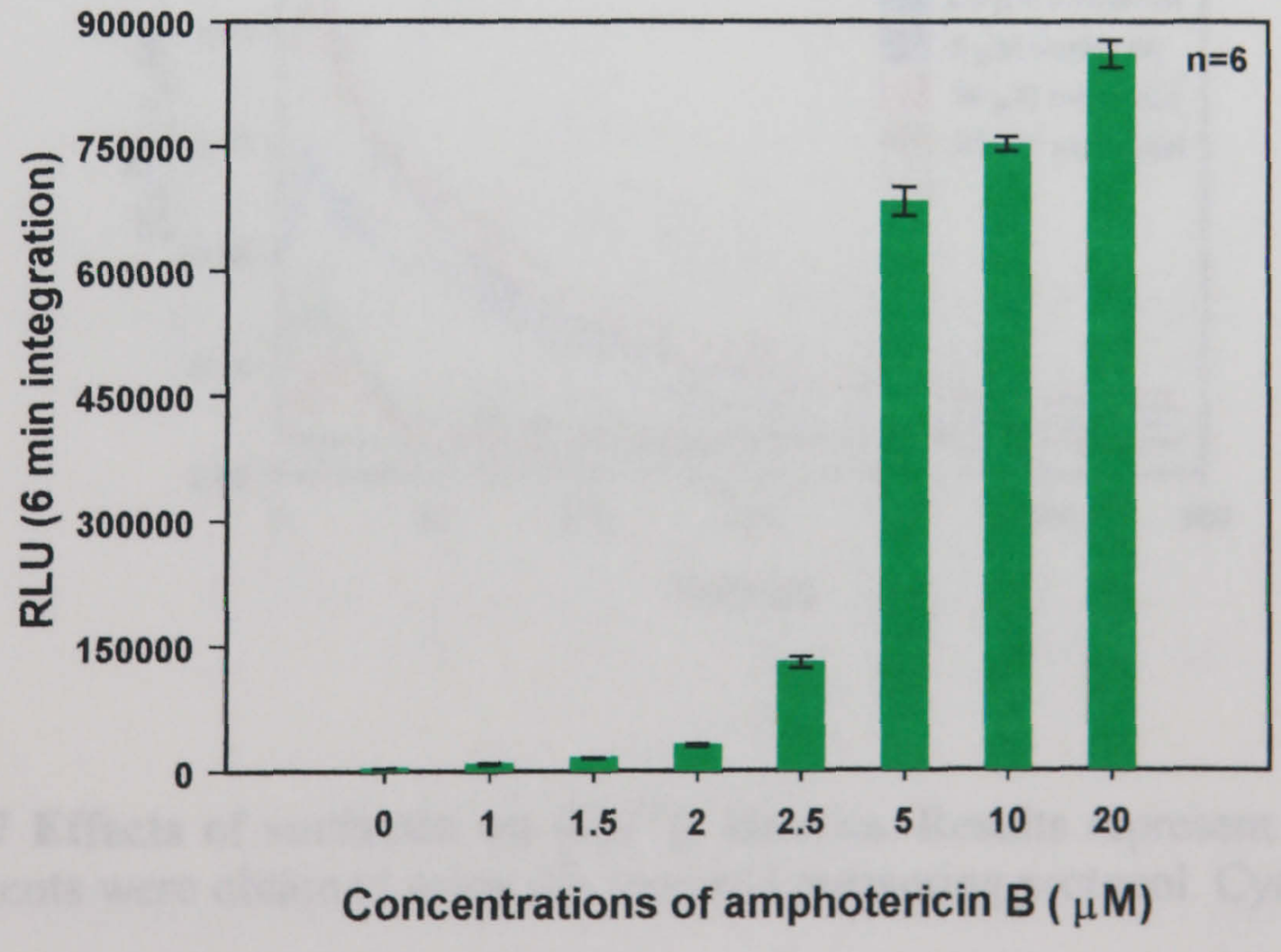

Figure 6.6 Dose-dependent effects of amphotericin B on $[Ca^{2+}]_c$. Data represent integration of the kinetics presented in Fig. 6.5. Results represent mean ± SE.

The $[Ca^{2+}]_c$ response to surfactin occurred immediately following addition of surfactin and was highly dose dependent (Figs. 6.7 and 6.8). After incubation with surfactin for 1 h most of the surfactin concentrations tested resulted in a small increase in the $[Ca^{2+}]_c$ resting level compared with the control (0 μM surfactin). The increase in the $[Ca^{2+}]_c$ resting level after 1 h with surfactin was significantly lower than that found with amphotericin B.

The $[Ca^{2+}]_c$ response to viscosinamide was dose-dependent but the $[Ca^{2+}]_c$ increases were not as great as found after the addition of amphotericin B or surfactin (cf. Figs. 6.9 and 6.10 with Figs. 6.5-6.8). The $[Ca^{2+}]_c$ response to viscosinamide was also prolonged compared with the $[Ca^{2+}]_c$ response to amphotericin B or surfactin. The $[Ca^{2+}]_c$ resting levels after a 1 h incubation with viscosinamide were higher with concentrations ≥ 5 μM (data not shown).

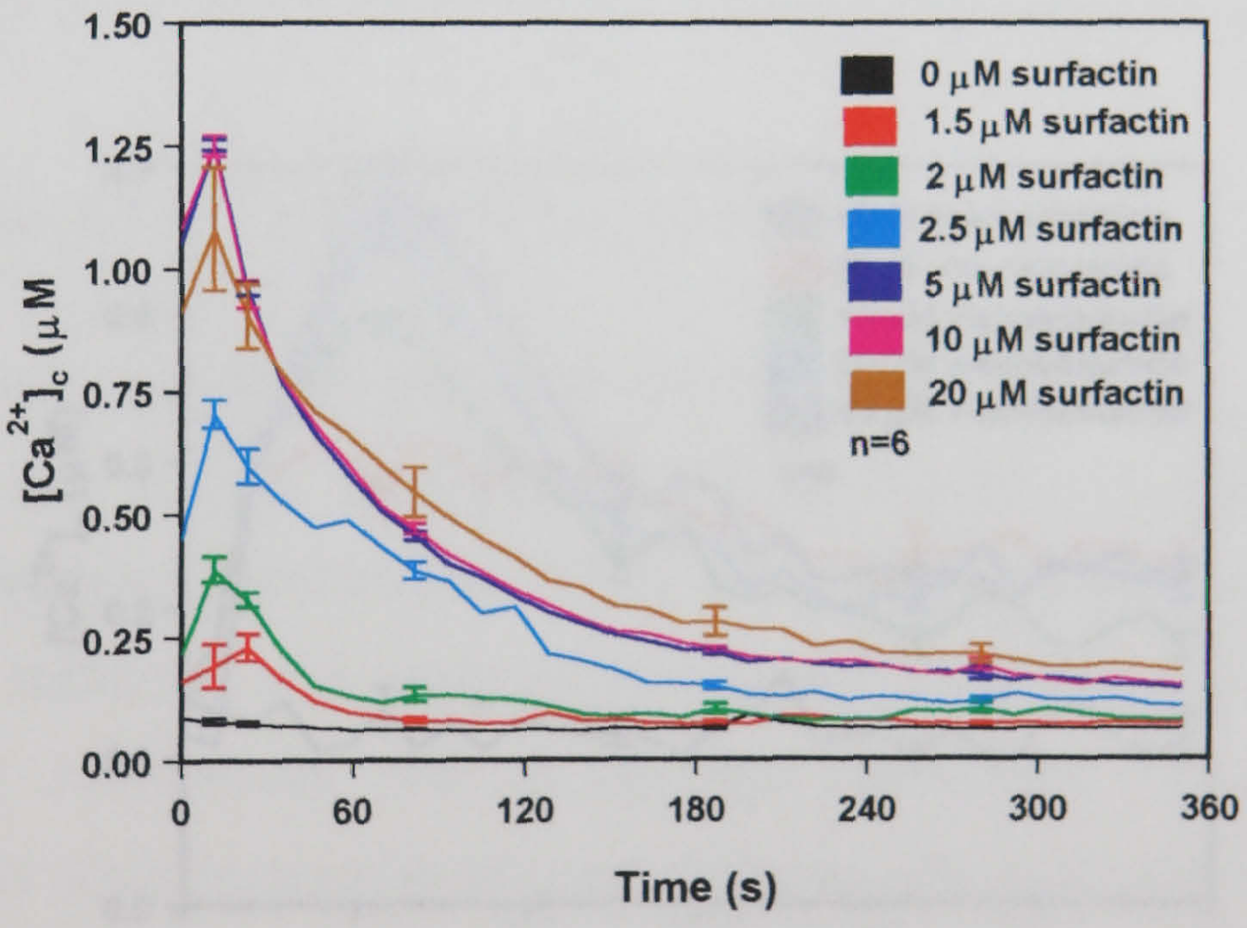

Figure 6.7 Effects of surfactin on $[Ca^{2+}]_c$ kinetics. Results represent mean ± SE. Measurements were obtained using the repeated measuring protocol. Cycle time 11.6 s.

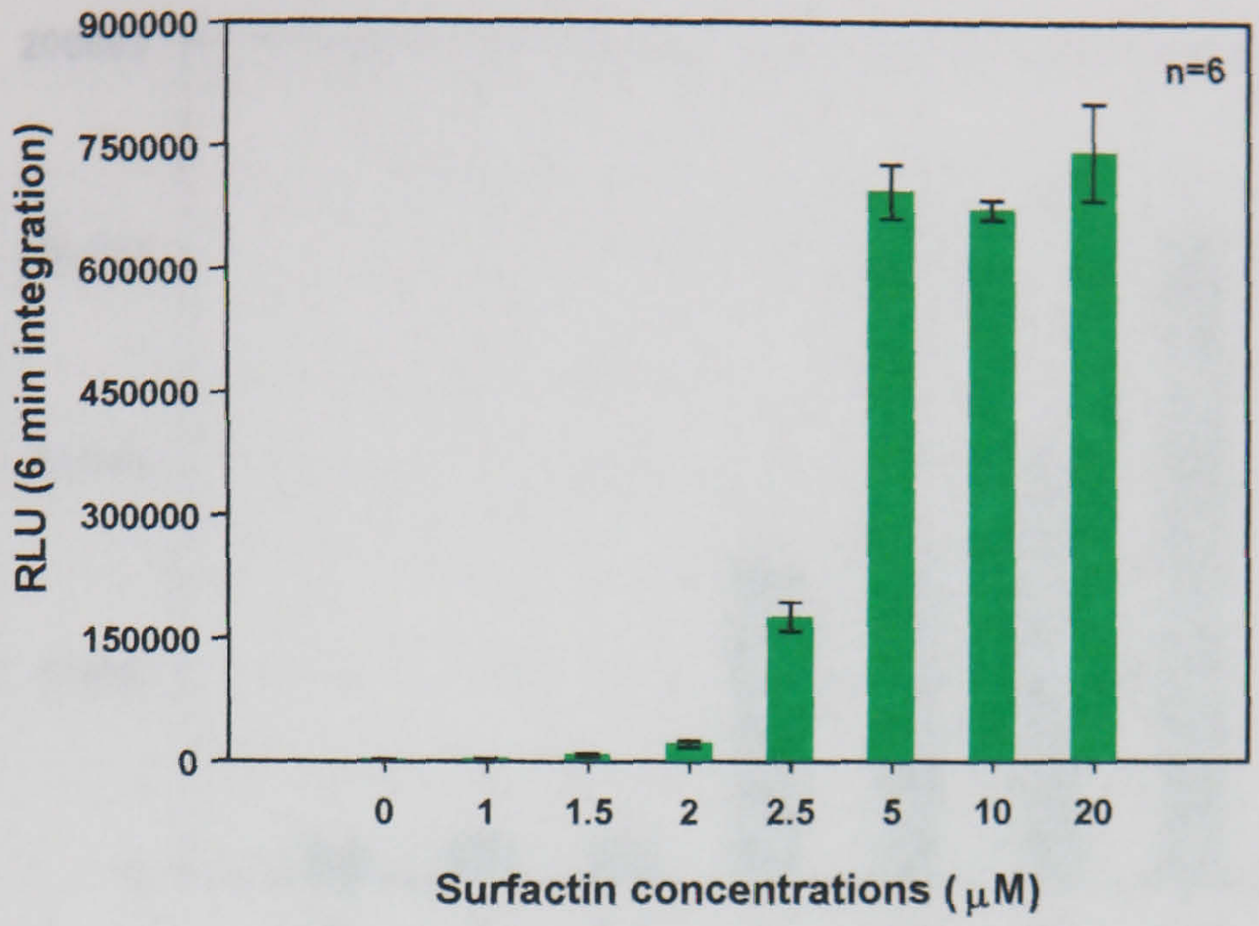

Figure 6.8 Dose-dependent effects of surfactin on $[Ca^{2+}]_c$. Data represent integration of the kinetics presented in Fig. 6.7. Results represent mean ± SE.

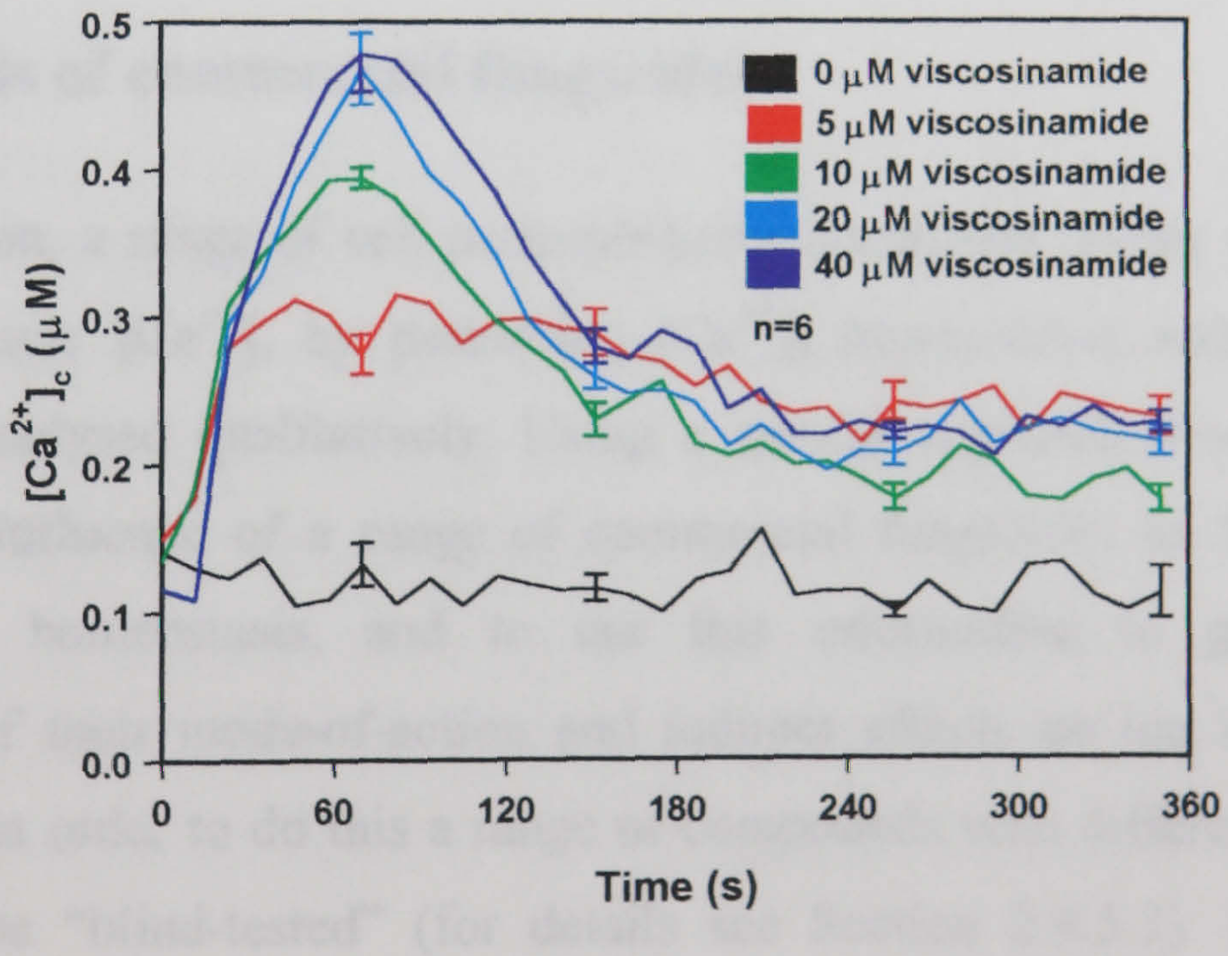

Figure 6.9 Effects of viscosinamide on $[Ca^{2+}]_c$ kinetics. Results represent mean ± SE. Measurements were obtained using the repeated measuring protocol. Cycle time 11.6 s.

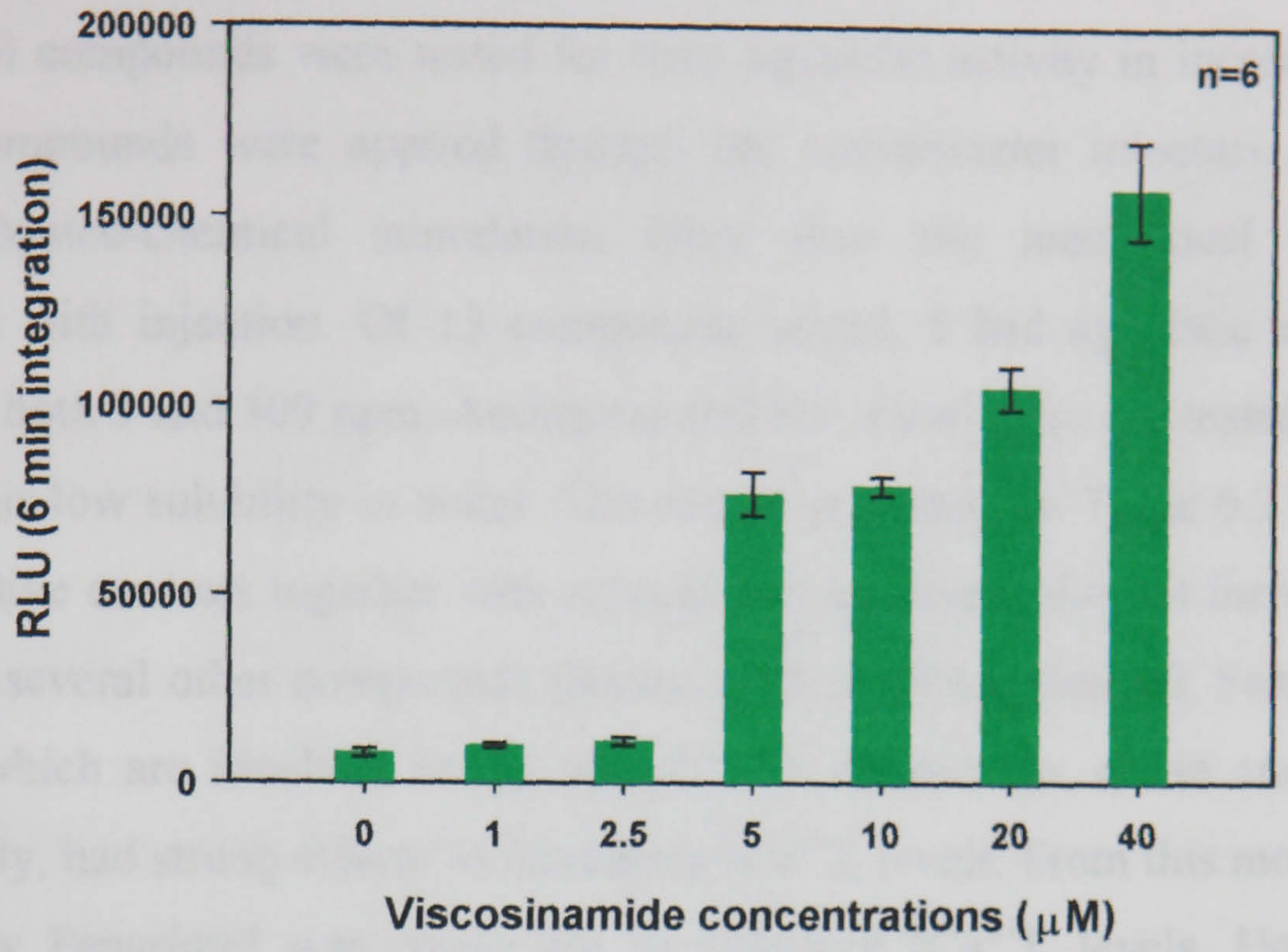

Figure 6.10 Dose-dependent effects of viscosinamide on $[Ca^{2+}]_c$. Data represent integration of the kinetics presented in Fig. 6.9. Results represent mean ± SE.

6.2.2 Analysis of commercial fungicides

In the last section, a range of cell permeabilizing antifungal agents were shown to transiently increase $[Ca^{2+}]_c$ by perturbing $[Ca^{2+}]_c$ homeostasis and these $[Ca^{2+}]_c$ changes were analysed qualitatively. Using a similar approach it was decided to investigate the influence of a range of commercial fungicides on their ability to perturb $[Ca^{2+}]_c$ homeostasis, and to use this information to gain a greater understanding of their mode-of-action and indirect effects on ion homeostasis in fungal hyphae. In order to do this a range of compounds with different specificities (Table 6.4) were "blind-tested" (for details see Section 2.4.5.3). Minoxidil and octopamine were included as two negative controls and CPA was included as positive control as it is a strong $[Ca^{2+}]_c$ agonist in *A. awamori* (Figs. 4.24 and 4.25).

6.2.2.1 Agonistic activity of commercial fungicides on $[Ca^{2+}]_c$

Initially all compounds were tested for their agonistic activity in increasing $[Ca^{2+}]_c$ levels. Compounds were applied through the luminometer injectors without any further physico-chemical stimulation other than the mechanical perturbation associated with injection. Of 13 compounds tested, 8 had agonistic effects when applied at both 3 and 100 ppm. Antimycin and Fenarimol were not tested at 100 ppm due to their low solubility in water. The results presented in Table 6.3 showed that both negative controls together with ridomil and antimycin did not increase $[Ca^{2+}]_c$. However, several other compounds (Beam, Captan, Chlorothalonil, Fenpropimorph, Nustar), which are involved in the biosynthesis of melanin, chitin and ergosterol, respectively, had strong effects in increasing $[Ca^{2+}]_c$ levels. From this mode-of-action group only Fenarimol was found not to influence $[Ca^{2+}]_c$ levels. However, it is important to note that only 3 ppm of Fenarimol were tested due to the compound precipitating at higher concentration. Another compound that had a significant effect on $[Ca^{2+}]_c$ at both low and 100 ppm was MBC, which is known to inhibit microtubule assembly.

Several parameters of the $[Ca^{2+}]_c$ signature associated with the primary $[Ca^{2+}]_c$ increase induced by the fungicide were analysed: lag period, rise time, amplitude and length of transient. These parameters were compared with the untreated control (mechanical perturbation). In many cases more than one $[Ca^{2+}]_c$ increase was observed after applying the compounds. The extent of the secondary $[Ca^{2+}]_c$ increases varied significantly. It was decided not to characterize various parameters of the signature of the secondary $[Ca^{2+}]_c$ increase but just to note its presence or absence. Another parameter analysed was the final $[Ca^{2+}]_c$ resting level.

Table 6.5 shows that none of the compounds influenced the lag period and rise time. The length of the $[Ca^{2+}]_c$ transient was affected only in the case of Captan. Beam and Captan caused an increase in the amplitude of the primary $[Ca^{2+}]_c$ increase. Beam, Fenpropimorph, Manzate, Nustar, MBC and Chlorothalonil caused a secondary $[Ca^{2+}]_c$ increase. The final $[Ca^{2+}]_c$ resting level was increased in all cases

in which a secondary $[Ca^{2+}]_c$ increase was observed. The only other fungicide which also increased the final $[Ca^{2+}]_c$ resting level was Captan.

Compound	Mode-of-action	Agonistic effect	
		3 ppm	100 ppm
Antimycin A	Complex III mitoch. electron transport inhibitor (Ox phos uncoupler at higher rates)	-	n.a.
Beam* (Tricyclazole)	Melanin biosynthesis inhibitor	+	++
Captan*	Possible chitin synthesis inhibitor	+	++
Chlorothalonil	Ergosterol biosynthesis inhibitor	+	++
CPA	Ca^{2+}-ATPase inhibitor (positive control)	-	+++
Fenarimol	Ergosterol biosynthesis inhibitor	-	n.a.
Fenpropimorph	Ergosterol biosynthesis inhibitor	+	++
Manzate*	Not known	++	++
MBC	Microtubule assembly inhibitor	++	++
Minoxidil	K^+-channel blocker (negative control)	-	-
Nustar Flusilazole	Ergosterol biosynthesis inhibitor	+	+
Octopamine	Biogenic amine agonist (negative control)	-	-
Ridomil* (Metalaxyl)	RNA synthesis inhibitor	-	-

Table 6.4 Effect of different concentrations of the compounds on $[Ca^{2+}]_c$. Abbreviations: * = trade name; - = no effect; +, ++, +++ = extent of agonistic effect; n.a. = not appropriate (compounds did not completely dissolve in water thus preventing their use in the luminometer injectors).

Compound	Primary $[Ca^{2+}]_c$ increase				Secondary $[Ca^{2+}]_c$ increase	Final $[Ca^{2+}]_c$ resting level
	Lag period	Rise time	Amplitude	Length of transient		
Antimycin A	- *	- *	- *	- *	- *	- *
Beam Tricyclazole	- -	- -	- ↑	- -	- +	- ↑
Captan	- -	- -	↑ ↑	- ↑	- -	↑ ↑
Chlorothalonil	- -	- -	- -	- -	+ +	↑ ↑
CPA	- -	- -	- -	- -	- +	- ↑
Fenarimol	- *	- *	- *	- *	- *	- *
Fenpropimorph	- -	- -	- -	- -	- +	- ↑
Manzate	- -	- -	- -	- -	- +	↑ ↑
MBC	- -	- -	- -	- -	+ +	↑ ↑
Minoxidil	- -	- -	- -	- -	- -	- -
Nustar Flusilazole	- -	- -	- -	- -	+ +	↑ ↑
Octopamine	- -	- -	- -	- -	- -	- -
Ridomil Metalaxyl	- -	- -	- -	- -	- -	- -

Table 6.5 Detailed analysis of the agonistic effects of compounds tested. Abbreviations: - = no effect (compared with untreated control), + = induction of secondary $[Ca^{2+}]_c$ increase, ↑ = increase in parameter with the compound at 3 ppm, ↑ = increase in parameter with the compound at 100 ppm, ↓ = decrease in parameter with the compound at 3 ppm, ↓ = decrease in parameter with the compound at 100 ppm, * = not tested because insolubility of compounds in water, MBC = Methyl 2-benzimidasolecarbamate, Captan = N-tricholomethylthio–4–cyclohexene–1,2-dicarboximide, Manzate = manganese ethylenebis dithiocarbamate (polymeric).

6.2.2.2 Dose-dependent and long-term effects on $[Ca^{2+}]_c$ of commercial fungicides

The compounds Manzate, MBC and Beam (not ergosterol inhibitors), which gave the most interesting $[Ca^{2+}]_c$ responses (Table 6.5) were analysed further for their dose-

dependent effects and long term effects on $[Ca^{2+}]_c$. Dose-dependent effects involved using different concentrations (1, 3, 10, 30 and 100 ppm) for each compound. Long term effects involved using 3 ppm and 100 ppm over three different incubation times (10, 30 and 60 min) with the luminescence measurements being carried out throughout the periods of incubation. The qualitative results obtained using these three compounds are summarized in Table 6.6.

Compound	**Primary $[Ca^{2+}]_c$ increase**		**Secondary $[Ca^{2+}]_c$ increase**	**Tertiary $[Ca^{2+}]_c$ increase**	**Final $[Ca^{2+}]_c$ resting level**
	Amplitude	Length of transient			
Manzate	- -	- -	++	- +	↑ ↑
MBC	- -	- -	+ +	- -	↑ ↑
Beam	- ↑	- -	- +	- -	-↑

Table 6.6 Detailed qualitative analysis of the agonistic effects on $[Ca^{2+}]_c$ on Manzate, MBC and Beam. - = no effect (compared with untreated control), + = induction of secondary $[Ca^{2+}]_c$ increase, ↑ = increase in parameter with the compound at 3 ppm, ↑ = increase in parameter with the compound at 100 ppm.

Manzate did not affect the amplitude of the primary $[Ca^{2+}]_c$ increase at all the concentrations tested, but did cause a secondary $[Ca^{2+}]_c$ increase. The higher the concentration of Manzate applied the higher the amplitude of the secondary $[Ca^{2+}]_c$ increase which was observed (Fig. 6.11). When cultures were treated with 100 ppm Manzate, secondary (after 4 min) and tertiary (after 12 min) $[Ca^{2+}]_c$ increases were observed (Figs 6.11 and 6.12). Treatment with 100 ppm Manzate almost doubled the final resting $[Ca^{2+}]_c$ level (Fig. 6.12).

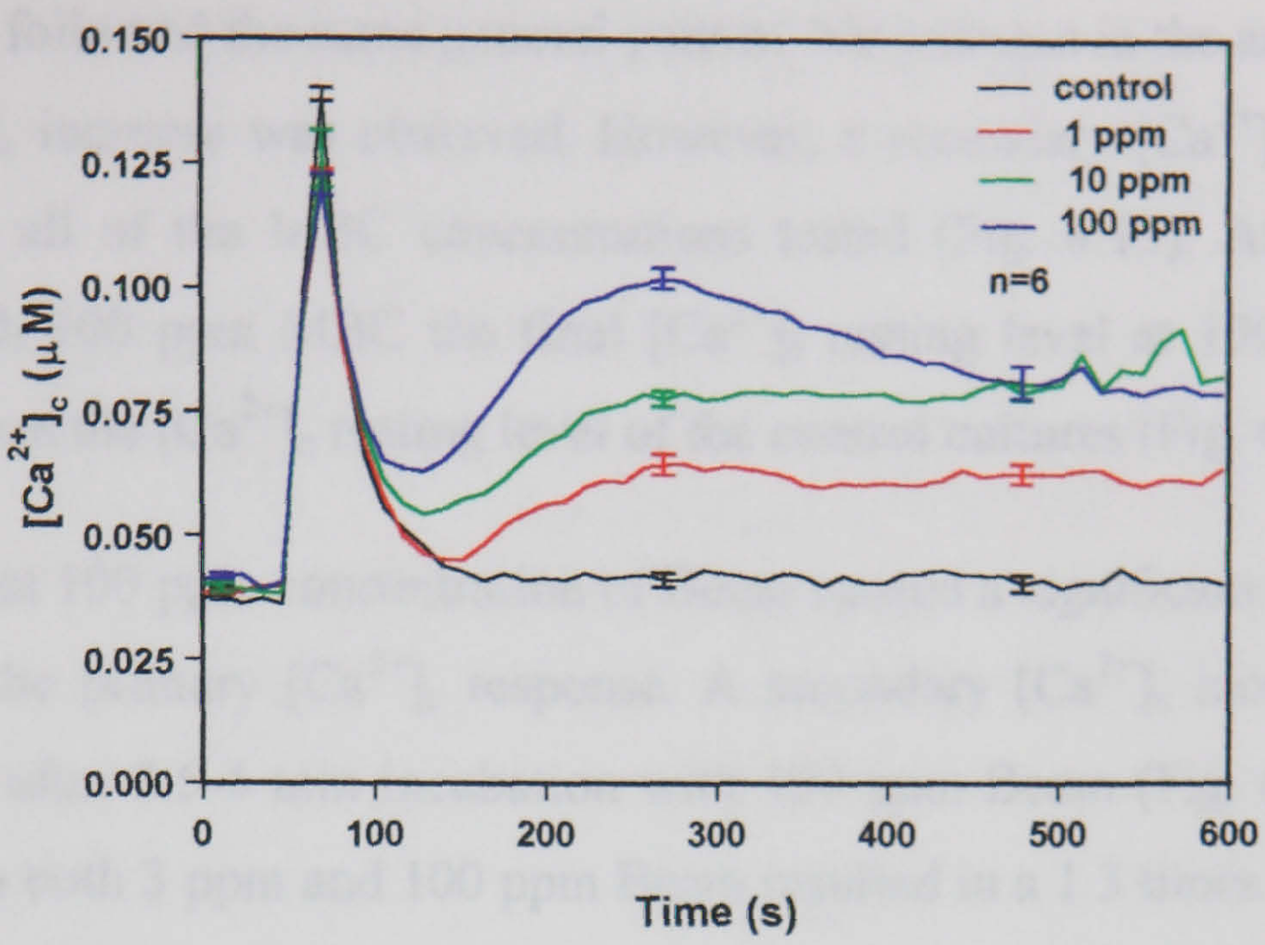

Figure 6.11 Effects of Manzate on $[Ca^{2+}]_c$ kinetics. Results represent mean ± SE. Measurements were obtained using the repeated measuring protocol. Cycle time 11.6 s.

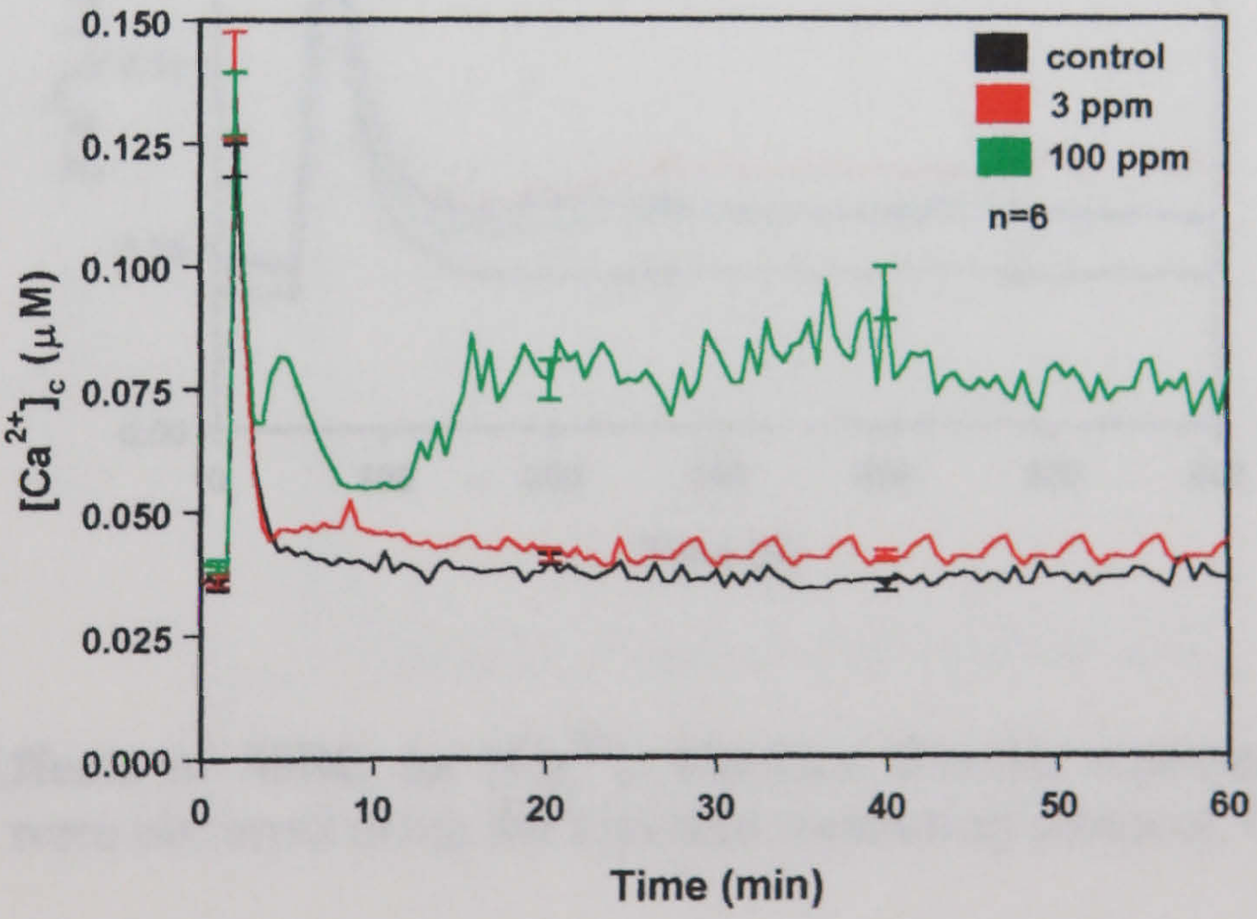

Figure 6.12 Effects of long term incubation (60 min) with Manzate on $[Ca^{2+}]_c$ kinetics. Results represent mean ± SE. Measurements were obtained using the repeated measuring protocol. Cycle time 60.1 s.

The changes in $[Ca^{2+}]_c$ caused by MBC were not as dramatic as with Manzate. However, they followed the same general pattern. No increase in the amplitude of the primary $[Ca^{2+}]_c$ increase was observed. However, a secondary $[Ca^{2+}]_c$ increase was observed with all of the MBC concentrations tested (Fig. 6.13). After 60 min of incubation with 100 ppm MBC the final $[Ca^{2+}]_c$ resting level at 100 ppm was 1.6 times higher than the $[Ca^{2+}]_c$ resting level of the control cultures (Fig. 6.14).

Only the highest 100 ppm concentration of Beam caused a significant increase in the amplitude of the primary $[Ca^{2+}]_c$ response. A secondary $[Ca^{2+}]_c$ increase was also only observed after 3.5-4 min incubation with 100 ppm Beam (Fig. 6.15). After 60 min incubation both 3 ppm and 100 ppm Beam resulted in a 1.3 times increase in the final $[Ca^{2+}]_c$ resting level (Fig. 6.16).

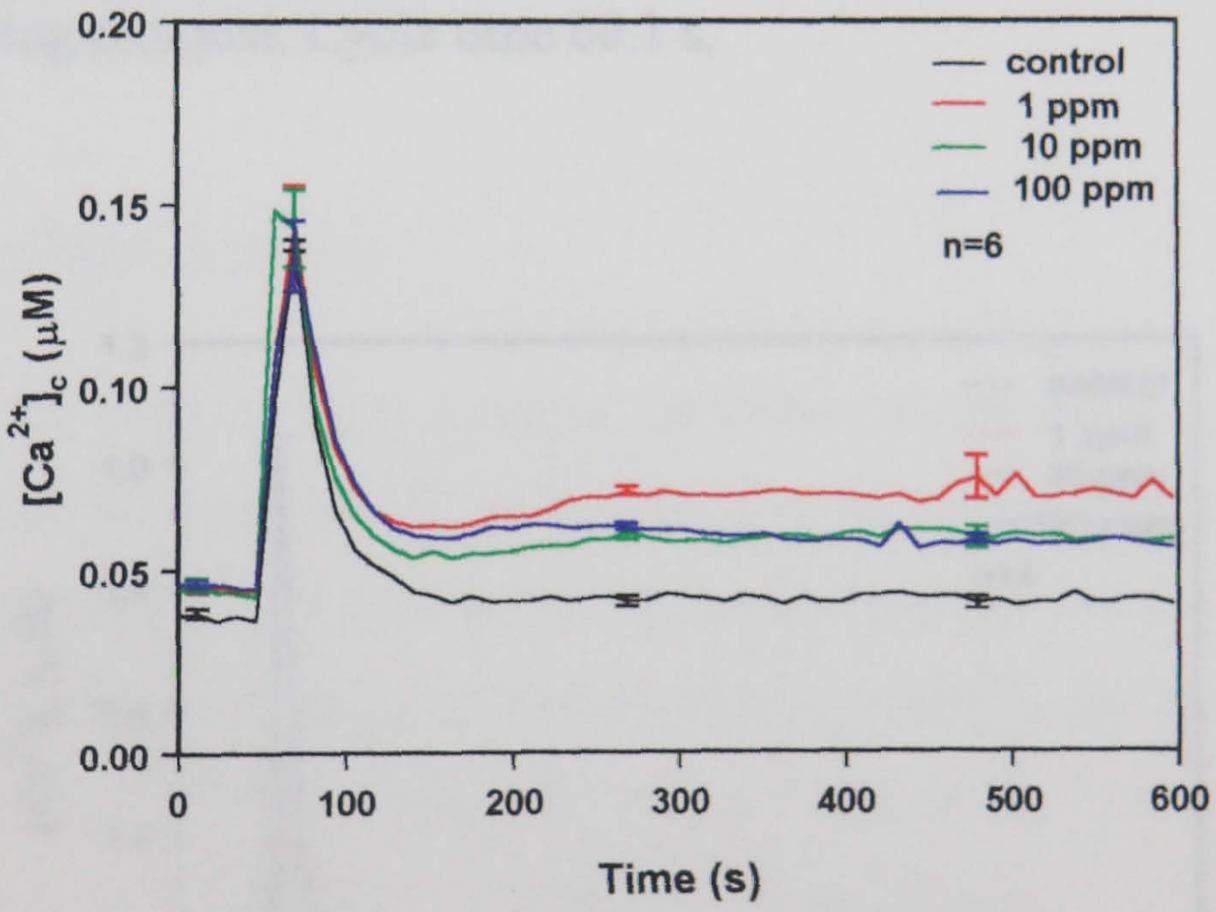

Figure 6.13 Effects of MBC on $[Ca^{2+}]_c$ kinetics. Results represent mean ± SE. Measurements were obtained using the repeated measuring protocol. Cycle time 11.6 s.

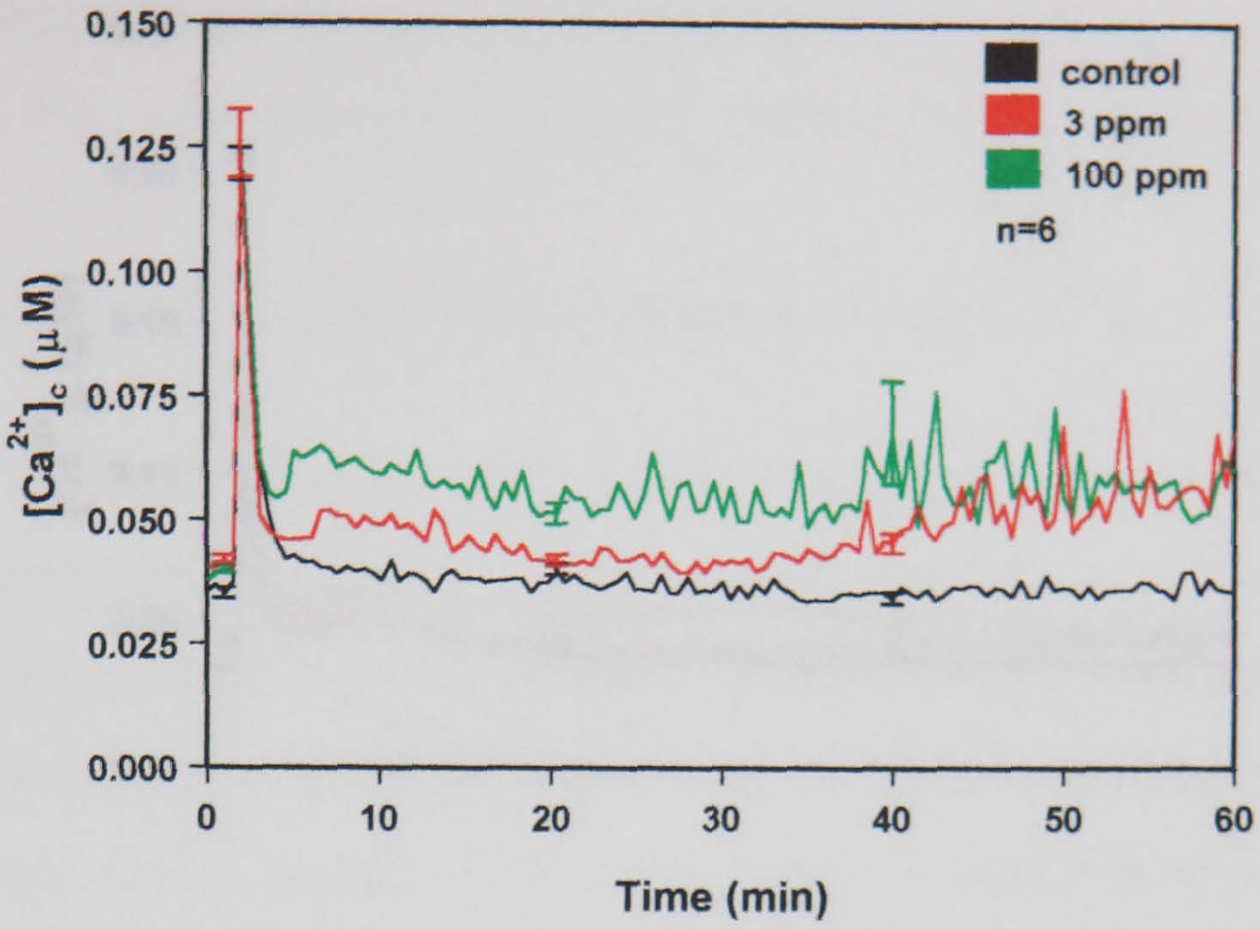

Figure 6.14 Effects of long term incubation (60 min) with MBC on $[Ca^{2+}]_c$ kinetics. Results represent mean ± SE. Measurements were obtained using the repeated measuring protocol. Cycle time 60.1 s.

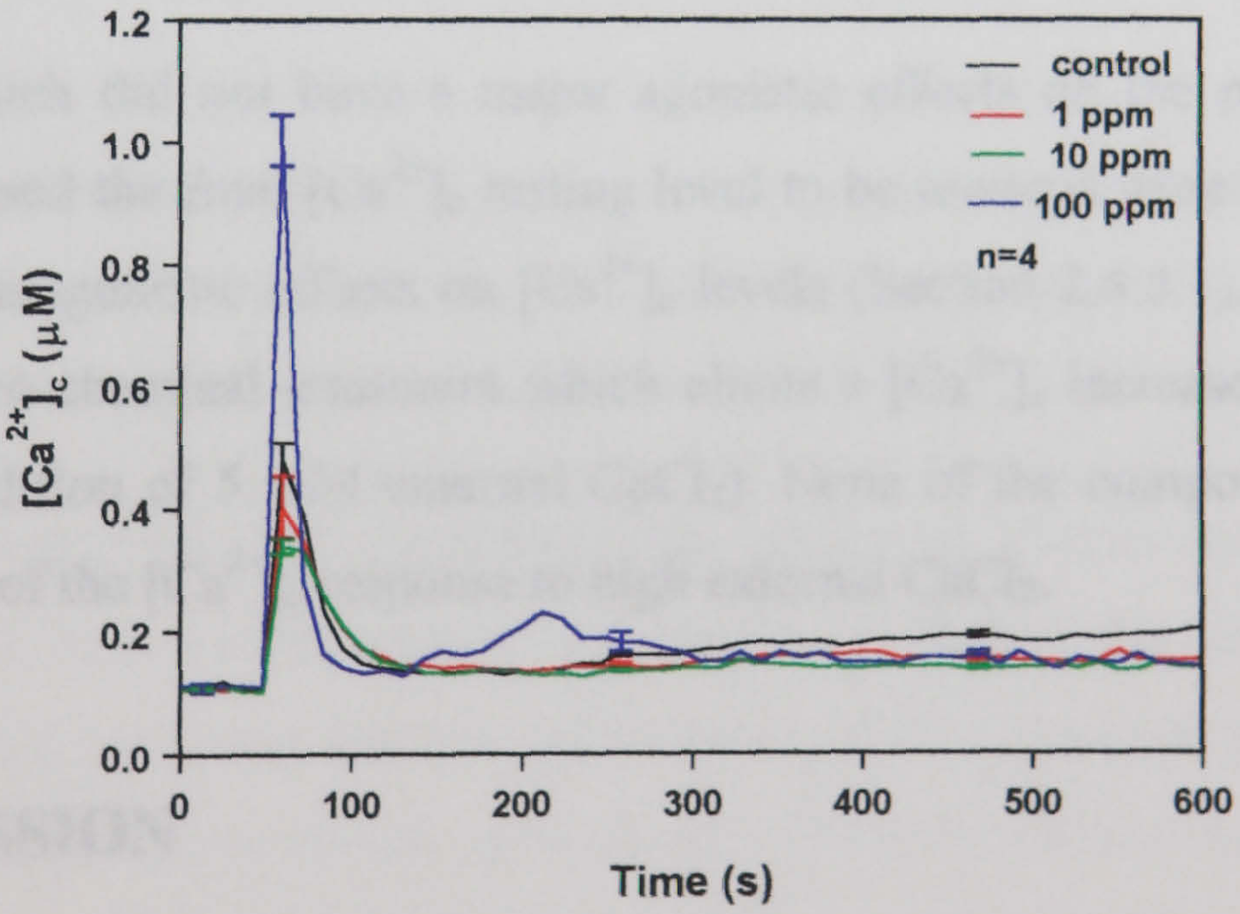

Figure 6.15 Effects of Beam on $[Ca^{2+}]_c$ kinetics. Results represent mean ± SE. Measurements were obtained using the repeated measuring protocol. Cycle time 11.6 s.

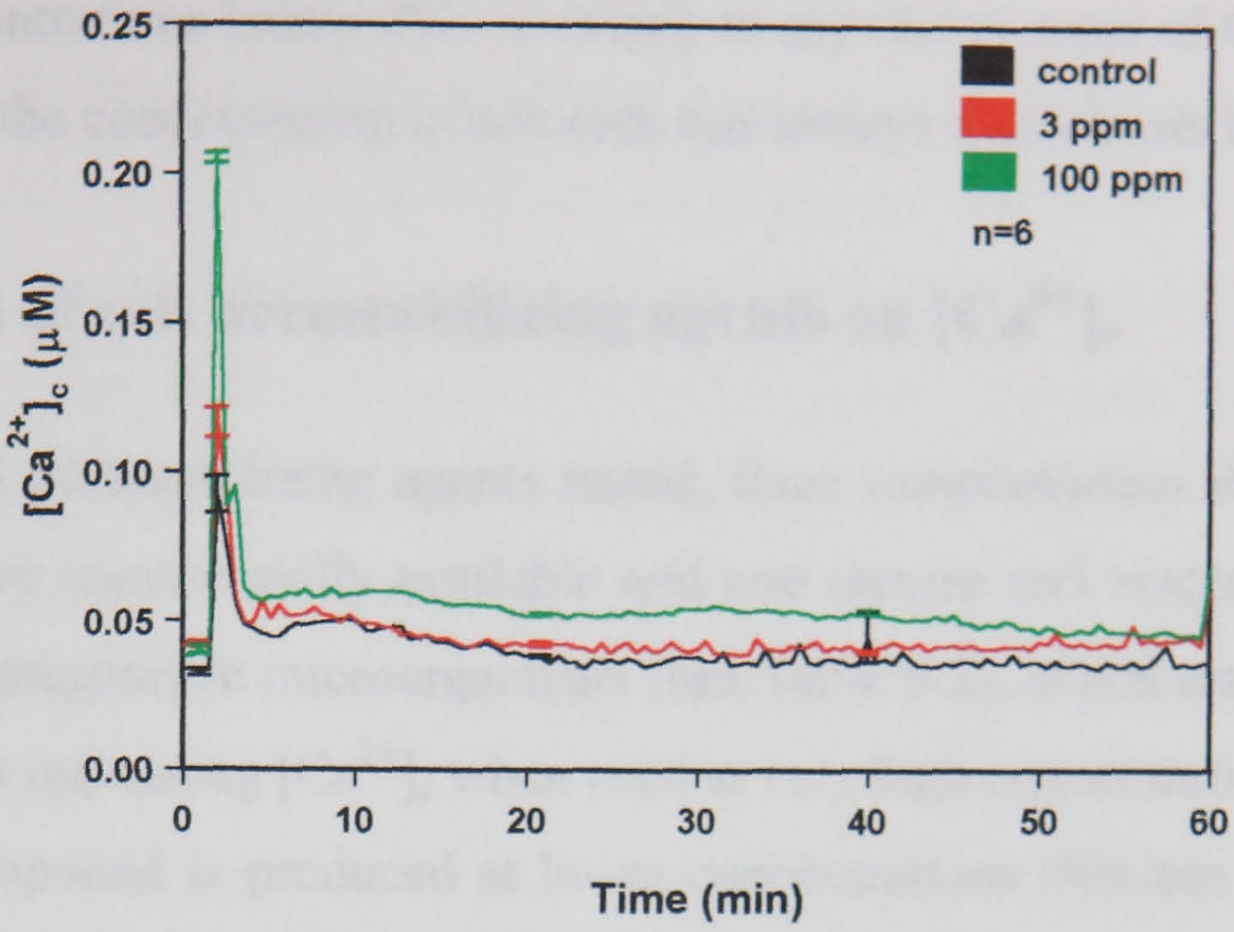

Figure 6.16 Effects of long term incubation (60 min) with Beam on $[Ca^{2+}]_c$ kinetics. Results represent mean ± SE. Measurements were obtained using the repeated measuring protocol. Cycle time 60.1 s.

6.2.3 Antagonistic activity

Compounds which did not have a major agonistic effects on the primary $[Ca^{2+}]_c$ response or caused the final $[Ca^{2+}]_c$ resting level to be lowered were then tested for their possible antagonistic effects on $[Ca^{2+}]_c$ levels (Section 2.4.5.1). Inhibition of only one physico-chemical treatment which elicits a $[Ca^{2+}]_c$ increase was analysed (namely the addition of 5 mM external $CaCl_2$). None of the compounds produced clear inhibition of the $[Ca^{2+}]_c$ response to high external $CaCl_2$.

6.3 DISCUSSION

6.3.1 Effects of solvents on $[Ca^{2+}]_c$

A lot of compounds possessing antifungal activities are insoluble in water. Therefore when analysing their effects on $[Ca^{2+}]_c$ levels it is important to know how these

solvents affect $[Ca^{2+}]_c$. When used on *A. awamori*, DMSO and MeOH did not affect $[Ca^{2+}]_c$ at concentrations below 5%. It is safe to say that in most of the experiments described here, the concentration of solvents was always much lower (<1%).

6.3.2 Effects of cell permeabilizing agents on $[Ca^{2+}]_c$

Of the five cell permeabilizing agents tested, three (amphotericin B, surfactin and gramicidin) were commercially available and two (tensin and viscosinamide) were purified from antagonistic microorganisms (see Table 6.2). When tested, tensin was only effective at increasing $[Ca^{2+}]_c$ when used at very high concentrations (> 80 µM). *In vivo* this compound is produced at lower concentrations (Nielsen et al. 2000). It therefore seems likely that changes in $[Ca^{2+}]_c$ observed in the experiments probably do not occur in nature. Thus the antifungal properties of tensin are probably not targeted at perturbing $[Ca^{2+}]_c$ unless *A. awamori* is particularly insensitive to this compound.

On the contrary, viscosinamide is produced in nature in substantial quantities (Nielsen et al. 1999). Also it was effective in increasing $[Ca^{2+}]_c$ at much lower concentrations (> 5 µM). Therefore the $[Ca^{2+}]_c$ changes, which were observed, may occur in fungal cells exposed to this compound in the soil. Thus this compounds may perturb the homeostasis of $[Ca^{2+}]_c$ and possibly other ions, and through this mechanism viscosinamide may be antagonistic to soil fungi.

Commercially available cell permeabilizing antifungal compounds were tested alongside tensin and viscosinamide. The common feature for amphotericin B, surfactin and gramicidin was that they all increased $[Ca^{2+}]_c$ levels to greater than 0.9 µM after being added at a very low concentration (20 µM). Each of these compounds had a long term effect in increasing the $[Ca^{2+}]_c$ resting level which remained abnormally high even after *A. awamori* was incubated with the compounds for 1 h. The hyphae therefore had difficulties in restoring $[Ca^{2+}]_c$ to its normal resting level in the presence of the compounds suggesting that the plasma membrane was severely permeabilized.

6.3.3 Fungicide mode-of-action studies

The idea of using the recombinant aequorin method to better understand the mode-of-action of commercially available fungicides proved successful because a large number of them increased $[Ca^{2+}]_c$ in *A. awamori*. Eight of the ten fungicides tested showed $[Ca^{2+}]_c$ agonistic properties. The negative controls (Minoxidil and Octopamine) showed no effect on $[Ca^{2+}]_c$ as either Ca^{2+} agonists or antagonists. However, the data confirmed that the positive control (CPA) was a Ca^{2+} agonist. None of the commercially available fungicides tested were found to possess Ca^{2+} antagonistic activity.

Except Fenarimol (which could only be tested at low concentration due to its low solubility in water), all the inhibitors of ergosterol biosynthesis (and thus involved in membrane synthesis) were found to affect $[Ca^{2+}]_c$ in the same manner. No effect on the parameters of the primary $[Ca^{2+}]_c$ transient was observed. However, all of the compounds caused a secondary $[Ca^{2+}]_c$ increase and the final $[Ca^{2+}]_c$ resting level was above its original level. The results suggest that these compounds cause the plasma membrane to become permeabilized. Interestingly, MBC (which is microtubule assembly inhibitor) had a similar effect on $[Ca^{2+}]_c$ as ergosterol synthesis inhibitors. This suggests that MBC may also have an effect in permeabilizing the plasma membrane.

On the contrary, Captan (which inhibits chitin biosynthesis) and Beam (which inhibits melanin biosynthesis) were shown to have a different effect on $[Ca^{2+}]_c$. These two compounds not only caused a secondary $[Ca^{2+}]_c$ increase and an increase in the final $[Ca^{2+}]_c$ resting level but they also caused an increase in the amplitude of the primary $[Ca^{2+}]_c$ increase and in the case of Captan, the length of the $[Ca^{2+}]_c$ transient. A possibility here is that the plasma membrane has again been perturbed by the compounds and this may in some way have affected the activity of Ca^{2+}-channels or other Ca^{2+} transport proteins.

When the data obtained with the ergosterol biosynthesis inhibitors were compared with the data on amphotericin B (which is known to interact with the ergosterols in the plasma membrane (Ghannoum and Rice 1999)) it was found that the increases in the $[Ca^{2+}]_c$ resting level observed was a similar feature of the $[Ca^{2+}]_c$ changes caused by both of these compounds. However, the ergosterol biosynthesis inhibitors lacked the strong affect of amphotericin B in increasing the amplitude and length of the $[Ca^{2+}]_c$ transient.

In summary, the main conclusions from the research described in this chapter were:

- Commercially available cell permeabilizing fungicides (amphotericin B, surfactin and gramicidin) caused $[Ca^{2+}]_c$ increases, which are both great in magnitude and long in duration. When fungal colonies were treated with high concentrations of these compounds hyphae were unable to restore their original $[Ca^{2+}]_c$ resting level. This suggests that these compounds may act by perturbing the homeostasis of $[Ca^{2+}]_c$ and possibly other ions in filamentous fungi.

- Of two recently purified cell permeabilizing compounds (tensin and viscosinamide) produced by antagonistic soil microorganisms, only viscosinamide increased $[Ca^{2+}]_c$ at concentrations likely to be present in the soil. It is therefore suggested that viscosinamide may inhibit the growth of soil fungi by perturbing the homeostasis of $[Ca^{2+}]_c$ or other ions.

7 USE OF THE AEQUORIN METHOD AS A BIOSENSOR FOR TOXICANT ANALYSIS

7.1 INTRODUCTION

The widespread use and release of natural and synthetic chemicals into the environment, singly or as complex domestic and industrial effluents, has necessitated the development of rapid and cost effective toxicity tests to protect humans and other organisms (Sherry et al. 1987). Short-term and long-term bioassays utilising microorganisms, invertebrates, higher plants and animals have been developed in order to diagnose the toxicity of pollutants. Short-term microbial toxicity tests involve bacteria, algae, protozoa and fungi, and, most of these can be regarded as biosensors (i.e. biological units linked to a transducer mechanism (de la Guardia 1995)). Bioluminescence is a particularly useful transducer because it can provide a microbial toxicity test which allows real time, non-destructive quantitative measurements of the effects of toxicants on living cells. One of the most widely used biosensors of this type is the Microtox® proprietary test utilising a natural light emitting marine bacterium, *Vibrio fischeri*. *Vibrio fischeri* is a gram negative free-living bacterium (Gellert et al. 1999) which is also found within the light organs of some species of fish and squid (Ruby and Lee 2001). Bioluminescence involves the emission of visible light mediated by the luciferin-luciferase enzyme system (Steinberg et al. 1995). Bacterial luciferase luminescence requires the activity of a branch of the electron transport chain (Wilson and Hastings 1998), and as the electron transport is involved in cell metabolism, any disruption to this system (e.g. due to the presence of toxins) will have an effect on light output. Luminescence is controlled by the *lux* operon (Meighen 1991) within *V. fischeri*, which emits blue light at 490 nm (Hastings et al. 1985; Wilson and Hastings 1998).

The general purpose of toxicity testing is to establish the potential impact of chemicals on organisms in the environment. The information gained can then be used to manage the treatment or release of chemicals. Whether a substance is toxic or not

depends on physico-chemical factors such as pH, temperature and salinity, but most importantly the test organism used and the concentration of the chemical. No one toxicity test can determine the effect of a toxicant on all organisms because organisms at different trophic levels respond to toxicants in different ways. Eukaryotic organisms can behave differently to prokaryotes although with the *V. fischeri* test a high correlation has been shown with other bioassays using eukaryotic organisms (Kaiser 1993).

The aims of the research described in this chapter were:

- To evaluate the use of recombinant aequorin as a biosensor in toxicant testing by analysing the effects of three representative toxic substances (3,5-dichlorophenol [3,5-DCP], chromium and zinc) on $[Ca^{2+}]_c$ in *A. awamori* expressing codon-optimised aequorin.

- To compare fungal aequorin and bacterial luciferase biosensors for the identification and analysis of toxic substances.

7.2 RESULTS

In this study I analysed the $[Ca^{2+}]_c$ response of *A. awamori* to different toxicant concentrations. Both changes in aequorin luminescence (RLU) and in $[Ca^{2+}]_c$ concentrations (μM) were analysed (Table 7.1; Figs 7.1-7.6). The concentrations of Zn^{2+}, Cr^{6+} and 3,5-DCP used in the experiments to assess toxicity were based on previous experience with *V. fischeri* bioassays (Prof. N. Christofi, personnel communication). Initially, these three chemicals were added to the fungus growing in microwell plates and luminescence was measured from the time of addition for 10 min periods. The $[Ca^{2+}]_c$ response was not significantly different from that obtained with the control solution which resulted in a $[Ca^{2+}]_c$ transient from mechanical perturbation (data not shown). A second approach studied the effects of preincubating the fungus for 5 and 30 min with the toxicants on the $[Ca^{2+}]_c$ response to external $CaCl_2$ (5 mM). All three toxicants influenced the $[Ca^{2+}]_c$ signature

resulting from this treatment (Table 7.1). Parameters of the Ca^{2+} signature which were assessed were the rise time, amplitude and full width half maximum (FWHM) (see Section 4.2.1.1), and the final resting level of $[Ca^{2+}]_c$ at the end of the experiment. 24 h old cultures in the multiwell plate were preincubated for 5 or 30 min before applying the 5 mM $CaCl_2$ stimulus. Comparisons were made with control (VS medium).

Treatment		**Features of $[Ca^{2+}]_c$ signatures**			
		Rise time (s)	Amplitude	FWHM	Final resting level
3,5-DCP	0.112 mg/l	7-9	↑	-	-
	11.2 mg/l	7-9	↓	-	↑
	112 mg/l	15-17	↓	↑	↑
Cr^{6+}	15 mg/l	7-9	↓	-	-
	120 mg/l	7-9	↓	-	-
	260 mg/l	7-9	↓	-	-
Zn^{2+}	0.18 g/l	7-9	↑	-	↑
	0.35 g/l	7-9	↓	-	↑
	0.7 g/l	7-9	↓	↑	↑
	1.3 g/l	7-9	↓	↑	↑

Table 7.1 Qualitative analysis of the effects of preincubating cultures of *A. awamori* with Zn^{2+}, Cr^{6+} and 3,5-DCP on $[Ca^{2+}]_c$ response to 5 mM external $CaCl_2$. Abbreviations: - = no effect (compared with untreated control), ↑ = increase in parameter, ↓ = decrease in parameter, FWHM - full width half maximum.

At low concentration (0.012 mg/l), 3,5-DCP caused a small increase in the amplitude of the $[Ca^{2+}]_c$ response. At higher concentrations (11.2 and 112 mg/l) the phenolic inhibited the amplitude of the $[Ca^{2+}]_c$ response (Figs. 7.1-7.4; Table 7.1). The high concentration of 3,5-DCP (112 mg/l) also increased the FWHM and rise time (Table 7.1). With 11.2 and 112 mg/l 3,5-DCP the final resting levels of $[Ca^{2+}]_c$ was elevated.

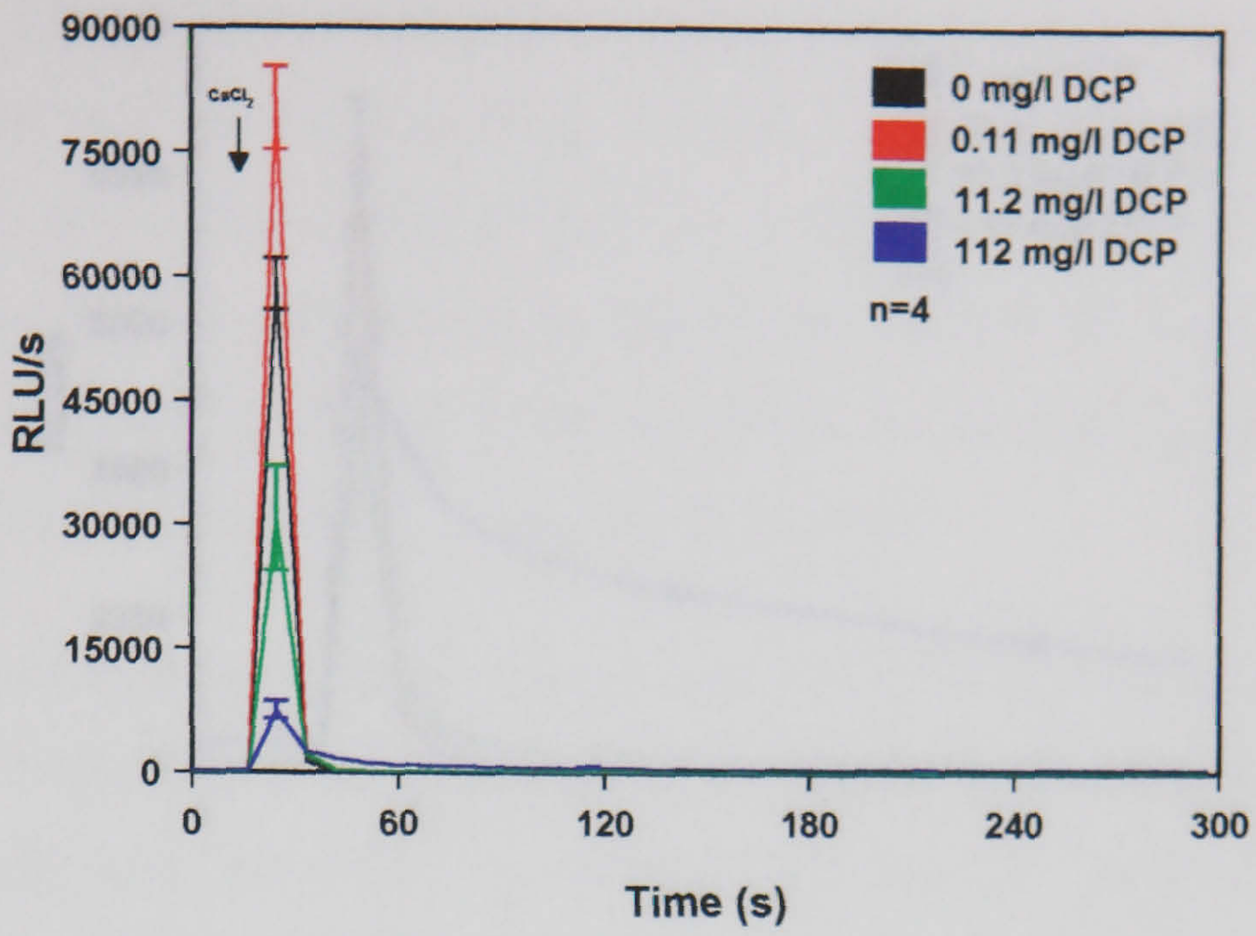

Figure 7.1 Effect of 3,5-DCP (5 min preincubation) on aequorin light emission in response to the addition of external $CaCl_2$ (5 mM). Results represent mean ± SE. Measurements were obtained using the repeated measuring protocol. Cycle time 11.6 s.

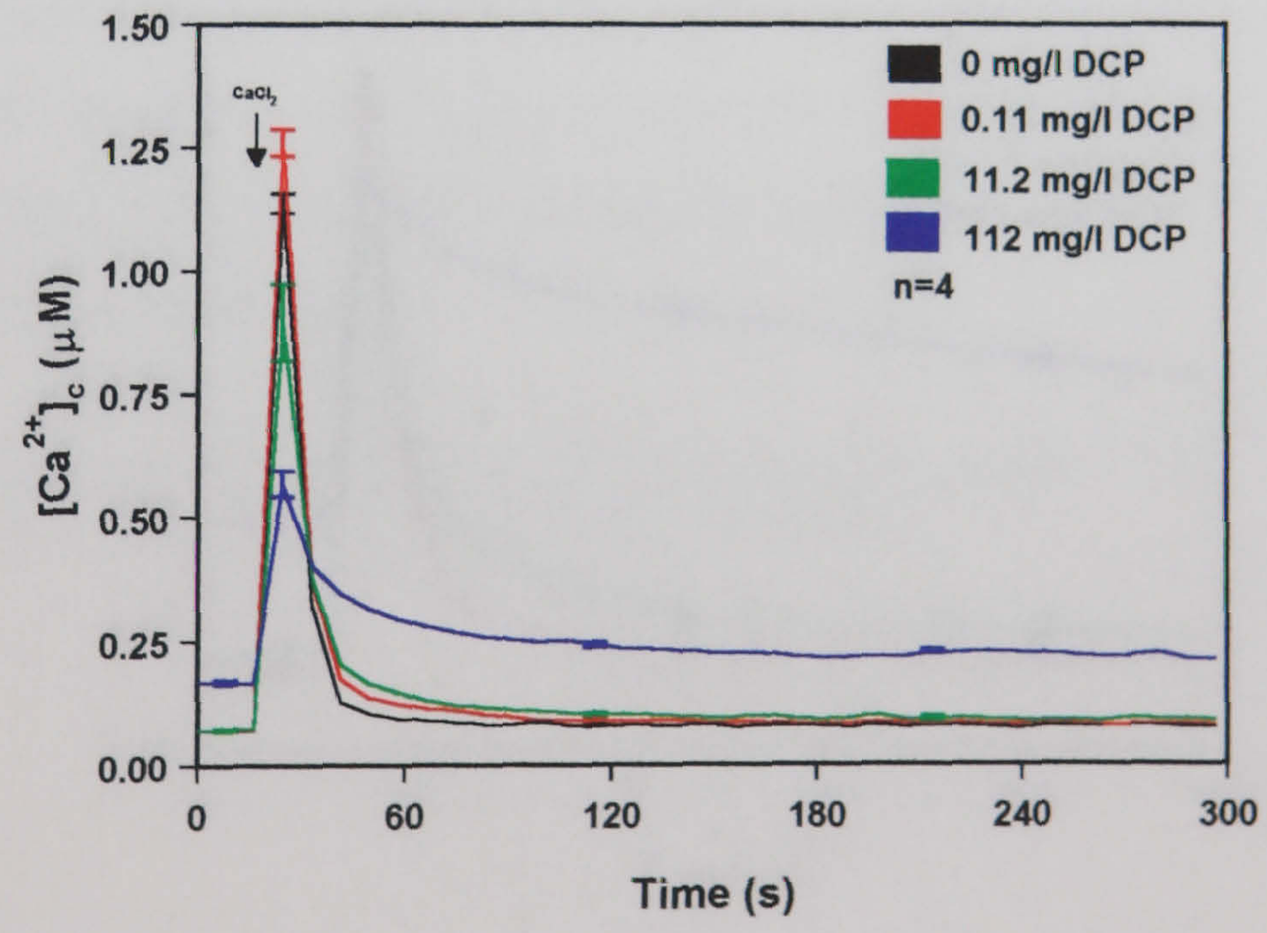

Figure 7.2 Effect of 3,5-DCP (5 min preincubation) on $[Ca^{2+}]_c$ in response to the addition of external $CaCl_2$ (5 mM). Results represent mean ± SE. Measurements were obtained using the repeated measuring protocol. Cycle time 11.6 s.

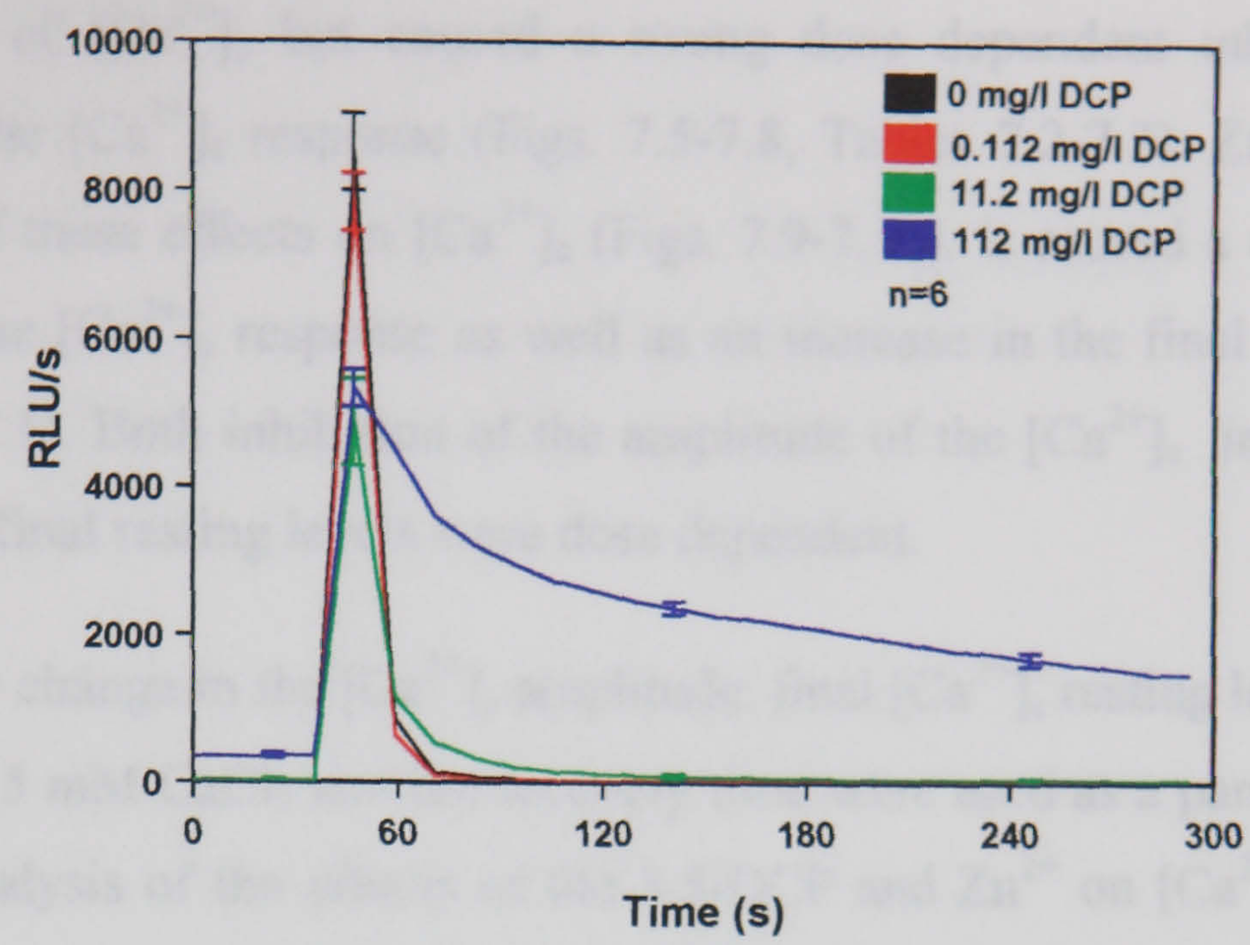

Figure 7.3 Effect of 3,5-DCP (30 min preincubation) on aequorin light emission in response to the addition of external $CaCl_2$ (5 mM). Results represent mean ± SE. Measurements were obtained using the repeated measuring protocol. Cycle time 11.6 s.

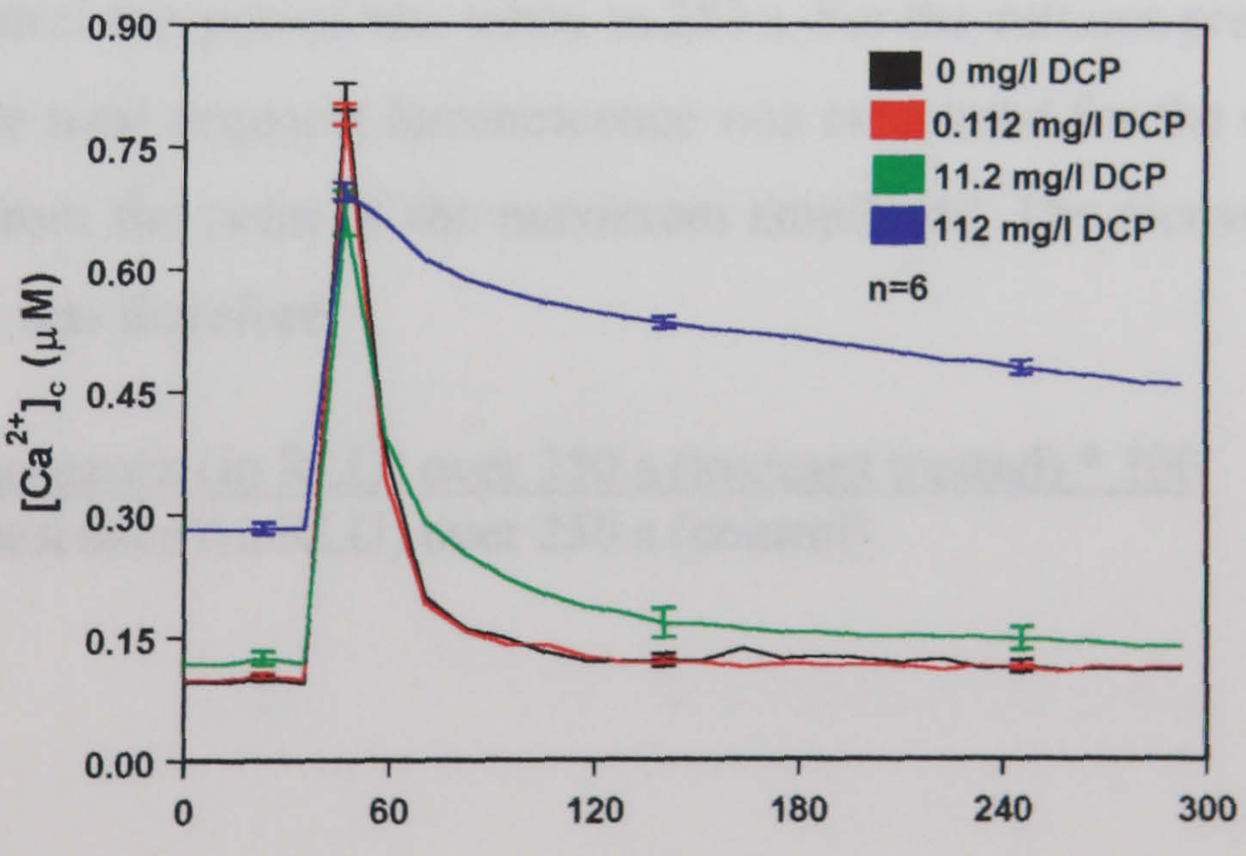

Figure 7.4 Effect of 3,5-DCP (30 min preincubation) on $[Ca^{2+}]_c$ in response to the addition of external $CaCl_2$ (5 mM). Results represent mean ± SE. Measurements were obtained using the repeated measuring protocol. Cycle time 11.6 s.

Chromium did not have significant affect ($P < 0.5$) the final $[Ca^{2+}]_c$ resting levels or recovery time of $[Ca^{2+}]_c$ but caused a strong dose dependent inhibition of the amplitude of the $[Ca^{2+}]_c$ response (Figs. 7.5-7.8, Tables 7.2-7.3). Zinc exhibited a combination of these effects on $[Ca^{2+}]_c$ (Figs. 7.9-7.12). It caused a decrease in the amplitude of the $[Ca^{2+}]_c$ response as well as an increase in the final $[Ca^{2+}]_c$ resting levels (Table 7.1). Both inhibition of the amplitude of the $[Ca^{2+}]_c$ increase and the increase in the final resting levels were dose dependent.

The percentage change in the $[Ca^{2+}]_c$ amplitude, final $[Ca^{2+}]_c$ resting levels following treatment with 5 mM $CaCl_2$ and the recovery time were used as a parameters for the quantitative analysis of the effects of the 3,5-DCP and Zn^{2+} on $[Ca^{2+}]_c$ (Tables 7.2 and 7.3). The percentage change in the $[Ca^{2+}]_c$ amplitude was calculated assuming that the amplitude of the control cultures was 100%. The percentage increase in the $[Ca^{2+}]_c$ resting level was calculated assuming that the $[Ca^{2+}]_c$ resting level of the control cultures was 100%. The recovery time was first calculated for control cultures. The term recovery time represents the total aequorin luminescence emitted during the period of time from the point when the maximum amplitude following $CaCl_2$ treatment was achieved to the point when the $[Ca^{2+}]_c$ reached its final resting level. In the control this period was taken as 250 s. For the cultures preincubated with the toxicants the total aequorin luminescence was calculated for the same period of 250 s starting from the point of the maximum amplitude. The recovery time of the control cultures was therefore:

$$\frac{\text{Aequorin luminescence (in RLU) over 250 s (toxicant treated)} * 100}{\text{Aequorin luminescence (in RLU) over 250 s (control)}}$$

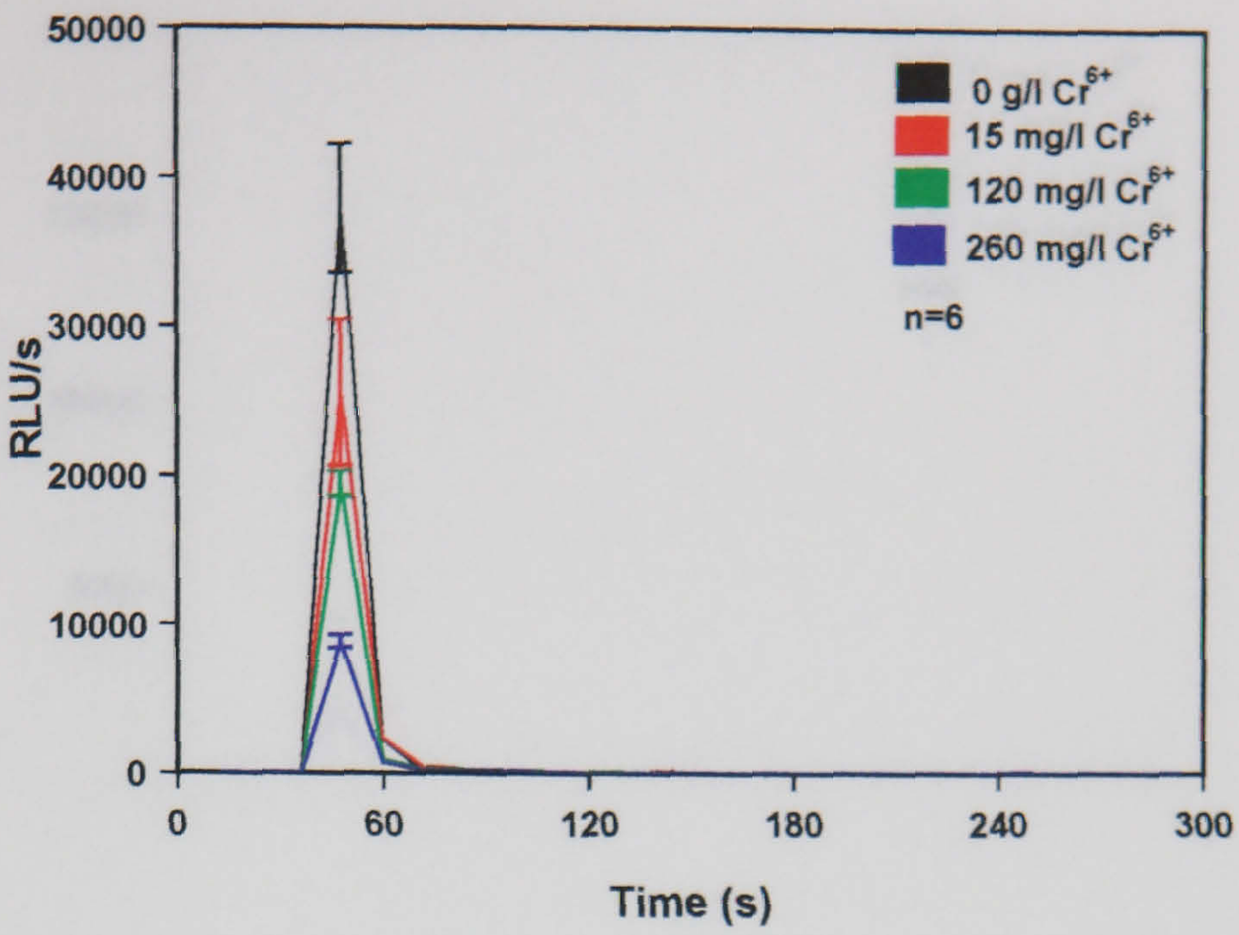

Figure 7.5 Effect of Cr^{6+} (5 min preincubation) on aequorin light emission in response to the addition of external $CaCl_2$ (5 mM). Results represent mean ± SE. Measurements were obtained using the repeated measuring protocol. Cycle time 11.6 s.

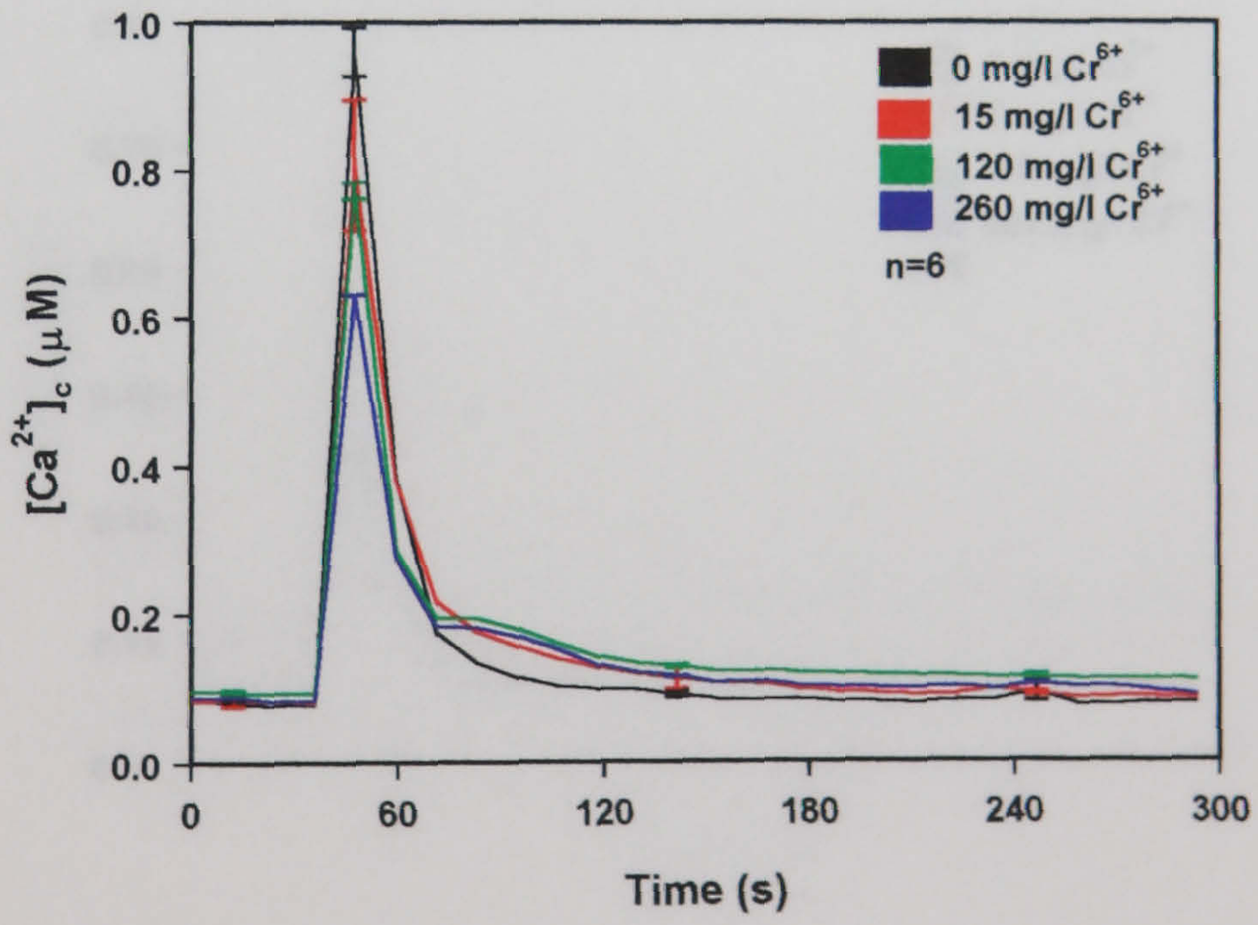

Figure 7.6 Effect of Cr^{6+} (5 min preincubation) on $[Ca^{2+}]_c$ in response to the addition of external $CaCl_2$ (5 mM). Results represent mean ± SE. Measurements were obtained using the repeated measuring protocol. Cycle time 11.6 s.

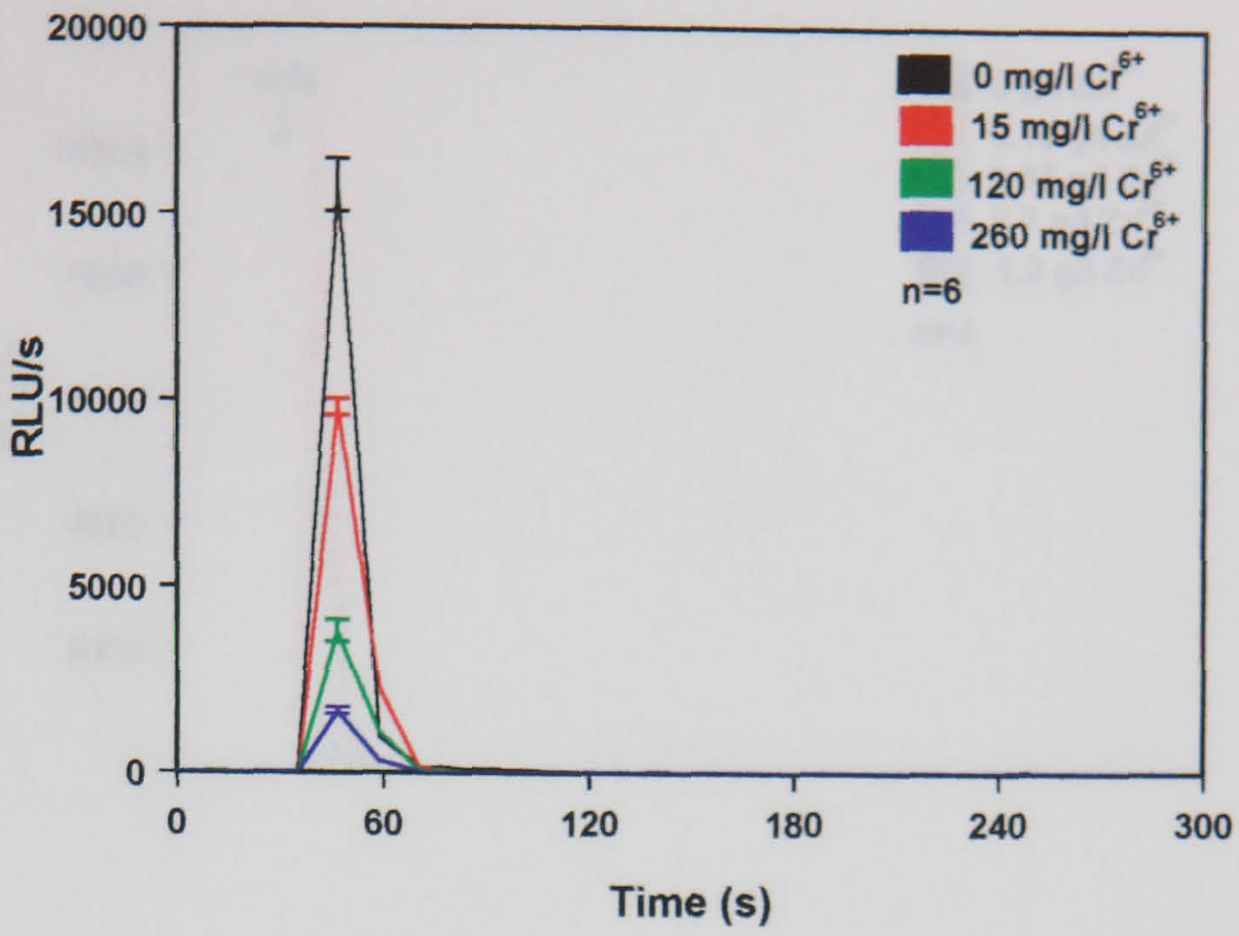

Figure 7.7 Effect of Cr^{6+} (30 min preincubation) on aequorin light emission in response to the addition of external $CaCl_2$ (5 mM). Results represent mean ± SE. Measurements were obtained using the repeated measuring protocol. Cycle time 11.6 s.

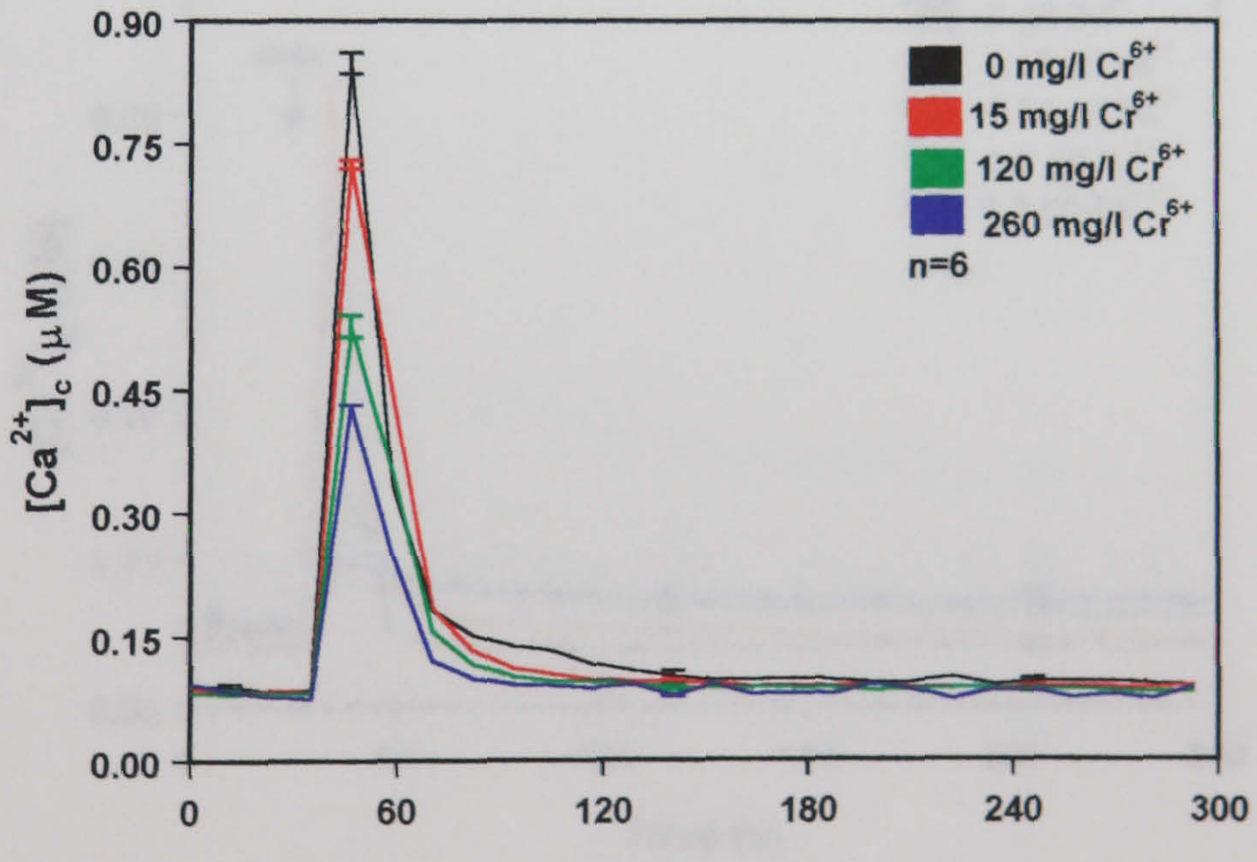

Figure 7.8 Effect of Cr^{6+} (30 min preincubation) on $[Ca^{2+}]_c$ in response to the addition of external $CaCl_2$ (5 mM). Results represent mean ± SE. Measurements were obtained using the repeated measuring protocol. Cycle time 11.6 s.

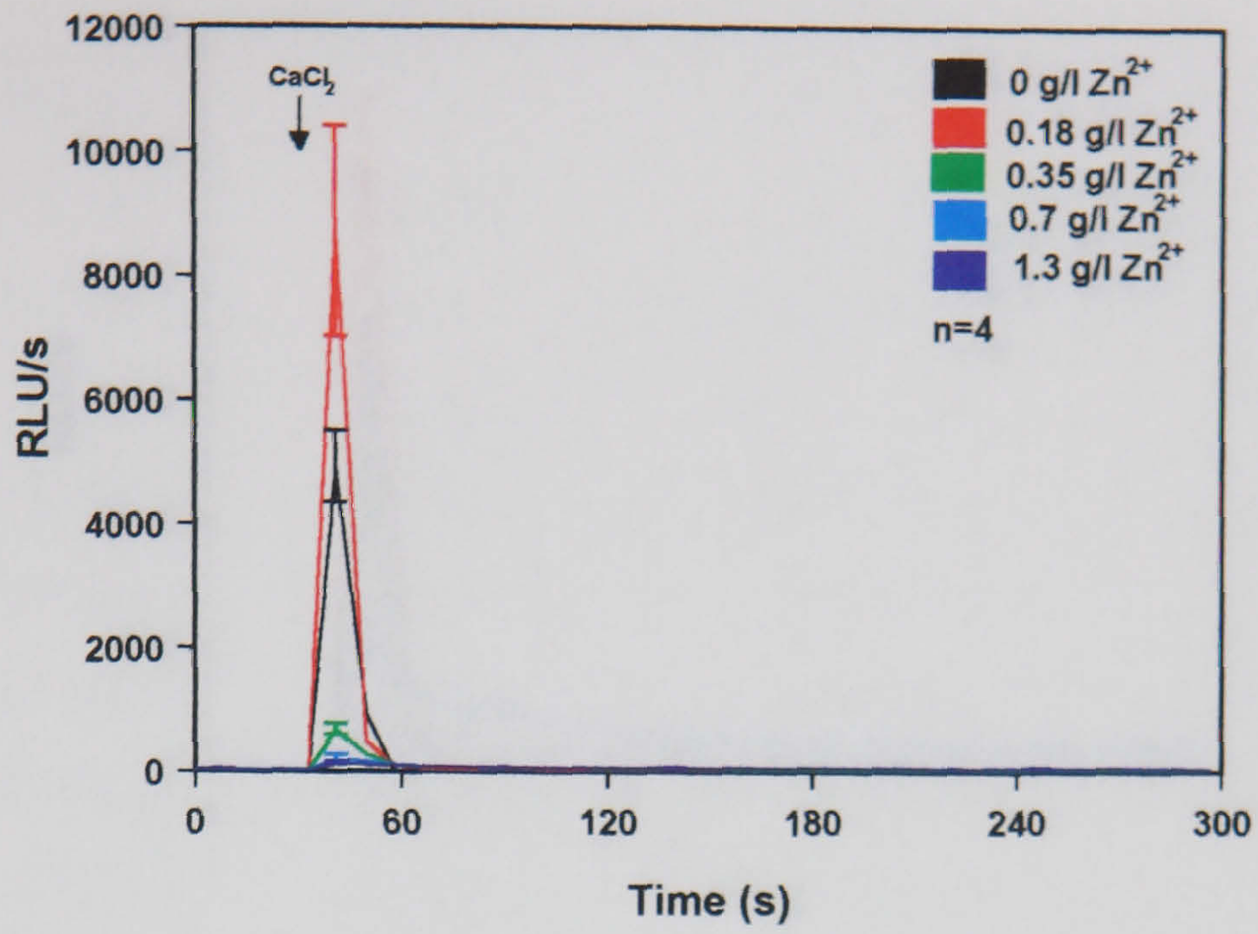

Figure 7.9 Effect of Zn^{2+} (5 min preincubation) on aequorin light emission upon the response to external $CaCl_2$ (5 mM). Results represent mean ± SE. Measurements were obtained using the repeated measuring protocol. Cycle time 11.6 s.

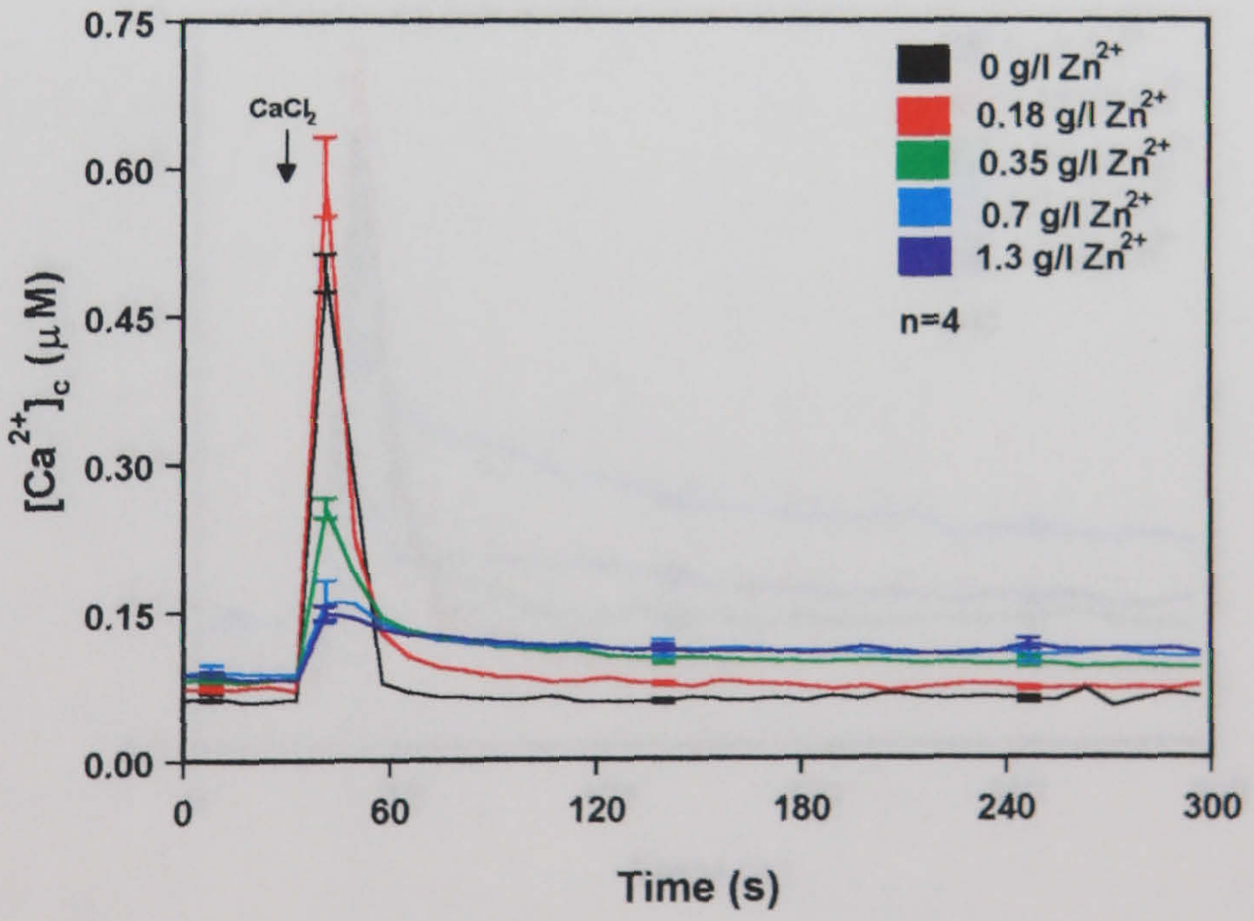

Figure 7.10 Effect of Zn^{2+} (5 min preincubation) on $[Ca^{2+}]_c$ upon the response to external $CaCl_2$ (5 mM). Results represent mean ± SE. Measurements were obtained using the repeated measuring protocol. Cycle time 11.6 s.

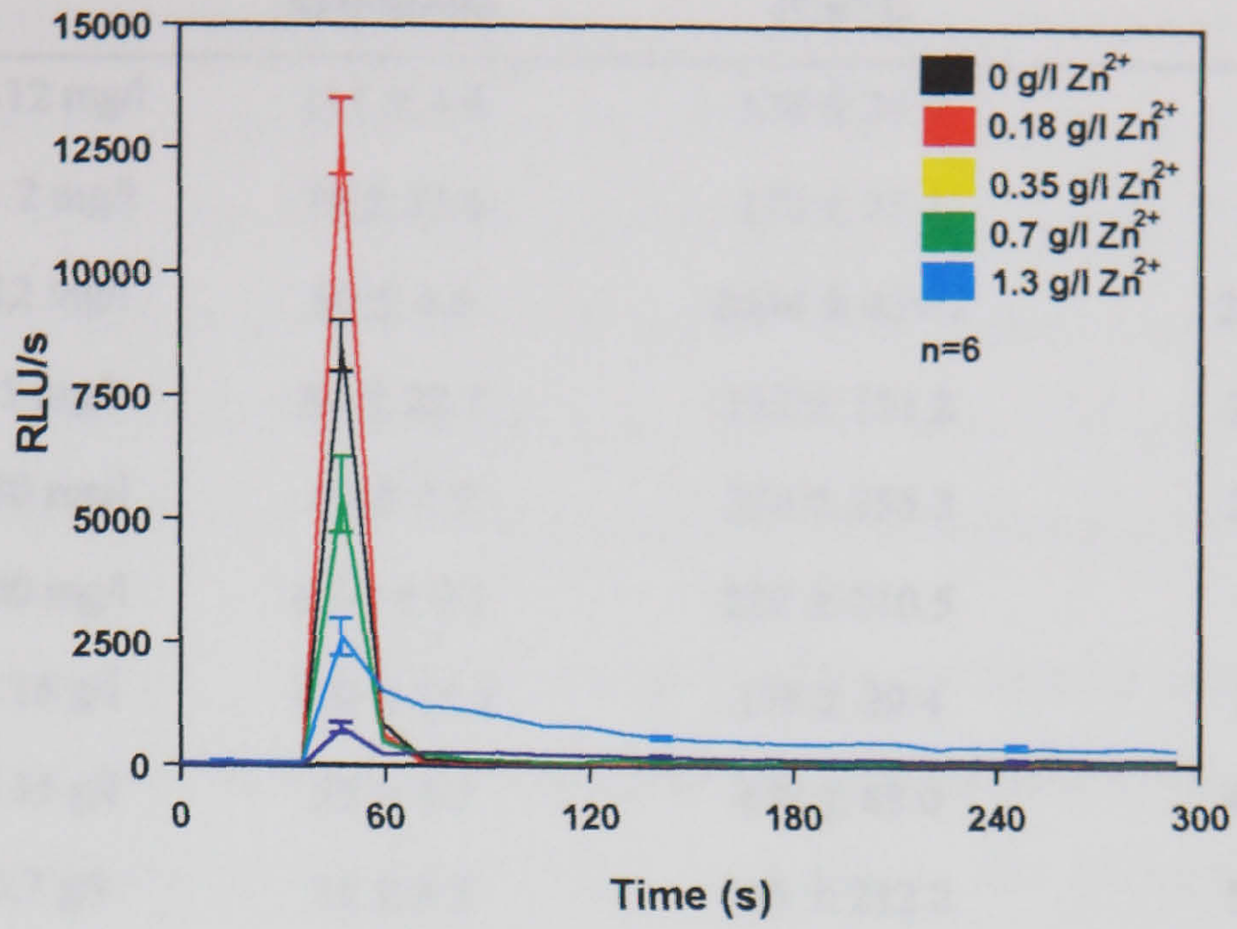

Figure 7.11 Effect of Zn^{2+} (30 min preincubation) on aequorin light emission upon the response to external $CaCl_2$ (5 mM). Results represent mean ± SE. Measurements were obtained using the repeated measuring protocol. Cycle time 11.6 s.

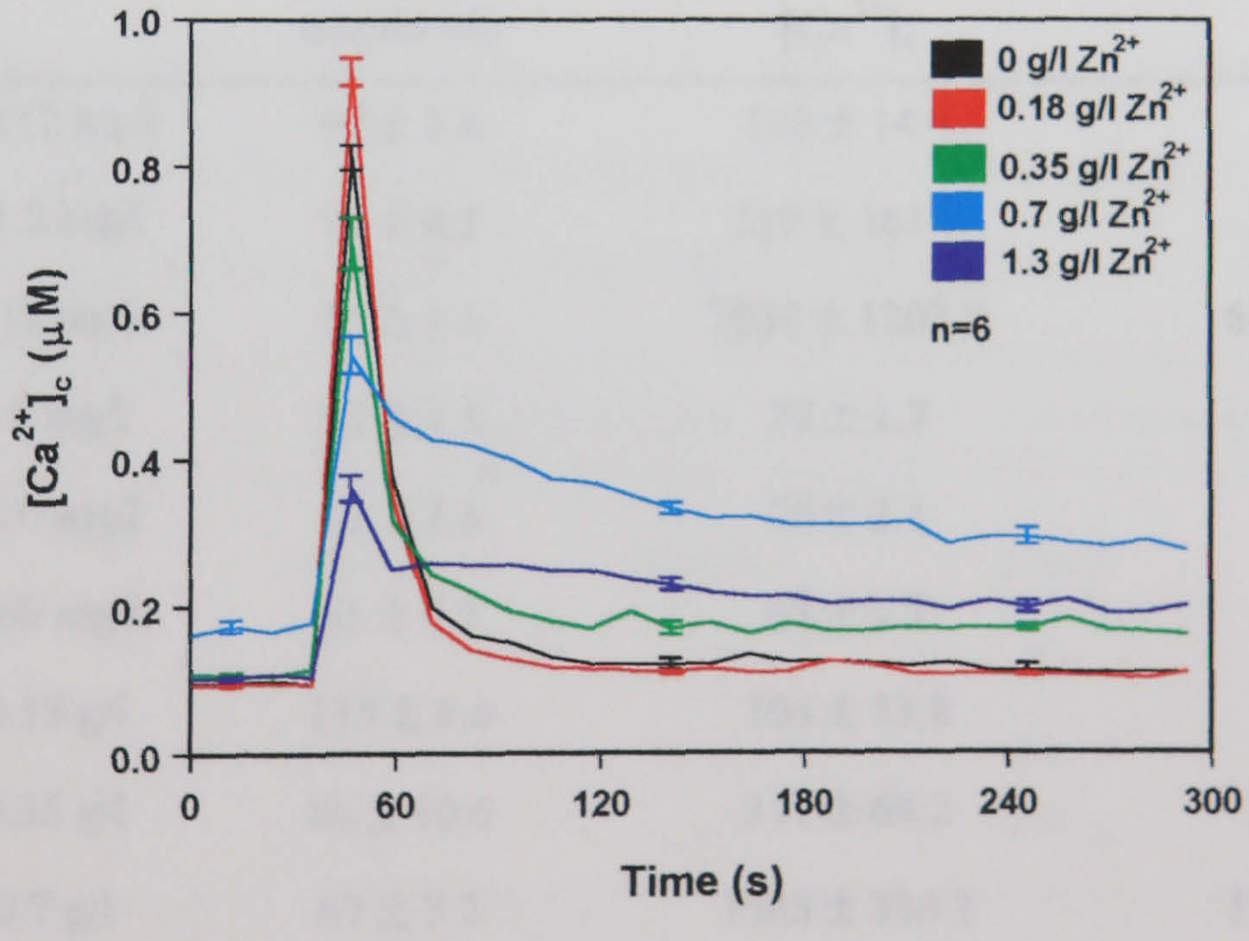

Figure 7.12 Effect of Zn^{2+} (30 min preincubation) on $[Ca^{2+}]_c$ upon the response to external $CaCl_2$ (5 mM). Results represent mean ± SE. Measurements were obtained using the repeated measuring protocol. Cycle time 11.6 s.

Treatment		% change in amplitude	% increase in final $[Ca^{2+}]_c$	% increase in recovery time
3,5-DCP	0.112 mg/l	111 ± 4.8	138 ± 30.9	143 ± 37.5
	11.2 mg/l	79 ± 13.6	172 ± 21.1	207 ± 23.2
	112 mg/l	50 ± 4.6	2444 ± 439.7	2547 ± 189.6
Cr^{6+}	15 mg/l	84 ± 22.7	157 ± 121.2	243 ± 256.7
	120 mg/l	80 ± 2.9	334 ± 255.3	254 ± 255.8
	260 mg/l	65.8 ± 0.1	220 ± 210.5	191 ± 87.2
Zn^{2+}	0.18 g/l	120 ± 16.2	176 ± 29.4	220 ± 33.5
	0.35 g/l	52 ± 4.2	430 ± 88.0	484 ± 123.0
	0.7 g/l	33 ± 8.5	585 ± 212.2	599 ± 238.2
	1.3 g/l	30 ± 2.9	661 ± 122.6	603 ± 102.0

Table 7.2 Inhibitory and stimulatory effects of Zn^{2+}, Cr^{6+} and 3,5-DCP on $[Ca^{2+}]_c$ amplitude, $[Ca^{2+}]_c$ resting levels and recovery time in *A. awamori* following stimulation with 5 mM $CaCl_2$. 5 min preincubation with toxicant. Results represent mean ± SD. Abbreviations: - = no effect (compared with untreated control). Control is estimated as 100%.

Treatment		% change in amplitude	% increase in final $[Ca^{2+}]_c$	% increase in recovery time
3,5-DCP	0.112 mg/l	97 ± 3.8	108 ± 14.4	88 ± 2.9
	11.2 mg/l	82 ± 8.2	219 ± 161.0	288 ± 231
	112 mg/l	86 ± 3.3	7030 ± 1207.8	6507 ± 739.9
Cr^{6+}	15 mg/l	85 ± 1.5	77 ± 1.7	71 ± 14.9
	120 mg/l	62 ± 3.8	76 ± 2.1	56 ± 25.2
	260 mg/l	51 ± 0.1	65 ± 2.7	43 ± 16.7
Zn^{2+}	0.18 g/l	115 ± 5.6	104 ± 53.8	74 ± 6.2
	0.35 g/l	86 ± 10.6	311 ± 64.2	276 ± 62.8
	0.7 g/l	67 ± 7.7	1563 ± 330.1	1710 ± 172.3
	1.3 g/l	44 ± 5.3	651± 370.3	519 ± 146.2

Table 7.3 Inhibitory and stimulatory effects of Zn^{2+}, Cr^{6+} and 3,5-DCP on $[Ca^{2+}]_c$ amplitude, $[Ca^{2+}]_c$ resting levels and recovery times in *A. awamori* following stimulation with 5 mM $CaCl_2$. 30 min preincubation with toxicant. Results represent mean ± SD. Abbreviations: - = no effect (compared with untreated control). Control is estimated as 100%.

Recovery of the $[Ca^{2+}]_c$ resting levels in *A. awamori* cultures preincubated with toxicants for 5 min was fairly rapid compared with that in the control cultures. This was not the case for *A. awamori* preincubated with toxicants for 30 min prior to $CaCl_2$ treatment. In this case there was a protracted recovery in $[Ca^{2+}]_c$ concentration at the higher toxicant concentrations in all systems. The highest concentration of 3,5-DCP used (112 mg/l) and all concentrations of Zn^{2+} above 0.35 g/l elevated $[Ca^{2+}]_c$ resting levels until the end of the 5 min period of luminescence measurements.

In order to calculate IC_{50} values (concentration of the compound which causes 50% inhibition of the parameter) for all the toxicants it was decided to use the amplitude of the $[Ca^{2+}]_c$ response to external $CaCl_2$ (5 mM) in the presence of different concentrations of each toxicant. Changes in $[Ca^{2+}]_c$ amplitude was chosen instead of effects on the final $[Ca^{2+}]_c$ resting level because the former exhibited a greater dynamic range in the presence of different concentration of the toxicant. Calculated IC_{50} values for the 5 and 30 min toxicant preincubations with *A. awamori* are presented in Table 7.4. The 30 min IC_{50} for 3,5-DCP, Cr^{6+} and Zn^{2+} were 36.7, 167.8 and 549.7 mg/l. These can be compared with values from the *V. fischeri* test which gave IC_{50} values of 3.6, 13.95 and 0.44 mg/l for the same period of preincubation with the toxicants. The toxicity values with the fungal aequorin system were higher than those obtained with the bacterial luciferase system indicating a lower bioassay sensitivity with the parameters used to calculate the IC_{50} values.

	***V. fischeri* luciferase**		***A. awamori* aequorin**	
Preincubation time with toxicant	**5 min**	**30 min**	**5 min**	**30 min**
3,5-DCP	3.62	3.13	46.7	36.7
Cr^{6+}	29.9	13.95	400.1	167.9
Zn^{2+}	95.56	0.44	237.2	549.7

Table 7.4 IC_{50} values (mg/l) for 3,5-DCP, Cr^{6+} and Zn^{2+} using *V. fischeri* luciferase and *A. awamori* aequorin. IC50 values are based on the inhibition of the amplitude of the $[Ca^{2+}]_c$ increase (RLU) in response to the addition of 5 mM $CaCl_2$.

7.3 DISCUSSION

The proprietary Microtox bioassay and other bacterial bioluminescence methods, which do not involve genetically modified bacteria, including that used in the present study, utilise *V. fischeri.* There is no doubt that transgenic *A. awamori* expressing codon-optimised aequorin responds to toxic chemical challenge in a reproducible way. A major advantage of aequorin system is that it has more parameters which can be assessed than other toxicant bioassays. In the present study six different parameters were used: final $[Ca^{2+}]_c$ resting level, recovery time and amplitude of $[Ca^{2+}]_c$ following chemical challenge for 5 or 30 min.

Final $[Ca^{2+}]_c$ resting levels and recovery time after addition of 0.112 mg/l 3,5-DCP were significantly higher than in the control (Tables 7.2 and 7.3). Interestingly, the values obtained after 5 min preincubation were higher than after a 30 min preincubation with 3,5-DCP. This suggests that the fungus may be able to adapt to low concentrations of the toxicant. A 30 min incubation period with 112 mg/l 3,5-DCP increased final $[Ca^{2+}]_c$ resting levels and recovery was prolonged. Such concentrations were too toxic for the fungus and apparently did not allow adaptation to occur.

Chromium affected only the amplitude of the $[Ca^{2+}]_c$ response and this was used to calculate IC_{50} values. All other parameters were not significantly different from the control. Zinc caused an increase in the $[Ca^{2+}]_c$ resting levels and recovery time at a concentration above 350 mg/l which is 3 orders of magnitude higher than the IC_{50} for *V. fischeri* (Table 7.4).

Aequorin luminescence in *A. awamori* was shown to respond to organic and inorganic compounds by a decrease in the amplitude of the $[Ca^{2+}]_c$ response to external $CaCl_2$ with increasing toxicant concentration. 3,5-DCP and Zn^{2+} also affected the final $[Ca^{2+}]_c$ resting levels in the fungus. In the case of a 30 min preincubation with either 112 mg/l DCP or 0.7 g/l Zn^{2+}, the final $[Ca^{2+}]_c$ resting levels were significantly higher than after 5 min preincubation with these toxicants indicating a greater toxicity to the fungus with longer contact with each toxicant.

This is similar to the response of the *V. fischeri* bioassay where it was generally observed that toxicity increases (IC_{50} values decrease) with longer incubation times. Also the IC_{50} values for Zn^{2+} calculated using the amplitude changes in $[Ca^{2+}]_c$ concentrations showed decreased toxicity at higher concentrations. The toxicity to 3,5-DCP in *V. fischeri* and *A. awamori* was almost complete after 5 min (Table 7.4).

With Zn^{2+} there was also evidence of toxicity recovery through adaptation with increasing times of incubation with the toxicant. This may be due to acquired resistance by the organism through synthesis of metal-binding proteins (metallothioneins) or constituents in the growth medium removing/immobilising the metal (e.g. EDTA or phosphate precipitation).

It was interesting to compare toxicity data obtained with the *A. awamori* aequorin system compared with those obtained with the *V. fischeri* luciferase. My results suggested that the bacterial luciferase biosensor may be more sensitive than the fungal aequorin one. The usual toxicity test is carried out using the IC_{50} parameter, so we attempted to calculate values for the aequorin assay. It is important to mention that IC_{50} values calculated on the basis of RLU are usually lower than IC_{50} values calculated on the basis of $[Ca^{2+}]_c$ concentrations. This is because aequorin luminescence is not directly proportional to $[Ca^{2+}]_c$ concentration. In this study it was decided to calculated the IC_{50} values using $[Ca^{2+}]_c$ concentrations (μM) because the changes in amplitude of the $[Ca^{2+}]_c$ response in RLU were very different from one experiment to another (data not shown). However, when RLU were converted into $[Ca^{2+}]_c$ concentrations, they were normalized.

The IC_{50} results with Cr^{6+} indicated that the fungal aequorin biosensor is less sensitive to this toxicant than the bacterial luciferase biosensor as the values were 12 times higher in the fungus. The IC_{50} values for the 30 min Zn^{2+} preincubations with the luciferase system were approximately 3 orders of magnitude lower for *V. fischeri*. Such insensitivity to Zn^{2+} has been observed previously with an ATP luminescence assay (Dalzell and Christofi 2001). Comparing the IC_{50} values for the fungus obtained with the 5 and 30 min incubation times, it is evident that with longer

preincubation the sensitivity of the organism is reduced possibly due to adaptation. This would negate the use of longer incubation times for assays. The results of the 5 min assay of Cr^{6+} using *A. awamori* gave an IC_{50} value of 400 mg l. This value is the same order of magnitude as the 15 min Microtox assay (339.6 mg/l) carried out by Codina et al (1993). Indeed the use of *V. fischeri* in various proprietary tests (LumisTox, Microtox, ToxAlert etc) has been shown to exhibit differences in sensitivity to different toxicants (Christofi et al. 2000). It is, therefore, difficult to state categorically that the *V. fischeri* luciferase biosensor is more sensitive to Cr^{6+} than the *A. awamori* aequorin one, particularly when different toxicant preincubation periods are used since the latter influence the ultimate IC_{50} value. My studies used toxicant preincubation times of 5 and 30 min for the *V. fischeri* assay and there was an increase in sensitivity when using the longer incubation with 3,5-DCP and Cr^{6+} toxicants but not with Zn^{2+} (Table 7.4). The Codina et al (1993) study showed an IC_{50} value for Zn^{2+} of 5.6 mg/l (15 min test) using Microtox whereas our studies obtained a value of 0.44 mg/l for a 30 min test. The response to toxicants by *A. awamori* is complete after about 6 min with respect to amplitude of response and final resting level of $[Ca^{2+}]_c$. My initial observations suggest that using a 30 min preincubation time for *V. fischeri*, the organism is more sensitive to Zn^{2+} and Cr^{6+} than *A. awamori* expressing aequorin. In future it may be possible to increase significantly the sensitivity of the aequorin biosensor using a higher concentration of $CaCl_2$ to stimulate the fungus following preincubation with the toxicant, by increasing the preincubation time with the toxicant or by using the final $[Ca^{2+}]_c$ level or recovery time to calculate the IC_{50}, especially if the preincubation time with the toxicant has been increased. Also obtaining a combination of different IC_{50} values from the effects on different parameters of the $[Ca^{2+}]_c$ signature could be useful for providing a more precise identification of the particular toxicant present.

Codina et al (1993) also used a yeast bioassay to test metal toxicity. The eukaryotic yeast was found to be less sensitive to metals than prokaryotic bacteria including *Vibrio* and *Pseudomonas* species. An IC_{50} value of 549.1 mg/l was obtained for Zn^{2+} using the yeast assay (Codina et al, 1993) which is comparable to some of the values obtained with the *A. awamori* aequorin system in our study. The yeast was slightly

more sensitive to Cr^{6+} (30.9 mg/l) than the filamentous *A. awamori* but this is not unusual among organisms at the same trophic level (see Codina et al, 1993).

An interesting observation is the enhanced stimulation of light output in some systems with a low concentration of toxicant. This was seen after 5 min preincubation with 0.112 mg/l 3,5-DCP (Fig. 7.1), 180 mg/l Zn^{2+} (Fig. 7.5) and also after 30 min preincubation with 180 mg/l Zn (Fig. 7.6). This stimulation is a common occurrence in toxicity bioassays (Christofi et al. 2000) referred to as hormesis. It is often observed in *V. fischeri* (N. Christofi, personnel communication).

It is not clear, based on these preliminary observations, what causes elevation of the final $[Ca^{2+}]_c$ resting level. In the case of 3,5-DCP it may be that this polar narcotic is affecting membrane permeability and the transport of Ca^{2+} out of the cytosol (e.g. by Ca^{2+}-ATPases and Ca^{2+}/H^+ antiporters). The metals may be competing with the transport mechanisms in membranes. The metals thus act by interacting with physiological ions affecting transport and its concomitant effect on $[Ca^{2+}]_c$.

In summary the main conclusions from the research described in this chapter were:

- The recombinant aequorin method can be used as a novel eukaryotic toxicant biosensor. It offers more parameters which can be readily analysed than the traditionally used bacterial biosensors.

- The fungal aequorin biosensor responded to toxic substances (3,5-DCP, Zn^{2+} and Cr^{6+}) by a decrease in the amplitude of the $[Ca^{2+}]_c$ response to 5 mM $CaCl_2$ and an increase in the $[Ca^{2+}]_c$ resting levels (Zn^{2+} and 3,5-DCP).

- Preliminary IC_{50} values obtained with the fungal aequorin system, and based on the inhibition of the $[Ca^{2+}]_c$ amplitude in response to external $CaCl_2$ treatment, indicate that it is less sensitive for detecting 3,5-DCP, Zn^{2+} and Cr^{6+} than the *V. fischeri* luciferase system.

8 FUTURE WORK

The recombinant aequorin method employed in this study was shown to be a very useful and powerful tool for the analysis of fundamental studies of Ca^{2+} signalling in filamentous fungi as well as in applied research (e.g. fungicide mode-of-action studies; as a biosensor) in which $[Ca^{2+}]_c$ levels are used as an indicator of hyphal physiology. Future work carrying on from the research described in this thesis, should be in the following areas.

- Analysis of $[Ca^{2+}]_c$ responses to other physiological treatments (e.g. anoxia, blue light, red light, oxidative stress, salinity, sugar and nitrogen starvation).

- Use of a wider range of Ca^{2+} agonists and antagonists to analyse the biochemical machinery which is involved in the different signal-response pathways which are Ca^{2+}-mediated.

- Analysis of the effects of CaM, cAMP, IP_3 and protein kinase agonists on $[Ca^{2+}]_c$ levels measured with aequorin in order to investigate the cross talk between Ca^{2+} signalling and other signalling pathways.

- Analysis of $[Ca^{2+}]_c$ responses in aequorin-transformed strains with mutations in genes encoding proteins (e.g. Ca^{2+}-channels, Ca^{2+}-ATPase, CaM etc.) which are believed to play important roles in Ca^{2+} signalling and Ca^{2+} homeostasis. Pharmacological agents may also be used with these strains to attempt to correct the phenotype or even enhance it.

- Screen a wider range of fungicides with different modes-of-action in order to construct a database of Ca^{2+} signatures specific for each typo of fungicide.

- Carry out a comprehensive testing of a wide range of metals and organic compounds to assess the value of *A. awamori* as a biosensor both in systems using pure chemicals and those involving real samples (e.g. complex effluents and soil water matrices). A database of Ca^{2+} signatures characteristic to each group of environmental pollutants may then be constructed.

- Image the aequorin luminescence in single hyphae using a low light camera. This may be facilitated by using coelenterazine analogues (*hcp*-coelenterazine) which produce more sensitive aequorins which can sense lower $[Ca^{2+}]_c$ levels (Knight et al, 1993).

- Target aequorin to different organelles by fusing to different organelles targeting sequences in order to measure organellar free Ca^{2+} (e.g. see Rizzuto et al, 1992) and to determine the roles that theses organelles play as Ca^{2+} stores in different Ca^{2+} signalling pathways.

9 REFERENCES

Aagaard-Tillery, K.M. and Jelinek, D.F. 1995. Differential activation of a calcium-dependent endonuclease in human B lymphocytes. *Journal of Immunology* **155:** 3297-3307.

Allen, D.G. and Blinks, J.R. 1978. Calcium transient in aequorin-injected frog cardiac muscle. *Nature* **273:** 509-513.

Allen, D.G., Blinks, J.R., and Prendergast, F.G. 1977. Aequorin luminescence: relation of light emission to calcium concentration - a calcium-independent component. *Science* **195:** 996-998.

Alsina, A. and Rodriguez-Del Valle, N. 1984. Effects of divalent cations and functionally related substances on the yeast to mycelium transition of *Sporothrix schenckii*. *Sabouraudia* **22:** 1-5.

Anraku, Y., Ohya, Y., and Iida, H. 1991. Cell cycle control by calcium and calmodulin in *Saccharomyces cerevisiae*. *Biochimica et Biophysica Acta* **1093:** 169-177.

Arora, D.S. and Ohlan, D. 1997. *In vitro* studies on antifungal activity of tea (*Camellia sinensis*) and cofee (*Coffea arabica*) against wood-rotting fungi. *Journal of Basic Microbiology* **37:** 159-165.

Azur. 1997. *Microtox Manual. Volume 1-4.* Azur Environmental, 2232 Rutherford Road Carlsbad, California, USA.

Batiza, A.F., Schulz, T., and Masson, P.H. 1996. Yeast respond to hypotonic shock with a calcium pulse. *Journal of Biological Chemistry* **271:** 23357-23362.

Bauer, C.D., Simonis, W., and Schonknecht, G. 1999. Different xanthines cause membrane potential oscillations in a unicellular green algae pointing to a

ryanodine/cADPR receptor Ca^{2+} channel. *Plant And Cell Physiology* **20:** 453-456.

Baum, G., Long, J.C., Jenkins, G.I., and Trewavas, A.J. 1999. Stimulation of the blue light phototropic receptor NPH1 causes a transient increase in cytosolic Ca^{2+}. *Proceedings of the National Academy of Sciences of the USA* **96:** 13554-13559.

Berridge, M.J. 1997a. Elementary and global aspects of calcium signalling. *Journal of Physiology* **499:** 291-306.

Berridge, M.J. 1997b. The AM and FM of calcium signalling. *Nature* **386:** 759-760.

Berridge, M.J. and Bottman, M.D. 1996. Calcium signalling. In Heldin, C.H. and Purton, M., editors, *Signal Transduction*. Chapman & Hall. London. 206-221.

Blinks, J.R. 1982. The use of photoproteins as calcium indicators in cellular physiology. *Techniques in Cellular Physiology*. Elsevier. Amsterdam. 1-38.

Bootman, M.D., Cheek, T.R., Moreton, R.B., Bennett, D.L., and Berridge, M.J. 1994. Smoothly graded Ca^{2+} release from inositol 1,4,5-trisphosphate-sensitive Ca^{2+} stores. *Journal of Biological Chemistry* **269:** 24783-24791.

Bootman, M.D., Collins, T.J., Pappiatt, C.M., Prothero, L.S., MacKenzie, L., De Smet, P., Travers, M., Tovey, S.C., Seo, J.T., Berridge, M.J., Ciccolini, F., and Lipp, P. 2001. Calcium signalling - an overview. *Seminars in Cell and Developmental Biology* **12:** 3-10.

Bootman, M.D., Young, K.W., Young, J.M., Moreton, R.B., and Berridge, M.J. 1996. Extracellular calcium concentration controls the frequency of intracellular calcium spiking independently of inositol 1,4,5- trisphosphate production in HeLa cells. *Biochemical Journal* **314:** 347-354.

Bosnjak, Z.J., Aggarwal, A., Turner, L.A., Kampine, J.M., and Kampine, J.P. 1992. Differential-effects of halothane, enflurane, and isoflurane on Ca^{2+} transients and papillary muscle tension in guinea pigs. *Anesthesiology* **76:** 123-131.

Bradford, M.M. 1976. A rapid and sensitive method for the quantification of microgram quantities of protein utilizing the principle of protein dye binding. *Analytical Biochemistry* **72:** 248-254.

Brini, M., Marsault, R., Bastianutto, C., Alvarez, J., Pozzan, T., and Rizzuto, R. 1995. Transfected aequorin in the measurement of cytosolic Ca^{2+} concentration $[Ca^{2+}]_c$. *Journal of Biological Chemistry* **270:** 9896-9903.

Bush, D.S. 1995. Calcium regulation in plant cells and its role in signaling. *Annual Review of Plant Physiology and Plant Molecular Biology.* **46:** 95-122.

Callaham, D.A. and Hepler, P.K. 1991. Measurements of free calcium in plant cells. In McCormack, J.G. and Cobbold, P.H., editors, *Cellular Calcium. A Practical Approach*. IRL Press. Oxford. 383-410.

Calvert, C.M. and Sanders, D. 1995. Inositol trisphosphate-dependent and triphosphate independent Ca^{2+} mobilisation pathways at the vacular membrane of *Candida albicans*. *Journal of Biological Chemistry* **270:** 7272-7280.

Campbell, A.K. 1983. *Intracellular Calcium. Its Universal Role as Regulator*. John Wiley and Sons. Chichester, England.

Campbell, A.K., Trewavas, A.J., and Knight, M.R. 1996. Calcium imaging shows differential sensitivity to cooling and communication in luminous transgenic plants. *Cell Calcium* **19:** 211-218.

Carafoli, E. 1987. Intracellular calcium homeostasis. *Annual Review of Biochemistry* **56:** 395-433.

Carlile, M.J. and Watkinson, S.C. 1996. *The Fungi.* Academic Press. Harcourt Brace & Company. London-Boston-San Diego-New York-Sydney-Tokyo.

Cessna, S.G., Chandra, S., and Low, P.S. 1998. Hypo-osmotic shock of tobacco cells stimulates Ca^{2+} fluxes deriving first from external and then internal Ca^{2+} stores. *Journal of Biological Chemistry* **273:** 27286-27291.

Christofi,N., Dalzell, D.J.B., Hoffmann, C.C., Sales, D., Morton, J., Arretxe, M., Heap, M., Obst, U., Alte, S., Etxebarria, J., de Las Fuentes, M., Gutierrez, M., de la Sota, A. and Aspichueta, E. DTOX-DIRECT toxicity assessment of complex industrial effluents discharged to sewer. 2000. Brussels. Final Report to the European Commission.

Clayton, H., Knight, M., Knight, H., McAinsh, M.R., and Hetherington, A.M. 1999. Dissection of the ozone-induced calcium signature. *Plant Journal* **17:** 575-579.

Cobbold, P.H. and Rink, T.J. 1987. Fluorescence and bioluminescence measurement of cytoplasmic free calcium. *Biochemical Journal* **248:** 313-328.

Codina, J.C., Perez-Garcia, A., Romero, P., and de Vicente, A. 1993. A comparison of microbial bioassays for the detection of metal toxicity. *Archives of Environmental Contamination and Toxicology.* **25:** 250-254.

Collis, A.J. 1996 The development of transgenic aequorin as an indicator for cytosolic free calcium in *Neurospora crassa.* PhD thesis, University of Edinburgh.

Cornelius, G., Gebauer, G., and Techel, D. 1989. Inositol triphosphate induces calcium release from *Neurospora crassa* vacuoles. *Biochemical and Biophysical Research Communications* **162:** 852-856.

Cornelius, G. and Nakashima, H. 1987. Vacuoles play a decisive role in calcium homeostasis in *Neurospora crassa*. *Journal of General Microbiology* **133:** 2341-2347.

Corzo, A. and Sanders, D. 1992. Inhibition of Ca^{2+} uptake in *Neurospora crassa* by La^{3+} - a mechanistic study. *Journal of General Microbiology* **138:** 1791-1795.

Cox, J.A., Ferraz, C., Demaille, J.G., Perez, R.O., Vantuinen, D., and Marme, D. 1982. Calmodulin from *Neurospora crassa* - general properties and conformational changes. *Journal of Biological Chemistry* **257:** 694-700.

Creton, R., Speksnijder, J.E., and Jaffe, L.F. 1998. Patterns of free calcium in zebrafish embryos. *Journal of Cell Science* **111:** 1613-1622.

Cunningham, K.W. and Fink, G.R. 1994a. Ca^{2+} transport in *Saccharomyces cerevisiae*. *Journal of General Microbiology* **196:** 157-166.

Cunningham, K.W. and Fink, G.R. 1994b. Calcineurin-dependent growth control in *Saccharomyces cerevisiae* mutants lacking *pmc1*, a homologue of plasma membrane Ca^{2+} ATPases. *Journal of Cell Biology* **124:** 351-363.

Cunningham, K.W. and Fink, G.R. 1996. Calcineurin inhibits VCX1-dependent H^+/Ca^{2+} exchange and induces Ca^{2+} ATPases in *Saccharomyces cerevisiae*. *Molecular and Cellular Biology* **16:** 2226-2237.

Czymmek, K.J., Whallon, J.H., and Klomparens, K.L. 1994. Confocal microscopy in mycological research. *Experimental mycology* **18:** 275-293.

Dalzell, D.J.B. and Christofi, N. 2001. An ATP luminescence method for direct toxicity assessment of pollutants impacting on the activated sewage sludge process. *Water Research* (in press).

Davis, T.N., Urdea, M.S., Masiarz, F.R., and Thorner, J. 1986. Isolation of the yeast calmodulin gene - calmodulin is an essential protein. *Cell* **47:** 423-431.

De la Guardia, M. 1995. Biochemical sensors: the state of the art. *Mikrochimika Acta* **120:** 243-255.

Deacon, J.W. 1997. *Modern Mycology.* Blackwell Science. Oxford-London-Edinburgh-Malden-Carlton.

Dicker, J.W. and Turian, G. 1990. Calcium deficiencies and apical hyperbranching in wild-type and the "frost" and "spray" morphological mutants of *Neurospora crassa*. *Journal of General Microbiology* **136:** 1413-1420.

Dolmetsch, R.E., Lewis R.S., Goodnow C.C. and Healy, J.I. 1997. Differential activation of transcription factors induced by Ca^{2+} response amplitude and duration. *Nature*. **386:** 855-858.

Dunn, T., Gable, K., and Beeller, T. 1994. Regulation of cellular Ca^{2+} by yeast vacuoles. *Journal of Biological Chemistry* **269:** 7273-7278.

Elad, Y. and Kirshner, B. 1992. Calcium reduces *Botrytis cinerea* damage to plants *Ruscus hypoglossum*. *Phytoparasitica* **20:** 285-291.

Fischer, M., Schnell, N., Chattaway, J., Davies, P., Dixon, G., and Sanders, D. 1997. The *Saccharomyces cerevisiae CCH1* gene is involved in calcium influx and mating. *FEBS Letters* **419:** 259-262.

Fluck, R.A., Miller, A.L., and Jaffe, L.F. 1992. High calcium zones at the poles of developing medaka eggs. *Biological Bulletin* **183:** 70-77.

Foyouzi-Youssefi, R., Arnaudeau, S., Borner, C., Kelley, W.L., Tschopp, J., Lew, D.P., Demaurex, N., and Krause, K.H. 2000. Bcl-2 decreases the free Ca^{2+} concentration within the endoplasmic reticulum. *Proceedings of the National Academy of Sciences of the USA* **97:** 5723-5728.

Frazer, L.N. and Moore, D. 1993. Antagonists and inhibitors of calcium accumulation do not impair gravity perception though they adversely affect

the gravity responses of *Coprinus cinereus* stipes. *Mycological Research* **97:** 1113-1118.

Fricker, M.D., Plieth, C., Knight, H., Blancaflor, E., Knight, M.R., White, N.S., and Gilroy, S. 1999. Fluorescence and Luminescence Techniques to Probe Ion Activities in Living Plant Cells. In Mason, W.T., editor, *Fluorescent and Luminescent Probes*. Academic Press. London. pp. 569-596.

Gadd, G.M. 1995. Signal transduction in fungi. In Gow, N.A.R. and Gadd, G.M., editors, *The Growing Fungus*. Chapman & Hall. London. 183-210.

Gadd, G.M. and Brunton, A.H. 1992. Calcium involvement in dimorphism of *Ophiostomac ulmi*, the Dutch elm disease fungus, and characterization of calcium uptake in yeast cells and germ tubes. *Journal of General Microbiology* **138:** 1561-1571.

Gage, M.J., Bruenn, J., Fischer, M., Sander, D., and Smith, T.J. 2001. KP4 fungal toxin inhibits growth in *Ustilago maydis* by blocking calcium uptake. *Molecular Microbiology* **41:** 775-785.

Gasbarrini, A., Borle, A.B., Farghali, H., Caraceni, P., and Vanthiel, D. 1993. Fasting enhances the effects of anoxia on ATP, $Ca_i(^{2+})$ and cell injury in isolated rat hepatocytes. *Biochimica et Biophysica Acta* **1178:** 9-19.

Gellert, G., Stommel, A., and Trujillano, A. 1999. Development of an optimal bacterial medium based on the growth inhibition assay with *V. fischeri*. *Chemosphere* **39:** 467-476.

Gelli, A. and Blumwald, E. 1993. Calcium retrieval from vacuolar pools. *Plant Physiology* **102:** 1139-1146.

Ghannoum, M.A. and Rice, L.B. 1999. Antifungal agents: mode of action, mechanisms of resistance and correlation of these mechanisms with bacterial resistance. *Clinical Microbiology Reviews* **12:** 501-517.

Ghislain, M., Goffeau, A., Halachmi, D., and Eilam, Y. 1990. Calcium homeostasis and transport are affected by disruption of *cta3*, a novel gene encoding Ca^{2+}-ATPase in *Schizosaccharomyces pombe*. *Journal of Biological Chemistry* **265:** 18400-18407.

Gibbon, B.C. and Kropf, D.L. 1994. Cytosolic pH gradients associated with tip growth. *Science* **263:** 1419-1421.

Gilroy, S. and Trewavas, A. 2001. Signal processing and transduction on plant cells: the end of the beginning? *Nature Reviews* **2:** 307-314.

Giri, S., Mago, N., Bindra, A., and Khuller, G.K. 1994. Possible role of calcium in phospholipid synthesis of *Microsporum gypseum*. *Biochemical and Biophysical Acta* **1215:** 337-340.

Gong, M., vanderLuit, A.H., Knight, M.R., and Trewavas, A.J. 1998. Heat-shock-induced changes in intracellular Ca^{2+} level in tobacco seedlings in relation to thermotolerance. *Plant Physiology* **116:** 429-437.

Gow, N.A.R., Miller, P.F.P., and Gooday, G.W. 1992. Life at the apex: growth of the hyphal tip. *Journal of Chemical Technology and Biotechnology* **56:** 217-219.

Grygorczyk, R., Feighner, S.D., Adam, M., Liu, K.K., LeCouter, J.E., Dashkevicz, M.P., Hreniuk, D.L., Rydverg, E.H., and Arena, J.P. 1996. Detection of intracellular calcium elevations in *Xenopus laevis* oocytes: Aequorin luminescence versus electrophysiology. *Journal of Neuroscience Methods* **67:** 19-25.

Gu, F., Khimani, A., Rane, S.G., Flurkey, W.H., Bozarth, R.F., and Smith, T.J. 1995. Structure and function of a virally encoded fungal toxin from *Ustilago maydis*: a fungal and mammalian Ca^{2+} channel inhibitor. *Structure* **3:** 805-814.

Halachmi, D. and Eilam, Y. 1996. Elevated cytosolic free Ca^{2+} concentrations and massive Ca^{2+} accumulation within vacuoles, in yeast mutant lacking PMR1, a homolog of Ca^{2+}-ATPase. *FEBS Letters* **392:** 194-200.

Hancock, J.T. 1997. Intracellular calcium: its control and role as an intracellular signal. *Cell signalling*. Wesley Longman. pp. 144-166.

Hasenfuss,G., Pieske, B., Castell, M., Kretschmann, B. and Maier, L.S. 1998. Influence of the novel inotropic agent levosimendan on isometric tension and calcium cycling in failing human myocardian. *Circulation* **98:** 2141-2147.

Hastings, J.W., Potrikus, C., Guptas, S., Kurfust, M., and Makemson, J. 1985. Biochemistry and physiology of bioluminescent bacteria. *Advances in Microbial Physiology* **26:** 235-291.

Hepler, P.K. and Waye, R.O. 1985. Ca^{2+} and plant development. *Annual Review of Plant Physiology* **36:** 397-439.

Hernandez, A., Cooke, D.T., and Clarkson, D.T. 1994. Ca^{2+} ATPase-driven calcium accumulation in *Ustilago maydis* plasma membrane vesicles. *Microbiology* **140:** 3047-3051.

Hirschi, K.D., Zhen, R.G., Cunningham, K.W., Rea, P.A., and Fink, G.R. 1996. CAX1, an H^+/Ca^{2+} antiporter from *Arabidopsis*. *Proceedings of the National Academy of Sciences of the USA* **93:** 8782-8786.

Hoshino, T., Mizutani, A., Shimizu, S., and Hidaka. 1991. Calcium-ion regulates the release of lipase of *Fusarium oxysporium* . *Journal of Biochemistry* **110:** 457-461.

Hudecova, D., Varecka, L., Vollek, V., and Betina, V. 1994. Growth and morphogenesis of *Botrytis cinerea*. Effects of exogenous calcium ions, calcium channel blockers and cyclosporin A. *Folia Microbiologica* **39:** 269-275.

Inouye, S., Noguchi, M., Sakaki, Y., Takagi, Y., Miyata, T., Iwanaga, S., and Tsuji, F.I. 1985. Cloning and sequence analysis of cDNA for the luminescent protein aequorin. *Proceedings of the National Academy of Sciences of the USA* **82:** 3154-3158.

Jackson, S.L. and Heath, I.B. 1989. Effects of exogenous calcium ions on tip growth, intracellular Ca^{2+} concentration, and actin arrays in hyphae of the fungus *Saprolegnia ferax*. *Experimental mycology* **13:** 1-12.

Johannes, E., Brosnan, J.M., and Sanders, D. 1991. Calcium channels and signal transduction in plant cells. *Bioessays* **13:** 331-336.

Kaiser, K.L.E. 1993. Qualitative and quantitative relationships of Microtox data with toxicity data for other aquatic species. In Richardson, M.L. editor, *Ecotoxicology Monitoring*. VCH Publishers, Weinheim. pp. 197-211.

Kendall, J.M., Badminton, M.N., Salanewby, G.B., Campbell, A.K., and Rembold, C.M. 1996. Recombinant apoaequorin acting as a pseudo-luciferase reports micromolar changes in the endoplasmic-reticulum free Ca^{2+} of intact cells. *Biochemical Journal* **318:** 383-387.

Klionsky, D.J., Herman, P.K., and Emr, S.D. 1990. The fungal vacuole - composition, function, and biogenesis. *Microbiological Reviews* **54:** 266-292.

Knight, H., Trewavas, A.J., and Knight, M.R. 1997. Calcium signalling in *Arabidopsis thaliana* responding to drought and salinity. *Plant Journal* **12:** 1067-1078.

Knight, H., Trewavas, A.J., and Read, N.D. 1993a. Confocal microscopy of living fungal hyphae microinjected with Ca^{2+}-sensitive fluorescent dyes. *Mycological Research* **97:** 1505-1515.

Knight, M., Campbell, A.K., Smith, S.M., and Trewavas, A. 1991a. Recombinant aequorin as a probe for cytosolic free Ca^{2+} in *Eschericia coli*. *FEBS Letters* **282:** 405.

Knight, M., Read, N.D., Campbell, A.K., and Trewavas, A. 1993b. Imaging calcium dynamics in living plants using semi-synthetic recombinant aequorins. *Journal of Cell Biology* **121:** 83-90.

Knight, M.R., Campbell, A.K., Smith, S.M., and Trewavas, A.J. 1991b. Transgenic plant aequorin reports the effects of touch and cold-shock and elicitors on cytoplasmic calcium. *Nature* **352:** 524-526.

Knight, M.R., Smith, S.M., and Trewavas, A.J. 1992. Wind-induced plant motion immediately increases cytosolic calcium. *Proceedings of the National Academy of Sciences of the USA* **89:** 4967-4971.

Koeppe, R.F., Killian, J.A., Bas Vogt, T.C., de Kruijff, B., Taylor, M.J., Mattice, G.Y., and Greathouse, D.V. 1995. Induced conformational changes of specific side chains in the gramicidin transmembrane channel. *Biochemistry* **34:** 9299-9306.

Koltin, K. and Day, R.P. 1975. Specificity of *Ustilago maydis* killer proteins. *Applied Microbiology* **30:** 694-696.

Krystofova, S., Varecka, L., and Betina, V. 1995. The Ca-45(2+) uptake by *Trichoderma viride* mycelium. Correlation with growth and conidiation. *General Physiology and Biophysics* **14:** 323-337.

Krystofova, S., Varecka, L., and Betina, V. 1996. Effects of agents affecting Ca^{2+} homeostasis on *Trichoderma viride* growth and conidiation. *Folia Microbiologica* **41:** 249-253.

Leung, C.F., Webb, S.E., and Miller, A.L. 1998. Calcium transients accompany ooplasmic segregation in zebrafish embryos. *Development Growth and Differentiation* **40:** 313-326.

Li, L.H., Wine, R.N., Miller, D.S., Reece, J.F., Smith, M., and Chapin, R.E. 1997. Protection against methoxyacetic-acid-induced spermatocyte apoptosis with calcium channel blockers in cultures rat seminiferous tubules: possible mechanisms. *Toxicology and Applied Pharmacology* **144:** 105-119.

Liang, F., Cunningham, K.W., Harper, J.F., and Sze, H. 1997. ECA1 complements yeast mutants defective in Ca^{2+} pumps and encodes an ER-type Ca^{2+}-ATPase in *Arabidopsis thaliana*. *Plant Physiology* **114:** 54.

Lu, K.P., Osmani, S.A., Osmani, A.H., and Means, A.R. 1992. Cooperative regulation of cell proliferation by calcium and calmodulin in *Aspergillus nidulans*. *Molecular Endocrinology* **6:** 365-374.

Lu, K.P., Osmani, S.A., Osmani, A.H., and Means, A.R. 1993. Essential roles for calcium and calmodulin in G2/M progression in *Aspergillus nidulans*. *Journal of Cell Biology* **121:** 621-630.

Luan, Y., Matsuura, I., and Yazawa, M. 1987. Yeast calmodulin: structural and functional differences compared with vertabrate calmodulin. *Journal of Biochemistry* **102:** 1531-1537.

Magalhaes, B.P., Wayne, R., Humber, R.A., Shields, E.J., and Roberts, D.W. 1991. Calcium-regulated appressorium formation of the entomopathogenic fungus *Zoophthora radicans*. *Protoplasma* **160:** 77-88.

Malho, R., Moutinho, A., van der Luit, A., and Trewavas, A.J. 1998. Spatial characteristics of calcium signalling: the calcium wave as a basic unit in plant cell calcium signalling. *Philosophical Transactions of the Royal Society Of London Series B - Biological Sciences* **353:** 1463-1473.

McAinsh, M.R. and Hetherington, A.M. 1998. Encoding specificity in Ca^{2+} signalling systems. *Trends in Plant Science* **3:** 32-36.

Meighen, E. 1991. Molecular-biology of bacterial bioluminescence. *Microbiological Reviews* **55:** 123-142.

Meuse, A.J., Perreault, C.L., and Morgan, J.P. 1992. Pathophysiology of cardiac-hypertrophy and failure of human working myocardium - abnormalities in calcium handling. *Basic Research In Cardiology* **87:** 223-233.

Miller, A.J., Vogg, G., and Sanders, D. 1990. Cytosolic calcium homeostasis in fungi - roles of plasma membrane transport and intracellular sequestration of calcium. *Proceedings of the National Academy of Sciences of the USA* **87:** 9348-9352.

Miller, A.L., Karplus, E., and Jaffe, L.F. 1994. Imaging $[Ca^{2+}]_i$ with aequorin using photon imaging detector. *Methods in Cell Biology*. Academic Press Inc. 305-358.

Mithofer, A., Ebel, J., Bhagwat, A.A., Boller, T., and NeuhausUrl, G. 1999. Transgenic aequorin monitors cytosolic calcium transients in soybean cells challenged with beta-glucan or chitin elicitors. *Planta* **207:** 566-574.

Muthukumar, G., Nickerson, A.W., and Nickerson, K.W. 1987. Calmodulin levels in yeasts and filamentous fungi. *FEMS Microbiology Letters* **41:** 253-255.

Muthukumar, G. and Nickerson, K.W. 1984. Ca(ii)-calmodulin regulation of fungal dimorphism in *Ceratocystis ulmi*. *Journal of Bacteriology* **159:** 390-392.

Nakajima-Shimada, J., Iida, H., Tsuji, F.I., and Anraku, Y. 1991a. Galactose-dependent expression of the recombinant Ca^{2+}-binding photoprotein aequorin in yeast. *Biochemical And Biophysical Research Communications* **174:** 115-122.

Nakajima - Shimada, J., Iida, H., Tsuji, F.I., and Anraku. Y. 1991b. Monitoring of intracellular calcium in *Saccharomyces cerevisiae* with an apoaequorin cdna expression system. *Proceedings of the National Academy of Sciences of the USA* **88:** 6878-6882.

Nakano, M.M., Marahiel, M.A., and Zuber, P. 1988. Identification of a genetic locus required for biosynthesis of the lipopeptide antibiotic surfactin in *Bacillus subtilis*. *Journal of Bacteriology* **170:** 5662-5668.

Nelson, G. 1999. Development of the recombinant aequorin method and its evaluation for calcium measurement in filamentous fungi. PhD thesis, University of Edinburgh.

Nelson,G., Kozlova, O.V., Collis, A.J., Knight, M., Fincham, J.R.S., Stanger, C., Renwick, A., Hessing, H., Punt, P., van der Hondel, C. and Read, N.D. 2001. Calcium measurement in living filamentous fungi expressing codon-optimised aequorin (in preparation).

Nelson, G., Stanger, C., Hessing, H., van der Hondel, C., Renwick, A. and Read, N.D. 1998. Calcium measurement in *Aspergillus* using recombinant aequorin. Abstract of the 6th International Mycological Congress, Jerusalem, Israel. p 9.

Nielsen, T.H., Christophersen, C., Anthoni, U., and Sorensen, J. 1999. Viscosinamide, a new cyclic depsipeptide with surfactant and antifungal properties produced by *Pseudomonas fluorescens* DR54. *Journal of Applied Microbiology* **86:** 80-90.

Nielsen, T.H., Thrane, C., Christophersen, C., Anthoni, U., and Sorensen, J. 2000. Structure, production characteristics and fungal antagonism of tensin- a new antifungal cyclic lipopepetide from *Pseudomonas fluorescens* strain 96.578. *Journal of Applied Microbiology* **89:** 992-1001.

Ohsumi,Y. and Anraku, Y. 1981. Active transport of basic amino acids driven by a proton motive force in vacuolar membrane vesicles of *Saccharomyces cerevisiae*. *Journal of Biological Chemistry* **256:** 2079-2082.

Ohya, Y., Ohsumi, Y., and Anraku, Y. 1986. Isolation and characterisation of Ca^{2+}-sensitive mutants of *Saccharomyces cerevisiae*. *Journal of General Microbiology* **132:** 979-988.

Ohya, Y., Umemoto, N., Tanida, I., Ohta, A., Iida, H., and Anraku, Y. 1991. Calcium-sensitive *cls* mutants of *Saccharomyces cerevisiae* showing a Pet phenotype are ascribable to defects of vacuolar membrane H^+-ATPase activity. *Journal of Biological Chemistry* **266:** 13971-13977.

Okorokov, L.A., Kuranov, A.J., Kuranova, E.V., and Silva, R.D. 1997. Ca^{2+}-transporting ATPase(s) of the reticulum type in intracellular membranes of *Saccharomyces cerevisiae*. Biochemical identification. *FEMS Microbiology Letters* **146:** 39-46.

Oparka, K.J. and Read, N.D. 1994. The use of fluorescent probes for studies in living plant cells. In Harris, N. and Oparka, K.J., editors, *Plant Cell Biology. A Practical Approach*. Oxford University Press, Oxford. pp. 27-50.

Parton, R.M. and Read, N.D. 1999. Calcium and pH imaging in living cells. In Lacey, A.J., editor, *Light Microscopy in Biology*. Oxford University Press. Oxford. pp. 211-264.

Pfeiffer, R.D., Reed, P.W., and Lardy, H.A. 1974. Ultraviolet and fluorescent spectral properties of the divalent cation ionophore A23187 and its metal ion complexes. *Biochemistry* **13:** 4007-4014.

Pietrobon, D., Di Virgilio, F.D., and Pozzan, T. 1990. Structural and functional aspects of calcium homeostasis in eukaryotic cells. *European Journal of Biochemistry* **193:** 599-662.

Pitt, D. and Barnes, J.C. 1993. Calcium homeostasis, signaling and protein-phosphorylation during calcium-induced conidiation in *Penicillium notamun*. *Journal of General Microbiology* **139:** 3053-3063.

Plieth, C., Hansen, U.P., Knight, H., and Knight, M.R. 1999. Temperature sensing by plants: the primary characteristics of signal perception and calcium response. *Plant Journal* **18:** 491-497.

Podczasy, J.J., Church, J.P., and Schoene, N.N. 1995. Effects of dietary fish-oil on calcium homeostasis in rat. *Journal of Nutrition* **6:** 327-333.

Prasher, D., McCann, R.O., and Cormier, M.J. 1985. Cloning and expression of the cDNA coding for aequorin, a bioluminescent calcium-binding protein. *Biochemical and Biophysical Research Communications* **126:** 1259-1268.

Price, A.H., Taylor, A., Ripley, S.J., Grippiths, A., Trewavas, A., and Knight, M. 1994. Oxidative signals in tobacco increase cytosolic calcium. *Plant Cell* **6:** 1301-1310.

Rao, J.P., Reena, G., and Subramanyam, C. 1997. Calmodulin-dependent protein phosphorylation during conidial germination and growth of *Neurospora crassa*. *Mycological Research* **101:** 1484-1488.

Read, N.D., Allan, W.T.G., Knight, H., Knight, M.R., Malho, R., Russell, A., Shacklock, P.S., and Trewavas, A.J. 1992. Imaging and measurement of cytosolic free calcium in plant and fungal cells. *Journal of Microscopy* **166:** 57-86.

Read, N.D., Shacklock, P.S., Knight, M.R., and Trewavas, A.J. 1993. Imaging calcium dynamics in living plant cells and tissues. *Cell Biology International* **17:** 111-125.

Reissig, J.L. and Kinney, S.G. 1983. Calcium as a branching signal in *Neurospora crassa*. *Journal of Bacteriology* **154:** 1397-1402.

Ribo, J.M. 1997. Interlaboratory comparison studies of the luminescent bacteria toxicity bioassay. *Environmental Toxicology and Water Quality* **12:** 283-294.

Rivera-Rodriguez, N. and Rodriguez-Del Valle, N. 1992. Effects of calcium ions on the germination of *Sporothrix schenckii* conidia. *Journal of Medical and Veterinary Mycology* **30:** 185-195.

Rizzuto, R., Brini, M., Pizzo, P., Murgia, M., and Pozzan, T. 1995. Chimeric green fluorescent protein as a tool for visualizing subcellular organelles in living cells. *Current Biology* **5:** 635-642.

Rizzuto, R., Simpson, A.W.M., Brini, M., and Pozzan, T. 1992. Rapid changes of mitochondrial Ca^{2+} revealed by specifically targeted aequorin. *Nature* **358:** 325-327.

Robert, V., Massimino, M.L., Tosello, V., Marsault, R., Cantini, M., Sorrentino, V., and Pozzan, T. 2001. Alteration in calcium handling at the subcellular level in mdx myotubes. *Journal of Biological Chemistry* **276:** 4647-4651.

Robson, G.D., Wiebe, M.G., and Trinci, A.P. 1991a. Involvement of Ca^{2+} in the regulation of hyphal extension and branching in *Fusarium graminearum* a-3/5. *Experimental mycology* **15:** 263-272.

Robson, G.D., Wiebe, M.G., and Trinci, A.P. 1991b. Low calcium concentrations induce increased branching in *Fusarium graminearum*. *Mycological Research* **95:** 561-565.

Roncal, T., Ugalde, U.O., and Irastorza, A. 1993. Calcium-induced conidiation in *Penicillium cyclosporium*: calcium triggers cytosolic alkalinization at the hyphal tip. *Journal of Bacteriology* **175:** 879-886.

Ruby, E. and Lee, K. 2001. The *Virrio fischeri-Euprymna scolopes* light organ association: current ecological paradigms. *Applied And Environmental Microbiology* **64:** 805-813.

Sadakane, Y. and Nakashima, H. 1996. Light-induced phase shifting of the circadian conidiation rhythm is inhibited by calmodulin antagonists in *Neurospora crassa*. *Journal of Biological Rhythms* **11:** 234-240.

Saladino, C.F., Warmhold, A.D., Vicente, L., and Jonas, E.A. 1996. Intracellular ionized calcium ($[Ca^{++}]_i$) mobilization in platelets from rats receiving atherogenic lipids. Modulation with nifedipine. *Artery* **22:** 80-92.

Sanders, D., Brownlee, C., and Harper, J.F. 1999. Communicating with calcium. *Plant Cell* **11:** 691-706.

Saporito, S.M. and Sypherd, P.S. 1991. The isolation and characterization of a calmodulin-encoding gene (cmd1) from the dimorphic fungus *Candida albicans*. *Gene* **106:** 43-49.

Saran, S., Nakao, H., Tasaka, M., Iida, H., Tsuji, F.I., Nanjundiah, V., and Takeuchi, I. 1994. Intracellular free calcium level and its response to cAMP stimulation in developing *Dictyostelium* cells transformed with jellyfish apoaequorin cDNA. *FEBS Letters* **337:** 173-183.

Schmid, J. and Harold, F. 1988. Dual role for calcium ions in apical growth of *Neurospora crassa*. *Journal of General Microbiology* **134:** 2623-2631.

Shaw, B., Kozlova, O., Read, N.D., Turgeon, B.G., and Hoch, H.C. 2001. Expression of recombinant aequorin as an intracellar calcium reporter in the phytopathogenic fungus *Phyllosticta ampecilida*. *Fungal Genetics and Biology* **34:** 207-215.

Sherry, J., Scott, B., and Dutka, B. 1987. Use of various acute, sublethal and early life-stage tests to evaluate the toxicity of refinery effluents. *Environmental Toxicology and Chemistry* **16:** 2249-2257.

Shimomura, O. 1986. Isolation and properties of various molecular forms of aequorin. *Biochemical Journal* **234:** 271-277.

Shimomura, O., Musicki, B., and Kishi, Y. 1988. Semi-synthetic aequorin. *Biochemical Journal* **251:** 405-410.

Shimomura, O., Musicki, B., Kishi, Y., and Inouye, S. 1993. Light-emitting properties of recombinant semi-synthetic aequorins and recombinant fluorescein-conjugated aequorin for measuring cellular calcium. *Cell Calcium* **14:** 373-378.

Silverman-Gavrila, L.B. and Lew, R.R. 2001. Regulation of the tip-high [Ca^{2+}] gradient in growing hyphae of the fungus *Neurospora crassa*. *European Journal of Cell Biology* **80:** 379-390.

Simkovic, M., Krystofova, S., and Varecka, L. 2000. Ca^{2+} fluxes in developing *Trichoderma viride* mycelium. *Canadian Journal of Microbiology* **46:** 312-324.

Steinberg, S., Poziomek, E., Engelmann, W., and Rogers, K. 1995. A review of environmental applications of bioluminescent measurement. *Chemosphere* **30:** 2155-2197.

Stowe, D.F., Sprung, J., Turner, L.A., Kampine, J.P., and Bosnjak, Z.J. 1994. Differential-effects of halothane and isoflurane on contractile force and calcium transients in cardiac purkinje fibers. *Anesthesiology* **80:** 1360-1368.

Strayle, J., Pozzan, T., and Rudolph, H. 1999. Steady-state free Ca^{2+} in the yeast endoplamic reticulum reaches only 10 μM and is mainly controlled by the secretory pathway pump Pmr1. *The EMBO Journal* **18:** 4733-4743.

Stroobant, P. and Scarborough, G.A. 1979. Active transport of calcium in *Neurospora* plasma membrane vesicles. *Proceedings of the National Academy of Science of the USA* **76:** 3102-3106.

Takahashi, K., Isobe, M., Knight, M.R., Trewavas, A.J., and Muto, S. 1997. Hypoosmotic shock induces increases in cytosolic Ca^{2+} in tobacco suspension-culture cells. *Plant Physiology* **113:** 587-594.

Takeda, T. and Yamamoto, M. 1987. Analysis and *in vivo* disruption of the gene coding for calmodulin in *Schizosaccharomyces pombe*. *Proceedings of the National Academy of Sciences of the USA* **84:** 3580-3584.

Torrecilla, I., Leganes, F., Bonilla, I., and Fernandez-Pinas, F. 2000. Use of recombinant aequorin to study calcium homeostasis and monitor calcium transients in response to heat and cold shock in cyanobacterial. *Plant Physiology* **123:** 161-175.

Vogel, H.J. 1956. A convenient growth medium for *Neurospora* (Medium N). *Microbial Genetics Bulletin* **51:** 107-124.

Wilson, T. and Hastings, J.W. 1998. Bioluminescence. *Annual Review of Cell and Developmental Biology* **14:** 197-230.

Wood, N.T., Haley, A., Viry-Moussaid, M., Johnson, C.H., van der Luit, A.H., and Trewavas, A.J. 2001. The calcium rhythms of different cell types oscillate with different circadian phases. *Plant Physiology* **125:** 787-796.